Table of Contents

Chapter		Page

Appendix

NASA Contractor Report 3103

Heat Transfer to a Full-Coverage, Film-Cooled Surface With Compound-Angle (30° and 45°) Hole Injection

H. K. Kim, R. J. Moffat, and W. M. Kays

CONTRACT NAS3-14336
FEBRUARY 1979

NASA

159

NASA Contractor Report 3103

Heat Transfer to a Full-Coverage, Film-Cooled Surface With Compound-Angle (30° and 45°) Hole Injection

H. K. Kim, R. J. Moffat, and W. M. Kays
Stanford University
Stanford, California

Prepared for
Lewis Research Center
under Contract NAS3-14336

NASA
National Aeronautics
and Space Administration

**Scientific and Technical
Information Office**

1979

Table of Contents

NOMENCLATURE

A	Heat transfer area, including hole area (see Fig. 1.1).
A_h	Hole cross-sectional area (see Fig. 1.1).
T_{tot}	Test section plate surface area.
β_h	Blowing parameter, $F/St(\theta = 1)$.
c	Specific heat, mainstream fluid.
c_f	Skin friction coefficient, $\tau_o = c_f/2\ \rho_\infty U_\infty^2$.
$\dot{E}_{supplied\ power}$	Electrical power supplied to plate.
E	Emissivity of plate to determine $\dot{Q}_{rad}$.
F	Blowing fraction $(\dot{m}_{jet}/A)/(\rho_\infty U_\infty)$.
h	Heat transfer coefficient, $\dot{q}_o''/(T_o - T_\infty)$, with wall mass flux (transpiration or film cooling)
h^*	Heat transfer coefficient, $\dot{q}_o''/(T_o - T_{aw})$, with film cooling.
h_o	Heat transfer coefficient, without wall mass flux.
H	Velocity profile shape factor, δ_1/δ_2.
k	Thermal conductivity.
K	Conductance between plate and cavity to determine $\dot{Q}_{cond}$.
KFL	Conductance to determine $\dot{Q}_{flow}$.
KCONV	Conductance-area product to determine T_2.
$\dot{m}$	Mass flow rate.
M	Blowing parameter, $(\rho_2 U_2)/(\rho_\infty U_\infty)$.
P	Hole spacing, or pitch (see Fig. 1.1).
Pr	Prandtl number, $\mu c/k$.
$\dot{Q}_o''$	Wall heat flux, $\dot{Q}_{CONV}/A_{tot}$.
$\dot{Q}_{cond}$	Heat transferred from plate to cavity and adjacent plates to determine $\dot{Q}_{losses}$.

$\dot{Q}_{CONV}$	Heat transferred from plate by convection to define Stanton number.
$\dot{Q}_{flow}$	Heat transferred from plate to secondary air flow.
$\dot{Q}_{losses}$	Heat transferred from plate other than by convection, $\dot{Q}_{cond} + \dot{Q}_{flow} + \dot{Q}_{rad}$.
$\dot{Q}_{rad}$	Heat transferred from plate by radiation.
r	Recovery factor, $Pr^{0.33}$.
Re_x	x-Reynolds number, $(x-x_{vo})U_\infty/\nu$.
Re_{δ_2}	Momentum thickness Reynolds number, $\delta_2 U_\infty/\nu$.
Re_{Δ_2}	Enthalpy thickness Rey-olds number, $\Delta_2 U_\infty/\nu$.
S	Conductance between adjacent plates to determine $\dot{Q}_{cond}$.
St	Stanton number, $h/(\rho_\infty c U_\infty)$, see Eqn. (2.1).
St_o	Stanton number at $M = 0$.
SCFM	Injectant flow rate through one tube.
T	Temperature.
T_g	Temperature of secondary air delivered to test section.
T^+	Non-dimensional temperature, $(T-T_\infty)\ \sqrt{c_f/2}/\{(T_o-T_\infty)St\}$.
$T_{\infty,r}$	Mainstream stagnation temperature, $T_\infty + \{rU_\infty^2\}/\{2g_c Jc\}$.
U	Velocity component, x-direction.
U_τ	Friction velocity, $\sqrt{g_c \tau_o/\rho_o}$, determined by Clauser plot method.
U^+	Non-dimensional velocity, U/U_τ.
x	Distance along surface, measured from nozzle exit.
x_{vo}	Distance, nozzle exit to virtual origin of turbulent boundary layer.
x^+	Non-dimensional distance, xU_τ/ν.
y	Distance normal to surface.
y^+	Non-dimensional distance, yU_τ/ν.

Greek Letters

α	Hole axis angle, measured from surface in the flow direction.
β	Hole axis angle, measured from surface in the spanwise direction.
$\delta(\ )$	Uncertainty in ( )
δ	Boundary layer thickness where $U/U_\infty = 0.99$.
δ_1	Displacement thickness, $\int_o^\infty \left(1 - \frac{\rho U}{\rho_\infty U_\infty}\right) dy$.
δ_2	Momentum thickness, $\int_o^\infty \frac{\rho U}{\rho_\infty U_\infty} \left(1 - \frac{U}{U_\infty}\right) dy$.
Δ_2	Entnalpy thickness, $\int_o^\infty \frac{\rho U}{\rho_\infty U_\infty} \left(\frac{T - T_\infty}{T_o - T_\infty}\right) dy$.
η	Adiabatic wall effectiveness, $(T_{aw} - T_\infty)/(T_2 - T_\infty)$.
θ	Temperature parameter, $(T_2 - T_\infty)/(T_o - T_\infty)$
μ	Dynamic viscosity.
ν	Kinematic viscosity.
ρ	Density.
σ	Stefan-Boltzmann constant.
ϕ	Function in $\theta = 1$ data correlation, $\{St(\theta = 1)/St_o\}/\{\ell n(1 + B_h)/B_h\}$.

SUMMARY

An experimental study of heat transfer was conducted on a turbulent boundary layer with full-coverage film cooling through an array of holes inclined at 30° to the surface and 45° to the flow direction (compound-angle injection). Heat transfer coefficients, based on $(t_{wall} - t_{stream})$, were measured over a range of injectant flows ($M = 0$ to $M = 1.5$) and Reynolds numbers ($1.6 \times 10^5 \leq Re_x \leq 2.5 \times 10^6$) at velocities between 9.8 and 16.8 m/s.

Compound-angle injection gives better thermal protection than in-line, slant-hole injection, but the beneficial effect is minimal in the first six rows of holes. For a value of $M = 0.37$ the heat transfer coefficient with compound-angle injection was the same as for the slant-angle injection after six rows, but was only one-half the slant-hole value after 11 rows.

The data for compound-angle injection show the same general features as for slant-angle and normal injection. Within the blown region, Stanton number decreases rapidly, with the minimum at the last row of holes. Recovery is rapid after the last row of holes, with the heat transfer returning to a conventional smooth-plate correlation. The data for $M = 0.4$ show the lowest values of Stanton number. Pitch-to-diameter ratio of 10 provides less thermal protection than 5, for the same value of M.

Stanton numbers are defined using the difference between wall temperature and stream temperature as the potential difference. Data are presented for injectant temperature equal to the wall temperature and injectant temperature equal to the stream temperature. Superposition can be used to predict the Stanton number for any intermediate temperature.

Chapter 1

INTRODUCTION

1.1 Background

When high-temperature gases pass over a surface there may be excessive heat transfer to the surface, and it is of practical interest to investigate various methods of thermal protection. Full-coverage film cooling is one such method. Film cooling is accomplished by injecting gaseous coolant through holes in the surface and into the boundary layer. The coolant, when distributed properly over the surface, acts as an effective heat sink and protects the surface from the high-temperature mainstream gases.

One application for film cooling is in protecting the blades and valves of high-temperature gas turbine engines. In high-pressure gas turbine engines it is desirable to increase the turbine inlet temperature, since this improves the thermodynamic efficiency. This raises problems, however, in internal protection. Accurate heat transfer data are critically important for the design of cooling systems. Esgar et al. [1] indicated that in the critical temperature range a reduction of about 20°F in the blade temperature could double the life of the blade. Cooling over the entire exterior of the surface may be accomplished either by transpiration (cooling using a porous blade surface) or by full-coverage film cooling through an array of small, discrete holes which cover the entire blade surface. Either method will allow a mainstream gas temperature well above that which would otherwise cause failure. Transpiration cooling appears to be impractical because of the low structural strength of the porous surface, and because of susceptibility to clogging of the pores by combustion products, especially during accidental engine backfires. Discrete-hole, full-coverage film cooling seems more practical, at the present stage of development.

The work reported herein is an experimental study of heat transfer to the turbulent boundary layer over a full-coverage film-cooled surface with compound angle (30° and 45°) hole injection.

1.2 Literature Review

The blade-cooling literature can be divided into two parts -- transpiration cooling (the limiting case where the individual holes are very close together and small relative to the sublayer of the boundary layer) and discrete-hole film cooling.

Transpiration cooling through a uniform porous plate has been very well investigated [2,3,4,5,6,7,8,9].

A general review of discrete-hold film cooling can be found in Goldstein [10] and, more recently, by Choe et al. [11] and Crawford et al. [12]. Only the most relevant topics will be treated in the present work.

1.2.1 Experimental Works

Wieghardt [13] investigated the de-icing problem on an airplane wing using a two-dimensional slot with injection nearly parallel to the surface. He correlated his experimental results in terms of an adiabatic wall effectiveness, η, and a parameter $X/(S\ M)$, where η is defined as

$$\eta \triangleq \frac{T_{aw} - T_\infty}{T_2 - T_\infty} \tag{1.1}$$

X is the distance downstream from the slot, S is the width of the slot, and M is the ratio of the injectant mass flux to the free-stream mass flux. T_∞ is the free-stream temperature, T_2 is the injectant temperature, and T_{aw} is the temperature assumed by an adiabatic wall downstream from the slot.

Le Brocq et al. [14] investigated the effects on η of hole-pattern arrangement, injectant angle, density ratio (coolant/mainstream), and blowing ratio. Their investigations were mainly carried out by plates with a pitch-diameter ratio of 8. Both in-line and staggered hole patterns were studied with normal injection (hole axis perpendicular to the surface). The staggered pattern was also tested with 45° downstream-angled injection. The results of their investigation concluded as follows: (i) the staggered hole pattern was more effective because the jets penetrated less into the boundary layer; (ii) there existed an optimum blowing ratio for which η was a maximum, and above which η decreased; and (iii) angled injection was more effective than normal injection.

Metzger et al. [15] investigated both effectiveness and heat transfer on a full-coverage surface with normal holes spaced 4.8 diameters apart and arranged in both in-line and staggered patterns. They based their values of heat transfer coefficient on the difference scheme -- local surface temperature and adiabatic wall temperature. Their investigation concluded that a staggered pattern yielded a higher effectiveness than did an in-line pattern, and that h^* could be 20 to 25 percent higher than h_o (without film cooling).

Mayle and Camarata [16] studied the effects of hole spacing and blowing ratio on heat transfer and film effectiveness for a staggered-hole array with compound-angle injection. The holes were angled 30° to the plate surface in the downstream direction and 45° to the flow direction in the spanwise direction, with P/D of 8, 10, and 14. They concluded that higher effectivenesses were obtained with P/D of 10 and 8 than with $P/D = 14$, regardless of coolant-flow ratio. They also found a blowing ratio that yielded a maximum η, and that the heat transfer coefficients, h^*, were significantly higher than h_o. Values of h^* were found to be almost constant for all M at $P/D = 8$, but only for high blowing ratios with a $P/D = 10$. Downstream of the last row of holes, h^* rapidly returned to h_o.

Choe et al. [11] investigated the effects on heat transfer of hole spacing, blowing ratio, mainstream velocity, and initial conditions upstream of the discrete-hole array, using normal injection at $P/D = 5$ and $P/D = 10$. Stanton number data were taken for two values of injectant temperature, and linear superposition was shown to predict Stanton number as a continuous function of injectant temperature. The two conditions tested were: injectant at surface temperature $(\theta = 1.0)$ and injectant at free stream temperature $(\theta = 0.0)$. The data were correlated using the same parameters used with transpiration investigations. Their results concluded that: (i) for a given injectant flow F, holes spaced at $P/D = 5$ produced better cooling than holes spaced at $P/D = 10$; (ii) in the initial region there was not much cooling and, in fact, St/St_o could be greater than unity; and (iii) the ratio St/St_o rapidly returned to unity in the downstream recovery region.

Crawford et al. [12] continued the series of Choe et al. [11] with 30° slant-hole injection, holding all other parameters identical to those used in [11]. Their study showed that, when the injectant temperature was equal to the plate temperature, a blowing ratio, M, of about 0.4 gave the minimum Stanton number, while higher blowing ratios resulted in higher Stanton numbers. Blowing ratios above 1.5 could produce Stanton number larger than that without film cooling. Within the first few rows of holes, Stanton number values were found to be affected by the upstream momentum thickness and by the ratio of thermal-to-momentum thickness. The data showed a slight dependence upon mainstream velocity, and spacing holes 10 diameters apart produced less effect on Stanton number for the same value of blowing ratio.

Metzger and Fletcher [17] investigated heat transfer and adiabatic wall effectiveness for discrete-hole injection, while Eriksen [18] measured laterally averaged heat transfer coefficients and cooling effectiveness. Launder and York [19] studied the effect of slant angle and acceleration on the same geometry as Le Brocq et al. [14]. Burggraf and Huffmeire [20] measured η and h^* for the case of two rows of holes. Nina and Whitelaw [21] studied cooling effectiveness with tangential injection through a row of circular holes.

Ramsey and Goldstein [22] measured temperature profiles, velocity profiles, and turbulence intensity profiles downstream of a single injection hole, with turbulence data and the velocity profiles taken by a hot-film probe. Metzger et al. [23] reported the heat transfer behavior on a full-coverage, film-cooled surface.

1.2.2 Analytical Works

Presently there are three methods available to predict wall temperature, film effectiveness, and heat transfer coefficient: (i) boundary layer finite-difference methods, (ii) energy integral equation methods, and (iii) superposition of single-jet effectiveness data.

Goldstein et al. [24] and Eriksen et al. [25] described a method for predicting cooling effectiveness for individual jets. Injection was modeled as a point heat source located above the wall, and a reduced form of the energy equation was solved and normalized to give effectiveness as a

function of both spanwise and streamwise distance. Mayle and Camarata [25] developed an improved superposition method to predict the full-coverage data. Their prediction equation contained two parameters, each a function of M and P/D.

Pai and Whitelaw [26] and Patankar et al. [27] investigated prediction of wall temperature and effectiveness downstream of two- and three-dimensional film-cooling slots. For two-dimensional slots, the boundary layer differential equations were solved using a mixing-length hypothesis to model the eddy viscosity. The mixing length was augmented algebraically to reflect the large increase in turbulent mixing associated with the injection process. For three-dimensional slots, the Navier-Stokes equations were reduced to elliptic in the cross-plane while held parabolic in the direction of flow, and then solved numerically. Again, a mixing-length hypothesis was used, with an algebraic augmentation to account for increased turbulent mixing.

Choe et al. [11] and Crawford et al. [12] developed both integral and differential analyses to predict their data. Choe et al. [11] developed a finite-difference method for predicting heat transfer with full-coverage film cooling. Their equations used local averaging, with models for the injection process, the nonlinear terms, and the augmented turbulent mixing. With local averaging, the area for averaging moves continuously, centered upon the nominal values of x. With this concept, they were able to model the injection process as transpiration rather than discrete injection. The nonlinear terms were modeled by decomposing them into two parts, interpreting one part to be a contribution to increased turbulent mixing and the second part as a momentum or energy source. The augmented turbulent mixing was modeled using an algebraic equation. Choe et al. [11] predicted most of their Stanton number data for low and moderate blowing ratios and $P/D = 5$ and 10. Crawford et al. [12] later used the same concepts in their prediction of Stanton number data for the blowing ratio range $0.2 \leq M \leq 0.75$ at $P/D = 5$.

1.3 Heat Transfer with Film Cooling

In full-coverage film cooling the injectant can leave the surface with a temperature, T_2, different from T_o, while in transpiration cooling the injectant temperature T_2 is always the same as that of the surface temperature T_o. Film cooling is a three-dempterature-potential problem.

The conventional convective rate equation is given as:

$$\dot{Q}_o'' = h_o(T_o - T_{aw}) \tag{1.2}$$

where T_o is wall temperature, T_{aw} is the adiabatic wall temperature, and h_o is the heat transfer coefficient in the absence of film cooling. In order to evaluate $\dot{Q}_o''$, the adiabatic wall effectiveness, η, must be known from experiment, as well as h_o (the value of h at the same x-Reynolds number with no blowing).

$$\eta \triangleq \frac{T_{aw} - T_\infty}{T_2 - T_\infty} \tag{1.5}$$

where T_∞ is the mainstream temperature and T_2 is the injectant coolant temperature. Thus two types of data are required, the first to establish η from the insulated surface as a function of blowing ratio M and the second to get h_o in the absence of film cooling.

Choe et al. [11] abandoned the η and h_o approach and used the following equation:

$$\dot{Q}_o'' = h(T_o - T_\infty) \tag{1.3}$$

where T_o is plate temperature, T_∞ is mainstream temperature. Thus h is the actual heat transfer coefficient. Using Eqn. (1.3), the dependence of the Stanton number upon injection temperature can be described in terms of the parameter, θ,

$$\theta = \frac{T_2 - T_\infty}{T_o - T_\infty} \tag{1.4}$$

The heat transfer Stanton number, St, can be obtained for an arbitrary value of θ (all other parameters fixed) using two fundamental experimental points: $\theta = 0$ and $\theta = 1$. Then, taking advantage of the linearity of the constant-property thermal energy equation, superposition can be used to determine St for any other values of θ:

$$St(\theta) = St(\theta{=}0) - \theta x[St(\theta{=}0) - St(\theta{=}1)] \tag{1.5}$$

One of the important hydrodynamic parameters is given in terms of blowing ratio, defined as the ratio of the injectant-to-mainstream mass flux:

$$M = \frac{\rho_2 u_2}{\rho_\infty U_\infty} \tag{1.6}$$

or averaged over the area associated with one hole, as shown in Fig. 1.1.

$$F = \frac{\dot{m}_{jet}/A}{\rho_\infty U_\infty} = M \frac{\pi D^2}{4P^2} \tag{1.7}$$

1.4 Objectives for the Present Research

The objective of the present study was to provide an experimental data base useful in developing methods of predicting surface heat flux on a full-coverage film-cooled surface with compound-angle injection.

The desired data consist of spanwise-averaged heat transfer coefficients within the discrete-hole array, and in the downstream (recovery) region after the final row of holes. Initial velocity and temperature profiles were to accompany the data. The range of conditions covers different blowing ratios and upstream initial conditions, with two injectant temperatures, $\theta = 0$ and $\theta = 1$ at each blowing ratio. The test surface configurations include $P/D = 5$ and $P/D = 10$.

A secondary objective was to test an integral analysis for correlating the data.

Mr. Ståle Rustad designed the Vortex Control Flow System and carried out a preliminary investigation of the flow field.

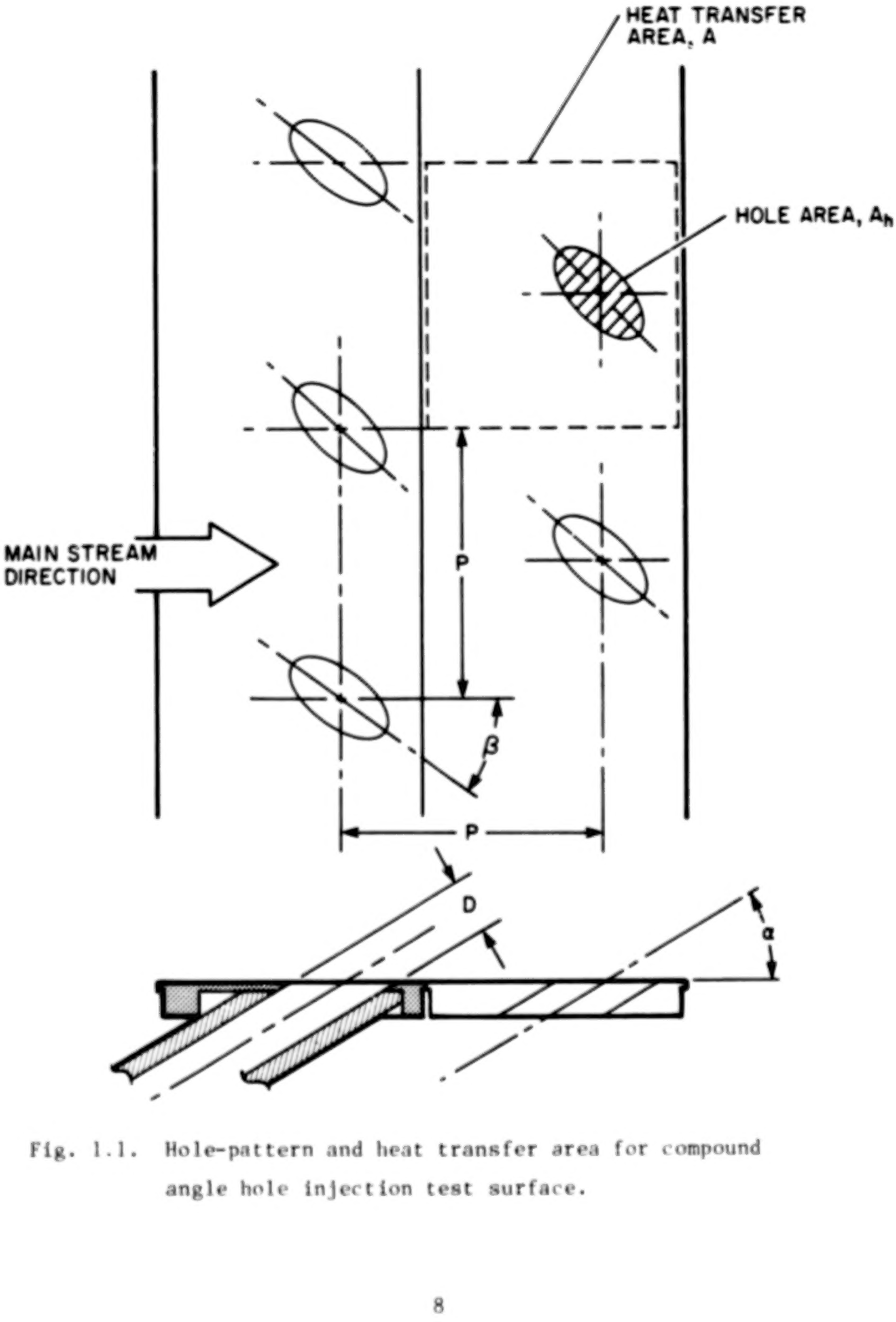

Fig. 1.1. Hole-pattern and heat transfer area for compound angle hole injection test surface.

Chapter 2

EXPERIMENTAL APPARATUS AND GENERAL APPROACH

2.1 Discrete Hole Rig

The heat transfer apparatus used in this experiment, the Discrete Hole Rig, was basically the same as that of Choe et al. [11] and Crawford et al. [12], except for the addition of a vortex control system. The Discrete Hole Rig is a closed-loop air tunnel which operates at ambient pressure and controlled, constant temperature. The test plates, foreplates, and afterplates can be heated as much as 20°C (36°F) above the temperature of mainstream air. A secondary system delivers the blowing air, heated or cooled, to the test section.

The vortex control system is a secondary loop which sucks air from one side of the test suction and injects it again at the opposite side wall, to control the cross flow inherent in compound-angle injection. Fig. 2.1 shows a schematic of the system. Fig. 2.2 shows the overall view.

2.1.1 Primary Air Supply System

The main loop is driven by a blower which delivers air through a uniform pressure header and a heat exchanger. The air then passes through a plenum chamber, a screen pack, and a rectangular nozzle before entering the test section. Flow leaves the test section through a plenum box serving both the secondary and the primary blower. The test duct is 20.3 cm (8 in.) high by 50.8 cm (20 in.) wide by 3.05 m (10 ft) long in the flow direction. The tunnel velocity is varied by changing pulleys and belts on the fan and motor in the range of 9 m/s (30 ft/sec) to 38 m/s (115 ft/sec).

The working section consists of an upstream foreplate, a test section, and a downstream afterplate. The sidewalls and topwall of the tunnel are plexiglass, with the topwall flexible so that any desired pressure gradient can be set in the flow direction. For the present experiments, the topwall was set to give a uniform static pressure in the flow direction

for each run. The deviation was not mroe than 0.25 mm of water pressure difference from the beginning of the test section to the downstream edge of the afterplate.

2.1.2 Secondary Air Supply System

The secondary loop is driven by a blower which delivers air through an oblique header into a secondary heat exchanger to control the blowing air temperature. The flow passes through the heat exchanger, a bank of finned heaters, and a screen pack, and then enters a plenum box.

A distribution manifold splits the secondary flow into 11 channels, one for each row of holes. Valves in each of the 11 channels regulate the flow, row by row. Hot-wire flowmeters installed in the delivery tubes measure the secondary air flow rates. Four of the delivery tubes had to be relocated for the present experiment, and all 11 were recalibrated. The results of the calibration of the flowmeters are documented in Appendix I. Each distribution manifold (also calibrated -- see Appendix II) contains eight or nine trim-adjust valves for assuring uniform flow rate, within 2 percent, to each of the eight or nine holes in the row.

2.1.3 Vortex Control System

The Vortex Control System sucks away the corner vortices built up by secondary flows on the sidewall and delivers the air to the opposite sidewall, where it is reinjected.

The flow rate can be regulated so as to "swallow" the corner vortex buildup. This allows the injected secondary air to achieve a uniformly vectored flow over the recovery region and test plates. Fig. 2.3 shows a plan view of the Vortex Control System.

2.1.4 Foreplate/Afterplate Heating System

The foreplate and afterplate are heated by a closed-loop hot water system which operates with continuous water flow. Recirculated water runs through two water heaters in series and is delivered to rectangular tubes built into the foreplate and afterplate. From the exit manifold the water

is returned to the recirculation pump. Water temperature is held constant using a proportional controller connected to one of the heaters. The preplate can be disconnected for tests with an unheated starting length.

2.1.5 Heat Exchanger Cooling Water System

The heat exchanger cooling system is a semi-closed loop system which continuously circulates water from an insulated holding tank. Flow rate is maintained high enough to ensure uniform temperature of the mainstream air being cooled. The secondary air heat exchanger is also part of this system. Temperature control of the cooling water is achieved by dumping a portion of the recirculated water and resupplying with make-up water from a cold water supply main.

2.1.6 Test Plate Electrical Power System

The test plate electrical power system delivers heater power to each of 12 plates that comprise the discrete-hole test section. Power is supplied from a 120 volt AC, 1ϕ source through two voltage stabilizers and 12 variable transformers. A switching circuit allows a wattmeter to be inserted for plate power measurements.

2.2 The Test Surface

The floor of the tunnel consists of three sections: a foreplate, a test section (blowing region), and an afterplate. The foreplate and afterplate are thermally isolated from the test section, and the three surfaces are leveled to have a continuous, smooth surface.

2.2.1 Discrete-Hole Test Section

The test section consists of 12 copper plates supported on an aluminum frame. The assembly is 56 cm wide and 62 cm long in the flow direction. The individual copper plates are 0.6 cm deep by 46 cm wide and are 5 cm long in the flow direction. The first plate has no holes. The 11 that do alternate nine holes and eight holes. Each of the 94 holes is connected to an individually adjusted flow tube. The holes are each

1.03 cm in diameter and are spaced 5.15 cm apart, to form a staggered-hole array. Fig. 2.4 shows an overall view of the test section.

The plates are heated by resistance wires installed in slots machined into the back side of each plate. Two resistance wires for each plate gives a desired uniform plate temperature, as copper is a good conductor. The wire is made of size AWG (28) Chromel wire, and bussed at one end with copper wire to give an overall resistance of about 8 Ohms. Four iron-constantan thermocouples, made of 30 AWG duplex wire, are embedded into the back side of each plate. Each thermocouple is located midway between two adjacent holes.

The plates are supported on phenolic cross ribs, except for the two end plates, which are supported from the aluminum end rails of the frame. The siderails of the frame have water passages for heating, to control conduction heat loss from the plates. Heating water tubes on the bottom plates, parallel to the cross ribs, serve to regulate the cavity temperature, again to control conduction heat loss.

The air delivery tubes are glued into recesses cut into the back side of each plate. The tubes, made of linen phenolic, extend back from the plate surface for a distance of 35 cm, and Gates Safety Stripe Heater Hose of 1.60 cm (5/8 in.) diameter is connected between each tube and its distribution manifold tube. Three tubes in each plate have iron-constantan thermocouples located upstream of the point where the tube enters the frame cavity. The cavity is loosely packed with insulating material to minimize heat loss from the back sides of the plates.

2.2.2 Foreplate and Afterplate

The foreplate and afterplate of the test surface are identical in design. Each plate has 48 cells 2.6 cm long in the flow direction, made of a rectangular tube (wave guide) insulated on the back and separated from each other with thin spacers. Hot water is run through 24 of the cells in each plate for temperature control. The heated halves of the foreplate and afterplate are adjacent to the test section (blowing region). Each cell is covered with three layers of thin bakelite and topped by a thin copper strip. The middle laminate was machined out to make room for a 5-cm-wide

heat flux transducer. An iron-constantan thermocouple is embedded in a groove in the back side of each thin copper plate, directly above the heat flux transducer, for plate temperature measurement.

2.3 Rig Instrumentation and Measurement

Measurement techniques for the various physical quantities used in computing Stanton numbers or velocity and temperature profiles are described in this section. The uncertainties in measurements are also given, obtained by the procedure described by Kline and McClintock [28].

2.3.1 Temperature

All temperatures were measured by iron-constantan thermocouples. The wires were calibrated against a precision quartz thermometer (Hewlett-Packard Quartz Thermometer), and the resulting calibration curves were used in the data-reduction program.

The thermocouple wires were brought into uniform temperature zone boxes and attached to selector switches. To eliminate sharp temperature gradients along the wires, all the wires were sheathed in polyflo tubing from the point of origin to the zone boxes.

Thermocouples were embedded in the test section plates, siderails, and endrails with adequate immersion depth, to elimiante conduction error. The four thermocouples in each plate were read individually, at first, to ensure that each plate did operate at near-isothermal conditions. The two middle thermocouples of each plate read the same, and they were connected in parallel.

The temperature of the mainstream air was measured with a thermocouple whose junction was normal to the flow. The indicated temperature was corrected for velocity error following the procedure described by Moffat [29], with the recovery factor of the gas taken to be the Prandtl number raised to the one-third power. The total temperature was used in formulating the Stanton number for high-velocity data.

Uncertainty in a thermocouple measurement is believed to be 0.14°C (0.25°F).

2.3.2 Velocity and Temperature Profiles

Velocity profiles were measured by traversing the boundary layer with a round, 0.5 mm outside diameter pitot probe. The resulting dynamic pressure was measured with a Validyne pressure transducer (Model DP45, Range ± 1" H_2O), which was calibrated against a Combist Manometer with an uncertainty of about 0.05 mm of water.

Temperature profiles were measured by traversing the boundary layer with an 0.08 mm diameter Chromel-constantan gooseneck thermocouple probe suggested by Moffat [33]. The probe was calibrated against a Hewlett-Packard precision quartz thermometer to give an uncertainty in temperature of 0.08°C.

2.3.3 Secondary Air Flow Rate

The hot-wire flowmeters used to measure secondary air flow rate were recalibrated for the experiments. Each flowmeter has a constant-current heating element and a thermocouple circuit which measures the temperature difference between the upstream air and the heating element. The flowmeters were installed at the downstream end of the delivery tubes and claibrated in place. The calibration constants of the flowmeters are incorporated into the data-reduction program. Uncertainty in secondary air flow rate for a row of holes was about 3 percent.

2.3.4 Pressure

Tunnel static pressure and mainstream dynamic pressure were measured with a Meriam inclined-tube manometer (Model 40GD10WM, Range 2" H_2O). The mainstream dynamic pressure was measured with a Kiel probe which was insensitive to the small changes of yaw angle. Uncertainty in these pressure measurements was 0.25 mm water. This also applies to the zero pressure gradient tunnel condition.

2.3.5 Afterplate Heat Flux

Heat flux from each afterplate cell was measured by a heat-flux meter previously calibrated by Choe [11] and Crawford [12] to account for heat loss through the meter to adjacent plates and to the plate surface. Their

calibrations are used in the present data-reduction program. Uncertainty in the heat-flux meter measurements was believed to be about 3 percent of calculated heat flux.

2.3.6 Test Plate Power

The power delivered to each of the discrete-hole test plates was measured by a precision AC wattmeter into the plate power circuit. A circuit analysis was carried out to account for insertion loss. The insertion loss analysis and the wattmeter calibration are incorporated into the data-reduction program. Uncertainty in plate power measurement was 0.24 watts.

2.3.7 Summary of Uncertainty Intervals

This section summarizes the uncertainty intervals already described.

Variables	Uncertainty Interval
Temperature, except probe	0.14°C
Temperature, probe	0.08°C
Dynamic pressure	0.25 mm of H_2O
Static pressure	0.25 mm of H_2O
Velocity profile	0.05 mm of H_2O
Secondary air flow rate	3%
Heat flux measurement	3%
Power measurement	0.24 watts

2.4 Formulation of the Heat Transfer Data

Experimental heat transfer data from the discrete-hole test plates will be described in terms of a Stanton number as:

$$St = \frac{\dot{Q}_{conv}}{A_{tot}\rho_\infty U_\infty C_p(T_o - T_{\infty r})} \tag{2.1}$$

where $\dot{Q}_{conv}$ is energy transfer from the test plate to the boundary layer by forced convection, A_{tot} is the planform area of one test plate (width × length), ρ_∞ is density of the mainstream air, U_∞ is the mainstream velocity, C_p is specific heat of the mainstream, T_o is plate temperature, and $T_{\infty r}$ is the mainstream stagnation temperature.

To evaluate $\dot{Q}_{conv}$ from the power supplied to the plate requires a model for the heat transfer behavior of the experimental system. The conservation of energy principle can be written as:

$$\begin{matrix}\text{Rate of} & & \text{Rate of} & & \text{Rate of} & & \text{Rate of Increase} \\ \text{Creation} & = & \text{Energy} & - & \text{Energy} & + & \text{of Storage of} \\ \text{of Energy} & & \text{Outflow} & & \text{Inflow} & & \text{Energy}\end{matrix} \tag{2.2}$$

Applying Eqn. (2.2) to the test plate, $\dot{Q}_{conv}$ becomes

$$\dot{Q}_{conv} = \underset{\substack{\text{power to} \\ \text{plate}}}{\dot{E}\ \text{supplied}} - \dot{Q}\ \text{losses} \tag{2.3}$$

The energy losses in Eqn. (2.3) are decomposed into

$$\dot{Q}\ \text{losses} = \dot{Q}_{rad} + \dot{Q}_{cond} + \dot{Q}_{flow} \tag{2.4}$$

where $\dot{Q}_{rad}$ is thermal radiation from the test plate top, $\dot{Q}_{cond}$ is heat conduction between adjacent plates (or between the end plates and the preplate and afterplate) and between plate and frame, and $\dot{Q}_{flow}$ is energy transfer by convection from plate to the secondary air as it passes through the plate.

Experimental heat transfer data from the afterplates are also presented in terms of a Stanton number by replacing $\dot{Q}_{conv}/A_{tot}$ in Eqn. (2.1) with the heat flux indicated by the imbedded meters. Eqn. (2.3) was used, in which $\dot{Q}$ losses consisted only of $\dot{Q}_{rad}$ and $\dot{Q}_{cond}$.

The following sub-sections will describe heat loss components and the secondary air exit temperature measurements, along with energy balance closure tests based on Eqns. (2.3) and (2.4). The uncertainty in Stanton number is also discussed. Values of the constants used in the following sections are contained in the Stanton Number Data-Reduction Programs in Appendix III.

2.4.1 Conduction Energy Balance

A conduction energy balance was performed by experiments of the type described by Choe et al. [11]. The sidewalls and top wall were removed and a 9 cm (3-1/2 in.) thick styrofoam block was placed on top of the test plates. The plates were then heated to a uniform temperature and the frame and cavity cooled by the cold water supply. In this mode, the only energy transfer is by conduction to the frame, and the electrical power supplied to each plate can be attributed to its conduction energy loss, modeled as:

$$Q_{cond,i} = K_i(T_{o,i} - T_{cav,i}) + S_i(T_{o,i} - T_{o,i+1}) + S_{i-1}(T_{o,i} - T_{o,i-1}) \qquad (2.5)$$

where the subscripts denote the plate under consideration and its adjacent plates, K and S are the conduction energy loss constants, and T_{cav} is effective cavity temperature.

The S conduction energy-loss constants between the last test plate and the afterplate, and the first plate and the foreplate, were measured during the process of heat-flux calibration, as described by Choe et al. [11]. The calibration unit contains three heaters, of which the middle one is heated by D.C. power and the other two by A.C. power. The calibration unit was placed over the area in which the last test plate (or the first test plate) joins the afterplate (or the foreplate), and the other two heaters over its adjacent plates. Then the heaters were operated in three modes:

- the same power to all heaters;
- one of the guard heaters off; and
- both guard heaters off.

An energy balance for the middle plate leads to three equations for three unknowns, so that the values for S between the cell and the plate can be obtained.

The S conduction energy loss constants between adjacent plates within the test section were calculated by Crawford et al. [12]. Heat transfer results are not very sensitive to these values at all, because

all the plates were kept at the same temperature within a fraction of a degree, during testing.

The conduction energy loss constants K_i were calculated from the measured plate and cavity temperatures and power delivered to the plate using Eqn. (2.5). In the calculations, energy loss through the styrofoam was considered to be 11 percent of the power provided, since the styrofoam had only 5 ∿ 6 times the thermal resistance of the insulation between the plate and the frame.

The definition of effective cavity temperature was based on an analysis of the frame-temperature distribution. The frame was instrumented with two thermocouples in both the front and rear aluminum rails of the frame, and three thermocouples along each of the two aluminum side rails. From the resulting temperature field, the effective cavity temperature was calculated by linear interpolation of the ten measured temperatures. Since the cavity was composed of low thermal conductivity packed insulation, the base plate temperatures had a negligible influence on the plate conduction energy losses. In the actual heat transfer run, the side rails, end rails, and bottom plates were heated nearly to plate temperature to minimize the conduction energy losses, and a precise formulation of the effective cavity temperature is not required.

2.4.2 Secondary Air Exit Temperature

The secondary air exit temperature was different from its inlet temperature due to energy transfer between the air and the test plates. An experiment was carried out with a 9 cm (3-1/2 in.) thick styrofoam block covering four adjacent copper plates. Machined holes in the block allowed secondary air to pass through the block. The block served as insulation to the secondary air stream and also as mixers for achieving the mixed mean temperature at the exit.

For the experiment, all 12 of the test section plates, the frame side walls, and the bottom plates were heated to the same temperature to minimize conduction loss. Hence, considering the four test plates, the only energy transfer was from the plate to the secondary air. To further guard against the effects of conduction between plates, only the data obtained from the inner two plates, out of the four test plates, were used for

determining the convection energy transfer. The following measurements were made: (i) power supplied to the four test plates under the styrofoam block, (ii) plate temperature, (iii) secondary air exit temperature leaving the styrofoam block, (iv) secondary air inlet temperature four inches upstream, and (v) the secondary air flow rate. The heating of the exit air temperature can be modeled by considering the system as a heat exchanger whose effectiveness, ε, is:

$$\varepsilon \triangleq \frac{T_2 - T_g}{T_{ave} - T_g} = 1 - e^{-N_{tu}} \tag{2.6}$$

where T_2 is secondary air exit temperature, T_g is the inlet temperature, and T_{ave} is the arithmetic average of the test plate and cavity temperautre, calculated by linear interpolation of the measured siderail temperatures, and

$$N_{tu} \triangleq \frac{UA}{\dot{m}C_p} = \frac{KCONV}{SCFM} \tag{2.7}$$

Here U is the total conductance of the system, A is the contact area, $\dot{m}$ is the mass flow rate, C_p is the specific heat, SCFM is the volume flow rate of the secondary air, and KCONV is a constant proportional to the conductance UA, which is a function of flow rate. From the measured temperature and flow rate, using Eqns. (2.6) and (2.7), KCONV was calculated. The following correlation was obtained:

$$KCONV = 0.1433\ SCFM^{0.5662} \tag{2.8}$$

This expression is valid for nine hole rows. If a row has n holes, SCFM was corrected by $9/n$ to get the proper flow rate in the individual holes; then KCONV was calculated.

It is necessary to know what portion of KCONV came directly from the copper plate and what portion came from the cavity, through the tube. Energy transfer by convection between the plates and secondary air as it passes through the plate can be modeled as

$$\dot{Q}_{flow} = KFL(T_o - T_2) \tag{2.9}$$

where KFL is the partial conductance area product (for the tube/lip region), T_o is the plate temperature, and T_2 is the secondary air exit temperature.

From the measured temperature and power supplied to the inner two plates under the styrofoam, using Eqn. (2.9), KFL was calculated. Then KFL was correlated as a function of flow rate as

$$KFL = 0.1472\ SCFM^{0.5480} \qquad (2.10)$$

This expression is also valid for nine hole rows, so that n hole rows should be adjusted in the same manner as KCONV.

Choe et al. [11] estimated KFL theoretically using the three different regions of flow rate; i.e., KFL had three separate functions according to the flow rate. But KCONV was correlated as one continuous function of flow rate from the experimental data.

Crawford et al. [12] determined both KCONV and KFL from the experimental data using the three regions of flow rate.

The present study of heat transfer to a full-coverage, film-cooled surface with compound-angle (30° and 45°) hole injection estimated both KCONV and KFL as one continuous function of flow rate.

2.4.3 Radiation Energy Loss

Radiation loss was calculated assuming the radiation shape factor, F, is 1.0, and the absorption of radiation by the air was negligible. Then radiation from the top surface is given by

$$\dot{Q}_{rad} = EA_{tot}\ \sigma(T_o^4 - T_{\infty,r}^4) \qquad (2.11)$$

where E is the emissivity of the test plate, A_{tot} is the total area of the plate including holes, σ is the Stefan-Boltzmann constant, T_o is the plate temperature, and $T_{\infty,r}$ is the mainstream recovery temperature.

There will be no radiation loss from the back side of the plate because the cavity is packed with insulation.

2.4.4 Energy Balance Closure Tests

After all the loss constants were determined and separately tested, they were incorporated into the Stanton number data reduction program shown in Appendix III. Energy balance closure tests were then performed to determine the validity of the models used to calculate the energy losses. The tunnel mainstream was operated without cooling, and the plate power was adjusted to bring each plate up to the mainstream temperature. Cold water was supplied to cool the frame of the test section, resulting in a plate-to-frame temperature potential of about 10°C (18°F). In this mode of operation of the wind tunnel, there was no convective or radiative energy transfer to the mainstream from the test plates. The main loss mechanisms were conduction loss and the flow loss due to the injected secondary airstream. Tests were made for $M = 0$, $M = 0.40$, and $M = 0.75$. For the blowing runs, the secondary air temperature was within 0.6°C (1°F) of the freestream temperature. The thermal boundary conditions for these tests were designed primarily to check the conduction loss constants. The energy balance closure tests showed how much imbalance existed for a given set of conditions and evaluated the accuracy of the energy measurement system. In principle, the energy balance closure equation of

$$\dot{Q}_{con} = \dot{E}_{\substack{\text{supplied}\\ \text{power to}\\ \text{test plate}}} - \dot{Q}_{losses}$$

should sum to zero. The accuracy of the power measurement is within ± 0.24 watts (typical power supplied to each plate during a Stanton number run was 10 to 30 watts). The results of these tests are shown in Fig. 2.5. The energy imbalance can be converted to a Stanton number uncertainty following the procedure described by Moffat [2].

$$\delta St = \frac{\delta\dot{E}}{A_{tot}\rho_\infty U_\infty C_p (T_o - T_{\infty,r})} \tag{2.17}$$

To evaluate St, typical operating values of 15°C (27°F) for $(T_o - T_{\infty,r})$ and 16.8 m/s (55 ft/sec) for U_∞ were used, along with properties for air. This converts to a Stanton number uncertainty, δSt, of $\pm 0.360 \times 10^{-4}$.

Following the procedure of Kline and McClintock [28] for propagation of uncertainty in Stanton number, uncertainty bands on the data are predicted to be ±3% for both $\theta = 1$ and for $\theta = 0$.

2.5 Rig Qualification

After the completion of energy balance closure tests, baseline checks were run for hydrodynamic and heat transfer performance. Earlier qualification tests of the wind tunnel were reported by Choe et al. [11] and Crawford et al. [12]. For the present study of heat transfer to a full-coverage film-cooled surface with compound-angle hole injection, even though the same wind tunnel as that of Choe et al. [11] and Crawford et al. [12] was used, there was the additional vortex control system which has been described in Section 2.1.3. Hydrodynamic qualification tests were required to evaluate the vortex control system.

2.5.1 Hydrodynamics of the Wind Tunnel without Operation of the Vortex Control System

The hydrodynamic qualification tests were conducted to determine that the tunnel flow was two-dimensional and that the approaching boundary velocity profiles were typically turbulent.

Free stream velocity was measured at two locations with a Kiel probe traversed with 2.54 cm (1 in.) increments in the channel height: (i) at 127.64 cm (50.25 in.) from the nozzle exit over the middle of the first test plate for five points across the channel, and (ii) at 202.72 cm (79.8 in.) from the nozzle exit over the middle of the seventh recovery plate for three points across the channel. The velocity variation was within ±1%.

The two-dimensionality of the boundary layer was demonstrated by taking the momentum thickness and the enthalpy thickness measurements across the channel. The momentum thickness was measured at two locations, the same as those of the free stream velocity measurement. The variation of momentum thickness at the two locations was within ± 1.5%. Momentum thicknesses were measured at a free stream velocity of 16.8 m/sec (55 ft/sec). The results of this measurement showed very uniform boundary layer growths over the center span of the channel within ± 1.5%.

To achieve low initial values of momentum thickness, the flow was accelerated over the preplate and allowed to recover to zero pressure gradient before reaching the test section. Fig. 2.6 shows the top wall configurations and boundary layer trip locations for these two types of run.

The data showed that the apparent value of momentum thickness upstream of the first row of holes increased as M increased, due to the flow blockage from the injected secondary air stream. In the evaluation of the virtual origin, the velocity profiles taken at $M = 0$ were used.

Figure 2.7 shows the velocity profiles for flat plate conditions. This velocity profile shows the accepted behavior in the logarithmic and wake regions compared with the known correlations. In addition, profile shape factors were measured. It was shown that the shape factor was between 1.29 and 1.50; thus the flow can be considered turbulent. The skin friction coefficient, used to form U^+ and Y^+, was found by fitting the velocity data to a logarithmic law of the wall in the range of 75 to 125 for Y^+ (Clauser plot).

2.5.2 Hydrodynamics of the Vortex Control Flow

Mayle and Camarata [16] conducted a flow visualization study of a multihole aircraft turbine blade. The results of the tests indicated that the injected secondary air flow drifted across the test surface to the channel side wall, where it rolled into a corner vortex which spread back onto the plate. In order to eliminate corner vortex buildups and to keep the flow uniformly vectored in the test section and the recovery section, a Vortex Control System was deemed necessary (see Section 2.1.3 for the description of the system). The function of the Vortex Control System was to suck away the corner vortex buildup and inject the fluid through the opposite wall without disturbing the mainstream and secondary flows.

Two criteria were used to identify the proper flow in the Vortex Control System: (i) in the beginning of the recovery region, there should be no corner vortex buildup, and (ii) in the recovery region, the injected secondary air should be uniformly vectored in the spanwise direction.

2.5.3 Heat Transfer Qualification

The final qualification tests consisted of unblown heat transfer runs. The free stream velocity was maintained approximately at 16.8 m/sec (55 ft/sec), with the plate temperature about 15°C (27°F) above the free-stream temperature.

Figure 2.8 shows the results of heat transfer runs with the free-stream velocity of 16.8 m/sec (55 ft/sec) for the heated foreplate. In the region continuing the holes, the heat transfer results are 7% to 10% higher than the accepted correlation of $St = 0.0128\ Pr^{-0.5}\ Re_{\Delta_2}^{-0.25}$. This effect is attributed to the roughness from open holes. For the author's own curiosity the roughness radius was estimated using Pimenta et al.'s correlation of $St = 0.0017\ (\Delta_2/r)^{-0.175}$ [30]. The equivalent roughness radius was found to be 0.005 cm (0.013 in.).

From Fig. 2.8 it can be seen that the heat transfer data in the recovery region have more scatter than in the blowing region. Since the heat flux meters are calibrated within 3% accuracy, this scatter is attributed to the inability of the hot water system to produce a uniform plate temperature, resulting in axial conduction losses not propertly dealt with by the data-reduction program.

The results of the heat transfer qualification tests gave confidence that the energy measurement was accurate within the experimental uncertainty and that the discrete hole rig itself could perform as required for the proposed experiemnt.

2.5.4 The Effects of Vortex Control Flow on Stanton Number

Since the secondary air was injected with compound angle (30° and 45°) direction, a corner vortex was generated by the secondary fluid impinging on the sidewall, and the secondary flow field was not uniform (see Section 2.5.2 for the Hydrodynamics of the Vortex Control Flow). Corner vortex buildups and non-uniformity of the secondary flow field might have resulted in non-uniform heat transfer in the spanwise direction. Four settings of vortex control flow at $M = 0.4$ were tested to see the effects on heat transfer. Two settings of vortex control flow at $M = 0.9$ were tested. In the lower range of the blowing ratio, $M \leq 0.8$, the vortex control flow system is effective, but at $M \geq 1.0$ its effects diminish, since it does

not have enough capacity. Initial conditions of the boundary layer for the tests were $Re_{\delta_2} \simeq 2500$ and $Re_{\Delta_2} \simeq 1800$.

For the blowing ratio of 0.4, the Stanton number data are plotted versus Re_x in Fig. 2.9 for $\theta = 1$ and $\theta = 0$. The $\theta = 1$ figure shows the Stanton number data for four different settings of vortex control flow. The optimum flow setting shows the data about 4% lower in the recovery region than those with no vortex control flow. The $\theta = 0$ figure shows the reverse effects. The Stanton number data for the optimum flow are about 5 to 8% higher in the blowing region than those with no vortex control flow. The data for all other settings of vortex control flow are about 10 to 15% lower in the blowing region than those with no vortex control flow.

The $M = 0.9$ data are plotted versus Re_x in Fig. 2.10 for $\theta = 1$ and $\theta = 0$. The $\theta = 1$ figure shows the effects of two settings of vortex control flow on Stanton number data. The case of no vortex control flow gives a value of Stanton number about 5% lower in the recovery region than those with the optimum vortex control flow. Here the optimum flow was considered to be a full flow setting. It has been observed that the effects of the Vortex Control System diminished for higher blowing ratio, $M \gtrsim 1$. The $\theta = 0$ figure shows the reverse effects. In the blowing region, the optimum setting of vortex flow gives about 9% lower Stanton number data than those of the no-flow case.

These two series of Stanton number runs gave a good experimental idea as to the optimum setting of the vortex control flow on heat transfer for each blowing ratio M. All the data presented in Chapter 3 were taken with the optimum setting of vortex control flow.

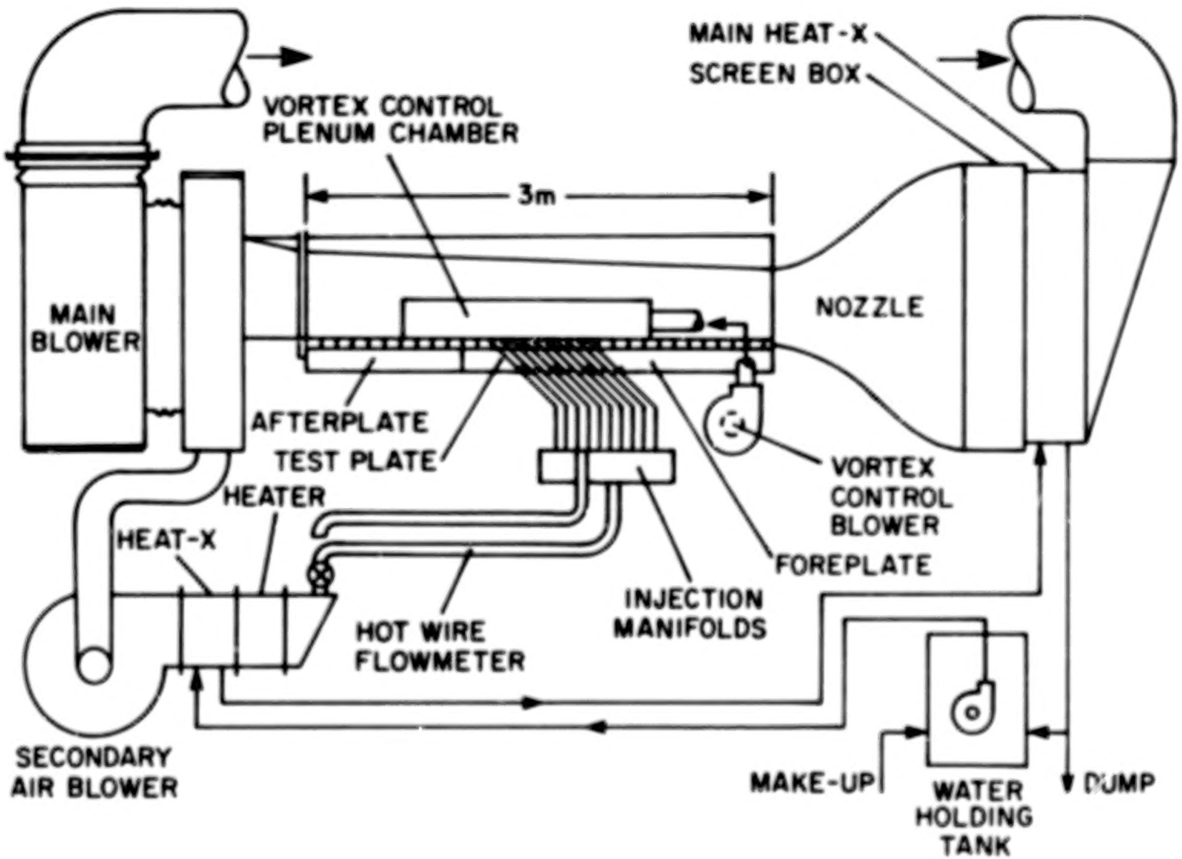

Fig. 2.1. Flow schematic of wind tunnel facility, the Discrete Hole Rig.

Figure 2.2 Overall view of Discrete Hole Rig

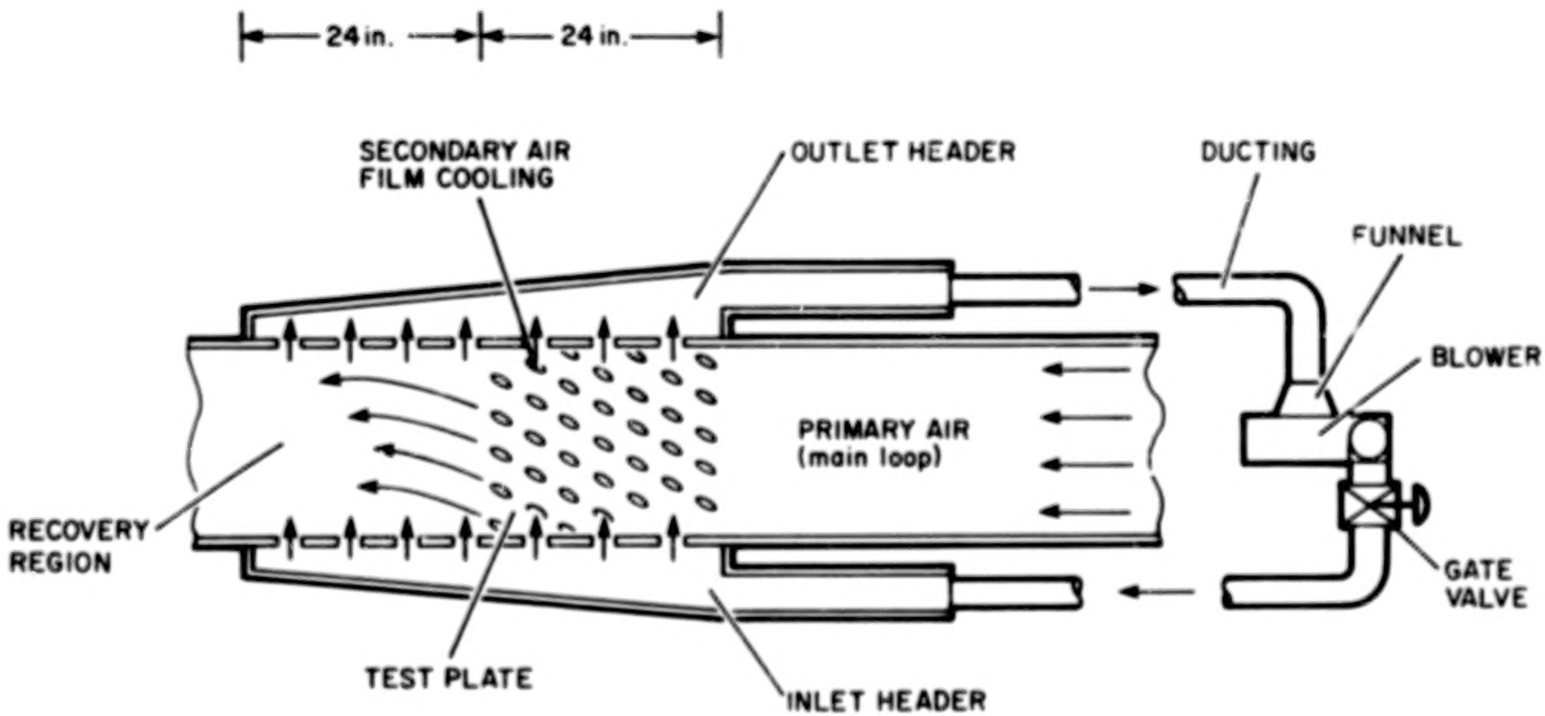

Fig. 2.3. Plan view of installed vortex control system

BLANK PAGE

BLANK PAGE

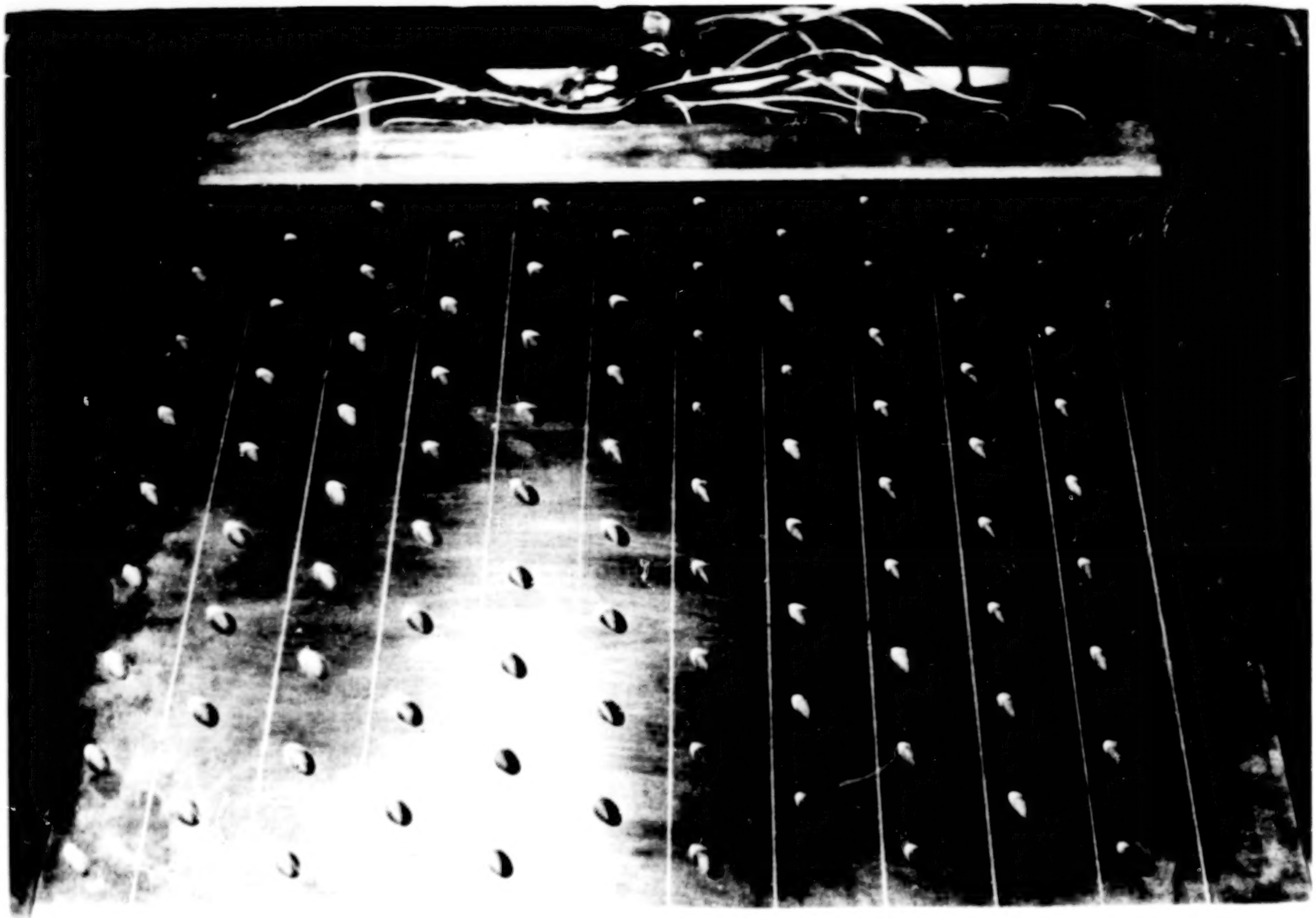

Figure 2.4 Photograph of compound angle hole injection test surface, showing staggered hole array

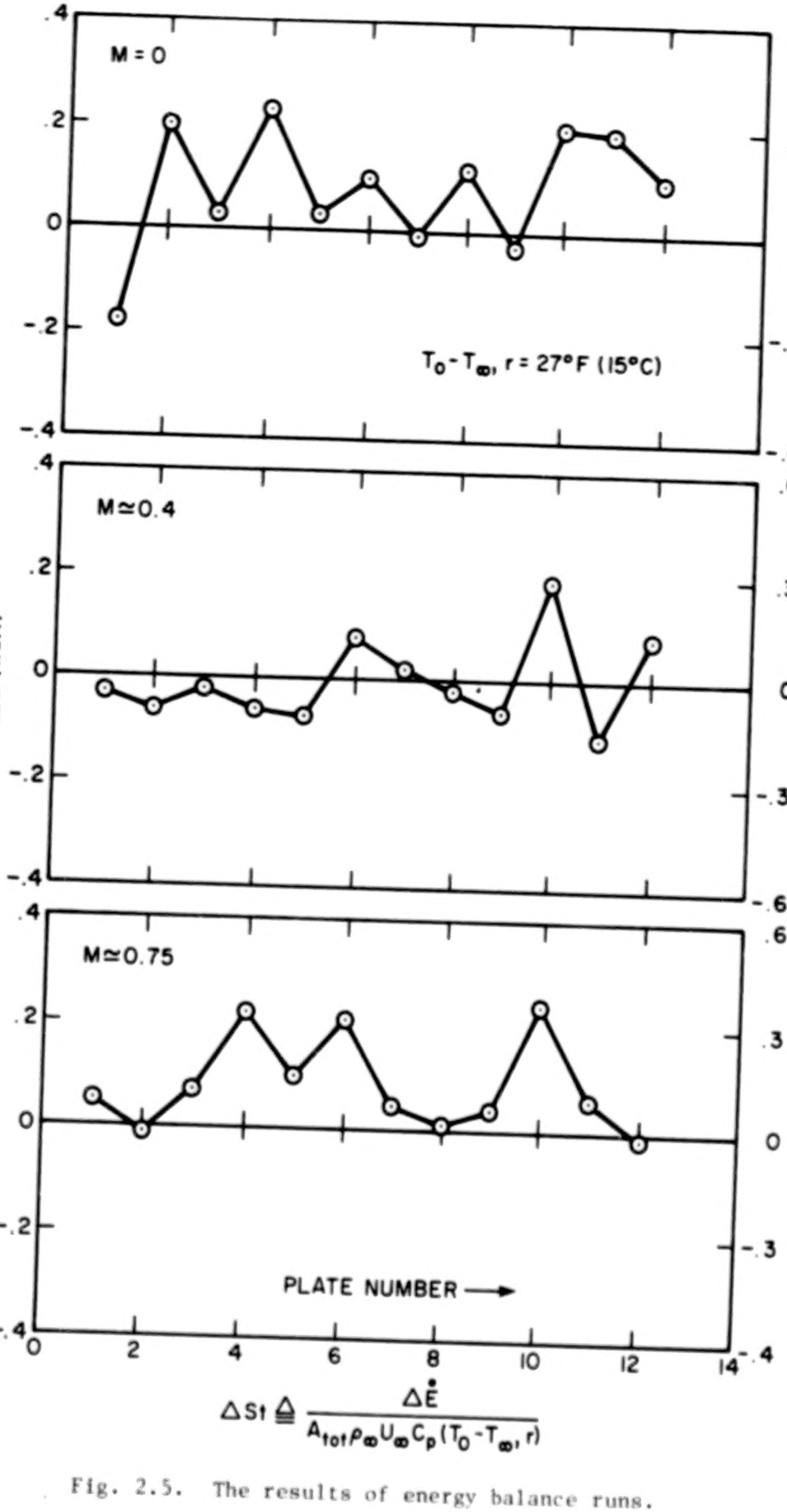

Fig. 2.5. The results of energy balance runs.

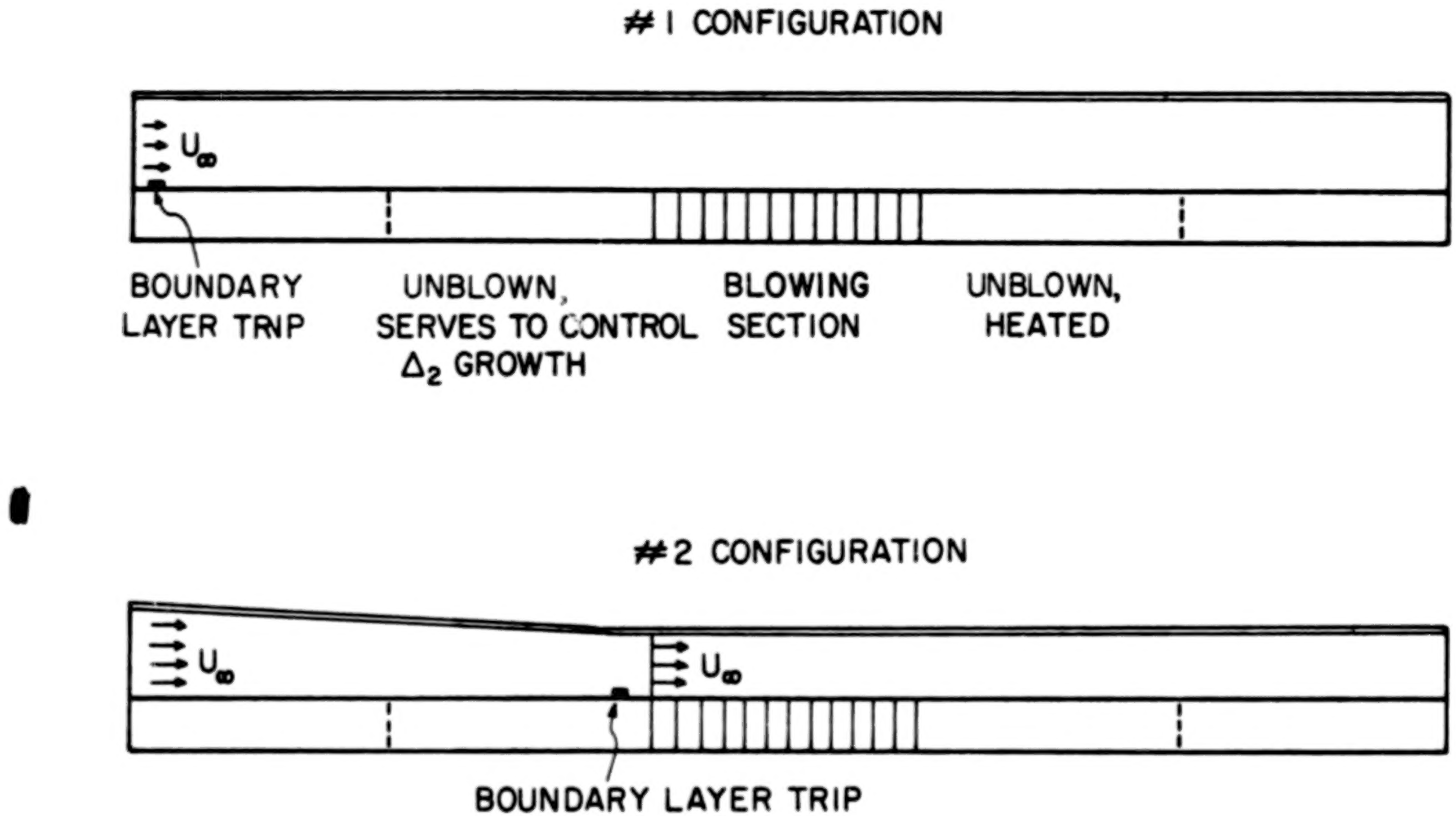

Figure 2.6. Configurations for tunnel topwall and boundary layer trip: #1 is for thick initial boundary layer; #2 is for thin initial boundary layer

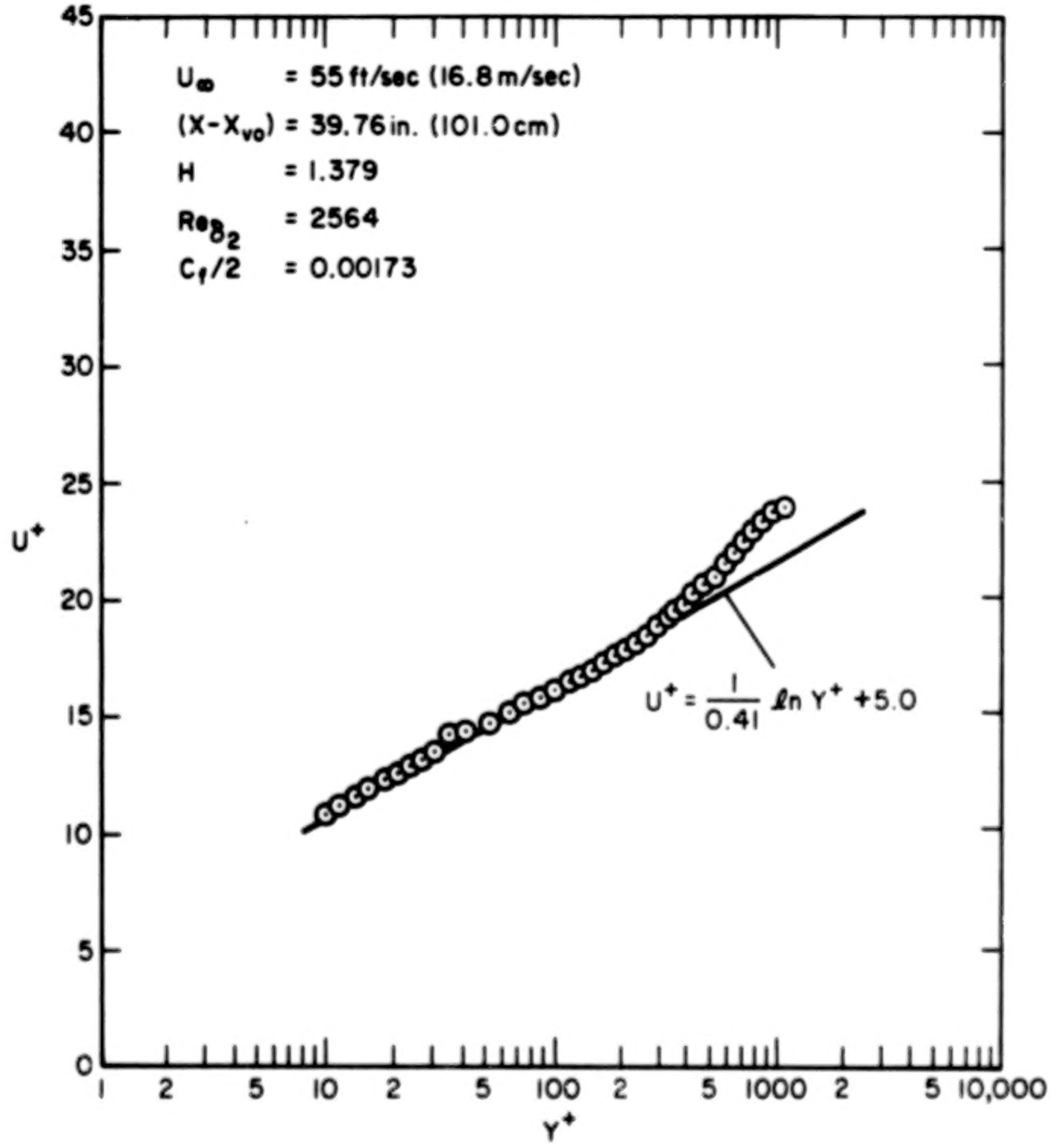

Fig. 2.7. Upstream velocity profile

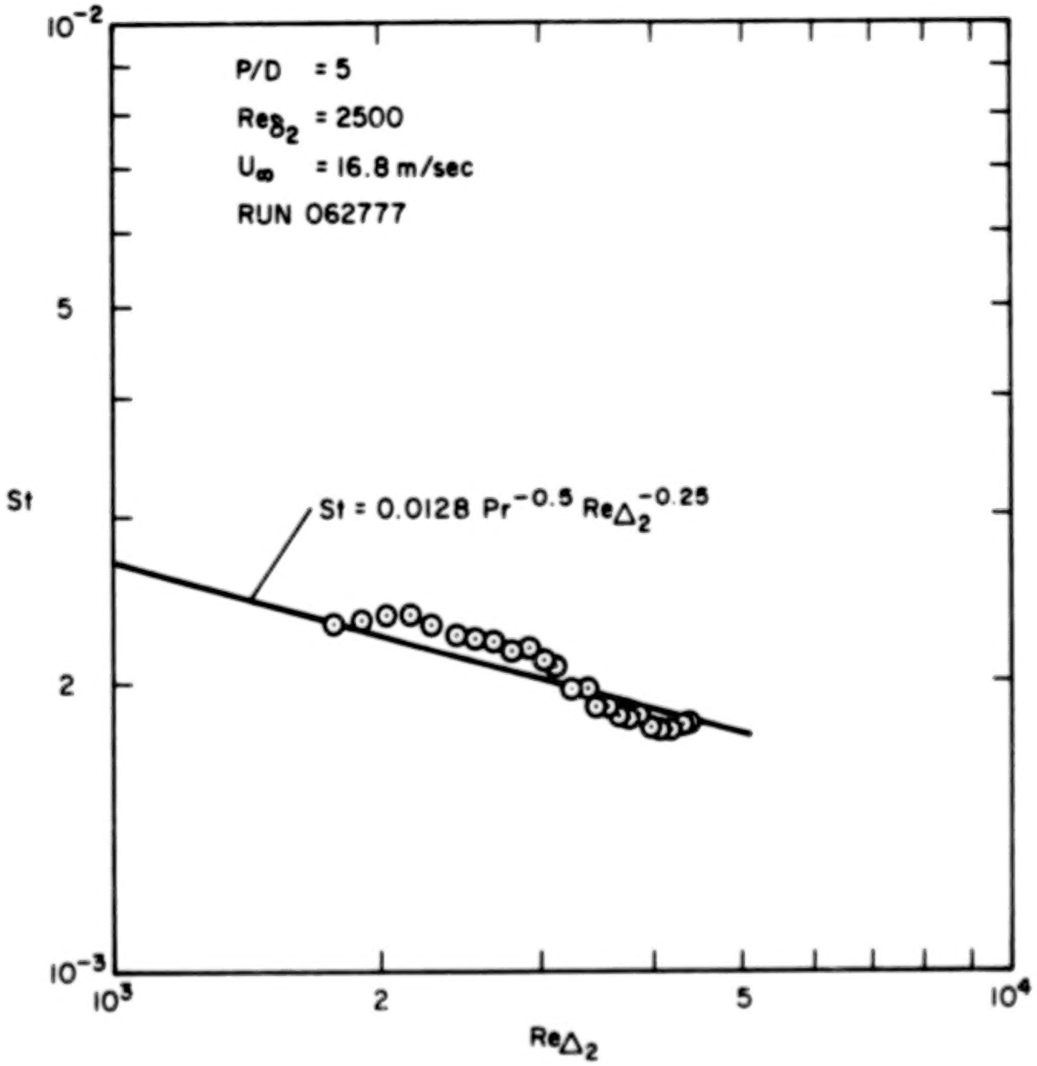

Fig. 2.8. St vs. Re_{Δ_2} for flat plate, heated starting length, with P/D = 5.

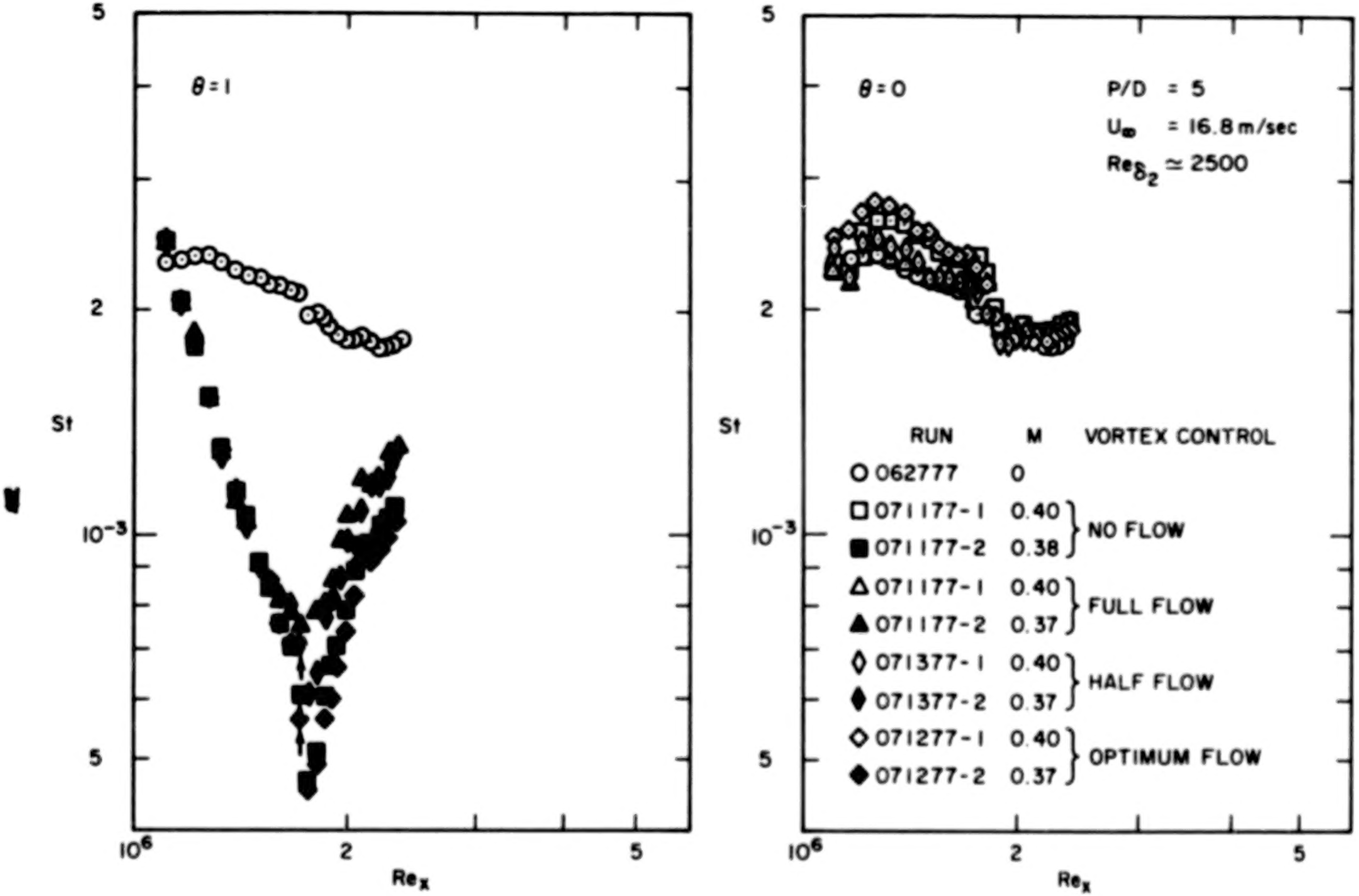

Fig. 2.9. St vs. Re_x for $\theta = 0$ and $\theta = 1$ with $P/D = 5$, heated foreplates, for the effect of vortex control flow on heat transfer.

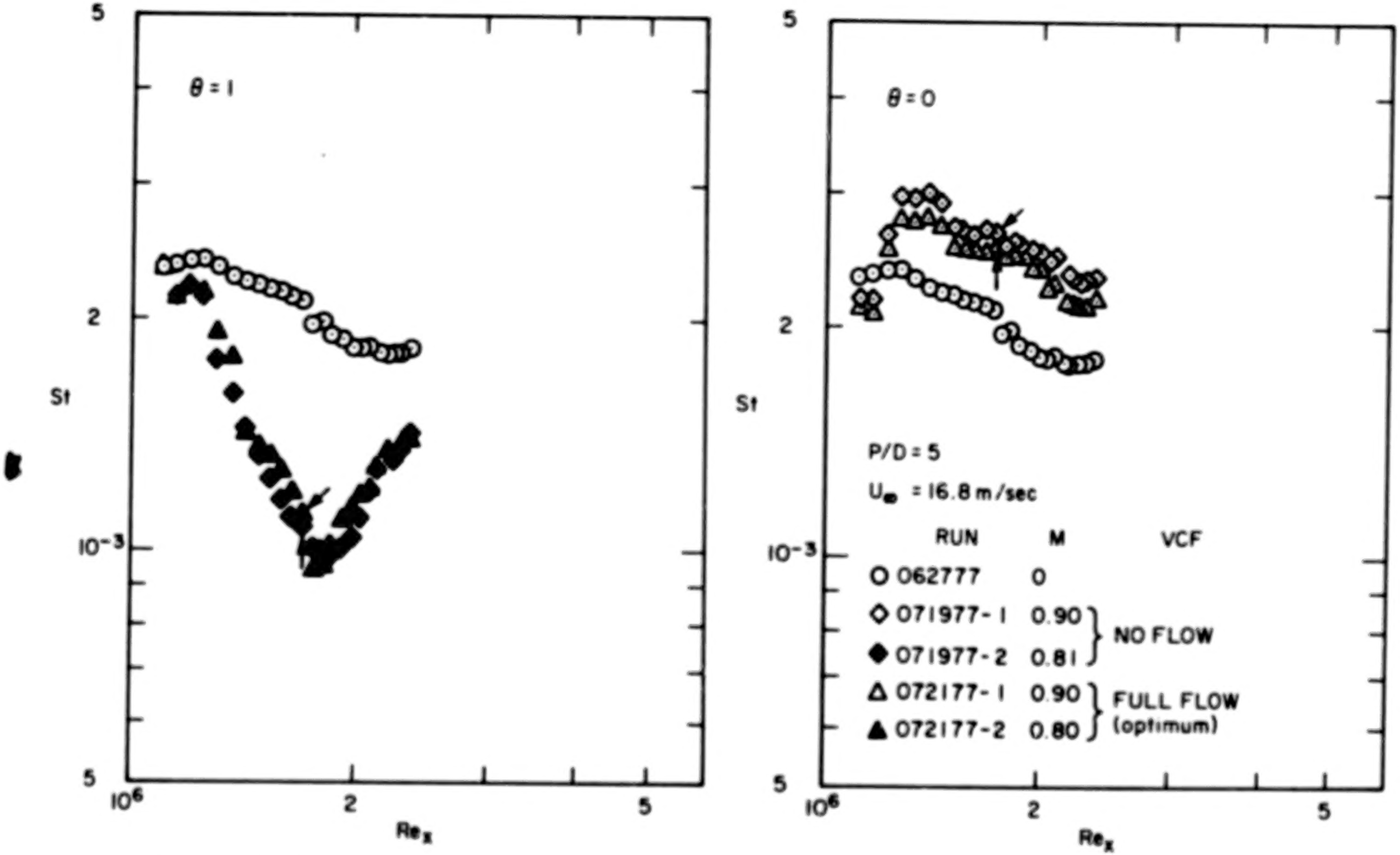

Fig. 2.10. St vs. Re_x for $\theta = 0$ and $\theta = 1$ with $P/D = 5$, heated foreplates, for the effect of vortex control flow on heat transfer.

Chapter 3

EXPERIMENTAL DATA

3.1 Types of Data

Stanton number data were obtained for a range of initial conditions and blowing ratios, with two injectant temperatures ($\theta = 0$ and $\theta = 1$) at each blowing ratio. The data were taken for two hole spacings: $P/D = 5$ and $P/D = 10$, both in the full-coverage region and in the recovery region. For the $P/D = 10$ case, only one set of initial conditions was used. Initial conditions are reported: mean velocity and temperature profiles of the boundary layer at the midpoint of the upstream guard plate. Table 3.1 summarizes the data range.

3.2 Description of the Stanton Number Data

The main experimental investigation was to examine the effects of the blowing ratio on Stanton number for $P/D = 5.0$ with a mainstream velocity of 16.8 m/s and an initial momentum thickness Reynolds number of about 2500, and with a heated preplate yielding an initial enthalpy thickness Reynolds number of 1800. All the data reported here are those with the optimum setting of the vortex control flow.

The effects of hole spacing on Stanton number were examined by plugging some holes in the array to give $P/D = 10$. A heated starting length initial condition was used, and tests were carried out for two blowing ratios of 0.4 and 0.9.

The effects on Stanton number of changing the initial hydrodynamic boundary layer was examined by tests with two different values of Re_{δ_2}, 1800 and 500. The ratio of initial boundary layer thickness-to-hole diameter for these tests varied from 2.4 to .53. For $Re_{\delta_2} = 1800$, tests were conducted with four values of blowing ratio M for $P/D = 5$. The upstream Re_{Δ_2} was about 1400. For thin initial boundary layers, $Re_{\delta_2} = 500$, two blowing ratios were used with initial $Re_{\Delta_2} = 600$. The initial boundary layer was about 0.5 hole diameter in thickness.

Table 3.1

SUMMARY OF COMPOUND-ANGLE HOLE INJECTION DATA

(Re_{δ_2} and Re_{Δ_2} are upstream initial conditions at guard plate midpoint)

Compound-Angle (30° and 45°) Hole Injection								
	Unheated Starting Length		Heated Starting Length					
U_∞ (m/s)	16.8		16.8		11.8		9.8	
Re_{δ_2}	2500		2500		600		1800	
Re_{Δ_2}	100		1800		600		1400	
P/D	5	10	5	10	5	10	5	10
M = 0	x		x	x	x		x	
M = 0.2								
M = 0.4	x		x[a]	x	x		x	
M = 0.6								
M = 0.75								
M = 0.9			x[b]	x	x		x	
M = 1.25			x				x	
M = 1.5							x.	

[a]For U_∞ = 16.8 m/s and M = 0.4 at P/D = 5, four sets of Stanton number data were taken in order to see the effect of vortex control flow (see Fig. 2.9).

[b]For U_∞ = 16.8 m/s and M = 0.9 at P/D = 5, two sets of Stanton number data were taken in order to determine the optimum value of vortex control flow (see Figs. 2.10).

At each blowing ratio, data were obtained with two injectant temperatures: (i) $0.0 < \theta < 0.2$, corresponding to the mainstream temperature fluid, and (ii) $0.9 < \theta < 1.1$, corresponding to the surface temperature fluid. The linear superposition equation, $St(\theta) = St(\theta=0) - \theta \times [St(\theta=0) - St(\theta=1)]$ was used with the two sets of data for a given blowing ratio M to adjust the data to Stanton numbers at $\theta = 0$ and $\theta = 1$. For the recovery region the average value of θ for blowing rows 10 and 11 were used.

The Stanton number data have been plotted both in terms of x-Reynolds number and enthalpy thickness Reynolds number. The x-Reynolds plot shows the Stanton number as a function of position, for fixed values of M and θ. Enthalpy thickness Reynolds number plots show Stanton number in "local boundary layer coordinates". Values of x-Reynolds numbers are based on virtual origin computed, using the initial value of momentum thickness and a conventional turbulent correlation.

On the Stanton number graphs, the first 12 points are for the test section plates. An arrow denotes the end of blowing (twelfth point). The remaining points are for every other recovery region plate. The reference lines shown on the x-Reynolds number and enthalpy-thickness Reynolds number graphs are accepted correlations for two-dimensional equilibrium flow over a smooth plate with constant wall temperature and with the hydrodynamic and thermal boundary layers beginning at the same point.

3.3 Stanton Number Data

The experimental Stanton number data have been divided into three sections for discussion.

3.3.1 Thick Initial Boundary Layer with Heated Starting Length

This section summarizes three series of Stanton number data. Each data set sequentially consists of the upstream initial conditions of velocity and temperature profiles, Stanton number versus Re_x for $\theta = 1$ and $\theta = 0$, and the same Stanton number versus Re_{Δ_2} for $\theta = 1$ and $\theta = 0$.

3.3.1.1 $Re_{\delta_2} \approx 2500$ and $Re_{\Delta_2} \approx 1800$ at $U_\infty = 16.9$ m/s with $P/D = 5$

Stanton number data were obtained for three blowing ratios: 0.4, 0.9, and 1.25, for $\theta = 0$ and $\theta = 1$.

M = 0. The first data obtained in each data set were with $M = 0$ to establish a baseline. Fig. 3.1 shows the initial velocity profile over the midpoint of the guard plate for this run. Fig. 3.2 shows the initial temperature profile. The velocity profile, Fig. 3.1, shows a typical turbulent boundary layer profile, with a boundary layer thickness of about two hole diameters.

The Stanton number data are plotted versus Re_x in Fig. 3.3, and versus Re_{Δ_2} in Fig. 3.4. In the latter figure, the data for the unblown case are seen to be 7 to 10% above the generally accepted correlation curve, hereafter called the equilibrium line. This effect is attributed to a roughness effect of the open holes on the boundary layer (see Section 2.5.3 for Heat Transfer Qualification). In the recovery region the Stanton number drops within 3% of the equilibrium line within a few boundary layer thicknesses. The roughness effect will be seen more clearly in conjunction with $P/D = 10$ data in the next section (3.3.1.2).

Figure 3.3 shows the Stanton number data versus Re_x for $\theta = 1$ and $\theta = 0$, and the data are replotted in Re_{Δ_2} coordinate in Fig. 3.4.

$\theta = 1$ ($T_2 = T_0$). The trends of the data for all blowing ratios are similar. The data sharply decrease toward the end of the blowing with the minimum value occurring downstream after the last row of holes. Downstream of the recovery region the data sharply increase toward the equilibrium line.

The decrease in Stanton number values in the blowing region may be due to the attachment of the secondary fluid to the surface, which will delay jet interaction with the free stream. In the recovery region the effects of the compound-angled flow field diminish quickly.

For the blowing ratio $M = 0.4$ the minimum value of Stanton number was about one-fourth the value shown by the equilibrium line.

$\theta = 0$ $(T_2 = T_\infty)$. The data from the first blowing row are about 2% lower than those of the guard plate. The data then sharply increase for the next few blowing rows. In the blowing region, three different data trends can be seen: the $M = 0.4$ data continuously decrease; the $M = 0.9$ data slowly decrease and then level out to an asymptotic value in the beginning of the recovery region; the $M = 1.24$ data level out to an asymptotic value, independent of the number of rows of holes. A nearly constant Stanton number for the highest blowing ratio, $M = 1.24$, may be due to a nearly constant turbulent transport or eddy viscosity/eddy conductivity with respect to the streamwise direction, independent of boundary layer growth. Asymptotic behavior for the $\theta = 0$ condition was also observed by Mayle and Camarata [16] for compound-angle injection with $P/D = 8$ and 10 for moderate blowing ratios.

In the recovery region, the Stanton number data rapidly decrease. Two different trends are clearly seen. For $M = 0.4$ the data approach the equilibrium line within about 2%. For $M = 1.24$, the data approach those of the blowing ratio $M = 0.91$ within 3%. Both these data are still about 22% higher, at the end of the recovery region, than those of the eqhilibrium line. The radical drops of Stanton number in the recovery region could be due to the removal of the intense mixing from the jet-mainstream interaction. This effect may be explained by comparing the data for $M = 0.4$ with those of $M = 0.91$ and 1.24. At the lowest value of the blowing ratio, $M = 0.4$, the mixing from the jet-mainstream interaction is weaker than that of the higher blowing ratios, $M = 0.91$ and $M = 1.24$.

3.3.1.2 $P/D = 10$ with $Re_{\delta_2} \simeq 2600$ and $Re_{\Delta_2} \simeq 1900$ at $U_\infty = 16.9$ m/s

The Stanton number runs for $P/D = 10$ were performed at only one set of initial conditions with two blowing ratios: $M = 0.4$ and $M = 0.9$.

$M = 0$. The initial velocity and temperature profiles for the unblown Stanton number run are shown in Figs. 3.5 and 3.6, respectively. The St_o data are plotted versus Re_x and Re_{Δ_2} in Figs. 3.7 and 3.8. In the Re_{Δ_2} plots the data within the blowing region are within 2% of the accepted correlation line, probably because the roughness effect of open holes diminishes, as discussed in Section 3.3.1.1.

Figure 3.7 shows the Stanton number versus Re_x for $\theta = 1$ and $\theta = 0$, and the data are replotted in Re_{Δ_2} coordinates in Fig. 3.8.

$\theta = 1$ ($T_2 = T_o$). The $M = 0.38$ data produce a minimum Stanton number in the blowing region with the $M = 0.84$ data lying above the low blowing ratio data. Stanton number variation in the blowing region could be due to alternate rows of holes being plugged. In the recovery region, the Stanton number for $M = 0.38$ is seen to return to the equilibrium line.

The recovery region data for $M = 0.84$ appear not to return to the equilibrium line. This could be attributed to a problem with the heat flux measurement in the recovery region. For $P/D = 10$ and high M, the flow should be much more three-dimensional than its counterpart at $P/D = 5$, because the secondary air jet penetrates farther due to the individuality of the jets for the wider spacing. The flow width for averaging of the heat flux with afterplate is 5 cm, and the discrete holes are spaced about 10 cm apart; any three-dimensional effects will greatly influence the sensor. A similar anomaly was also observed by Choe et al. [11] and by Crawford et al. [12] for the data obtained with the natural transition over the blowing region, indicating the heat flux sensors do not give a spanwise-averaged heat transfer coefficient.

Comparing the $P/D = 10$ data (Figs. 3.7 and 3.8) with the $P/D = 5$ data (Figs. 3.3 and 3.4), the major effect of increased hole spacing is to reduce the effect of blowing: i.e., to reduce the Stanton number departure from the equilibrium line, St_o.

$\theta = 0$ ($T_2 = T_\infty$). The $M = 0.45$ data stay almost constant within the first half of the blowing region and then sharply drops to approach to an almost asymptotic value at the end of the blowing. The data for the higher blowing ratio, 0.87, stay almost constant within the blowing region. In the recovery region the $M = 0.45$ data approach the equilibrium line within 2%.

Comparing the $P/D = 10$ data with the $P/D = 5$ data, the major effect of increased hole spacing is, once again, to reduce the overall amount of the Stanton number departure from the equilibrium line.

3.3.1.3 $Re_{\delta_2} \approx 1800$ and $Re_{\Delta_2} \approx 1400$ at $U_\infty = 9.9$ m/s with $P/D = 5$

This section summarizes the Stanton number data for the moderately thick initial boundary layer for the blowing ratios of 0.4, 0.93, 1.25, and 1.48.

M = 0. The initial velocity and temperature profiles for the unblown Stanton number run are shown in Figs. 3.9 and 3.10, respectively. The St_o data are plotted in Re_x and Re_{Δ_2} in Figs. 3.11 and 3.12. In the Re_{Δ_2} plots the data trends are the same as those with $Re_{\delta_2} \approx 2500$ and with $Re_{\Delta_2} \approx 1800$. The blowing region data are about 7 to 10% above the generally accepted correlation curve, with the recovery region data within 2% of the curve.

Figure 3.11 shows the Stanton number versus Re_x for $\theta = 1$ and $\theta = 0$, and the data are replotted in Re_{Δ_2} coordinates in Fig. 3.12.

$\theta = 1$ ($T_2 = T_o$). In Figure 3.11 (Re_x coordinate), the Stanton number data for the higher blowing ratios increase for the first few blowing rows as M increases, and then rapidly decrease toward the end of the blowing. The M = 0.37 data continuously decrease to the minimum value at the end of the blowing. In the recovery region, the common trends of the data for all blowing ratios are similar, such that the data rise toward the equilibrium line. A visual comparison of the data with those with the thick boundary layer reveals that the overall level of the Stanton number departure from the St_o is reduced with the thin boundary layer.

$\theta = 0$ ($T_2 = T_\infty$). In the blowing region, the data rise for the first few blowing rows, with the slope dependent on M, and then decrease. In the recovery region, all the data display an apparent asymptotic value. The M = 1.48 data are about 10% lower than those with M = 0.93 and 1.25.

3.3.2 Thin Initial Boundary Layer ($Re_{\delta_2} \approx 500$ and $Re_{\Delta_2} \approx 600$ at $U_\infty = 11.3$ m/s) with Heated Starting Length and $P/D = 5$

The last data set for the heated starting length is a study of the effects of the upstream hydrodynamics for the blowing ratios of 0.44 and 0.93.

Figure 3.13 shows the initial velocity profile. Fig. 3.14 shows the corresponding temperature profile. The velocity profile, Fig. 3.13, exhibits the outer region similarity, but the inner region differences, plus the shape factor information for the velocity profile, indicate that the flow is still transitional on the guard plate. An acoustic probe in the boundary layer confirmed that the flow over the second plate was turbulent.

$\underline{M = 0}$. The unblown Stanton number data are plotted versus Re_x and Re_{Δ_2} in Figs. 3.15 and 3.16. The St_o are seen to be about 5 to 10% above the equilibrium line in the test plate region. The recovery region data lie slightly below the equilibrium line, in either Re_x or Re_{Δ_2} coordinate.

Figure 3.15 shows the Stanton number versus Re_x for $\theta = 1$ and $\theta = 0$, and the data are replotted in Re_{Δ_2} coordinates in Fig. 3.16.

$\underline{\theta = 1\ (T_2 = T_o)}$. The blowing region data drop toward the end of the blowing, and then the data rise toward the equilibrium line. The $M = 0.4$ data show the lowest values of Stanton number, with the higher blowing ratio causing an increase in the Stanton number over the blowing region and the recovery region.

$\underline{\theta = 0\ (T_2 = T_\infty)}$. In the blowing region the data slowly rise within a few blowing rows and then continuously decrease toward the end of the recovery region, with the $M = 0.4$ data slowly returning to the equilibrium line. This slow return may be due to the thin momentum boundary layer and its effect on turbulent mixing.

3.3.3 Unheated Starting Length with Thick Initial Boundary Layer ($Re_{\delta_2} \approx$ 2500 and $Re_{\Delta_2} \approx 100$ at $U_\infty = 16.8$ m/s) with P/D = 5

For the unheated starting length, only one Stanton number data set was obtained ($M = 0.43$). The primary purpose of this run was to see the effects of unheated starting length on heat transfer.

Figure 3.17 shows the Stanton number versus Re_x for $\theta = 0$ and $\theta = 1$, and the data are replotted in Re_{Δ_2} coordinates in Fig. 3.18.

In Fig. 3.17, comparing the data for $\theta = 1$ with those of the heated starting length for the same hydrodynamic condition, the former data are approximately 20% higher in both the blowing region and the recovery region. The trends of the data are very similar to those of the heated starting length

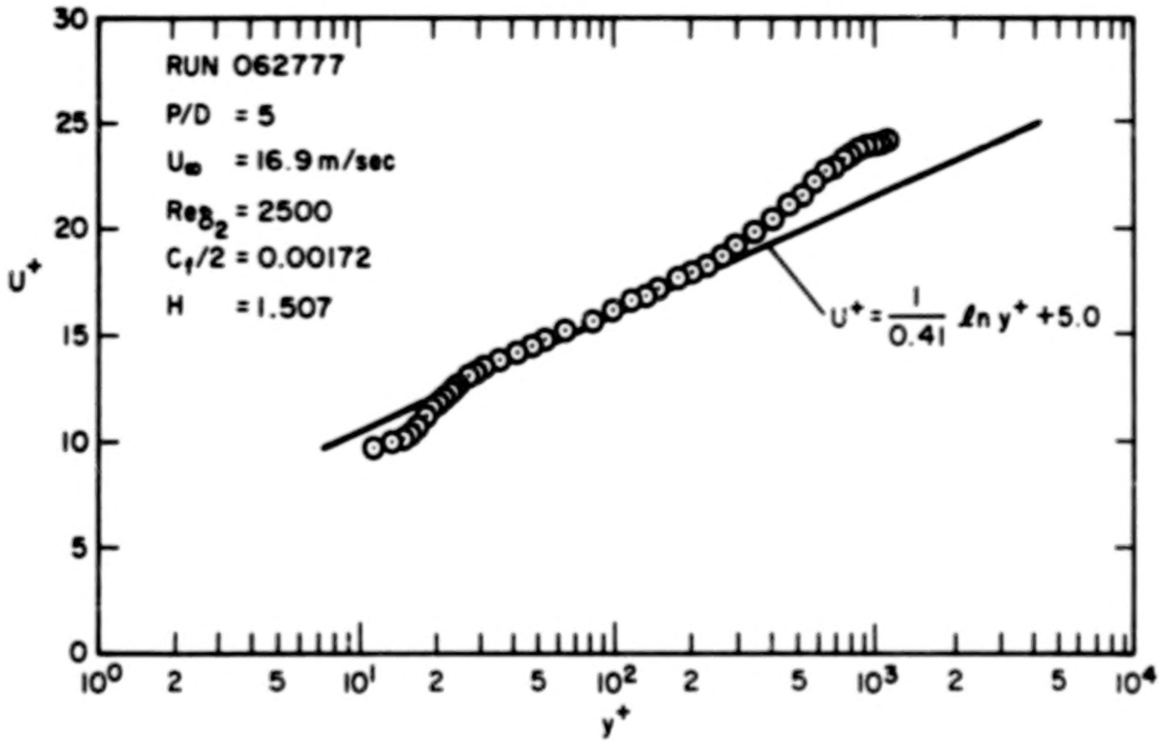

Fig. 3.1. Upstream velocity profile for initially high Re_{δ_2}, heated starting length runs, for Figs. 3.3 to 3.4.

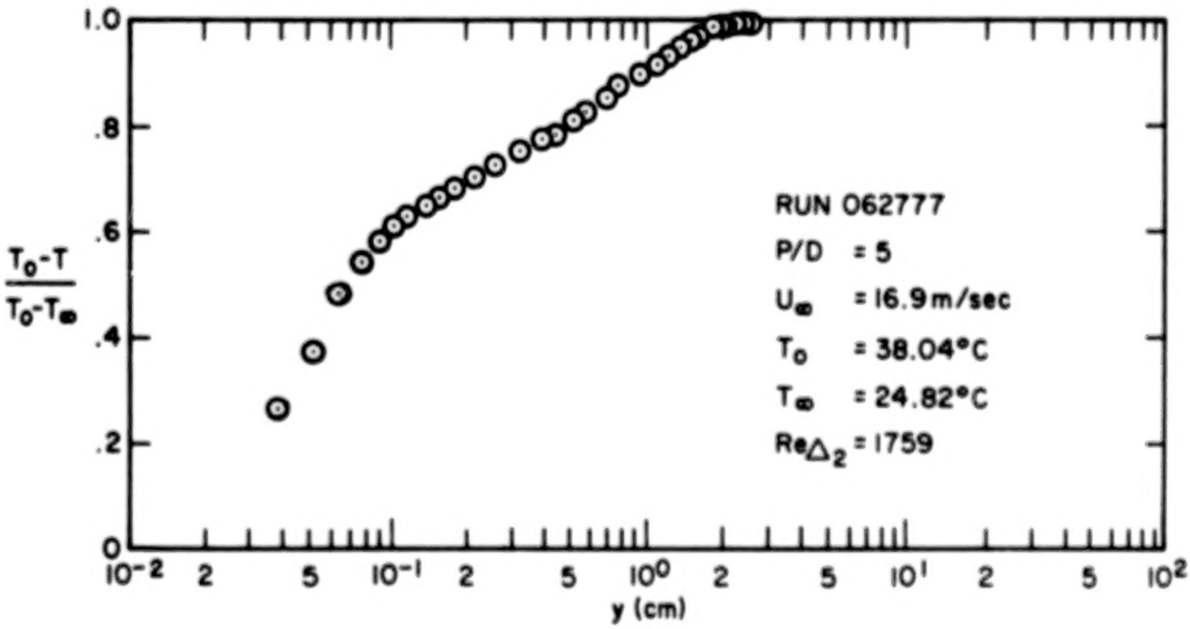

Fig. 3.2. Upstream temperature profile for initially high Re_{δ_2}, heated starting length runs, for Figs. 3.3 to 3.4.

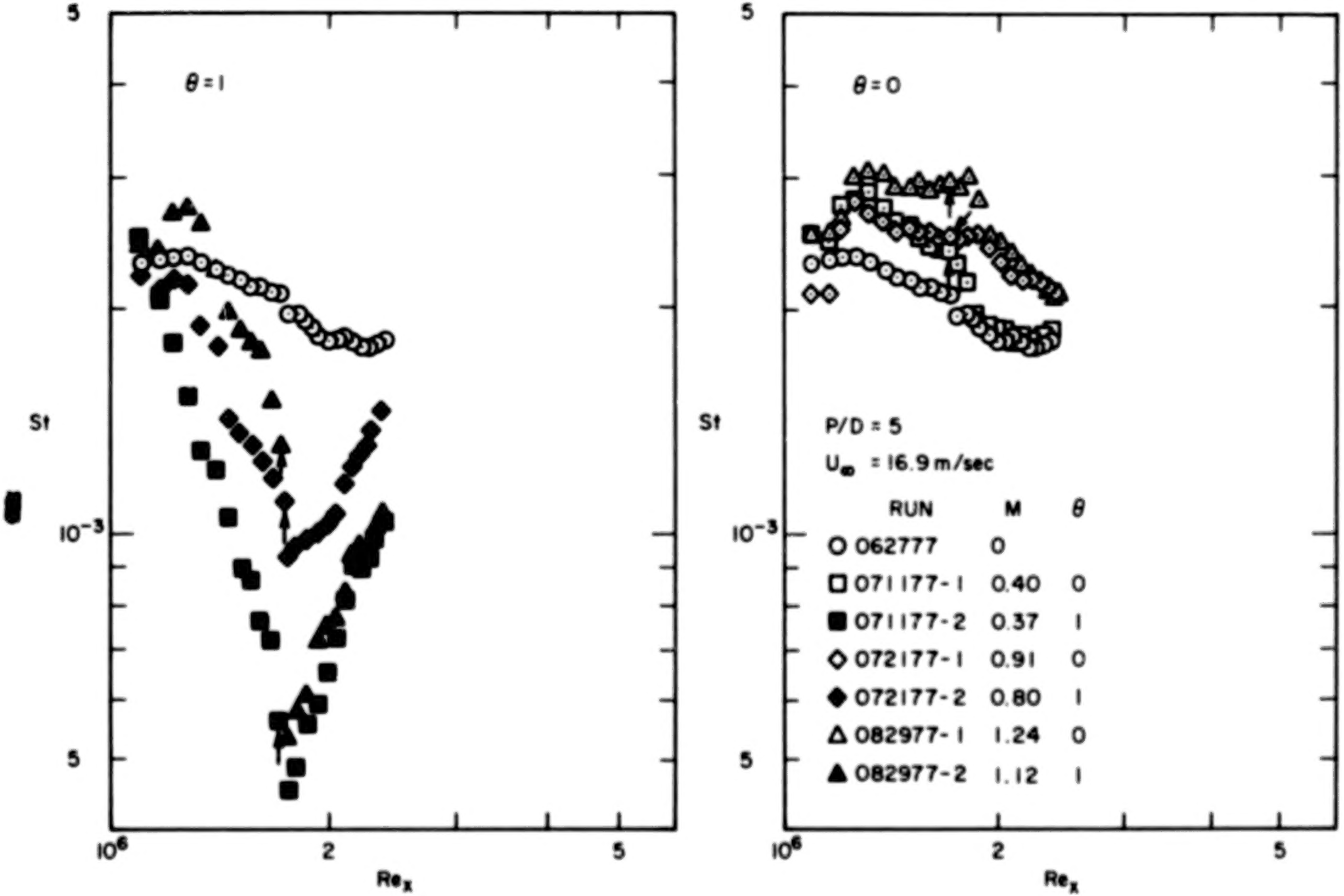

Fig. 3.3. St vs. Re_x for $\theta = 0$ and $\theta = 1$ with $P/D = 5$, heated foreplates.

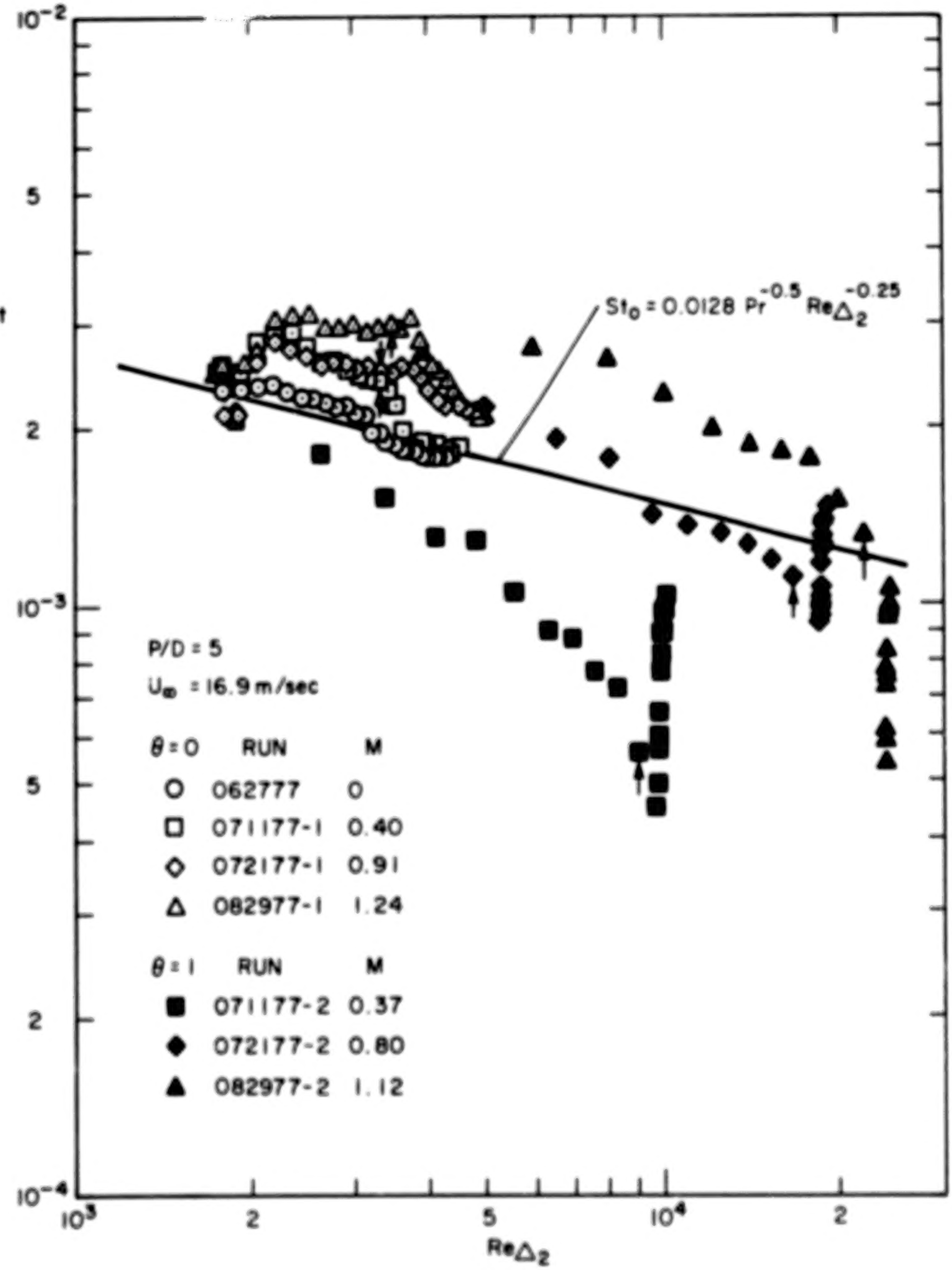

Fig. 3.4. St vs. Re_{Δ_2} for $\theta = 0$ and $\theta = 1$ with P/D = 5, heated foreplates (same data as in Fig. 3.3)

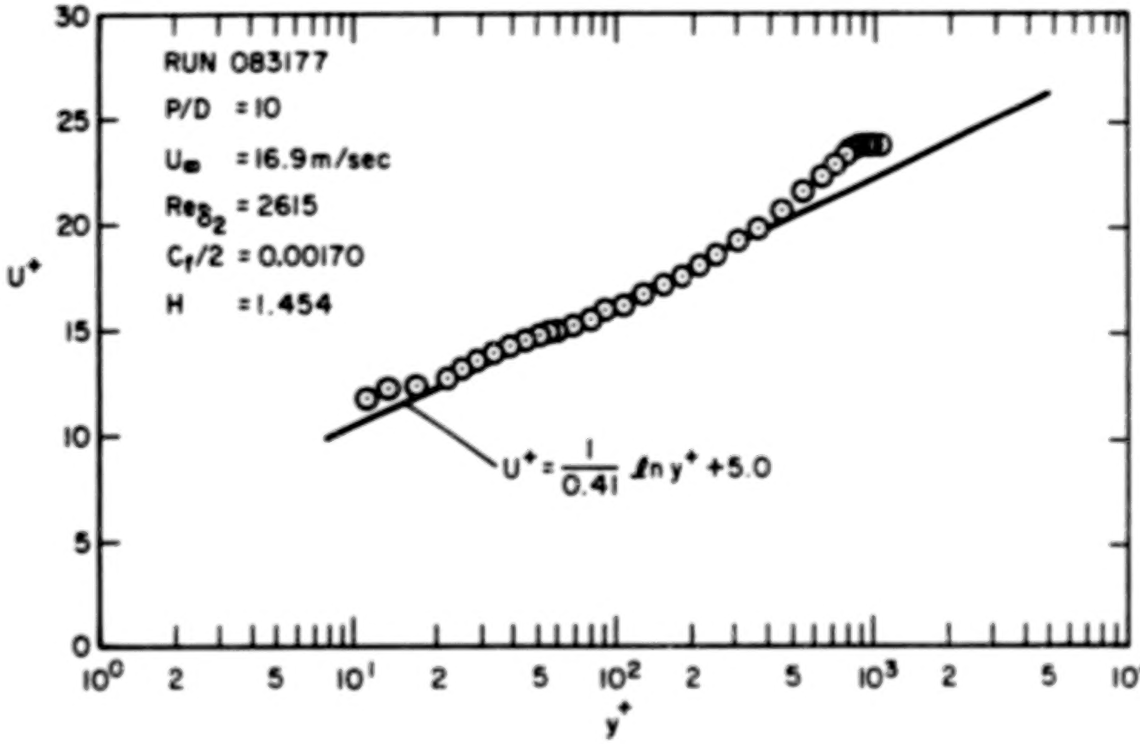

Fig. 3.5. Upstream velocity profile for initially high Re_{δ_2}, heated starting length runs, for Figs. 3.7 and 3.8.

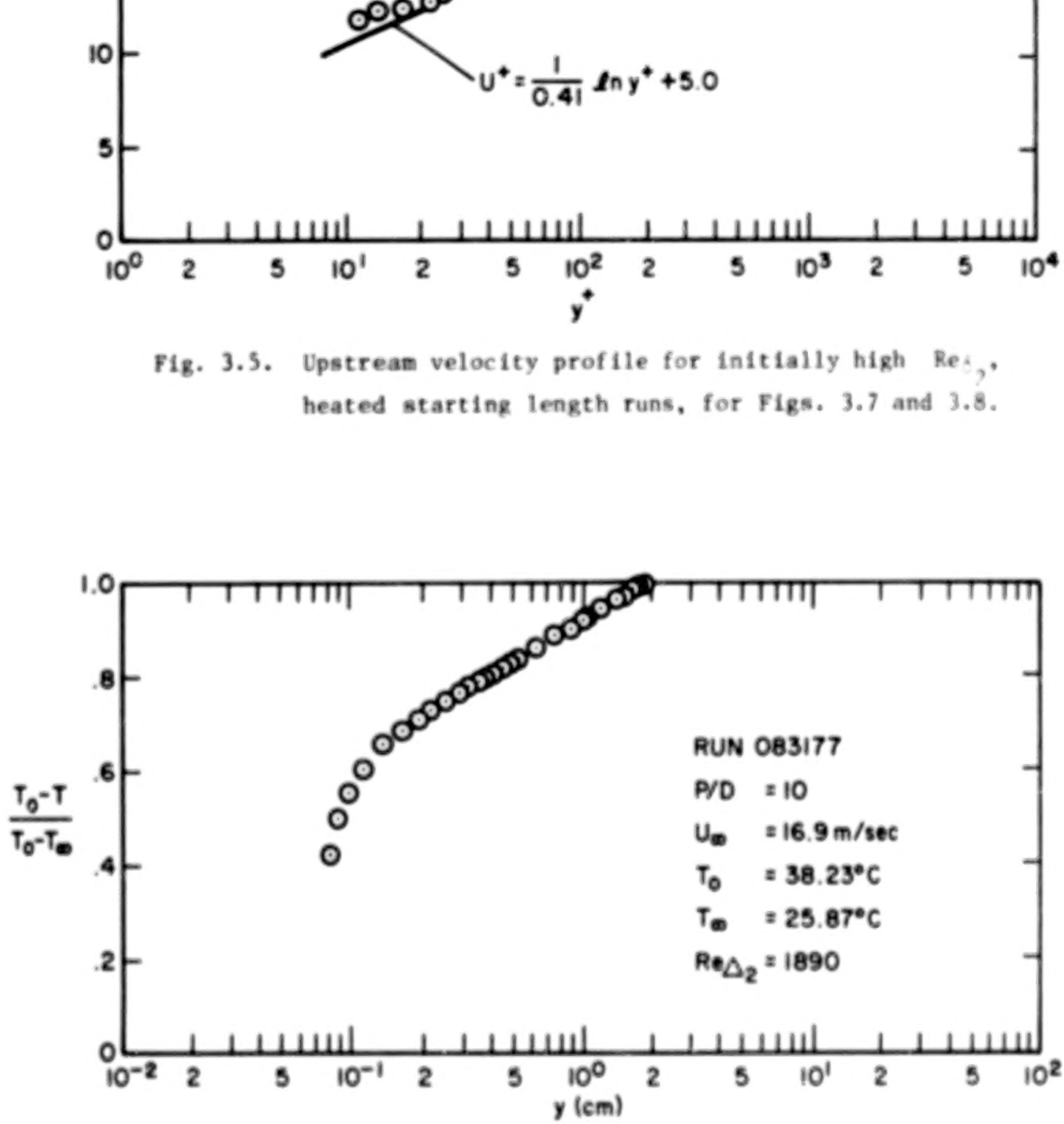

Fig. 3.6. Upstream temperature profile for initially high Re_{Δ_2}, heated starting length runs, for Figs. 3.7 and 3.8.

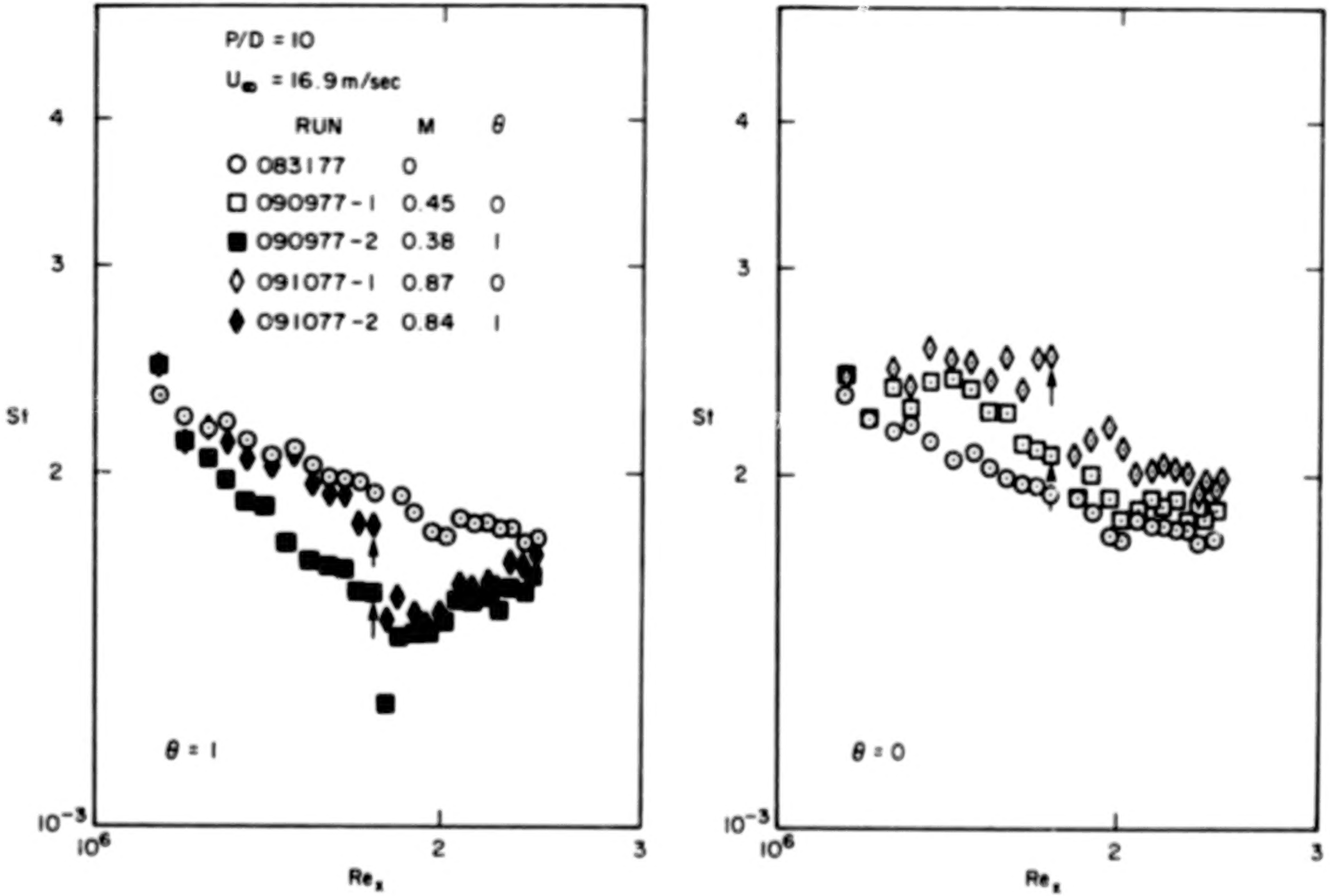

Fig. 3.7. St vs. Re_x for θ = 0 and θ = 1 with P/D = 10, heated foreplates.

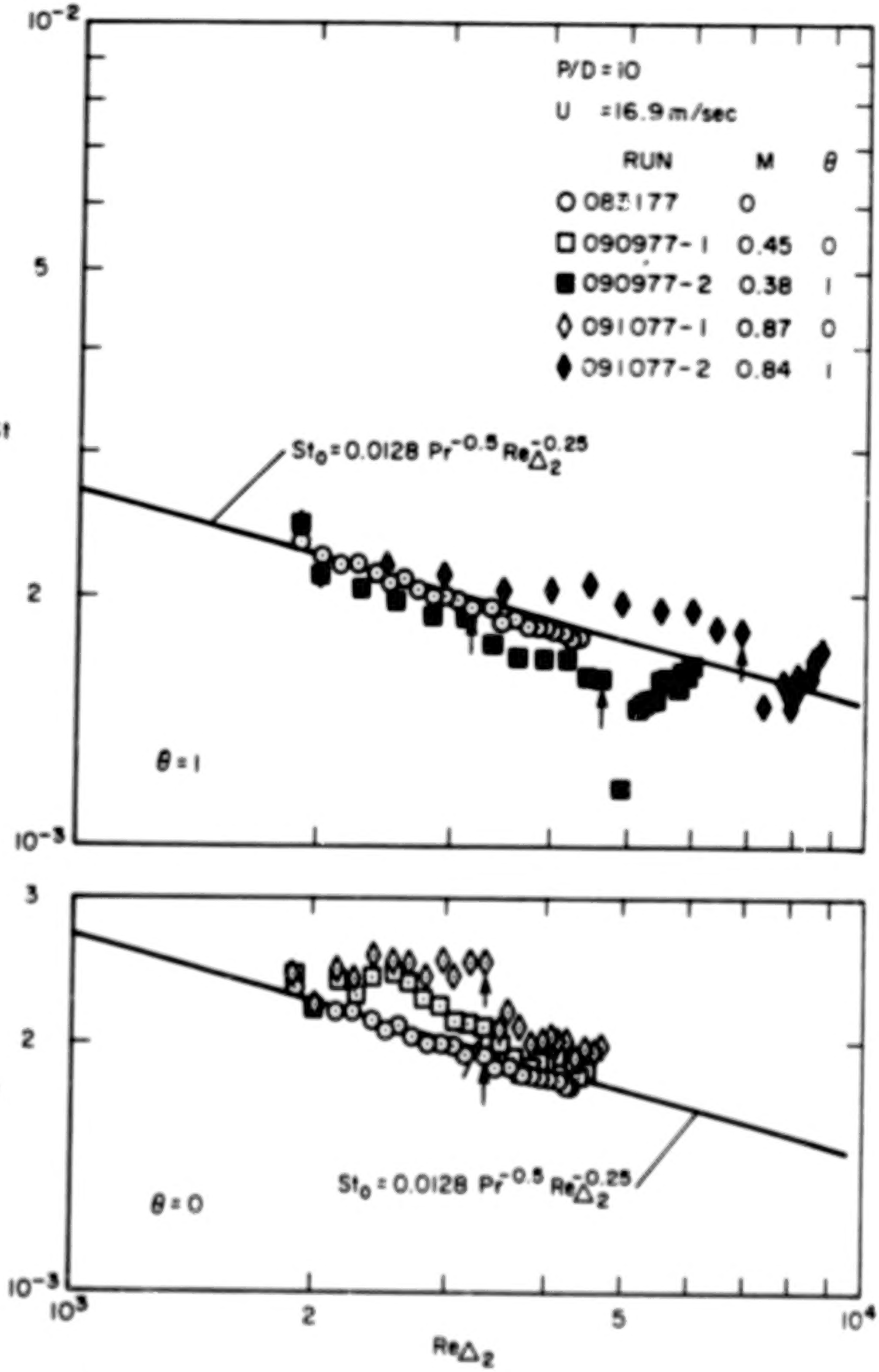

Fig. 3.8. St vs. Re_{Δ_2} for $\theta = 0$ and $\theta = 1$ with P/D = 10, heated foreplates (same data as in Fig. 3.7).

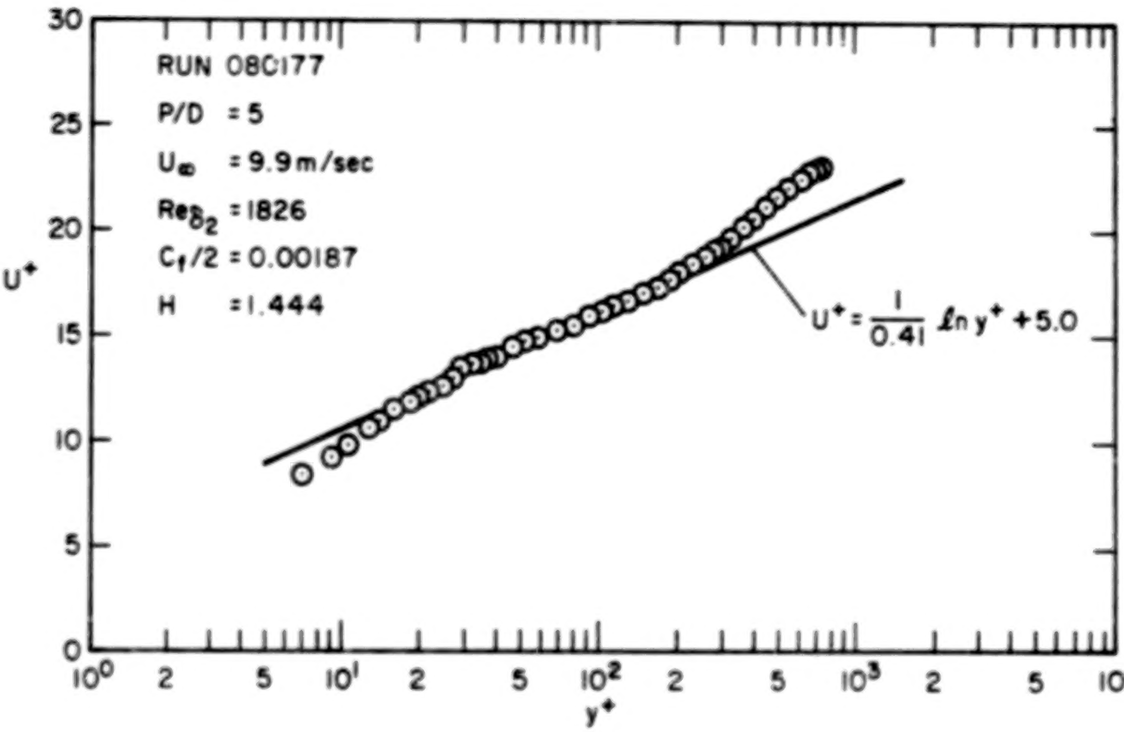

Fig. 3.9. Upstream velocity profile for initially high Re_{δ_2}, heated starting length runs, for Figs. 3.11 and 3.12.

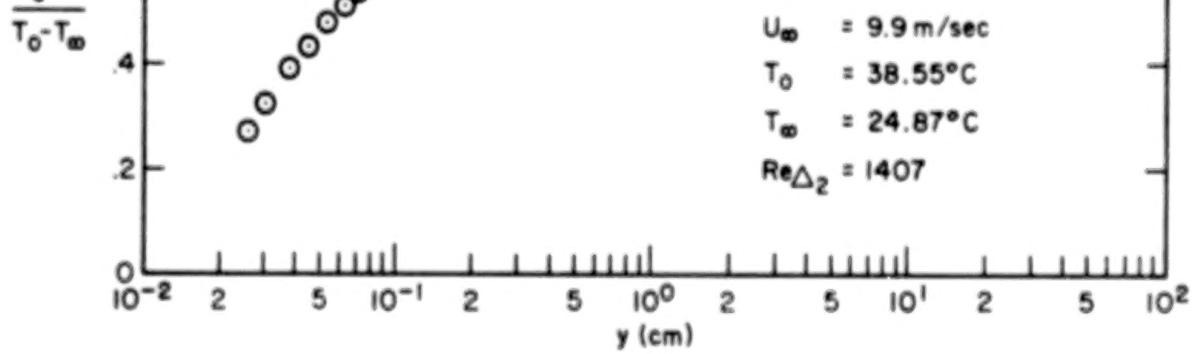

Fig. 3.10. Upstream temperature profile for initially high Re_{δ_2}, heated starting length runs, for Figs. 3.11 and 3.12.

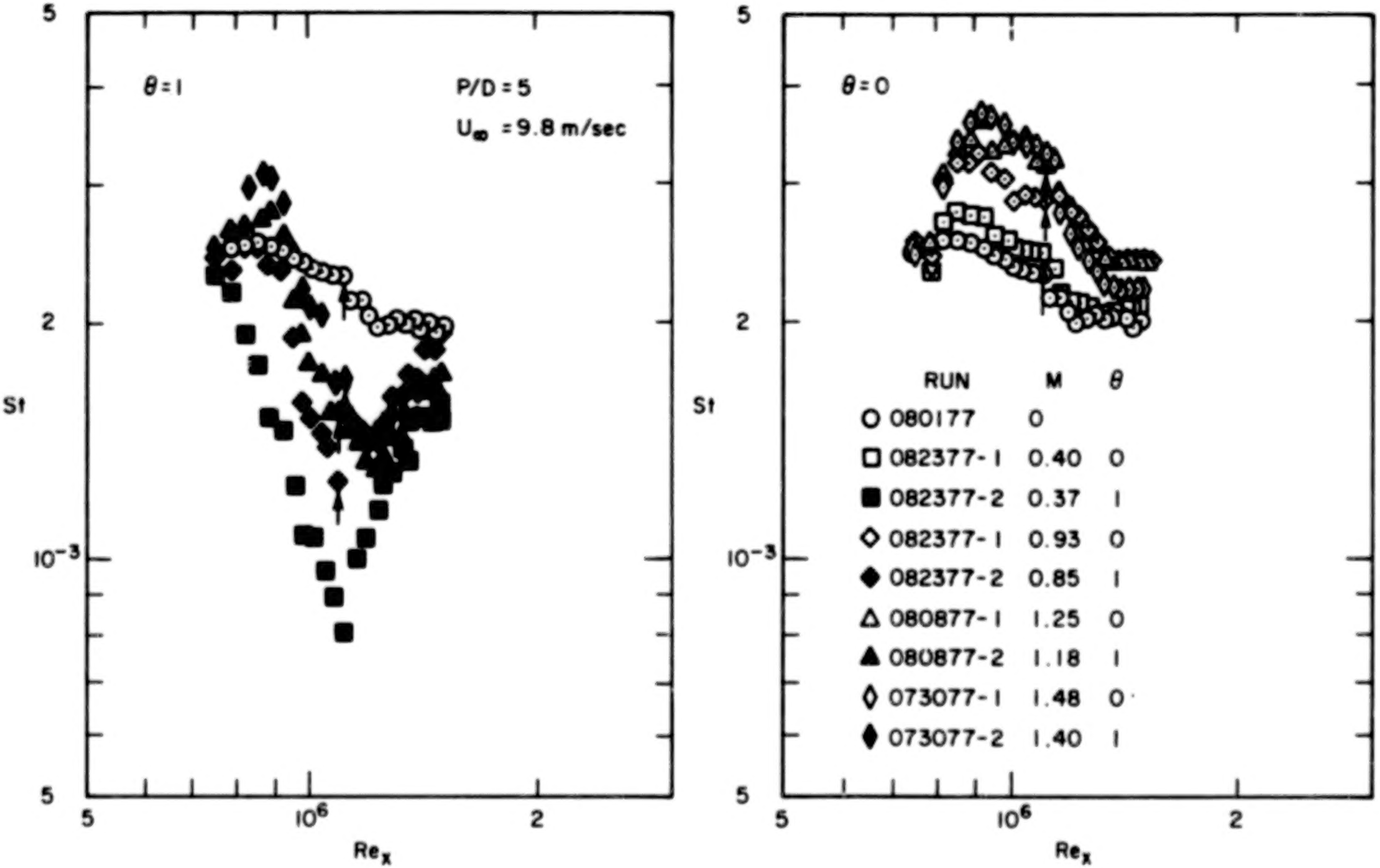

Fig. 3.11. St vs. Re_x for $\theta = 0$ and $\theta = 1$ with P/D = 5, heated foreplates.

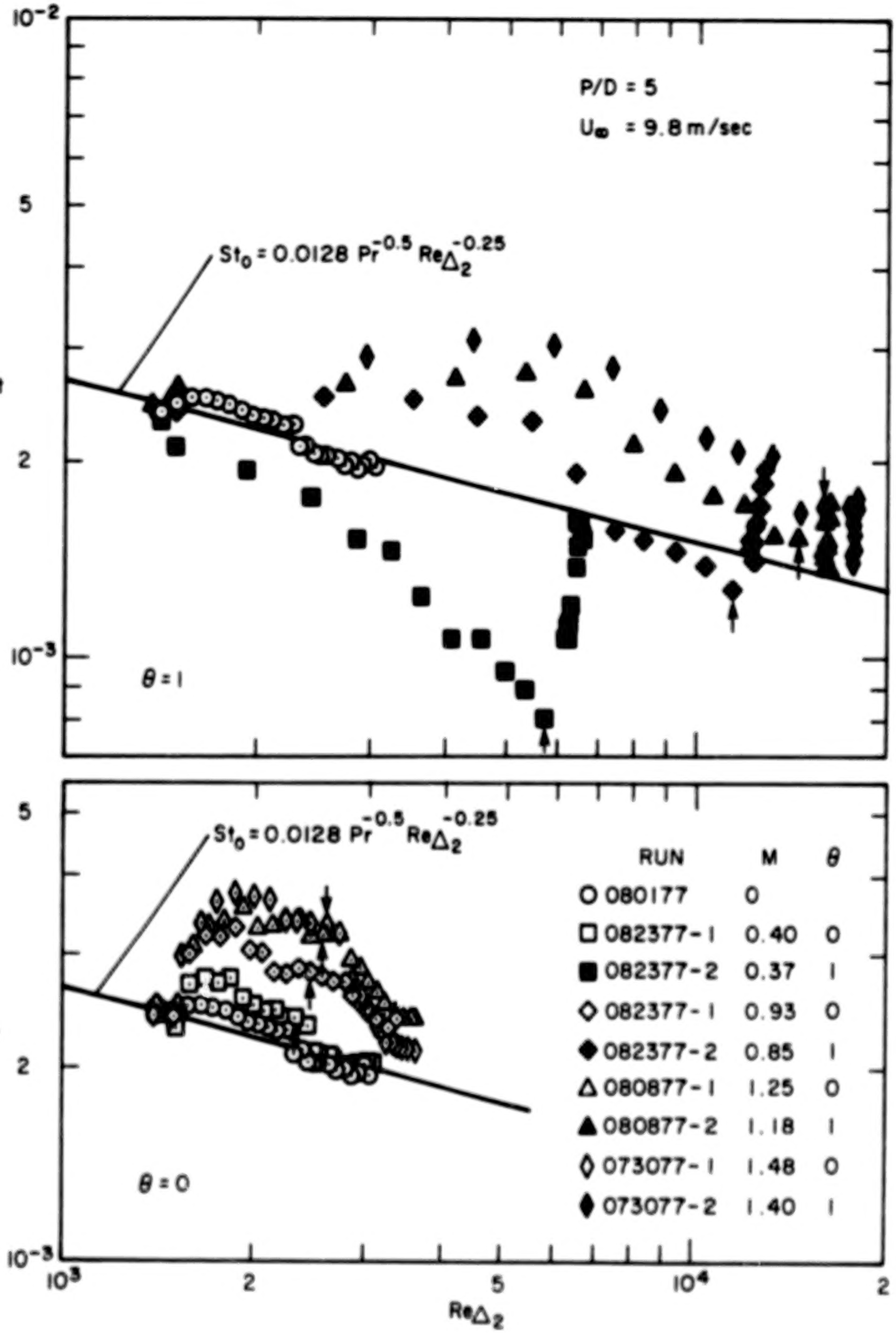

Fig. 3.12. St vs. Re_{Δ_2} for $\theta = 0$ and $\theta = 1$ with $P/D = 5$, heated foreplates (same data as in Fig. 3.11).

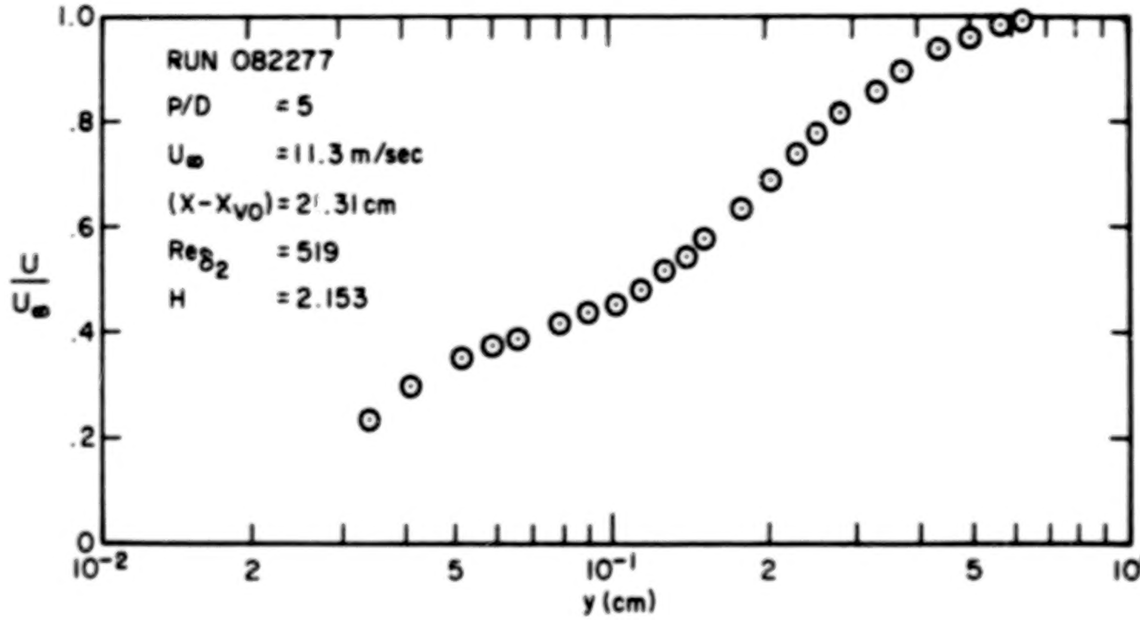

Fig. 3.13. Upstream velocity profile for initially low Re_{δ_2}, heated starting length runs, for Figs. 3.15 and 3.16.

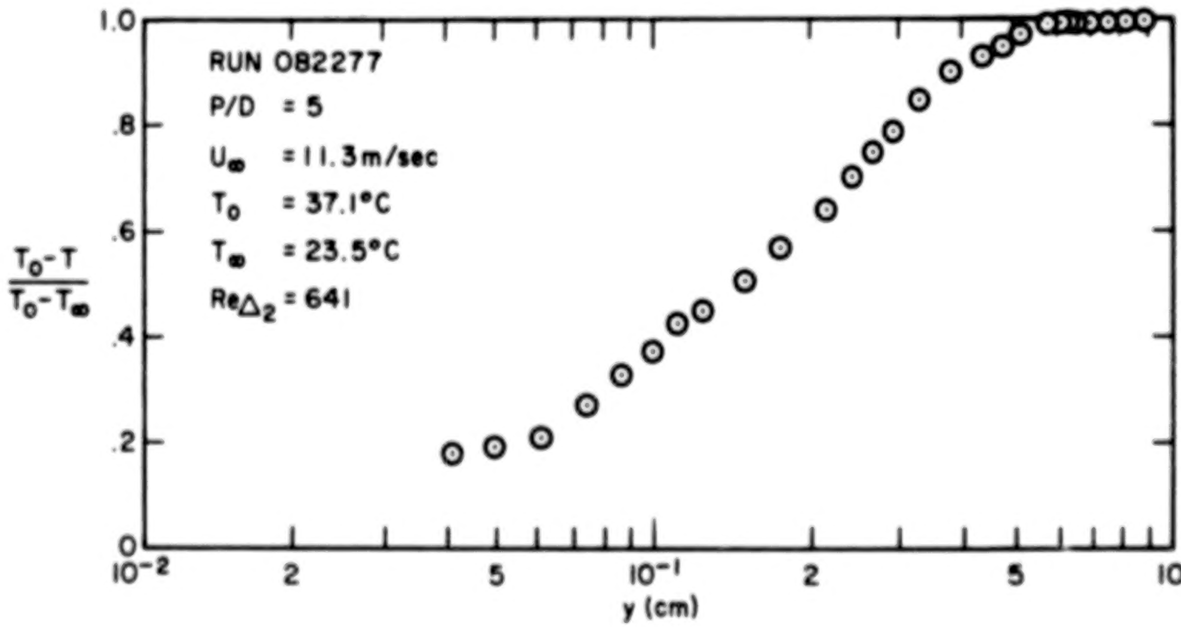

Fig. 3.14. Upstream temperature profile for initially low Re_{δ_2}, heated starting length runs, for Figs. 3.15 and 3.16.

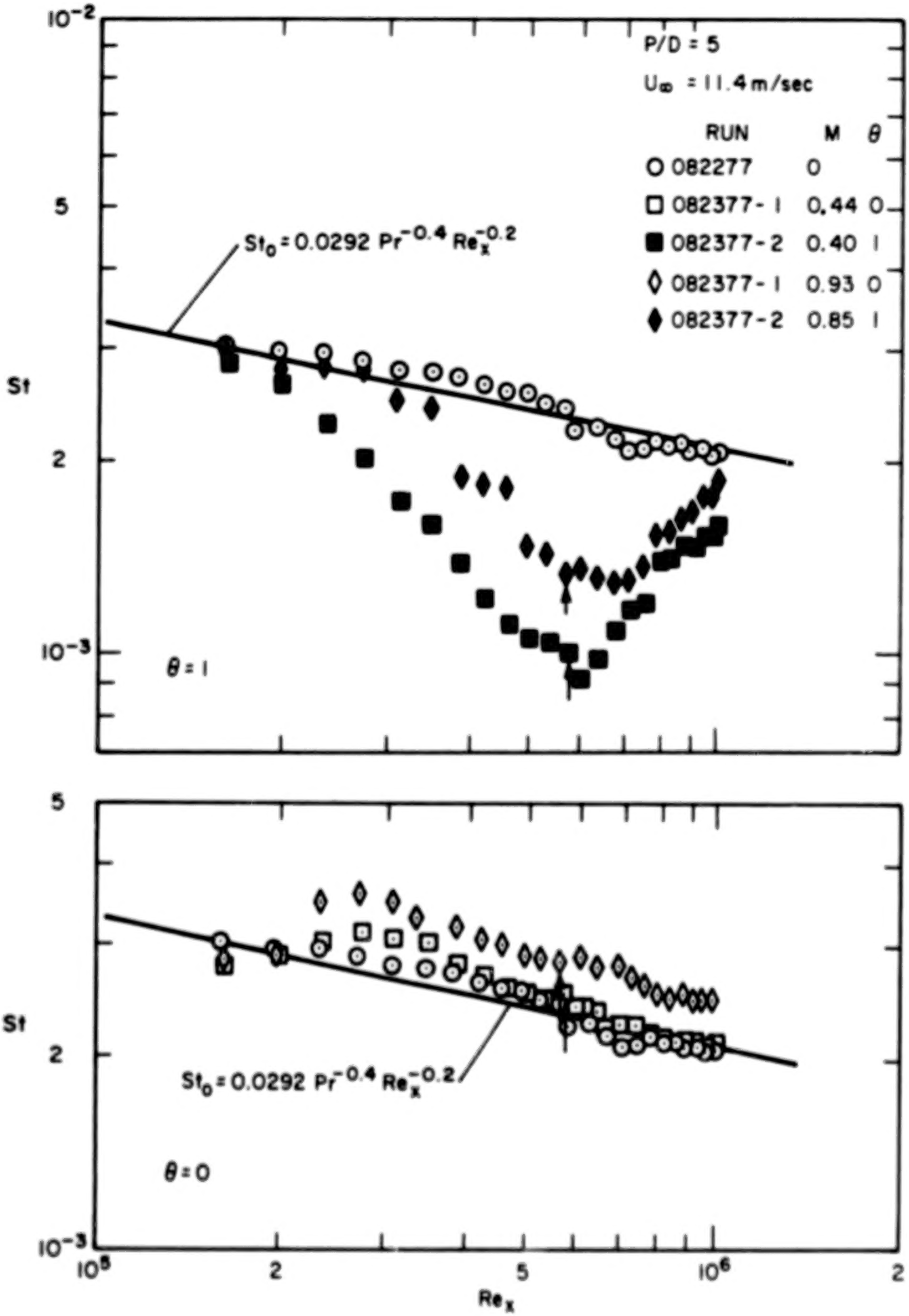

Fig. 3.15. St vs. Re_x for $\theta = 0$ and $\theta = 1$ with $P/D = 5$, heated foreplates.

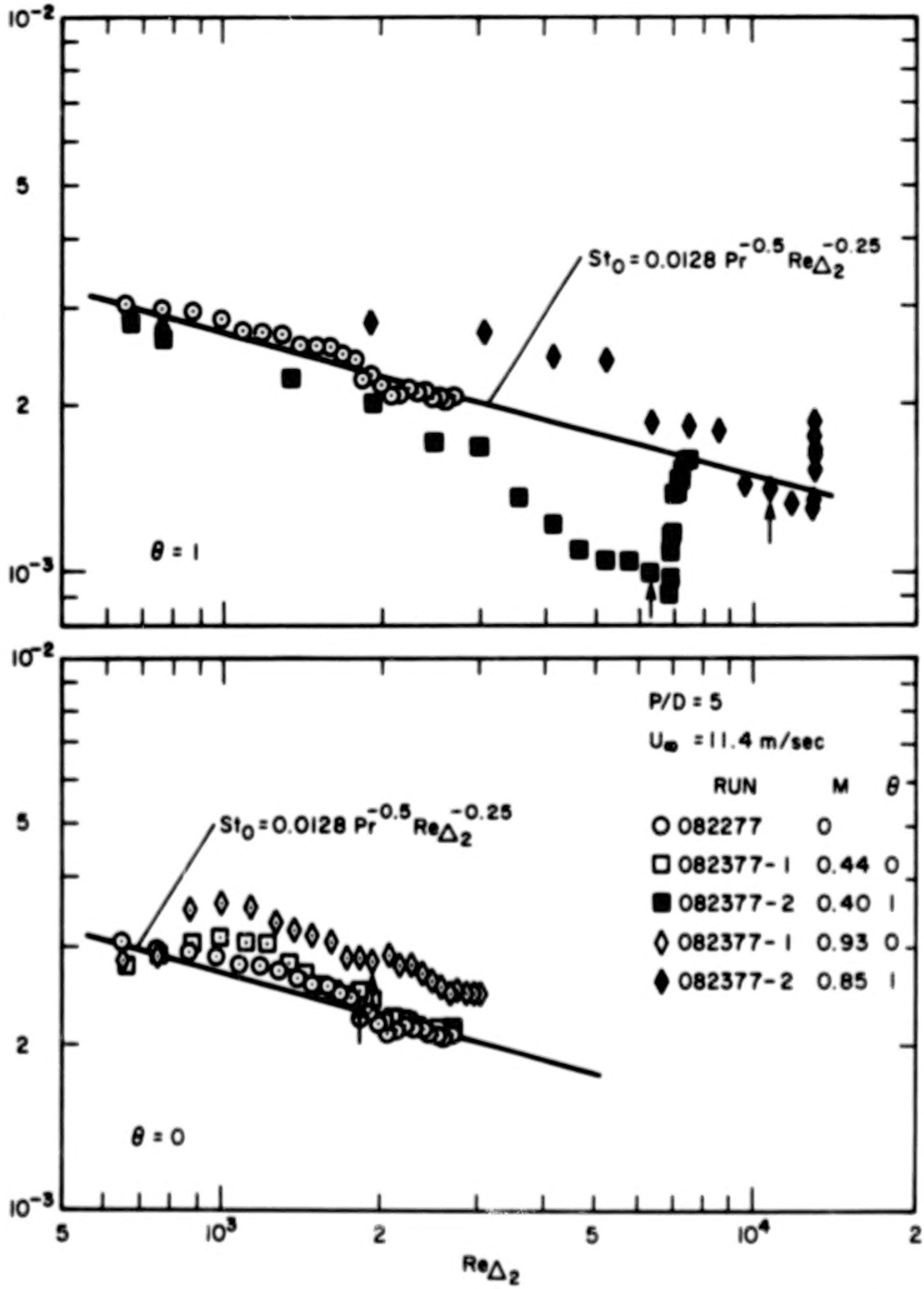

Fig. 3.16. St vs. Re_{Δ_2} for $\theta = 0$ and $\theta = 1$ with P/D = 5, heated foreplates (same data as in Fig. 3.15).

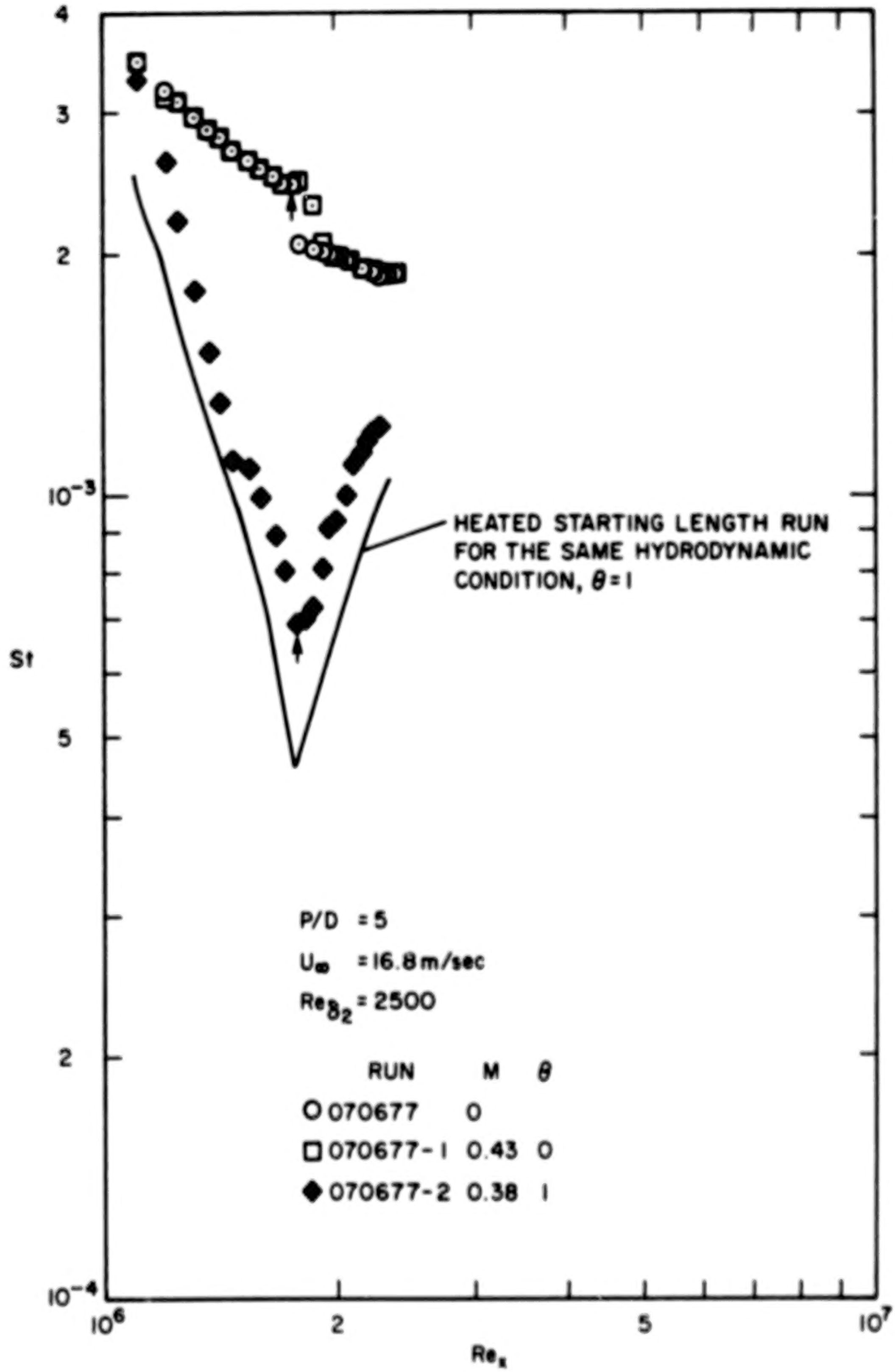

Fig. 3.17. St vs. Re_x for $\theta = 0$ and $\theta = 1$ with P/D = 5, unheated foreplates.

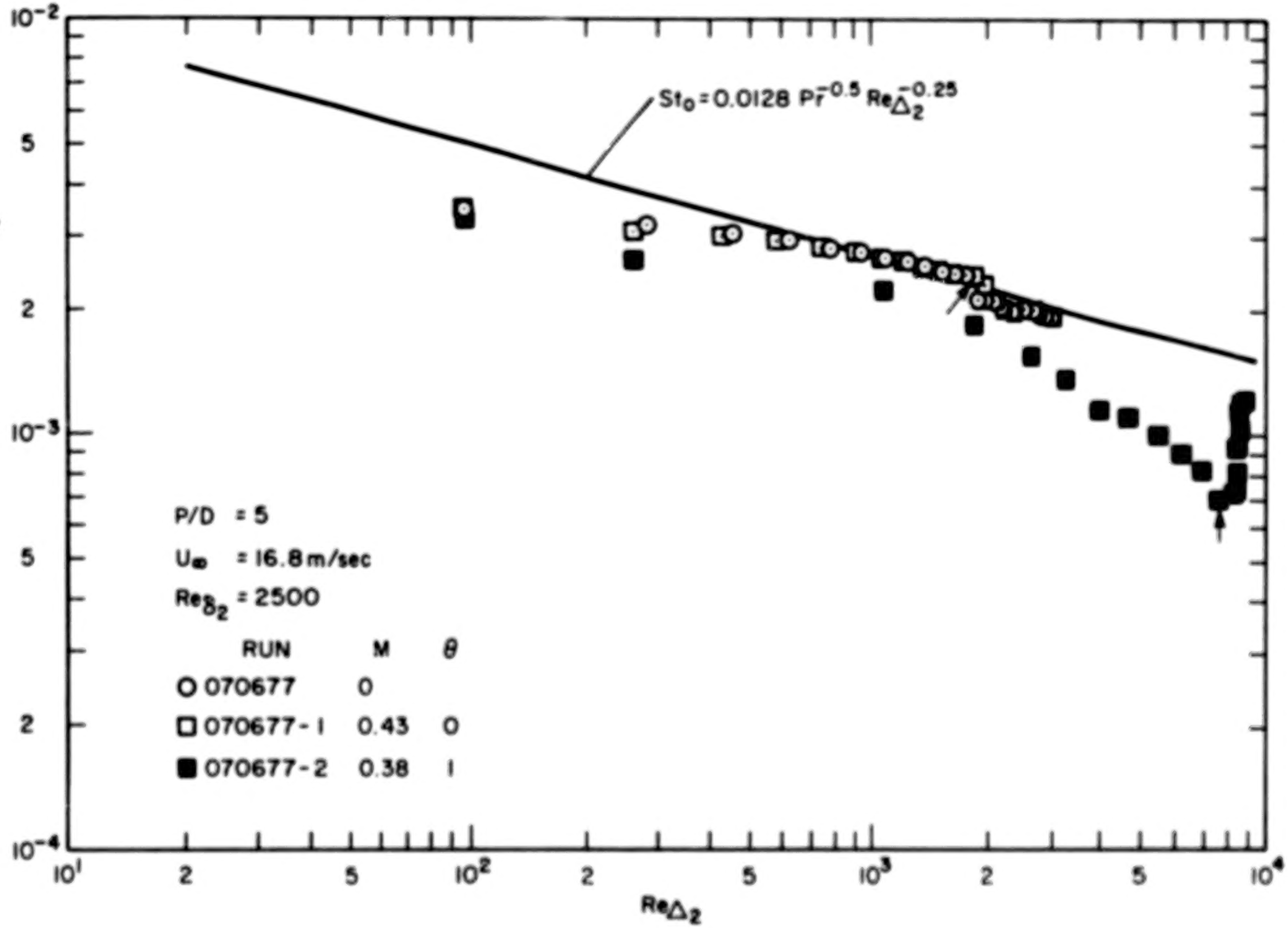

Fig. 3.18. St vs. Re_{Δ_2} for $\theta = 0$ and $\theta = 1$ with P/D = 5, unheated foreplates (same data as in Fig. 3.17).

Chapter 4

DISCUSSION OF THE DATA

4.1 Effects of Full-Coverage Film Cooling on Stanton Number

The results of the experimental Stanton number data have been presented in detail in the previous chapter. In this section of Chapter 4, the following items are summarized in order to see their effects on Stanton number (or heat transfer): (i) upstream initial conditions and free stream velocity, (ii) injectant temperature and blowing ratio, and (iii) hole spacing.

4.1.1 Upstream Initial Conditions and Free Stream Velocity

Free stream velocity and the initial conditions of the turbulent boundary layer were varied to study their effects on Stanton number. Fig. 4.1 shows all the data for $M = 0.4$ and $P/D = 5$, replotted as $St(\theta)/St_o$ versus the downstream distance x. St_o is the Stanton number for $M = 0$ with the same upstream initial conditions as $St(\theta)$.

In Fig. 4.1 the Stanton number ratios for $\theta = 1$ drop below unity in a fairly tight band for the blowing region, suggesting little or no effect of either the initial temperature or the free stream velocity. In the recovery region, the data do not order according to their initial layers but do show to order on free stream velocity.

Also shown in Fig. 4.1 are Stanton number ratios for $\theta = 0$. The recovery region data are quite coherent, while the blowing region data are separated. There is no ordering by velocity. Overall, the change in St by injection is much less for $\theta = 0$ than for $\theta = 1.0$. This is attributed to the fact that injecting $\theta = 0$ fluid does not directly contribute to the growth of Re_{Δ_2}, so until the thermal boundary layer grows beyond the penetration height of the jets, the Stanton number is only marginally different from St_o.

4.1.2 Injectant Temperature and Blowing Ratio

The injectant temperature level, T_2, is one of the important factors in heat transfer with full-coverage film cooling, compared with the surface and mainstream temperatures. For small temperature differences, the governing energy equation is linear so that the heat transfer is also a linear function of T_2. Stanton number data obtained for two injectant temperatures (all other parameters fixed) provide sufficient information to define the Stanton number as a continuous function of T_2. For the steady-state heat transfer tests described herein, the injectant temperatures were $T_2 = T_\infty(\theta = 0)$ and $T_2 = T_o$ $(\theta = 1)$. Colladay [31] indicated that for gas turbine applications, $T_2 < T_o < T_\infty$, a θ parameter was slightly larger than unity. Therefore the $\theta = 1$ data trends described in Chapter 3 should give an indication of the Stanton number behavior on a full-coverage turbine blade.

Although Stanton number is a simple function of θ, it is a very complex function of blowing ratio. Fig. 4.2 shows the Stanton numbers from Fig. 3.11, plotted versus blowing ratio. The data show a nonlinear dependence of St on M for $P/D = 5$. Also shown in Fig. 4.2 are predicted Stanton numbers for a typical θ operating condition to demonstrate the superposition principle. The predicted Stanton number decreases to a minimin at $M = 0.4$ and then rises as M increases. This minimum in Stanton number for a typical θ operation condition is clearly seen in the $\theta = 1$ data. This minimum appears to be independent of upstream initial conditions.

The drop in Stanton number for low M and $\theta = 1$ is similar to that found in transpiration cooling. With both cooling schemes the heat transfer is reduced due to addition of wall temperature fluid which significantly alters the temperature profile in the near-wall region. The cooling effect is diminished with full-coverage cooling because of increased turbulent transport. The full-coverage jets affect the transport over a range from the wall to at least two hole diameters, while the transpiration affects only the sublayer. Therefore, for an equivalent wall mass flux of coolant (equal F), the Stanton number with film cooling will be higher.

The increase in Stanton number with M for M 0.4 indicates that the film cooling jets are transporting the coolant farther out in the boundary layer. This increased penetration distance has two effects: (1) By

delivering the coolant farther away from the surface, the coolant must be convected or diffused back into the near-wall region in order to reduce the wall heat transfer. During this process the coolant entrains boundary layer fluid, and equilibration with the entrained fluid significantly reduces the effectiveness of the coolant. (ii) The increased penetration of the coolant farther out in the boundary layer causes increasing turbulence production. The resulting increased turbulent transport in the outer layer may intensify the coolant diffusion back to the surface, but it also intensifies the jet entrainment process which dilutes the coolant.

In the recovery region the Stanton number data for $\theta = 1$ rise rapidly for all blowing ratios, with almost the same slope.

4.1.3 Hole Spacing

Stanton numbers were obtained primarily for $P/D = 5$, but some data were taken for $P/D = 10$. Only one set of upstream initial conditions was tested in order to study the effects of hole spacing on Stanton number data. The visual comparison of these data in Chapter 3 revealed a much diminished effect for the same M with wider hole spacing.

4.2 Correlation of the Stanton Number Data

One way to evaluate film-cooling performance is by obtaining surface heat flux with and without film cooling, $\dot{Q}''(\theta)/\dot{Q}''_o$, at the same location on the surface. Since both heat fluxes are defined using the same convective rate equation, the film-cooling performance can be simplified to evaluation of $h(\theta)/h_o$ or $St(\theta)/St_o$. The $St(\theta)$ data can be obtained by applying superposition to correlations of the fundamental Stanton number data sets at $\theta = 0$ and $\theta = 1$.

The data for $\theta = 1$ were correlated based on a Couette flow analysis developed by Choe et al. [11] and Crawford et al. [12].

$$\left.\frac{St(\theta = 1)}{St_o}\right|_{Re_x} = \frac{\ln(1 + Bh)}{Bh} \cdot \phi \qquad (4.1)$$

where Bh is the blowing parameter, defined as $Bh = F/St(\theta = 1)$, and ϕ

is a functional measure of departure from the ideal case of transpiration cooling (for which value is a unity).

Figure 4.3 shows all data for $\theta = 1$ plotted versus F for $P/D = 5$ with heated starting length. As F increases, ϕ also continuously increases: as the blowing ratio increases, the cooling scheme rapidly departs from the transpiration cooling.

Correlations of the $\theta = 1.0$ data for $P/D = 5$ are as follows:

$$\left.\frac{St(\theta = 1)}{St_o}\right|_{Re_x} = [1 + 112.5\ F]\ \frac{\ln(1 + Bh)}{Bh} \tag{4.2}$$

or, in Re_{Δ_2} coordinates suggested by Whitten, Kays, and Moffat [4],

$$\left.\frac{St(\theta = 1)}{St_o}\right|_{Re_{\Delta_2}} = [1 + 112.5\ F]^{1.25} \left[\frac{\ln(1 + Bh)}{Bh}\right]^{1.25} [1 + Bh]^{0.25} \tag{4.3}$$

Here the values for St_o in Eqns. (4.2) and (4.3) are the typical smooth flat-plate values.

For $\theta = 0$, the Stanton number data are correlated in terms of F for three upstream initial conditions by the following heuristic equations:

- For $Re_{\delta_2} = 2500$, the correlating equation for $P/D = 5$ data is

$$St(\theta = 0) = 2.512 \times 10^{-3}\ e^{3.801\,F} \quad \text{for} \quad 0.40 \le M \le 1.24 \tag{4.4}$$

- For $Re_{\delta_2} = 1800$, the correlating equation for $P/D = 5$ data is

$$St(\theta = 0) = 2.437 \times 10^{-3}\ e^{7.677\,F} \quad \text{for} \quad 0.40 \le M \le 1.48 \tag{4.5}$$

- For $Re_{\delta_2} = 500$, the correlating equation for $P/D = 5$ data is

$$St(\theta = 0) = 2.762 \times 10^{-3}\ e^{4.463\,F} \quad \text{for} \quad 0.44 \le M \le 0.93 \tag{4.6}$$

4.3 The Comparison of Stanton Number Data for Compound-Angle Hole Injection with Those for 30° Slant-Hole Injection at $M = 0.4$ and $\theta = 1$

This section summarizes the comparison of two fundamental data sets, for compound-angle injection and for 30° slant-hole injection [12] at $M = 0.4$ and $\theta = 1$ for $P/D = 5$ and heated starting length.

Figure 4.4 shows the Stanton number data versus Re_x for the two cooling injection schemes described above, for the same hydrodynamic conditions. The compound-angle data at the minimum point (same location of the test surfaces) are about half those of the 30° slant-hole data. This trend is seen for all blowing ratios, when the two geometries are tested at the same hydrodynamic conditions. Thus, with compound-angle injection, the heat transfer coefficients were only one-half as high as with 30° slant-hole injection.

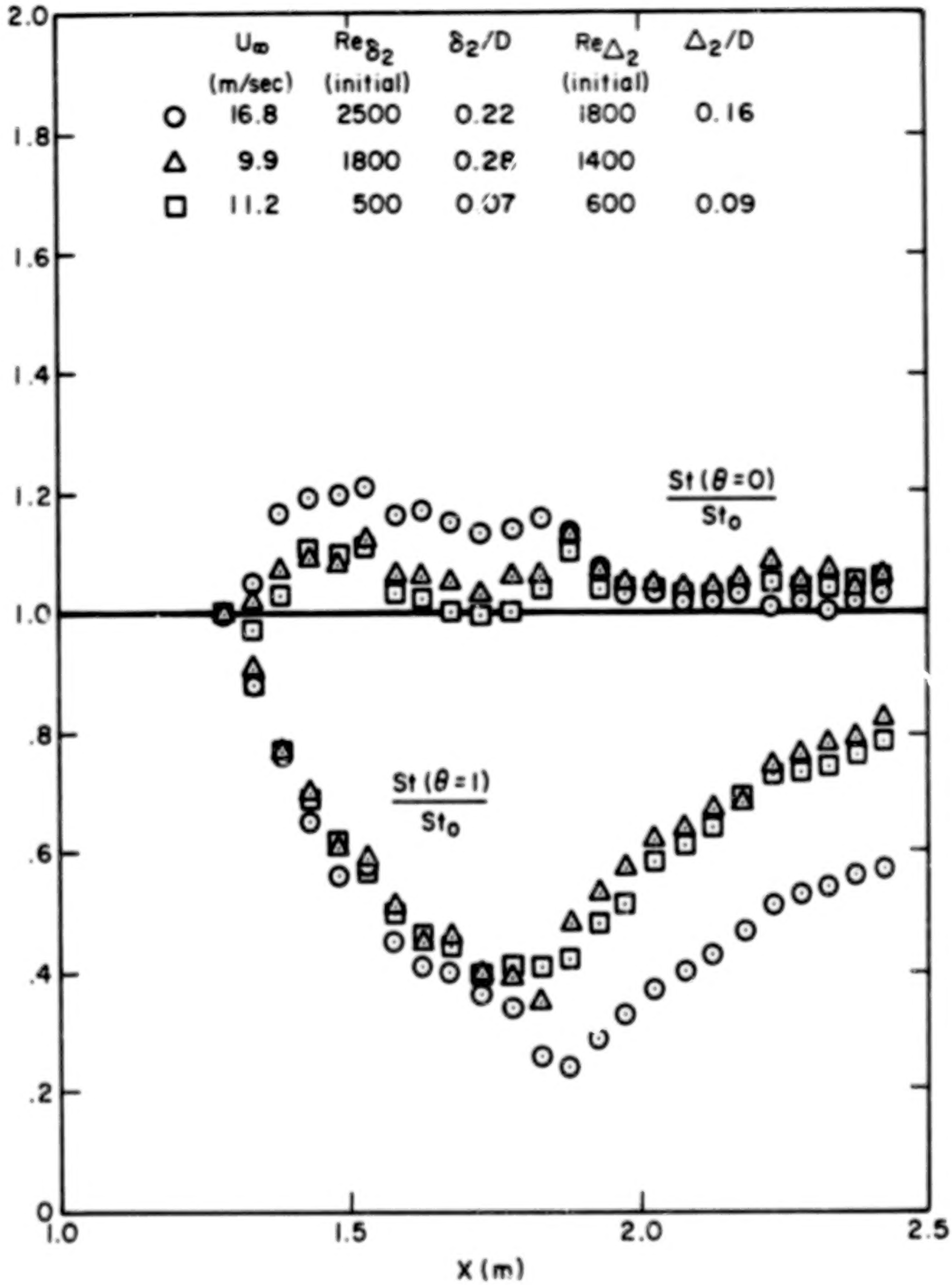

Fig. 4.1. Stanton number ratios for all M = 0.4 data and P/D = 5 with heated foreplates.

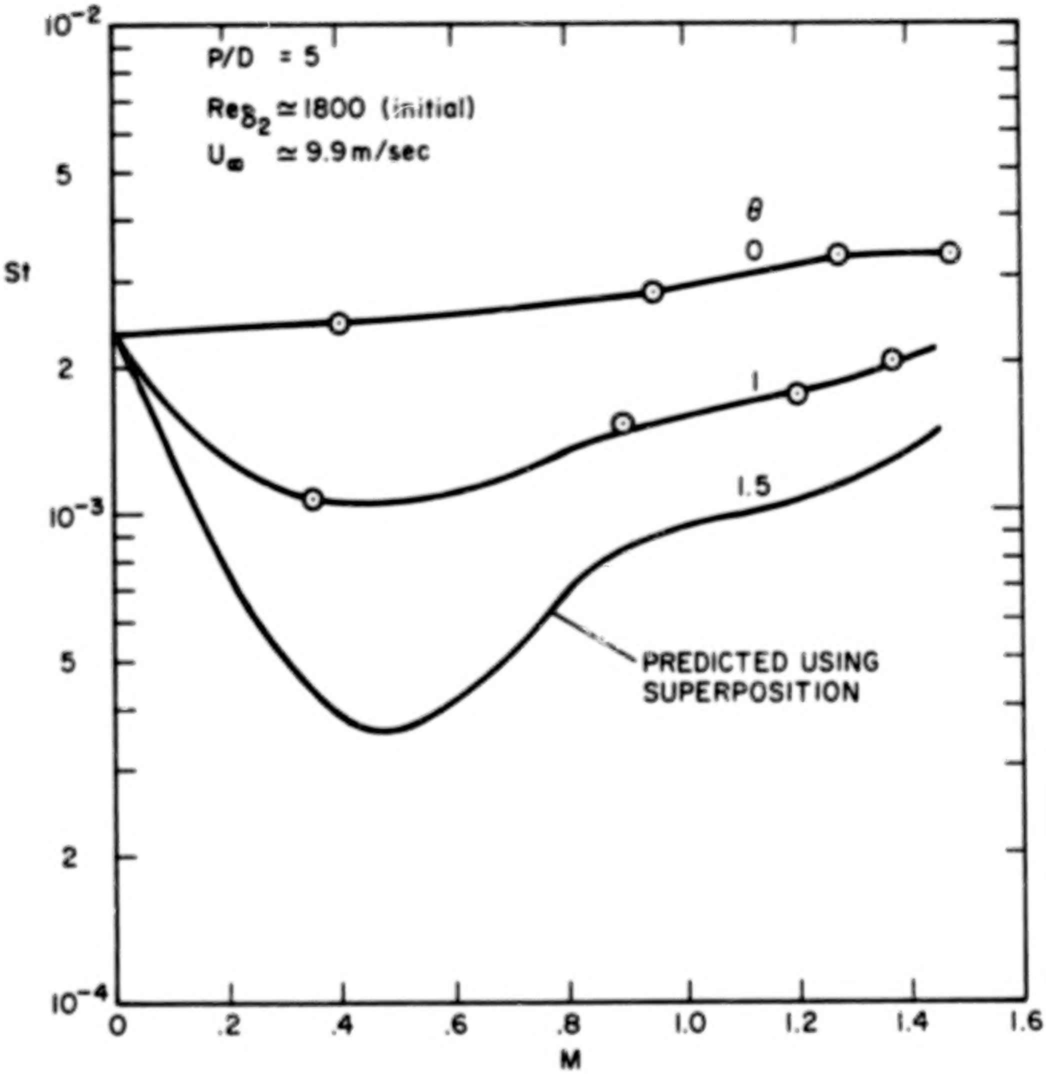

Fig. 4.2. Prediction of Stanton number for $\theta = 1.5$ by applying superposition to fundamental data sets, Fig. 3.11 (plate 9).

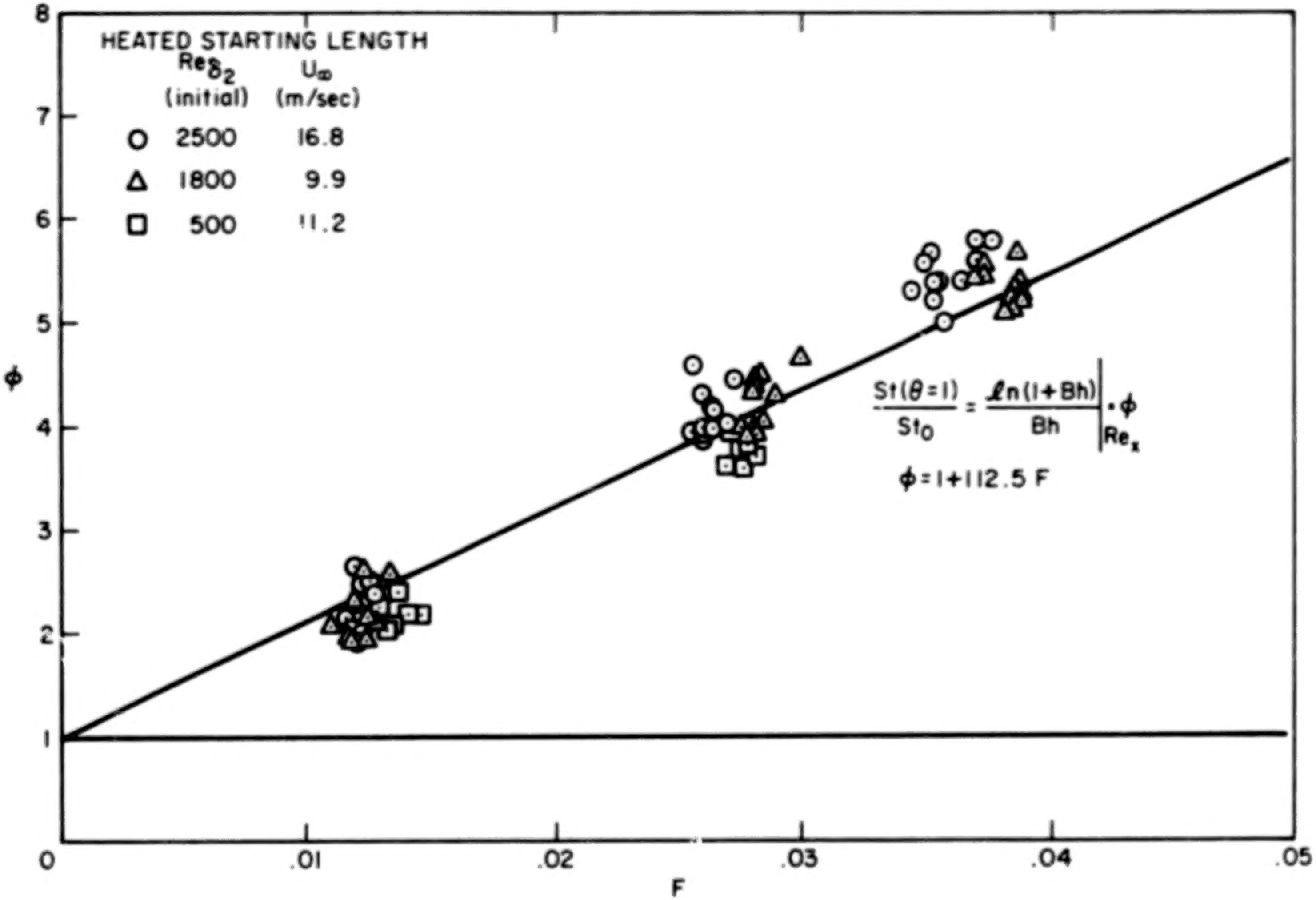

Fig. 4.3. Correlation of the Stanton number data at $\theta = 1$.

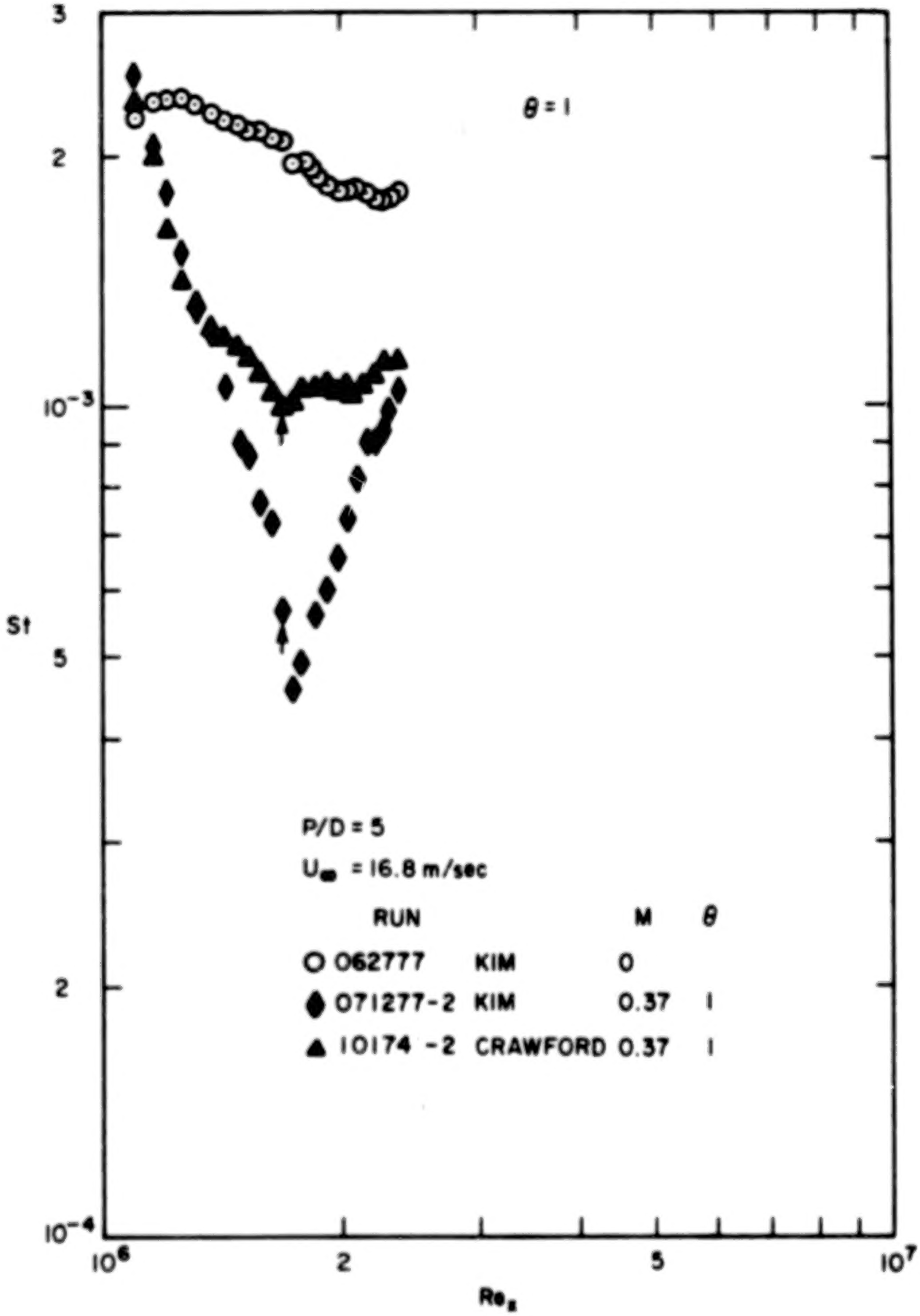

Fig. 4.4. Comparison of St vs. Re_x with Crawford's data [12] for the same hydrodynamic conditions.

Chapter 5

SUMMARY AND RECOMMENDATIONS

An experimental investigation of heat transfer to the boundary layer over a full-coverage, film-cooled surface has been performed. Injection of the coolant was from an array of staggered holes with hole spacing-to-hole diameter ratios of 5 and 10. The $P/D = 10$ data were obtained for only one set of upstream initial conditions. The holes were angled 30° to the surface in the downstream direction and 45° to the surface in the spanwise direction. In summary:

1. Experimental Stanton number data have been obtained by using two injectant temperatures ($\theta = 0$ and $\theta = 1$) at each blowing ratio, yielding two fundamental data sets. The data are defined using a wall temperature-to-mainstream temperature driving potential, which allows direct comparison of wall heat fluxes in terms of Stanton numbers, with and without film cooling, to describe film-cooling performance. Superposition can be applied to the two fundamental data sets to obtain Stanton number as a continuous function of injectant temperature.

2. When the injectant temperature, T_2, equals plate temperature, T_o, the lowest Stanton number is obtained for a blowing ratio $M = U_2/U_\infty$ of about 0.4. Higher ratios resulted in higher Stanton numbers. The data obtained in this experimental program for the highest blowing ratio of 1.48 are still smaller than those without film cooling.

3. Comparison of the data for the two hole spacings indicates that a wider hole spacing (10 hole diameters) gives less effect on Stanton number for the same value of blowing ratio. In other words the wider hole spacing reduces the film-cooling for the same blowing ratio.

4. The effects on Stanton number of changing the free stream velocity and the initial conditions showed the following effects: (i) at $\theta = 1$ U_∞ had a slight effect on Stanton number in the blown region; (ii) the $\theta = 1$ data in the recovery region were strongly dependent on U_∞.

5. For prediction of heat transfer data using integral equation relationships, the following formulae are recommended:

i) For $\theta = 1$ (injectant temperature equal to plate temperature)

$$\left.\frac{St(\theta=1)}{St_o}\right|_{Re_x} = [1+112.5\ F]\ \frac{\ln(1+Bh)}{Bh}$$

or in Re_{Δ_2} coordinates

$$\left.\frac{St(\theta=1)}{St_o}\right|_{Re_{\Delta_2}} = [1+112.5\ F]^{1.25}\left[\frac{\ln(1+Bh)}{Bh}\right]^{1.25}\ [1+Bh]^{0.25}$$

ii) For $\theta = 0$ (injectant temperature equal to mainstream temperature)

- At $Re_{\delta_2} = 2500$,

$$St(\theta=0) = 2.512 \times 10^{-3}\ e^{3.801\ F} \quad \text{for} \quad 0.40 \leq M \leq 1.24$$

- At $Re_{\delta_2} = 1800$,

$$St(\theta=0) = 2.437 \times 10^{-3}\ e^{7.677\ F} \quad \text{for} \quad 0.40 \leq M \leq 1.48$$

- At $Re_{\delta_2} = 500$,

$$St(\theta=0) = 2.762 \times 10^{-3}\ e^{4.463\ F} \quad \text{for} \quad 0.40 \leq M \leq 0.93$$

6. When the injectant temperature was equal to plate temperature, two distinct data trends were seen. The data within the blown region dropped rapidly to a minimum value at the last row of blowing. In the recovery region (60 hole diameters downstream of the last blowing row), the data rose rapidly toward the baseline data.

7. An examination of two data sets for the compound-angle hole injection and the 30° slant-hole injection at $\theta = 1$ and $M = 0.4$ with $P/D = 5$ and heated starting length revealed that compound-angle injection yielded heat transfer coefficients only one-half as high as those for 30° slant-hole injection.

The work reported here represents the third phase of an experimental heat transfer investigation into full-coverage, film-cooled boundary layers on a flat plate at Stanford: the first was normal-hole injection; the second was 30° slant-hole injection; and the last one was with compound-angle (30° and 45°) hole injection.

For further study of the compound-angled hole injection, it is recommended that:

- Detailed investigation of mean velocity, mean temperature, and turbulence profiles around the discrete holes should be carefully examined. The flow within the blown region and the recovery region is highly three-dimensional, a situation not experienced in previous test plates (the normal-angle hole and the 30° slant-hole). Such a study would provide details of the variation of velocity, temperature and turbulence level around the holes and also would provide data for a higher-level turbulence closure model for future numerical prediction programs.

- The effects of high mainstream turbulence level on heat transfer should be investigated. The importance of this effect may be confined to the recovery region. High turbulence levels may cause a more rapid recovery to unblown Stanton number conditions.

Appendix I

HOT-WIRE FLOWMETER CALIBRATION

Introduction

The hot-wire flowmeters [11] installed in the secondary air delivery pipes of the discrete hole rig had not been calibrated for approximately three years [32] in February of 1977. Also four of the secondary air delivery pipes had been relocated for the present heat transfer study of the compound-angle test plate. Therefore, all the hot-wire flowmeters needed to be recalibrated for the accurate measurement of flow rate.

Choe et al. [11] have described the hot-wire flowmeter. It has a thermocouple loop for measuring the temperature difference between the heater element and the incoming air stream. The thermocouple is made of iron-constantan with one junction at the middle of the heater element inside the brass tubing and the other junction in the air stream 1/2 inch upstream with 90° rotation. The calibration curve for hot-wire flowmeters [11] has shown the flow rate X plotted as a function of the voltage E. The functions X and E are expressed as:

$$X = SCFM \cdot \left(\frac{T}{530}\right)^{-0.76} \cdot (1+0.7\,w) \qquad (I-1)$$

$$E = emf. \cdot \left(\frac{I_o}{I}\right)^{2} \cdot \left(\frac{T}{530}\right)^{0.7} \cdot (1+0.22\,w)\,K_i \qquad (I-2)$$

where

SCFM = theoretical flow rate in CFM,

w = specific humidity in lbs/lb of D.A.

emf = the emf of the thermocouple signal,

I_o = 30.00 mv,

K_i = flowmeter calibration constant.

For the present calibration of hot-wire flowmeters, the same slope of the calibration curve shown in [11] has been used to determine the calibration constant, K_i, rather than constructing a new calibration

curve, because the initial calibration showed that all the calibration curves collapse by the horizontal shift of some distance on log-log coordinates. The values for the calibration constant, K_i, determined here cause the horizontal shift of some distance of each flowmeter into the same calibration curve shown in [11].

Instrumentation

The Meriam laminar flow meter was used in the experiment. Its flow rate was accurately known as a function of the pressure drop across the flowmeter with the temperature and absolute pressure correction factors upstream of the flowmeter. The actual flow rate was converted into the corresponding voltage using Eqns. (I-1) and (I-2) with the same slope of the calibration curve shown [11]. Then the emf of the thermocouple signal was compared with the actual flow rate voltage obtained by the Meriam laminar flow meter, in order to determine the calibration constant K_i. For each flowmeter, three sets of K_i at different flow rates were obtained to establish the experimental confidence. Then the final calibration constant K_i was determined from the arithmetic average of the three values.

Figure I-1 shows the arrangement of the experimental apparatus.

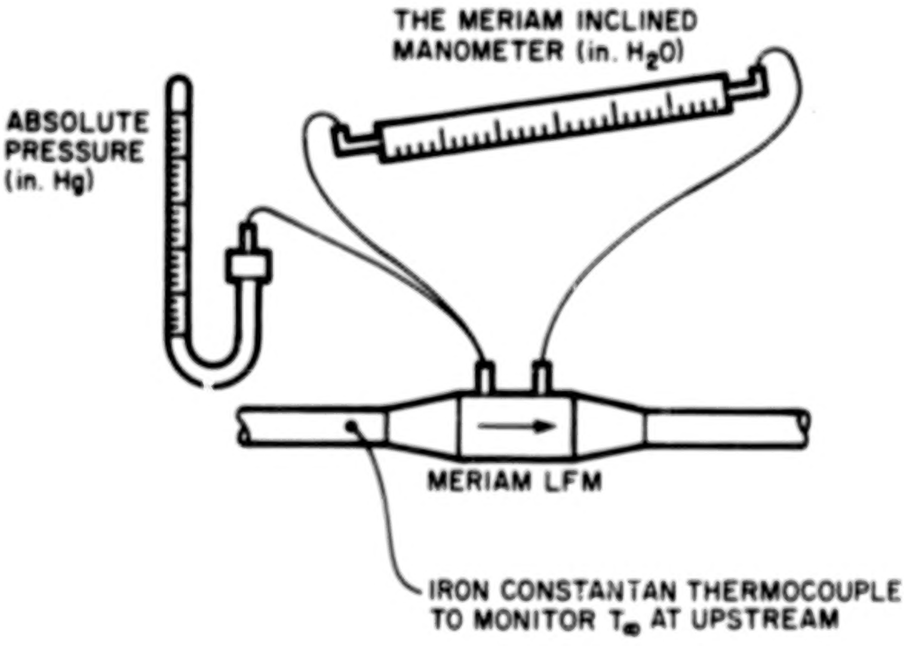

Fig. I-1. The experimental apparatus.

Instruments required:

- o Meriam laminar flow meter; Model 50MH10-2, Type 1,
- o Hewlett-Packard 2401C with 100K impedance,
- o Meriam inclined manometer (9-8" H_2O)
- o Mercury vertical manometer (in. Hg).

If there is no absolute pressure gauge, the Mercury vertical manometer can be used, because it gives the relative pressure reading. Then add the barometric pressure to the relative pressure reading to obtain the absolute pressure upstream of the Meriam laminar flow meter.

Data-Reduction Procedure

From the accurately known flow rate obtained by the Meriam laminar flow meter, the equivalent voltage can be determined in the following way. The calibration curve shown [11] gives the slope as:

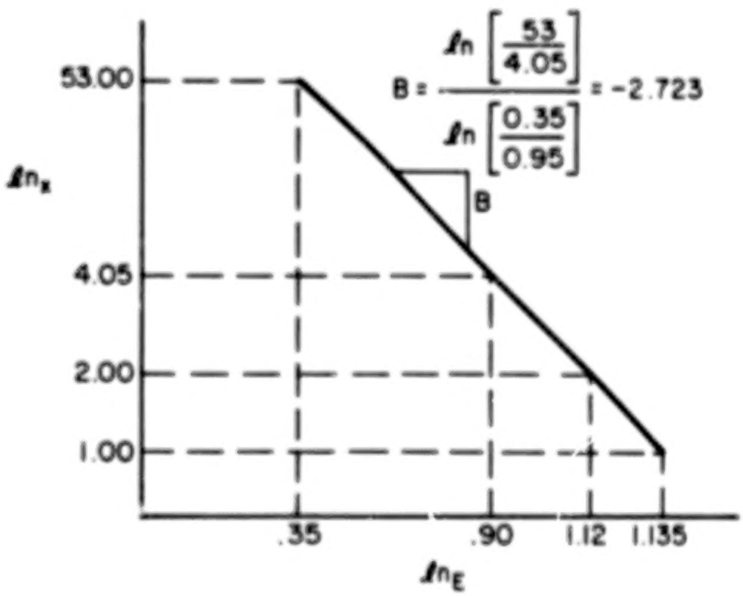

$$E = X_i \left[\frac{X}{Y_i}\right]^{1/B} = 0.35 \left[\frac{X}{53}\right]^{-\frac{1}{2.723}} \qquad \text{(I-3)}$$

For a sample data reduction, the following table shows data on the hot-wire flowmeter #2, for ω = 0.0047 lbm vapor/lbm dry air and C(I) = 30.00 mv,

Table I-1

SAMPLE DATA OF HOT-WIRE FLOWMETER CALIBRATION

Flow-meter Signal (mv)	No Power Signal (mv)	LFM P (in. H_2O)	P_{abs} (in. Hg)	T-C (°F)	CF_p	CF_T	CFM at P	CFM with CF's
0.376	-0.002	5.45	30.60	1312 (78.3)	0.02270	0.97284	30.60	30.44466

Using Eqn. (I-3), the flow rate can be converted into the equivalent voltage.

$$E = 0.35\left[\frac{30.44466}{53}\right]^{-\frac{1}{2.723}} = 0.42903$$

From Eqn. (I-2), the corresponding property corrections can be made:

$$\text{emf} \quad K_2 = \frac{0.42903}{\left[\frac{30}{30}\right]^2 \left[\frac{538.7}{530}\right]^{0.7} [1+0.22 \times 0.0047]} = 0.42395$$

$$K_2 = \frac{0.42395}{\text{emf}} = \frac{0.42395}{0.378} = 1.122$$

<u>Experimental Results</u>

The calibration constant of each hot-wire flowmeter has been obtained from averaging the values of three different flow rates. The following table shows the final calibration constants, which are compared with those of Choe and Crawford.

Table I-2

CALIBRATION CONSTANT OF FLOWMETER

	K_2	K_3^*	K_4^*	K_5^*	K_6^*	K_7	K_8	K_9	K_{10}	K_{11}	K_{12}
A	1.220	0.920	0.988	0.928	0.906	0.907	1.010	0.918	0.901	0.920	0.929
B	1.122	0.912	0.985	0.975	0.927	0.905	1.017	0.912	0.893	0.915	0.923
% of deviation:											
	8.7	0.9	0.3	-5	-2.3	0.2	-0.7	0.7	0.9	0.5	0.7

A = Choe and Crawford results, B = the results of the present work.
* signifies relocation of delivery pipes.

From the results of the hot-wire flowmeter calibration, it has been shown that, except for K_2 and K_5, the deviations are within the experimental uncertainty of 4%, as will be shown in the uncertainty analysis section.

Uncertainty Analysis

In order to determine the experimental confidence level, an uncertainty analysis was performed following the procedure described by Kline and McClintock [28].

The uncertainty intervals of the Meriam laminar flow meter were determined as:

$$\delta P \text{ (across LFM)} = 0.02'' \, H_2O \rightarrow \delta X = 0.1 \text{ CFM}$$

$$\delta T \text{ (upstream)} = 0.25°F \rightarrow \delta CF_T = 0.0008$$

$$\delta P_{abs} \text{ (upstream)} = 0.02'' \text{ Hg} \rightarrow \delta CF_p = 0.0007$$

The flow rate, X, is given as:

$$X = X \, CF_T \, CF_p$$

$$\delta X = \left[\left(\frac{\partial X}{\partial X} \delta X CF_F CF_p \right)^2 + \left(\frac{\partial X}{\partial C_F} \delta CF_T \cdot CF_p \right)^2 + \left(\frac{\partial X}{\partial CF_p} \delta CF_p \cdot CF_T \right)^2 \right]^{1/2}$$

Table of Contents

$$\frac{\delta X}{\delta CF_T} = XCF_p \quad , \quad \frac{\partial X}{\partial CF_p} = XCF_T$$

$$\delta X = \left[(0.1\ CF_T\ CF_p)^2 + (0.0008\ X^2\ CF_p^2)^2 + (0.0007\ X^2\ CF_T^2)^2 \right]^{1/2} \tag{I-4}$$

CFM converted into E:

$$E = 0.35 \left(\frac{X}{53}\right)^{-0.36724}$$

$$\delta E = \left[0.35(-0.36724)\left(\frac{X}{53}\right)^{-1.36724} \frac{\delta X}{53} \right] = 2.425 \times 10^{-3} \cdot \left(\frac{X}{53}\right)^{-1.36724} \cdot \delta X \tag{I-5}$$

E is corrected for the property changes:

$$K_i = \frac{E}{\left(\frac{I_o}{I}\right)^2 (1 + 0.22w)\ \mathrm{emf}\left(\frac{T}{530}\right)^{0.7}}$$

$(I_o/I)^2\ (1 + 0.22w)$ will be treated as a constant, α, because data were taken such that $I_o/I = 1.0$.

$$K_i = \frac{1}{\alpha} E\ \mathrm{emf}^{-1} \left(\frac{1}{530}\right)^{-0.7}$$

$$\delta k_i = \frac{1}{\alpha} \left[\left\{ \frac{\partial K_i}{\partial E}\ \delta E\ \mathrm{emf}^{-1} \left(\frac{T}{530}\right)^{-0.7} \right\}^2 + \left\{ \mathrm{emf}^{-2}\ \delta\ \mathrm{emf}\ E\left(\frac{T}{530}\right)^{-0.7} \right\}^2 + \left\{ 1.321 \times 10^{-2}\ E\ \mathrm{emf}^{-1} \left(\frac{T}{530}\right)^{-1.7} \delta T \right\}^2 \right]^{1/2}$$

where

$$\frac{\delta K_i}{\delta E} = \frac{1}{\alpha} \frac{1}{\mathrm{emf}} \left(\frac{1}{530}\right)^{-0.7} \tag{I-6}$$

Equation (I-6) is the final equation to get the uncertainty in K_i. Let emf = 0.005.

For the typical data on K_2 which shows the largest deviation from the previous calibration by Choe and Crawford,

$$CF_p = 1.01776, \quad CF_T = 0.97888, \quad X = 30.28645 \text{ CFM} \; ,$$

$$E = 0.42561, \quad T = 76.4°F, \quad emf = 0.383, \quad w = 0.0069$$

Using Eqn. (I-6), K_2 is calculated to be:

$$\delta K_2 = 0.03$$

$$\frac{\delta K_2}{K_2} = 0.034$$

Summary and Conclusions

The calibration constants of hot-wire flowmeters determined in this experiment were shown in the experimental results section. From the results it has been shown that, except for K_2 and K_5, all the calibration constants are within the experimental uncertainty. A possible explanation for the largest deviations in K_2 and K_5 from the previous calibration by Choe and Crawford could be that the oxidation of thermocouples, resulted in a change of heat transfer mode. However, there is no explanation why K_2 and K_5 should have been oxidized more than the others.

The calibration constants for hot-wire flowmeters obtained in this experiment were used to set the blowing ratio of the compound-angle test plate.

It is believed that the calibration constants obtained here could be used successfully for the next three years without recalibration, unless the insulation of the hot-wire flowmeters is accidentally changed.

Appendix II

MANIFOLD FLOW RATE DISTRIBUTION CHECK

In order to assure the uniformity of flow rate through each hole in the manifold, the flow rate of each hole needed to be determined. If the flow rate of each hole is too scattered, the valves of the manifold must be adjusted such that the flow rate distribution is as uniform as possible.

For the flow rate measurement, the Meriam laminar flow meter was used; it has a capacity of 3 CFM (0.944 ℓ/sec). The instrumentation was the same as for the hot-wire flowmeter calibration.

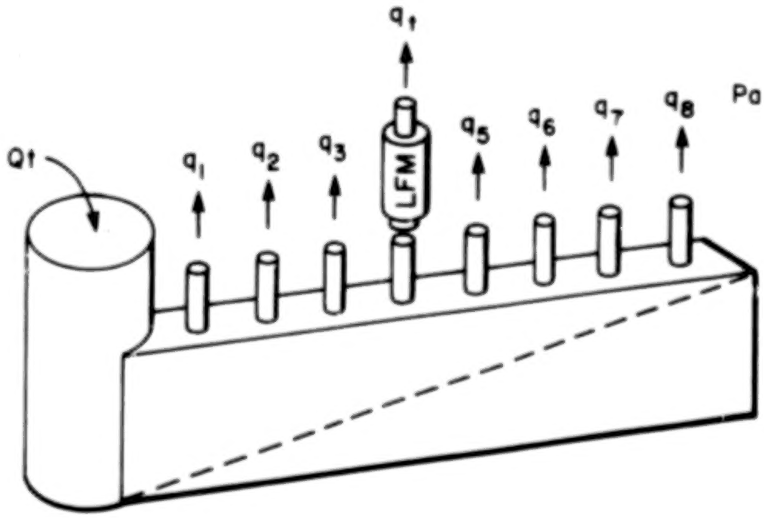

Fig. II-1. Sketch of manifold.

Before the valve adjustment of the manifold, the flow rate of each hole in all eleven manifolds was measured. Manifold #7 gave the largest flow distribution of 6%, so the valves were adjusted until the flow rate distribution was within 2%. The results of the manifold valve adjustment gave the flow rate uniformity within 2% at most.

The following table summarizes the results of the manifold valve adjustment.

Table II-1

FLOWRATE DISTRIBUTION OF THE MANIFOLD

Manifold Number	Flow Rate (CFM) Distribution	Uniformity (%)
1	0.200 - 0.204	2
2	0.220 - 0.224	2
3	0.206 - 0.208	1
4	0.228	-
5	0.200 - 0.204	2
6	0.216	-
7	0.212 - 0.216	2
8	0.220 - 0.224	2
9	0.211 - 0.212	0.5
10	0.224	-
11	0.208	-

It may be a concern that the flow rate may possibly be changed due to thermocouple installation in some of the delivery tubing to monitor the temperature of the gas. Assume that the flow rate could be decreased by 1/2%. The secondary air flow rate in each hole in one manifold is uniform within ±2 1/2% accuracy.

Appendix III

STANTON NUMBER DATA-REDUCTION PROGRAM

```
$WATFIV        LIST
C
C     STANTON NUMBER DATA REDUCTION PROGRAM
C     DISCRETE HOLE RIG   NAS-3-14336
C     THIS PROGRAM USES THE LINEAR SUPERPOSITION  PRINCIPLE TO
C     CALCULATE STANTON NUMBERS AND OTHER INTEGRAL PARAMETERS AT THETA=
C     0. AND 1.
C     REVISED JUNE 1977
C
      REAL K
      COMMON/ BLK1 /PAMB,PSTAT,TRECOV,RHUM,PDYN
      COMMON/ BLK2 /UINF,TINF,TADIAB,RHOG,VISC,PR,CP,W
      COMMON/ BLK3 /SAFR(12),CI(12),SM(12),F(12),KM,AH,THEAT
      COMMON/ BLK4 /TO(45),TG(12),T2(12),TCAST(12),TCAV(12),TH(12)
      COMMON/ BLK5 /Q(12),HM(45),VAR(12),QDOT(36)
      COMMON/ BLK6 /DXVO,DEND2,DF,DREEN(36),DST(36),DQDOT(36),DTH(12)
      DIMENSION NRN(4),KOMMNT(40), ST(36),QFLOW(12),
     1  X(36),REX(36),REEN(36),STNOB(36),STD(36),STCOL(36),STHOT(36),
     2  STS(36),STSF(36),STCR(36),STHR(36),STSR(36),SMO(12),FO(12),
     3  BHCOL(12),BHOT(12),REXD(36),RENCOL(36),RENHOT(36),THO(12),
     4  FB(12),D2HOT(36),DTHO(12),DSTO(36),ETA(36),FH(12),SF(12),SFO(12)
      DIMENSION NRNO(4),STHRB(12),KOMNTO(40)
      DATA X/50.3,52.3,54.3,56.3,58.3,60.3,62.3,64.3,66.3,68.3,
     1      70.3,72.3,73.82,74.85,75.88,76.915,77.95,78.98,80.01,81.04,
     2      82.07,83.1,84.13,85.165,86.2,87.23,88.26,89.29,90.32,91.35,
     3      92.38,93.415,94.45,95.48,96.51,97.54/
C
C *1*    READ RUN NUMBER AND CONTROL PARAMETERS
C
C        NRN     8 DIGIT RUN NUMBER
C        IOUT    PARAMETER TO TERMINATE PROGRAM
C                IOUT=0 TO READ DATA SET
C                IOUT NE 0 TO TERMINATE PROGRAM
C        KT      DATA TYPE FOR LINEAR SUPERPOSITION
C                KT=0  FLAT PLATE OR M(TH=0)
C                KT=1 M(TH=1)
C        KM      PITCH/DIAMETER RATIO OF HOLE ARRAY
C                KM=0 P/D FIVE
C                KM=1 P/D TEN
C        L       TYPE OF FLAT PLATE STANTON NUMBER FOR ST NO RATIO
C                REQUIRED TO SPECIFY L FOR TH=1 RUN ONLY
C                L=0 STANTON NUMBER BASED ON ST-REX HEATED STARTING
C                   LENGTH CORRELATION
C                L=1 STANTON NUMBER BASED ON ST-REX UNHEATED STARTING
C                   LENGTH CORRELATION
C                L=2 FLAT PLATE STANTON NUMBER TEST DATA
C
C        NOTE: DATA SETS MUST BE STACKED FLAT PLATE,M(TH=0),M(TH=1),
C              M(TH=0),M(TH=1),...
C
      WRITE (6,900)
C * * * * * * * * * * * * * * * * *
C      IPRINT=0 TO PRINT SUMMARY DATA SET ONLY
C      IPRINT=1 TO PRINT ENTIRE DATA REDUCTION
C
       IPRINT=1
C * * * * * * * * * * * * * * * * *
    5 READ (5,10)    (NRN(I),I=1,4),IOUT,KT,KM,L
   10 FORMAT(4A2,I2,I2,I2,I2)
      IF (IOUT.NE.0) GO TO 2000
```

```
C
C *2*    READ DATA RUN DESCRIPTION, A FORMAT  COL 1-80
C
      READ (5,2) (KOMMNT(I), I=1,40)
    2 FORMAT (40A2)
C
C *3*    READ TEST CONDITIONS
C
C        TAMB    AMBIENT TEMPERATURE (DEG F)
C        PAMB    AMBIENT PRESSURE (INCHES HG CORRECTED TO 32 DEG F)
C        RHUM    RELATIVE HUMIDITY (PERCENT)
C        THEAT   SECONDARY AIR TEMP, HEATER BOX (I-C TC, MV)
C        CI(1)   SECONDARY AIR FLOWMETER CURRENT SIGNAL (MV)
C
      READ (5,20) TAMB,PAMB,RHUM,THEAT,CI(1)
   20 FORMAT (7F10.0)
      DO 22 I=2,12
   22 CI(I)=CI(1)
C
C *4*    READ TUNNEL CONDITIONS
C
C        TRECOV  TUNNEL AIR RECOVERY TEMPERATURE (I-C TC, MV)
C        PDYN    TUNNEL AIR VELOCITY DYNAMIC PRESSURE (INCHES H2O)
C        PSTAT   TUNNEL GAGE STATIC PRESSURE (INCHES H2O)
C        XVO     VIRTUAL ORIGIN, TBL, FROM PGM PROFILE (INCHES)
C        END2    ENTHALPY THICKNESS, FROM PGM PROFILE (INCHES)
C        DXVO    UNCERTAINTY IN XVO, FROM PGM PROFILE (INCHES)
C        DEND2   UNCERTAINTY IN END2, FROM PGM PROFILE (INCHES)
C
      READ (5,20) TRECOV,PDYN,PSTAT,XVO,END2,DXVO,DEND2
C
C *5*    READ TEST SECTION CONDITIONS
C
C        TG(I)   SECONDARY AIR TEMPERATURE (I-C TC,MV)
C        TO(I)   PLATE TEMPERATURE (I-C TC, MV)
C        Q(I)    PLATE POWER (WATTS)
C        VAR(I)  VARIAC SETTING
C        SAFR(I) SECONDARY AIR FLOWMETER SIGNAL (MV)
C
      READ (5,25) (TG(I),TO(I),Q(I),VAR(I),SAFR(I), I=1,12)
   25 FORMAT (5F10.0)
C * * * * * * * * * * * * * * * * * * * *
C     IF (SAFR(2).NE.0.) L=2
C * * * * * * * * * * * * * * * * * * * * * *
C
C *6*    READ RECOVERY SECTION CONDITIONS
C
C        TO(I)   PLATE TEMPERATURE (I-C TC, MV)
C        HM(I)   HEAT FLUX METER SIGNAL (MV)
C
      READ (5,26) (TO(I),HM(I),I=13,45)
   26 FORMAT(2F10.0)
C
C *7*    READ TEMPERATURE
C
C        TCAST(I) TEST SECTION SIDERAIL TEMPEMPERATURES (I-C TC,MV)
C
      READ (5,27) (TCAST(I), I=1,8)
   27 FORMAT ( F10.0)
C
```

```
C         WRITE OUT ALL RAW DATA
C
          IF(IPRINT.NE.0) WRITE (6,900)
          WRITE (6,40) (NRN(I), I=1,4)
      40 FORMAT (10X,'RUN ',4A2,' *** DISCRETE HOLE RIG *** NAS-3-14336'
        1 ,10X,'STANTON NUMBER DATA'/)
          WRITE (6,610) (KOMMNT(I), I=1,40)
     610 FORMAT (10X,40A2/)
          IF (IPRINT.EQ.0) GO TO 7772
          WRITE (6,45)
      45 FORMAT (10X,'UNITS: PAMB(DEG F),PAMB(IN HG), RHUM(PCT)'/17X,
        1 'PSTAT(IN H2O), TRECOV(MV), PDYN(IN H2O), XVO(IN), TPLATE(MV)'/17
        2X,'TGAS(MV), QDOT(WATTS), SAFR(MV),HM(MV), CI(MV), THEAT(MV)'/)
          WRITE (6,50) TAMB,PAMB,RHUM,THEAT
      50 FORMAT(10X,'TAMB=', F6.1,5X,'PAMB=',F6.2, 5X,'RELHUM=',F5.1,6X,
        1  'THEATER=',F6.3/)
          WRITE (6,60) PSTAT,TRECOV,PDYN,XVO,END2,DXVO,DEND2
      60 FORMAT (10X,'PSTAT=',F6.2,5X,'TRECOV=',F6.3,5X,'PDYN=',F6.3,5X,
        1 'XVO=',F6.2,5X,'END2=',F6.4,5X,'DXVO=',F6.4,5X,'DEND2=',F6.4//)
          WRITE (6,70)
      70 FORMAT (10X,'PLATE',6X, 'TPLATE',6X,'TGAS',6X,'QDOT',4X,'VARIAC',
        1 5X,'SAFLOW',5X,'CURRENT',6X,'TCAST'/)
          NP1=1
          WRITE (6,75) NP1,TO(1),Q(1),VAR(1),TCAST(1)
      75 FORMAT (10X,I3,7X,F7.3,13X,F7.2,3X,F7.1, 27X,F7.3)
          WRITE (6,80) (I,TO(I),TG(I),Q(I),VAR(I),SAFR(I),CI(I),TCAST(I),
        1                I=2,12)
      80 FORMAT (10X,I3,7X,F7.3,3X,F7.3,3X,F7.2,3X,F7.1,3X,F8.3,3X,F8.3,
        1 5X,F7.3)
          WRITE(6,71)
      71 FORMAT(/,10X,'PLATE',6X,'TPLATE',6X,'HM')
          WRITE(6,72)(I,TO(I),HM(I),I=13,45)
      72 FORMAT(10X,I3,7X,F7.3,3X,F7.3)
    7772 CONTINUE
C
C         DATA CONVERSION BLOCK
C
C         CONVERT ALL TEMPERATURES FROM MV TO DEG F
          TRECOV=TC(TRECOV)
          THEAT=TC(THEAT)
          DO 90 I=1,12
          TO(I)=TC(TO(I))
          TG(I)=TC(TG(I))
      90 CONTINUE
          DO 93 I=1,8
    93    TCAST(I)=TC( TCAST(I) )
          DO 91 I=13,45
      91 TO(I)=TC(TO(I))
C         PLATE AREAS
C         HOLE AREA
          A=18.*1.968750/144.
          AH=(3.141593*0.406*0.406*0.25)/144.
C         COMPUTE WIND TUNNEL FLOW CONDITIONS
          CALL TUNNEL
C         COMPUTE SECONDARY AIR FLOW RATE
          CALL FLOW (KERROR)
          IF (KERROR.GT.0) RETURN
C         COMPUTE SECONDARY AIR FLOW TEMPERATURES AND QFLOW LOSS
          CALL T2EFF (QFLOW)
C         COMPUTE NET ENERGY TRANSFER FROM TEST SECTION AND RECOVERY
```

```
C          REGION
      CALL POWER (TINF,QFLOW,A)
C
C          WRITE ALL CONVERTED DATA
      IF (IPRINT.EQ.0) GO TO 1108
C
      WRITE (6,610) (KOMMNT(I), I=1,40)
      WRITE (6,100)
  100 FORMAT (//,10X,'UNITS: TPLATE(DEGF), TGAS(DEG F), QDOT(WATTS),',
     1 /17X,'SAFLOW(CFM),QFLUX(BTU/HR/SQFT),TEFF2(DEG F)'/)
      WRITE (6,102)
  102 FORMAT (10X,'PLATE',6X, 'TPLATE',5X,'TEFF2',5X,'QDOT',
     1 6X,'QFLUX',6X,'SAFLOW',6X,'TCAST',6X,'TGAS',6X,
     2       'TCAV'/)
      WRITE (6,105) NP1,TO(1),Q(1),QDOT(1),TCAST(1),TCAV(1)
  105 FORMAT(10X,I3,7X,F7.1,13X,F7.2, 5X,F7.2,14X,F7.1,9X,F10.1)
      WRITE (6,110) (I,TO(I),T2(I),Q(I),QDOT(I),SAFR(I),
     1 TCAST(I),TG(I),TCAV(I), I=2,12)
  110 FORMAT(10X,I3,7X,F7.1,3X,F7.1,3X, F7.2,5X,F7.2,1X,F8.2,
     1  5X,F7.1,2F10.1)
      WRITE (6,106)
  106 FORMAT(/,10X,'PLATE',6X,'TPLATE',6X,'HM',5X,'QFLUX'/)
      WRITE(6,107) (I,TO(I),HM(I),QDOT(I),I=13,36)
  107 FORMAT (10X,I3,7X,F7.3,3X,F7.3,3X,F7.2)
      I=108
      WRITE (6,108) I,TO(45)
  108 FORMAT (10X,I3,7X,F7.3)
C
C          COMPUTE STANTON NUMBER
C
 1108 CONTINUE
      XVI=X(1)-XVO-1.0
      IPD=5
      IF (KM.EQ.1) IPD=10
C     X REYNOLDS NUMBER BASED ON VIRTUAL ORIGIN TBL
  201 FACT=UINF/(VISC*12.)
      DREX=FACT*DXVO
      DO 210 I=1,36
  210 REX(I)=FACT*(X(I)-XVO)
C     COMPUTE STANTON NUMBERS
      DENOM=RHOG*UINF*CP*3600.
      DO 220 I=1,35
      ST(I)=QDOT(I)/(DENOM*(TO(I)-TADIAB))
C    DST(I):  UNCERTAINTY IN ST(I)
C     DP : UNCERTAINTY IN  MANOMETER PRESSURE  , IN H2O
      DP=0.008
C    DT: UNCERTAINTY IN TEMPERATURE, F
      DT=0.25
      DST(I)=ST(I)*SQRT(DQDOT(I)*DQDOT(I)/(QDOT(I)*QDOT(I))+DP*DP/(4.*
     1PDYN*PDYN)+DT*DT/((TO(I)-TINF)*(TO(I)-TINF)))
  220 CONTINUE
C        COMPUTE DEL2 AND REDEL2 BASED ON ACTUAL ST-DATA
      CALL ENTHAL (FACT,ST,REEN,END2)
C
      IF (IPRINT.EQ.0) GO TO 3310
       WRITE (6,900)
      WRITE (6,40) (NRN(I), I=1,4)
      TADBC=5.*(TADIAB-32.)/9.
       TINFC=5.*(TINF-32.)/9.
      UINFMS=UINF*0.3048
```

```
      XVOCM=XVO*2.54
      RHOKM3=RHOG*16.02
      VISCI=VISC*0.0929
      CPJKGK=CP*4184.
      WRITE (6,300) TADBC,UINFMS,TINFC,RHOKM3,VISCI,XVOCM,CPJKGK,PR
  300 FORMAT(10X,'TADB=',F6.2,' DEG C     UINF=',F12.2,' M/S       TINF=',
     1 F6.2,' DEG C'/10X,'RHO=',F7.3,' KG/M3     VISC=',E12.5,' M2/S
     2XVO=',F7.1,' CM'/10X,'CP=',F8.0,' J/KGK     PR=',F14.3/)
      WRITE(6,600) (KOMMNT(I),I=1,40)
 600  FORMAT(10X,40A2/)
 3310 CONTINUE
C     IF 2ND PLATE HAS NO SECONDARY INJECTION , THIS PROGRAM ASSUMES THAT
C     IT IS A NO-BLOWING CASE.
      IF (SM(2).EQ.0.) GO TO 400
      IF (IPRINT.EQ.0) GO TO 345
      WRITE (6,310)
  310 FORMAT(10X,'PLATE',3X,'X',5X,'REX',9X,'TO',6X,'REENTH',7X,
     1'STANTON NO', 6X,'DST',6X,'DREEN',4X,'M',4X,'F',6X,'T2',2X,
     2'THETA',3X,'DTH')
      XCM=X(1)*2.54
      TEMPC=5.*(TO(1)-32.)/9.
      WRITE (6,320) NP1,XCM,REX(1),TEMPC,REEN(1),ST(1),DST(1),DREEN(1)
  320 FORMAT(10X,I3,2X,F5.1,1X,E12.5,1X,F6.2,2(2X,E12.5),2X,E9.3,2X,
     1F5.0)
      DO 340 I=2,12
      XCM=X(I)*2.54
      TEMPC=5.*(TO(I)-32.)/9.
      TEMP2=5.*(T2(I)-32.)/9.
      WRITE (6,330)  I,XCM,REX(I),TEMPC,REEN(I),ST(I),DST(I),DREEN(I),
     1SM(I),F(I),TEMP2,TH(I),DTH(I)
  330 FORMAT(10X,I3,2X,F5.1,1X,E12.5,1X,F6.2,2(2X,E12.5),2X,E9.3,2X,F5.0
     1,2X,F5.2,F7.4,F6.2,F6.3,2X,F5.3)
  340 CONTINUE
      DO 341 I=13,36
      XCM=X(I)*2.54
      TEMPC=5.*(TO(I)-32.)/9.
      WRITE (6,331) I,XCM,REX(I),TEMPC,REEN(I),ST(I),DST(I),DREEN(I)
  331 FORMAT(10X,I3,2X,F5.1,1X,E12.5,1X,F6.2,2(2X,E12.5),2X,E9.3,2X,
     1F5.0)
  341 CONTINUE
      WRITE (6,334) DREX,DF
  334 FORMAT (/12X,'UNCERTAINTY IN REX=',F6.0,9X,'UNCERTAINTY IN F=',
     1F7.5,' IN RATIO')
      GO TO 345
C
C     STORE FLATPLATE EXPERIMENTAL DATA FOR STANTON NUMBER RATIO
C
  400 DO 401 I=1,36
      STNOB(I)=ST(I)
  401 CONTINUE
      WRITE (6,410)
  410 FORMAT(10X,'PLATE',3X,'X',5X,'REX',9X,'TO',6X,'REENTH',7X,'STANTON
     1NO',6X,'DST',6X,'DREEN',5X,'ST(THEO)',6X,'RATIO')
      DO 420 I=1,36
      STT=.0295*PR**(-.4)*(REX(I))**(-.2)
      IF (L.EQ.1)STT=STT*(1.-(XVI/(X(I)-XVO))**.9)**(-1./9.)
      RATIO=ST(I)/STT
      XCM=X(I)*2.54
      TEMPC=5.*(TO(I)-32.)/9.
      WRITE (6,430)  I,XCM,REX(I),TEMPC,REEN(I),ST(I),DST(I),DREEN(I),
```

```
     1  STT.RATIO
  430 FORMAT(10X,I3,2X,F5.1,1X,E12.5,1X,F6.2,2(2X,E12.5),2X,E9.3,2X,
     1F5.0,E15.5,F9.3)
  420 CONTINUE
      IF (IPRINT.EQ.0) WRITE (6,900)
      GO TO 5
C
C
C     STORE VALUES FOR TH=0
  345 IF (KT.EQ.1) GO TO 360
C
  350 DO 351 I=1,12
      SMO(I)=SM(I)
      FO(I)=F(I)
      THO(I)=TH(I)
      DTHO(I)=DTH(I)
      STO(I)=ST(I)
      DSTO(I)=DST(I)
      REXO(I)=REX(I)
  351 CONTINUE
      DO 352 I=13,36
      STO(I)=ST(I)
      DSTO(I)=DST(I)
      REXO(I)=REX(I)
  352 CONTINUE
      FACTO=FACT
      DFO=DF
      DO 353 I=1,4
  353 NRNO(I)=NRN(I)
       DO 354 I=1,40
  354 KOMNTO(I)=KOMMNT(I)
      GO TO 5
C
C        COMPUTE STANTON NUMBER AT TH=0 AND TH=1 BY LINEAR SUPERPOSITION
C
  360 FAVO=0.
      FAV=0.
      THAVO=0.
      THAV=0.
      DO 361 I=2,12
      THAVO=THAVO+THO(I)
      THAV=THAV+TH(I)
      FAVO=FAVO+FO(I)
      FAV=FAV+F(I)
  361 CONTINUE
      THAVO=(THO(11)+THO(12))/2.
      THAV=(TH(11)+TH(12))/2.
      FAVO=FAVO/11.
      FAV=FAV/11.
      FBAV=.5*(FAVO+FAV)
      STNOB(1)=STO(1)
      STCR(1)=STO(1)/STNOB(1)
      STNOB(1)=ST(1)
      STHR(1)=ST(1)/STHOB(1)
      STHRB(1)=STHR(1)
      TH(1)=TH(2)
      THO(1)=THO(2)
      DO 362 I=2,12
      DENOM=(TH(I-1)+TH(I))/2.-(THO(I-1)+THO(I))/2.
      STS(I)=(STO(I)-ST(I))/DENOM
```

```
      DNUM=(THO(I-1)+THO(I))/2.
      STCOL(I)=STO(I)+DNUM*STS(I)
      DNUM=(TH(I-1)+TH(I))/2.-1.
      STHOT(I)=ST(I)+DNUM*STS(I)
      FB(I)=0.5*(FO(I)+F(I))
      ETA(I)=STS(I)/STCOL(I)
C     COMPUTE STANTON NUMBER RATIO FOR TH=1 (IF L=2 USE FLAT PLATE
C     EXPERIMENTAL DATA)
      IF (L.EQ.2) GO TO 374
      STNOB(I)=.0295*PR**(-.4)*(REX(I))**(-.2)
      IF (L.EQ.1)STNOB(I)=STNOB(I)*(1.-(XVI/(X(I)-XVO))**(0.9))**
     1(-1./9.)
  374 STHR(I)=STHOT(I)/STNOB(I)
C     COMPUTE STANTON NUMBER RATIO FOR TH=0 (IF L=0 USE FLAT PLATE
C     EXPERIMENTAL DATA)
      IF (L.EQ.2) GO TO 375
      STNOB(I)=STNOB(I)*(REX(I)/REXO(I))**(0.2)
      IF (L.EQ.1)STNOB(I)=STNOB(I)*(1.-(XVI*FACTO/REXO(I))**(0.9))**
     1(-1./9.)
  375 STCR(I)=STCOL(I)/STNOB(I)
      STSR(I)=STHOT(I)/STCOL(I)
      BHCOL(I)=FO(I)/STCOL(I)
      BHOT(I)=F(I)/STHOT(I)
      STSF(I)=ALOG(1.+BHOT(I))/BHOT(I)
C     CORRECT STANTON NUMBER RATIO FOR TH=1 TO COMPARABLE TRANSPIRATION
C     CASE USING ALOG(1.+B)/B EXPRESSION
      STHRB(I)=STHR(I)/STSF(I)
      STSR(I)=STSR(I)/STSF(I)
      SF(I)=F(I)*STHOT(I)
      SFO(I)=FO(I)*STCOL(I)
  362 CONTINUE
      DO 363 I=13,16
      STS(I)=(STO(I)-ST(I))/(THAV-THAVO)
      STCOL(I)=STO(I)+THAVO*STS(I)
      STHOT(I)=ST(I)+(THAV-1.0)*STS(I)
      ETA(I)=STS(I)/STCOL(I)
C     COMPUTE STANTON NUMBER RATIO FOR RECOVERY REGION, TH=1
      IF (L.EQ.2) GO TO 372
      STNOB(I)=.0295*PR**(-.4)*(REX(I))**(-.2)
      IF (L.EQ.1)STNOB(I)=STNOB(I)*(1.-(XVI/(X(I)-XVO))**(0.9))**
     1(-1./9.)
  372 STHR(I)=STHOT(I)/STNOB(I)
C     COMPUTE STANTON NUMBER RATIO FOR RECOVERY REGION, TH=0
      IF (L.EQ.2) GO TO 373
      STNOB(I)=STNOB(I)*(REX(I)/REXO(I))**(0.2)
      IF (L.EQ.1)STNOB(I)=STNOB(I)*(1.-(XVI*FACTO/REXO(I))**(0.9))**
     1(-1./9.)
  373 STCR(I)=STCOL(I)/STNOB(I)
      STSR(I)=STHOT(I)/STCOL(I)
  363 CONTINUE
C         COMPUTE DEL2 AND REDEL2 BASED ON ST-DATA AT TH=0 AND TH=1
      STCOL(1)=STO(1)
      STHOT(1)=ST(1)
      STS(1)=STO(1)-ST(1)
      DO 370 I=1,12
      FH(I)=F(I)
  370 TH(I)=1.0
      CALL ENTHAL (FACT,STHOT,RENHOT,END2)
      DO 450 I=1,12
      F(I)=FO(I)
```

```
      TH(I)=0.
  450 DTH(I)=DTHO(I)
      DF=DFO
      DO 460 I=1,36
  460 DST(I)=DSTO(I)
      CALL ENTHAL (FACTO,STCOL,RENCOL,END2)
C
      IF (IPRINT.NE.1) GO TO 462
      WRITE (6,900)
      WRITE (6,40) (NRNO(I), I=1,4)
      WRITE (6,610) (KOMNTO(I), I=1,40)
      WRITE (6,40) (NRN(I), I=1,4)
      WRITE (6,610) (KOMMNT(I), I=1,40)
  462 WRITE (6,371) (NRNO(I), I=1,4),(NRN(I), I=1,4)
  371 FORMAT (10X,'LINEAR SUPERPOSITION IS APPLIED TO STANTON NUMBER',
     1' DATA FROM'/10X,'RUN NUMBERS ',4A2,' AND ',4A2,' TO OBTAIN'
     2,' STANTON NUMBER DATA AT TH=0 AND TH=1'/)
      WRITE(6,364)
  364 FORMAT   (/,7X,'PLATE',3X,'REXCOL',4X,'RE DEL2',3X,'ST(TH=0)',4X,
     1'REXHOT',4X,'RE DEL2',3X,'ST(TH=1)',4X,'ETA',4X,'STCR',4X,'F-COL',
     25X,'STHR',4X,'F-HOT',4X,'LOGB'/)
      WRITE(6,365)  (I,REXO(I),RENCOL(I),STCOL(I),REX(I),RENHOT(I),
     1STHOT(I),ETA(I),STCR(I),FO(I),STHR(I),FH(I),STHRB(I),I=1,12)
  365 FORMAT((10X,I2,2(2X,F9.1),1X,F9.6,2(2X,F9.1),1X,F9.6,2(2X,F5.3),
     12X,F7.4,2X,F7.3,2X,F7.4,F8.3))
      WRITE(6,366)  (I,REXO(I),RENCOL(I),STCOL(I),REX(I),RENHOT(I),
     1STHOT(I),ETA(I),STCR(I),STHR(I),I=13,36)
  366 FORMAT((10X,I2,2(2X,F9.1),1X,F9.6,2(2X,F9.1),1X,F9.6,2(2X,F5.3),
     111X,F7.3))
      IF (L.EQ.0) WRITE (6,505)
  505 FORMAT (//,10X,'STANTON NUMBER RATIO BASED ON ST*PR**0.4=0.0295*RE
     1X**(-.2)')
      IF (L.EQ.1) WRITE (6,510)
  510 FORMAT (//,10X,'STANTON NUMBER RATIO BASED ON ST*PR**0.4=0.0295*RE
     1X**(-.2)*(1.-(XI/(X-XVO))**0.9)**(-1./9.)')
      IF (L.EQ.2) WRITE (6,515)
  515 FORMAT (//,10X,'STANTON NUMBER RATIO BASED ON EXPERIMENTAL FLAT PL
     1ATE VALUE AT SAME X LOCATION')
      WRITE (6,520)
  520 FORMAT (//,10X,'STANTON NUMBER RATIO FOR TH=1 IS CONVERTED TO COMP
     1ARABLE TRANSPIRATION VALUE '/10X,'USING ALOG(1 + B)/B EXPRESSION I
     2N THE BLOWN SECTION')
      IF (IPRINT.EQ.0) WRITE (6,900)
      GO TO 5
 2000 WRITE (6,900)
  900 FORMAT (1H1)
      RETURN
      END

      FUNCTION TC(T)
C     FUNCTION CONVERTS TEMP FROM IRON-CONSTANTAN MV TO DEG F
      TM=-2220.703+781.25*SQRT(7.950782+0.256*T)
      TC=TM+49.97-1.26E-03*TM-.32E-04*TM*TM
      RETURN
      END

      SUBROUTINE TUNNEL
C
C          THIS ROUTINE COMPUTES THE WIND TUNNEL FLOW CONDITIONS
C
```

```
C          UINF        FREE STREAM VELOCITY (FT/SEC)
C          TINF        FREE STREAM STATIC TEMPERATURE (DEG F)
C          RHOG        FREE STREAM DENSITY (LBM/FT3)
C          VISC        FREE STREAM KINEMATIC VISCOSITY (FT2/SEC)
C          CP          FREE STREAM SPECIFIC HEAT (BTU/LBM/DEG R)
C          PR          FREE STREAM PRANDTL NUMBER
C          W           FREE STREAM ABSOLUTE HUMIDITY (LBM H2O/LBM DRY AIR)
C
      COMMON/ BLK1 /PAMB,PSTAT,TRECOV,RHUM,PDYN
      COMMON/ BLK2 /UINF,TINF,TADIAB,RHOG,VISC,PR,CP,W
C
C     SATURATION DATA FROM K AND K 1969 STEAM TABLES
      DIMENSION TEMP(10),PSAT(10),RHOSAT(10)
      DATA TEMP/      40.,      50.0,      60.0,      70.0,      80.0,
     1     90.0,      100.0,     110.0,     120.0,     130.0/
      DATA PSAT/      17.519,    25.636,    36.907,    52.301,    73.051,
     1     100.627,   136.843,   183.787,   244.008,   320.400/
      DATA RHOSAT/    .0004090,  .0005868,  .0008286,  .0011525,  .0015803,
     1     .0021381,  .0028571,  .0037722,  .0049261,  .0063625/
      REAL NU,MFA,MFV,MWA,MWV,JF
      TAMB=TRECOV
      DO 10 N=1,9
      IF(TEMP(N).GT.TAMB) GO TO 20
   10 CONTINUE
   20 T = TEMP(N)
      EPS = T - TAMB
      VAPH = PSAT(N)
      VAPL = PSAT(N-1)
      VEPS = VAPH - VAPL
      RHOH = RHOSAT(N)
      RHOL = RHOSAT(N-1)
      REPS = RHOH - RHOL
      RHOG = RHOL + (10.0 - EPS)*REPS/10.
      RA=1545.32/28.970
      PG = VAPL + (10.0 - EPS)*VEPS/10.0
      PUNITS=2116.21/33.932/12.
      P=PAMB*2116.21/29.9213 + PSTAT*PUNITS
      RHUM=RHUM/100.
      PVAP = RHUM*PG
      PA = P - PVAP
      RHOA = PA/(RA*(TAMB + 459.67))
      RHOV = RHUM*RHOG
      W=RHOV/RHOA
      RHOM = RHOA + RHOV
      MWA = 28.970
      MWV = 18.016
      MFV = RHOV/RHOM
      MFA = 1.0 - MFV
      RM = 1545.32*(MFA/MWA + MFV/MWV)
      CP = MFA*0.240 + MFV*0.445
      GC=32.1739
      JF=778.26
      RCF=0.7**0.33333
C      RECOVERY FACTOR FOR WIRE NORMAL TO FLOW
      RTC=0.68
      RHOG=(P/RM+PDYN*PUNITS*RCF/(CP*JF))/(TRECOV+459.67)
      UINF=SQRT(2.*GC*PDYN*PUNITS/RHOG)
      TINF=TRECOV-RTC*UINF*UINF/(2.*GC*JF*CP)
      VISC=(11.+0.0175*TINF)/(1.E06*RHOG)*(1.-.7*W)
      PR=.710*(530./(TINF+459.67))**(.1)*(1.+.9*W)
```

```
C      NOTE FOR HIGH VELOCITY THIS ROUTINE SHOULD BE ITERATED
C       CONVERT TO ADIABATIC WALL TEMPERATURE
        RCF=PR**0.33333
        TADIAB=TINF+RCF*UINF*UINF/(2.*GC*JF*CP)
       RETURN
       END

       SUBROUTINE FLOW (KERROR)
C
C         THIS ROUTINE COMPUTES SECONDARY AIR FLOW RATES
C
C         SAFR(I) SECONDARY AIR FLOW RATE CORRECTED FOR TEMPERATURE
C                 AND HUMIDIY (CFM)
C
       COMMON/ BLK1 /PAMB,PSTAT,TRECOV,RHUM,PDYN
       COMMON/ BLK2 /UINF,TINF,TADIAB,RHOG,VISC,PR,CP,W
       COMMON/ BLK3 /SAFR(12),CI(12),SM(12),F(12),KM,AH,THEAT
       COMMON/ BLK4 /TD(45),TG(12),T2(12),TCAST(8),TCAV(12),TH(12)
       DIMENSION X(5),Y(5),B(4),FMC(12),TM(12)
       DATA FMC/  1.0,  1.122, .906, .989, .924, .905, .905, 1.017,
      1            .912, .893, .915, .923/
C      CALIBRATION CURVE DATA
       DATA X,Y /0.35, 0.90, 1.12, 1.35, 1.5,
      1          53.0, 4.05, 2.00, 1.00, 0.69/
       KERROR=0
       DO 10 I=1,4
    10 B(I)=ALOG(Y(I)/Y(I+1))/ALOG(X(I)/X(I+1))
       FACT=1.0+0.22*W
       DO 20 I=2,12
       IF (SAFR(I).EQ.0.) GO TO 20
C      TM IS ESTIMATE OF SECONDARY AIR TEMPERATURE AT FLOWMETER STATION
       TM(I)=.5*(TG(I)+THEAT)
       SAFR(I)=SAFR(I)*(((TM(I)+459.67)/530.)**0.7)*FACT*(30.00/CI(I))**2
      1        *FMC(I)
    20 CONTINUE
       FACT=1.0+0.7*W
       DO 40 I=2,12
       IF (SAFR(I).EQ.0.) GO TO 40
       IF (SAFR(I).LT.X(1).OR.SAFR(I).GT.X(5)) GO TO 100
       DO 30 K=1,5
       IF (X(K).GT.SAFR(I)) GO TO 35
    30 CONTINUE
    35 Z=Y(K-1)*(SAFR(I)/X(K-1))**B(K-1)
       SAFR(I)=Z/((530./(TM(I)+459.67))**0.76)/FACT
    40 CONTINUE
C      NOTE UNCERTAINTY CALCULATION FOR FLOWRATE COMPUTED IN
C      SUBROUTINE T2EFF
       RETURN
   100 WRITE (6,200) SAFR(I)
   200 FORMAT (10X,'FLOWMETER READING OUT OF RANGE, EMF=',E12.5,//10X,
      1 'DATA SET REDUCTION TERMINATED')
       KERROR=2
       RETURN
       END


       SUBROUTINE T2EFF (QFLOW)
C
C         THIS ROUTINE COMPUTES
C
```

```
C          KFL(I)     EXPERIMENTAL CONDUCTANCE FOR COMPUTING QFLOW
C          KCONV(I)   EXPERIMENTAL CONDUCTANCE FOR COMPUTING T2EFF
C          T2(I)      EFFECTIVE SECONDARY AIR TEMPERATURE
C          QFLOW(I)   ENERGY LOSS FROM PLATE TO SECONDARY AIR
C          TH(I)      THETA=(T2-TINF)/(TO-TINF)
C          SM(I)      VELOCITY*DENSITY RATIO, SECONDARY AIR TO MAINSTREAM
C          F(I)       MASS FLUX RATIO, SECONDARY AIR TO MAINSTREAM, WHERE
C                     F=M*AH/(P*P)
C
      COMMON/ BLK1 /PAMB,PSTAT,TRECOV,RHUM,PDYN
      COMMON/ BLK2 /UINF,TINF,TADIAB,RHOG,VISC,PR,CP,W
      COMMON/ BLK3 /SAFR(12),CI(12),SM(12),F(12),KM,AH,THEAT
      COMMON/ BLK4 /TO(45),TG(12),T2(12),TCAST(12),TCAV(12),TH(12)
      COMMON/ BLK6 /DXVO,DEND2,DF,DREEN(36),DST(36),DQDOT(36),DTH(12)
      REAL KCONV(12),KFL(12),KL,KR
      DIMENSION QFLOW(12)
      KL=.5
      KR=.5
      CALL CAVITY (KL,KR)
      FACT=.074843*.24*60.
      QFLOW(1)=0.0
      HOLE9=9.
      HOLE8=8.
      DO 16 I=2,12,2
      KCONV(I)=0.
      KFL(I)=0.
      IF (SAFR(I).EQ.0.) GO TO 16
      IF (KM.NE.1) GO TO 8
      HOLE9=5.
      IF (I.EQ.4.OR.I.EQ.8.OR.I.EQ.12) HOLE9=4.
    8 SAFR(I)=SAFR(I)*9./HOLE9
      KFL(I)=0.0177*SAFR(I)**0.5480*HOLE9
      KCONV(I)=0.0179*SAFR(I)**0.5662*HOLE9/FACT
   16 CONTINUE
C     KFL COMPUTED FOR 8 HOLE ROW USING FACTOR HOLE9 INSTEAD OF HOLE8
      DO 26 I=3,12,2
      KCONV(I)=0.
      KFL(I)=0.
      IF (SAFR(I).EQ.0.) GO TO 26
      SAFR(I)=SAFR(I)*9./HOLE8
      KFL(I)=0.0177*SAFR(I)**0.5480*HOLE9
      KCONV(I)=0.0179*SAFR(I)**0.5662*HOLE9/FACT
   26 CONTINUE
CC     EFFECTIVE  'T2',AND 'QFLOW'.
      DO 30 I=2,12,2
      IF (SAFR(I).EQ.0.) GO TO 31
      IF (KM.NE.1) GO TO 33
      HOLE9=5.
      IF (I.EQ.4.OR.I.EQ.8.OR.I.EQ.12) HOLE9=4.
   33 SAFR(I)=SAFR(I)*HOLE9/9.
      TBAR=(TO(I)+TCAV(I-1))*0.5
      IF (I.EQ.2) TBAR=TO(I)
      IF (I.EQ.2) KCONV(I)=KFL(I)/FACT
      T2(I)=TG(I)+(TBAR-TG(I))*(1.-EXP(-KCONV(I)/SAFR(I)))
      QFLOW(I)=KFL(I)*(TO(I)-T2(I))
      GO TO 30
   31 T2(I)=TO(I)
      QFLOW(I)=0.
   30 CONTINUE
      DO 40 I=3,12,2
```

```
      IF (SAFR(I).EQ.0.) GO TO 41
      SAFR(I)=SAFR(I)*HOLE8/9.
      TBAR=(TO(I)+TCAV(I-1))*0.5
      IF (I.EQ.3) TBAR=TO(I)
      T2(I)=TG(I)+(TBAR-TG(I))*(1.-EXP(-KCONV(I)/SAFR(I)))
      QFLOW(I)=KFL(I)*(TO(I)-T2(I))
      GO TO 40
   41 T2(I)=TO(I)
      QFLOW(I)=0.
   40 CONTINUE
C
C     COMPUTE THETA=(T2-TINF)/(TO-TINF)
      TH(1)=0.
      DTH(1)=0.
C    DT: UNCERTAINTY IN TEMPERATURE, F
      DT=0.25
C     DT2, UNCERTAINTY IN T2, DEG F
      DT2=0.5
      DO 200 I=2,12
      TH(I)=(T2(I)-TINF)/(TO(I)-TINF)
C   DTH(I): UNCERTAINTY IN TH(I)
  200 DTH(I)=SQRT(DT2**2+(TH(I)*DT)**2+((1.-TH(I))*DT)**2)/(TO(I)-TINF)
C
      FACT=AH/(2.*2./144.)
      IF (KM.EQ.1) FACT=AH/(4.*4./144.)
      DO 50 I=2,12,2
      IF (KM.NE.1) GO TO 48
      HOLE9=5.
      IF (I.EQ.4.OR.I.EQ.8.OR.I.EQ.12) HOLE9=4.
   48 F9=AH*60.*UINF*HOLE9*RHOG
      RHOS=RHOG*(TINF+459.67)/(T2(I)+459.67)
      SM(I)=SAFR(I)*RHOS/F9
      F(I)=SM(I)*FACT
   50 CONTINUE
      F8=AH*60.*UINF*HOLE8*RHOG
      DO 60 I=3,11,2
      RHOS=RHOG*(TINF+459.67)/(T2(I)+459.67)
      SM(I)=SAFR(I)*RHOS/F8
      F(I)=SM(I)*FACT
C     ADJUST F,TH FOR P/D=10
      IF (KM.EQ.1) F(I)=F(I-1)
      IF (KM.EQ.1) TH(I)=TH(I-1)
   60 CONTINUE
      SM(1)=0.
      F(1)=0.
C
C     DP : UNCERTAINTY IN  MANOMETER PRESSURE  , IN H2O
      DP=0.008
C     DSAFR:  UNCERTAINTY IN SECONDARY FLOW RATE,RATIO
      DSAFR=0.05
C   DF: UNCERTAINTY IN  F , RATIO
      DF=SQRT(DSAFR*DSAFR+DP*DP/(4.*PDYN*PDYN))
      IF (SM(2).EQ.0.0) DF=0.0
      RETURN
      END

      SUBROUTINE CAVITY (KL,KR)
C
C         THIS ROUTINE COMPUTES TEST SECTION CAVITY TEMPERATURES
C
```

```
      REAL KL,KR
      COMMON/ BLK4 /TO(45),TG(12),T2(12),TCAST(12),TCAV(12),TH(12)
      DELT1= TCAST(5)-TCAST(3)
      DELT2= TCAST(4)-TCAST(2)
      TCAV(1)=KL*(.982*TCAST(3)+.987*TCAST(2))
      TCAV(2)=KL* (TCAST(3)+TCAST(2))
      TCAV(3)=KL*(TCAST(3)+.4*DELT1)+KR*(TCAST(2)+.4*DELT2)
      TCAV(4)=KL*(TCAST(3)+.6*DELT1)+KR*(TCAST(2)+.6*DELT2)
      TCAV(5)=KL*(TCAST(3)+.833*DELT1)+KR*(TCAST(2)+.833*DELT2)
      TCAV(6)=KL*(TCAST(5)+TCAST(4))
      DELT3=TCAST(7)-TCAST(5)
      DELT4=TCAST(6)-TCAST(4)
      TCAV(7)=KL*(TCAST(5)+.333*DELT3)+KR*(TCAST(4)+.333*DELT4)
      TCAV(8)=KL*(TCAST(5)+.5*DELT3)+KR*(TCAST(4)+.5*DELT4)
      TCAV(9)=KL*(TCAST(5)+.667*DELT3)+KR*(TCAST(4)+.667*DELT4)
      TCAV(10)=KL*(TCAST(5)+.833*DELT3   )    +KR*(TCAST(4)+.833*DELT4)
      TCAV(11)=KL*(TCAST(7)+TCAST(6))
      TCAV(12)=KL*(1.002*TCAST(7)+1.002*TCAST(6))
      RETURN
      END

      SUBROUTINE POWER (TINF,QFLOW,A)
C
C        THIS ROUTINE :
C
C             (1) CORRECTS THE INDICATED PLATE POWER READING FOR
C                 WATTMETER CALIBRATION AND CIRCUIT INSERTION LOSSES
C             (2) COMPUTES NET ENERGY LOST FROM PLATES BY FORCED
C                 CONVECTION HEAT TRANSFER
C             (3) COMPUTES HEAT FLUX FROM RECOVERY REGION PLATES
C
      COMMON/ BLK4 /TO(45),TG(12),T2(12),TCAST(12),TCAV(12),TH(12)
      COMMON/ BLK5 /Q(12),HM(45),VAR(12),QDOT(36)
      COMMON/ BLK6 /DXVO,DEND2,DF,DREEN(36),DST(36),DQDOT(36),DTH(12)
      REAL KL,KR,K
      DIMENSION RO(12),RBO(12),RR(12),RLOD(12),RWAT(12),RON(12),RL(12)
      DIMENSION XB(12),QFLOW(1)     ,K(39),S(40)
C        CONDUCTION LOSS CONSTANTS FOR TEST SECTION
      DATA K/    .8711, .6615, .6495, .5457, .5147, .4901,
     1           .4770, .4795,.4325, .4865, .4287, .4772,
C        HEAT FLUX METER CALIBRATION CONSTANTS NO 13-36
     2           34.00,   35.30,   35.04,   34.04,   33.64,   32.25,
     3           24.83,   34.04,   27.55,   31.55,   31.09,   31.80,
     4           34.01,   34.24,   32.21,   31.09,   24.50,   31.46,
     5           33.02,   39.35,   32.73,   23.60,   36.27,   33.24,
C        HEAT FLUX METER CALIBRATION CONSTANTS NO 106-108
     6           32.53,  32.62,  36.65/
C        AXIAL CONDUCTION LOSS CONSTANTS
      DATA  S/ 1.200 ,  11*2.3,  .950 ,  6.23,   4.962,  5.014,  4.965,
     1           5.118,  5.183,  4.777,  4.494,  5.480,  5.020,  5.597,
     2           5.254,  5.169,  5.254,  5.356,  5.211,  5.370,  5.583,
     3           4.990,  5.433,  4.872,  5.557,  5.545,  5.585,
     4           4.983,  5.056,  6.34 /
C        WATTMETER CIRCUIT RESISTANCES
      DATA RO  /     8.476,  8.595,  8.500,  8.506,  8.478,  8.571,
     1               8.549,  8.641,  8.590,  8.638,  8.481,  8.504/
      DATA RBO /     8.386,  8.502,  8.426,  8.418,  8.386,  8.471,
     1               8.445,  8.574,  8.509,  8.528,  8.391,  8.393/
      DATA RR  /     0.0408, 0.0541, 0.0406, 0.0411, 0.0413, 0.0412,
     1               0.0410, 0.0415, 0.0409, 0.0409, 0.0406, 0.0406/
```

```
      DATA RLOD/     8.256,  8.331,  8.237,  8.221,  8.239,  8.269,
     1               8.227,  8.238,  8.250,  8.253,  8.240,  8.248/
      DATA RWAT/     8.400,  8.484,  8.379,  8.367,  8.405,  8.429,
     1               8.422,  8.541,  8.544,  8.413,  8.386,  8.411/
      DATA RON /     8.313,  8.387,  8.281,  8.282,  8.316,  8.335,
     1               8.330,  8.455,  8.451,  8.428,  8.296,  8.291/
      DATA RL  /     7.946,  7.946,  7.946,  7.946,  7.946,  7.946,
     1               7.946,  7.946,  7.946,  7.946,  7.946,  7.946/
      DATA XB  /     12*0./
      DATA RA,XA,RV,RVM/     0.064,  0.063,  7500.0, 5300.0/
C
C          THIS BLOCK CORRECTS INDICATED WATTMETER READING USING
C          WATTMETER CALIBRATION EQUATION
      DO 10 I=1,12
      QP=Q(I)/75.
      QCOR=QP*(0.0728*QP-0.0427*QP*QP-0.0292)
      QCOR=0.99*Q(I)+QCOR*75.
C
C          THIS BLOCK CORRECTS FOR WATTMETER INSERTION LOSSES
      VARR=RR(I)*VAR(I)
      SUMRO=RO(I)+VARR
      SUMRBQ=RBO(I)+VARR
      FP1=RWAT(I)/RVM+1.
      ZROSQ=SUMRO*SUMRO+(XB(I)+XA/FP1)*(XB(I)+XA/FP1)
      ZRBOSQ=SUMRBO*SUMRBO+XB(I)*XB(I)
      RVMONS=(RVM/(RVM+RON(I)))*(RVM/(RVM+RON(I)))
      ZVALSQ=(RV+RA+RLOD(I))*(RV+RA+RLOD(I))+XA*XA
      Q(I)=QCOR*(ZROSQ/ZRBOSQ)*(ZVALSQ/RV/RV)*RVMONS
     1 *FP1*FP1*(RL(I)/(RA+RLOD(I)))
   10 CONTINUE
C
C          THIS BLOCK CORRECTS POWER DELIVERED TO PLATES
C          IN TEST SECTION FOR CONDUCTION,RADIATION, AND QFLOW LOSSES
      SF=1.
      EMIS=0.15
      TAR=(TINF+460.)/100.
      KL=0.5
      KR=0.5
      CALL CAVITY (KL,KR)
      TUP=TO(45)
      TDOWN=TO(13)
      TW1=TO(45)+K(39)*HM(45)/20.5
      TW12=TO(13)+K(13)*HM(13)/20.5
      TO(13)=0.75*TO(13)+0.25*TW12
      TO(45)=0.75*TO(45)+0.25*TW1
      IF (HM(13).EQ.0.) TO(13)=0.5*(TO(12)+TO(13))
      IF (HM(45).EQ.0.) TO(45)=0.5*(TO(1)+TO(45))
      DO 109 I=1,12
      TOR=(TO(I)+460.)/100.
      IF(I.EQ.1)  GO TO  98
      QCOND=K(I)*(TO(I)-TCAV(I))+S(I)*(TO(I)-TO(I-1))+S(I+1)*(TO(I)-
     1   TO(I+1))
      GO TO 100
   98 QCOND=K(I)*(TO(I)-TCAV(I))+S(I)*(TO(I)-TO(45))
     1  +S(I+1)*(TO(I)-TO(I+1))
  100 QRAD=A*SF*EMIS*.1714*(TOR*TOR*TOR*TOR-TAR*TAR*TAR*TAR)
C
C     ENERGY BALANCE IS APPLIED TO PLATE
      QLOSS=QCOND+QRAD+QFLOW(I)
      Q(I)=Q(I)-QLOSS/3.4129
```

```
      QDOT(I)=Q(I)*3.4129/A
  109 CONTINUE
      TO(45)=TUP
      TO(13)=TDOWN
C
C        THIS BLOCK COMPUTES HEAT FLUX FROM RECOVERY REGION PLATES
      SF=1.0
      EMIS=0.15
      TO(37)=TO(36)-.333*(TO(36)-TO(37))
      S(13)=7.0*S(13)
      TAR=(TINF+460.)/100.
      DO 200 I=13,36
      TOR=(TO(I)+460.)/100.
  200 QDOT(I)=K(I)*HM(I)*(1.+(80.-TO(I))/700.)
     1-S(I)*(TO(I)-TO(I-1))-S(I+1)*(TO(I)-TO(I+1))
     2  -SF*EMIS*.1714*(TOR*TOR*TOR*TOR-TAR*TAR*TAR*TAR)
      S(13)=S(13)/7.0
C
C    ASSUME ALL PROPERTIES CORRECT, AFTER TEMPERATURE-HUMIDITY CORRECTION.
C    DQ:  ENERGY BALANCE ERROR, WATT
      DQ=0.3
C   DHM:  UNCERTAINTY IN HM(I),MV
      DHM=0.025
C    DK:  UNCERTAINTY IN HEAT FLUX METER CALIBRATION,RATIO
      DK=0.03
C    DS:  UNCERTAINTY IN CONDUCTION CORRECTION ON HEAT FLUX METER,RATIC
      DS=0.05
C    DT: UNCERTAINTY IN TEMPERATURE, F
      DT=0.25
C   DQDOT: UNCERTAINTY IN HEAT FLUX,BTU/HR.SQFT
      DO 711 I=1,12
  711 DQDOT(I)=DQ*3.4129/A
      DO 712 I=13,36
  712 DQDOT(I)=SQRT(DK*DK*K(I)*K(I)*HM(I)*HM(I)+K(I)*K(I)*DHM*DHM+DT*DT
     1*(S(I)*S(I)+S(I+1)*S(I+1))+DS*DS*(S(I)*S(I)*(TO(I)-TO(I-1))*(TO(I)
     2-TO(I-1))+S(I+1)*S(I+1)*(TO(I)-TO(I+1))*(TO(I)-TO(I+1))))
       RETURN
      END

      SUBROUTINE ENTHAL (FACT,ST,REEN,END2)
C     COMPUTE ENTHALPY THICKNESS, ASSUMING THERMAL BL BEGINS AT
C
C        MIDDLE       OF PLATE 1. COMPUTATION BASED ON CONTROL
C        VOLUME FOR ENERGY ADDITION WITH BOUNDRIES PLATE CENTER
C        TO PLATE CENTER(EXCEPT PLATE 1)
C
      COMMON/ BLK3 /SAFR(12),CI(12),SM(12),F(12),KM,AH,THEAT
      COMMON/ BLK4 /TO(45),TG(12),T2(12),TCAST(12),TCAV(12),TH(12)
      COMMON/ BLK6 /DXVO,DEND2,DF,DREEN(36),DST(36),DQDOT(36),DTH(12)
      DIMENSION ST(1),REEN(1),D2(36),DD2(36)
      TH(1)=0.0
      DTH(1)=0.
      F(1)=0.0
      DX=1.
      DWX=.515625
C   DDX: UNCERTAINTY IN DX, IN
      DDX=0.005
      D2(1)=END2
      DD2(1)=DEND2
      IF (END2.EQ.0.) D2(1)=ST(1)*DX
```

```
      IF(.NOT.END2.EQ.0.)  GO TO 229
C   DD2(I):  UNCERTAINTY IN ENTHALPY THICKNESS, D2, IN
      DD2(1)=SQRT(DX*DX*DST(1)*DST(1)+ST(1)*ST(1)*DDX*DDX)
  229 DO 230 I=2,12
      D2(I)=D2(I-1)+(ST(I-1)+ST(I)+2.*F(I-1)*TH(I-1))*DX
      AL=ST(I)*ST(I)+ST(I-1)*ST(I-1)+F(I)*F(I)*TH(I)*TH(I)+F(I-1)*
     1F(I-1)*TH(I-1)*TH(I-1)
      BE=DST(I)*DST(I)+DST(I-1)*DST(I-1)+F(I)*F(I)*DTH(I)*DTH(I)+
     1F(I-1)*F(I-1)*DTH(I-1)*DTH(I-1)+DF*DF*(F(I)*F(I)*TH(I)*TH(I)+
     2F(I-1)*F(I-1)*TH(I-1)*TH(I-1))
  230 DD2(I)=SQRT(DD2(I-1)*DD2(I-1)+DDX*DDX*AL+DX*DX*BE )
      D2(13)=D2(12)+(ST(12)+2.*F(12)*TH(12))*DX+ST(13)*DWX
      DD2(13)=SQRT(DD2(12)*DD2(12)+DDX*DDX*(ST(12)*ST(12)+ST(13)*ST(13)
     1+F(12)*F(12)*TH(12)*TH(12)) +DWX*DWX*DST(13)*DST(13)+  DX*DX*(
     2DST(12)*DST(12)+F(12)*F(12)*DTH(12)*DTH(12)+DF*DF*F(12)*F(12)*
     3TH(12)*TH(12)))
      DO 231 I=14,36
      D2(I)=D2(I-1)+(ST(I-1)+ST(I))*DWX
      IF (I.EQ.14.AND.KM.EQ.1)D2(14)=D2(14)+2.*F(12)*TH(12)*DX
  231 DD2(I)= SQRT(DD2(I-1)*DD2(I-1)+DDX*DDX*(ST(I)*ST(I)+ST(I-1)*
     1ST(I-1))+ DWX*DWX*(DST(I)*DST(I)+DST(I-1)*DST(I-1)))
C     COMPUTE ENTHALPY THICKNESS REYNOLDS NUMBER FOR CENTER
C        OF PLATE BASED ON D2(I) FOR ENERGY ADDED TO THAT POINT
      DO 240 I=1,36
      REEN(I)=FACT*D2(I)
  240 DREEN(I)=FACT*DD2(I)
      RETURN
      END

@DATA
```

Appendix IV

STANTON NUMBER DATA

Contained in this appendix is a numerical tabulation of the Stanton number data. Initial velocity and temperature profiles precede the data, and the sequence of data follows the discussions in Sections 3.3.1 through 3.3.4. For the Stanton number data at each blowing ratio the experimental data at $\theta = 1$ and $\theta = 0$ are given first, followed by a sheet with the superposition-adjusted data to values at $\theta = 0, 1$.

Nomenclature

CF/2	$c_f/2$, friction coefficient
CP	c , specific heat
DEL	velocity or thermal boundary layer thickness (see DEL99 or DELT99)
DEL1	δ_1 , displacement thickness
DEL2	δ_2 , momentum thickness
DEL99	velocity boundary layer thickness
DELT99	thermal boundary layer thickness
DREEN	uncertainty in Re_{Δ_2}
DST	uncertainty in St
DTM	uncertainty in θ
ETA	$\{1 - St(\theta = 1)\}/St(\theta = 0)$
F	blowing fraction
F-COL	F at $\theta = 0$
F-HOT	F at $\theta = 1$
H	velocity shape factor
LOGB	ϕ function in $\theta = 1$ data correlation

M	blowing parameter
PORT	topwall location where profile is obtained
PR	Pr , Prandtl number
RE DEL2 REENTH REH	Re_{Δ_2} , enthalpy thickness Reynolds number
REM	Re_{δ_2} , momentum thickness Reynolds number
REX	Re_x , x-Reynolds number, based on (X - XVO)
RHO	density
ST	Stanton number
STCR	$St(\theta = 0)/St_o$. Note, St_o is defined at bottom of each summary data sheet.
STHR	$St(\theta = 1)/St_o$
T	recovery temperature of temperature probe
T2	T_2 , secondary air temperature
TADB	T_{∞} , r , temperature to define Stanton number
TBAR	$(T_o-T)/(T_o-T_{\infty})$ (or one minus that quantity in the second tabulated data column)
THETA	θ , temperature parameter
TINF	mainstream thermocouple temperature
TO TPLATE	T_o , plate temperature
U	velocity
U+	U^+ , non-dimensional velocity
UINF	U_{∞} , mainstream velocity
VISC	ν , kinematic viscosity
XLOC	x , distance from nozzle exit to probe tip

XVO	x_{vo} , distance from nozzle exit to virtual origin, turbulent boundary layer
Y	y , distance normal to surface
Y+	y^+ , non-dimensional y distance

RUN 062777 VELOCITY AND TEMPERATURE PROFILES

```
REX  = 0.10626E 07       REM  =        2451.      REH    =       1759.

XVO  =        26.12 CM   DEL2 =        0.229 CM   DEH2    =       0.162 CM
UINF =        16.98 M/S  DEL99=        1.994 CM   DELT99  =       1.862 CM
VISC = 0.15830E-04 M2/S  DEL1 =        0.344 CM   UINF    =       16.76 M/S
PORT =            3      H    =        1.507      VISC    = 0.15476E-04 M2/S
XLOC =       125.22 CM   CF/2 = 0.17160E-02       TINF    =       24.82 DEG C
                                                  TPLATE  =       38.04 DEG C
```

Y(CM)	Y/DEL	U(M/S)	U/UINF	Y+	U+	Y(CM)	T(DEG C)	TBAR	TBAR
0.025	0.013	6.57	0.411	11.3	9.91	0.0127	35.21	0.214	0.786
0.030	0.015	7.00	0.412	13.5	9.95	0.0254	31.99	0.458	0.542
0.033	0.017	7.06	0.416	14.7	10.04	0.0381	30.66	0.558	0.442
0.036	0.018	7.28	0.425	15.8	10.35	0.0508	30.09	0.601	0.399
0.038	0.019	7.60	0.448	16.9	10.81	0.0635	29.74	0.628	0.372
0.041	0.020	7.89	0.465	18.1	11.22	0.0762	29.55	0.642	0.358
0.043	0.022	8.13	0.479	19.2	11.56	0.0889	29.36	0.657	0.343
0.046	0.023	8.32	0.490	20.3	11.83	0.1016	29.13	0.674	0.326
0.048	0.024	8.51	0.501	21.4	12.10	0.1143	29.03	0.681	0.319
0.051	0.025	8.67	0.510	22.6	12.32	0.1270	28.82	0.697	0.303
0.053	0.027	8.80	0.518	23.7	12.52	0.1397	28.77	0.701	0.299
0.056	0.028	8.99	0.529	24.8	12.76	0.1524	28.64	0.711	0.289
0.061	0.031	9.24	0.544	27.1	13.13	0.1651	28.56	0.717	0.283
0.066	0.033	9.35	0.551	29.3	13.29	0.1778	28.45	0.725	0.275
0.071	0.036	9.53	0.561	31.6	13.54	0.1905	28.35	0.733	0.267
0.081	0.041	9.76	0.575	36.1	13.87	0.2032	28.26	0.739	0.261
0.094	0.047	10.05	0.592	41.7	14.28	0.2159	28.22	0.743	0.257
0.107	0.053	10.25	0.604	47.4	14.57	0.2286	28.14	0.749	0.251
0.119	0.060	10.43	0.614	53.0	14.83	0.2413	28.09	0.753	0.247
0.145	0.073	10.75	0.633	64.3	15.28	0.2540	28.02	0.757	0.243
0.183	0.092	11.08	0.652	81.2	15.75	0.2667	27.93	0.765	0.235
0.221	0.111	11.38	0.670	98.2	16.18	0.2794	27.90	0.767	0.233
0.259	0.130	11.66	0.687	115.1	16.58	0.2921	27.82	0.773	0.227
0.297	0.149	11.84	0.697	132.0	16.83	0.3048	27.77	0.777	0.223
0.335	0.168	12.09	0.712	148.9	17.19	0.3302	27.66	0.785	0.215
0.399	0.200	12.44	0.733	177.1	17.69	0.3556	27.58	0.791	0.209
0.450	0.225	12.66	0.745	199.7	17.99	0.3937	27.42	0.803	0.197
0.513	0.257	12.92	0.761	227.9	18.37	0.4318	27.29	0.813	0.187
0.577	0.289	13.22	0.779	256.1	18.80	0.4699	27.14	0.821	0.179
0.653	0.327	13.54	0.798	290.0	19.25	0.5207	26.99	0.835	0.165
0.780	0.391	14.05	0.827	346.4	19.97	0.5969	26.81	0.850	0.150
0.907	0.455	14.47	0.852	402.8	20.58	0.6604	26.64	0.862	0.138
1.034	0.518	14.88	0.877	459.2	21.16	0.7239	26.48	0.874	0.126
1.161	0.582	15.25	0.898	515.6	21.67	0.7874	26.33	0.885	0.115
1.288	0.646	15.59	0.918	572.0	22.16	0.8509	26.21	0.895	0.105
1.415	0.709	15.92	0.937	628.4	22.63	0.9779	25.97	0.913	0.087
1.542	0.773	16.23	0.956	684.8	23.07	1.1049	25.75	0.930	0.070
1.669	0.837	16.46	0.970	741.2	23.41	1.3589	25.39	0.957	0.043
1.796	0.901	16.66	0.981	797.7	23.69	1.6129	25.12	0.977	0.023
1.923	0.964	16.81	0.990	854.1	23.90	1.8669	24.95	0.990	0.010
2.050	1.028	16.92	0.996	910.5	24.05	2.1209	24.85	0.998	0.002
2.177	1.092	16.99	1.001	966.9	24.15	2.3749	24.82	1.000	-0.000
2.304	1.155	17.02	1.002	1023.3	24.20				
2.431	1.219	16.98	1.000	1079.7	24.14				

RUN 062777 *** DISCRETE HOLE RIG *** NAS-3-14336 STANTON NUMBER DATA

TADB= 24.86 DEG C UINF= 16.80 M/S TINF= 24.74 DEG C
RHO= 1.178 KG/M3 VISC= 0.15469E-04 M2/S XVO= 26.1 CM
CP= 1013. J/KGK PR= 0.716

****2500 FLAT PLATE HSL P/D=5****

PLATE	X	REX	TO	REENTH	STANTONNO	DST	DREEN	ST(THEO)	RATIO
1	127.8	0.11036E 07	38.08	0.17819E 04	0.22412E-02	0.563E-04	6.	0.20858E-02	1.075
2	132.8	0.11588E 07	38.06	0.19084E 04	0.23452E-02	0.570E-04	6.	0.20655E-02	1.135
3	137.9	0.12135E 07	38.04	0.20386E 04	0.23747E-02	0.573E-04	6.	0.20464E-02	1.160
4	143.0	0.12651E 07	38.04	0.21695E 04	0.23728E-02	0.573E-04	7.	0.20283E-02	1.170
5	148.1	0.13243E 07	38.04	0.22991E 04	0.23223E-02	0.570E-04	7.	0.20111E-02	1.155
6	153.2	0.13754E 07	38.02	0.24254E 04	0.22561E-02	0.567E-04	7.	0.19947E-02	1.131
7	158.2	0.14346E 07	38.02	0.25495E 04	0.22432E-02	0.566E-04	8.	0.19792E-02	1.133
8	163.3	0.14859E 07	38.00	0.26725E 04	0.22173E-02	0.565E-04	8.	0.19643E-02	1.129
9	168.4	0.15444E 07	37.96	0.27936E 04	0.21732E-02	0.564E-04	8.	0.19502E-02	1.114
10	173.5	0.16001E 07	37.94	0.29130E 04	0.21541E-02	0.564E-04	9.	0.19364E-02	1.112
11	178.6	0.16553E 07	37.92	0.30310E 04	0.21246E-02	0.563E-04	9.	0.19233E-02	1.105
12	183.6	0.17104E 07	37.94	0.31483E 04	0.21281E-02	0.562E-04	9.	0.19108E-02	1.114
13	187.5	0.17524E 07	37.47	0.32349E 04	0.19634E-02	0.688E-04	9.	0.19015E-02	1.033
14	190.1	0.17900E 07	37.37	0.32897E 04	0.18868E-02	0.694E-04	10.	0.18954E-02	0.995
15	192.7	0.18052E 07	37.39	0.33447E 04	0.19627E-02	0.711E-04	10.	0.18894E-02	1.049
16	195.4	0.18377E 07	37.64	0.33993E 04	0.18351E-02	0.676E-04	10.	0.18835E-02	0.974
17	198.0	0.18663E 07	37.66	0.34513E 04	0.18773E-02	0.663E-04	10.	0.18777E-02	1.000
18	200.6	0.18947E 07	37.66	0.35051E 04	0.18712E-02	0.661E-04	10.	0.18721E-02	1.000
19	203.2	0.19231E 07	37.68	0.35572E 04	0.17919E-02	0.653E-04	10.	0.18665E-02	0.960
20	205.8	0.19515E 07	37.71	0.36092E 04	0.18639E-02	0.675E-04	10.	0.18610E-02	1.001
21	208.5	0.19799E 07	37.66	0.36616E 04	0.18211E-02	0.660E-04	10.	0.18557E-02	0.981
22	211.1	0.20083E 07	37.68	0.37135E 04	0.18258E-02	0.674E-04	10.	0.18504E-02	0.987
23	213.7	0.20368E 07	37.51	0.37666E 04	0.19079E-02	0.687E-04	10.	0.18452E-02	1.034
24	216.3	0.20653E 07	37.64	0.38190E 04	0.17769E-02	0.661E-04	11.	0.18401E-02	0.966
25	218.9	0.20934E 07	37.62	0.38706E 04	0.18527E-02	0.640E-04	11.	0.18350E-02	1.010
26	221.6	0.21223E 07	37.23	0.39213E 04	0.17116E-02	0.613E-04	11.	0.18301E-02	0.935
27	224.2	0.21507E 07	37.66	0.39722E 04	0.18660E-02	0.691E-04	11.	0.18252E-02	1.023
28	226.8	0.21791E 07	37.85	0.40258E 04	0.19029E-02	0.704E-04	11.	0.18204E-02	1.045
29	229.4	0.22075E 07	37.62	0.40783E 04	0.17894E-02	0.639E-04	11.	0.18157E-02	0.986
30	232.0	0.22359E 07	37.92	0.41294E 04	0.18051E-02	0.674E-04	11.	0.18111E-02	0.997
31	234.6	0.22643E 07	37.89	0.41813E 04	0.18419E-02	0.676E-04	11.	0.18065E-02	1.020
32	237.3	0.22929E 07	37.71	0.42330E 04	0.17966E-02	0.658E-04	11.	0.18020E-02	0.997
33	239.9	0.23214E 07	37.70	0.42842E 04	0.18008E-02	0.667E-04	11.	0.17975E-02	1.002
34	242.5	0.23498E 07	37.41	0.43352E 04	0.17827E-02	0.638E-04	11.	0.17932E-02	0.994
35	245.1	0.23782E 07	37.64	0.43867E 04	0.18383E-02	0.686E-04	12.	0.17889E-02	1.028
36	247.8	0.24067E 07	37.66	0.44354E 04	0.15906E-02	0.686E-04	12.	0.17846E-02	0.891

RUN 071277-1 *** DISCRETE HOLE RIG *** NAS-3-14336   STANTON NUMBER DATA

TADB= 24.31 DEG C   UINF=   17.09 M/S   TINF= 24.18 DEG C
RHO= 1.142 KG/M3   VISC= 0.15928E-04 M2/S   XVO= 23.3 CM
CP= 1014. J/KGK   PR=   0.717

25CC HSL M=0.4 P/D=5 TH=0 W/VCF(OPTIMUM)

PLATE	X	REX		TO	REENTH		STANTON NO	DST	CREEN	M	F	T2	THETA	DTH
1	127.8	0.11209E	07	37.07	0.17602E	04	0.25446E-02	0.607E-04	11.					
2	132.8	0.11754E	07	37.05	0.18938E	04	0.23605E-02	0.556E-04	15.	0.40	0.0130	27.62	0.268	0.023
3	137.9	0.12255E	07	37.12	0.22173E	04	0.25412E-02	0.604E-04	20.	0.40	0.0131	27.41	0.249	0.023
4	143.0	0.12844E	07	37.14	0.25326E	04	0.25120E-02	0.601E-04	24.	0.41	0.0132	27.41	0.249	0.023
5	148.1	0.13389E	07	37.24	0.28466E	04	0.24162E-02	0.591E-04	28.	0.39	0.0127	27.47	0.252	0.023
6	153.2	0.13934E	07	37.28	0.31526E	04	0.23823E-02	0.588E-04	30.	0.40	0.0129	27.29	0.237	0.023
7	158.2	0.14479E	07	37.24	0.34455E	04	0.22338E-02	0.581E-04	33.	0.40	0.0129	27.32	0.241	0.023
8	163.3	0.15024E	07	37.20	0.37354E	04	0.22347E-02	0.580E-04	36.	0.39	0.0127	27.21	0.233	0.023
9	168.4	0.15569E	07	37.22	0.40150E	04	0.21183E-02	0.575E-04	38.	0.39	0.0128	27.22	0.233	0.023
10	173.5	0.16114E	07	37.26	0.42903E	04	0.20452E-02	0.569E-04	40.	0.40	0.0129	27.14	0.226	0.023
11	178.6	0.16659E	07	37.28	0.45601E	04	0.20265E-02	0.567E-04	42.	0.40	0.0129	27.28	0.237	0.023
12	183.6	0.17204E	07	37.28	0.48380E	04	0.20376E-02	0.568E-04	44.	0.39	0.0126	27.18	0.229	0.023
13	187.5	0.17618E	07	36.50	0.50770E	04	0.18672E-02	0.647E-04	45.					
14	190.1	0.17899E	07	36.44	0.51277E	04	0.17449E-02	0.656E-04	45.					
15	192.7	0.18179E	07	36.52	0.51771E	04	0.17724E-02	0.652E-04	45.					
16	195.4	0.18461E	07	36.76	0.52250E	04	0.16362E-02	0.618E-04	45.					
17	198.0	0.18743E	07	36.80	0.52711E	04	0.16395E-02	0.613E-04	45.					
18	200.6	0.19024E	07	36.84	0.53169E	04	0.16205E-02	0.608E-04	45.					
19	203.2	0.19304E	07	36.88	0.53616E	04	0.15628E-02	0.585E-04	45.					
20	205.8	0.19585E	07	36.36	0.54065E	04	0.16365E-02	0.605E-04	45.					
21	208.5	0.19866E	07	36.86	0.54514E	04	0.15554E-02	0.583E-04	45.					
22	211.1	0.20146E	07	36.86	0.54956E	04	0.15962E-02	0.604E-04	45.					
23	213.7	0.20427E	07	36.78	0.55410E	04	0.16343E-02	0.611E-04	45.					
24	216.3	0.20704E	07	36.84	0.55860E	04	0.15546E-02	0.597E-04	45.					
25	218.9	0.20991E	07	36.86	0.56308E	04	0.16227E-02	0.613E-04	45.					
26	221.6	0.21272E	07	36.65	0.56752E	04	0.15444E-02	0.576E-04	45.					
27	224.2	0.21552E	07	36.90	0.57200E	04	0.16424E-02	0.621E-04	45.					
28	226.8	0.21833E	07	37.01	0.57671E	04	0.17066E-02	0.643E-04	45.					
29	229.4	0.22114E	07	36.82	0.58134E	04	0.15912E-02	0.585E-04	45.					
30	232.0	0.22394E	07	37.05	0.58587E	04	0.16303E-02	0.622E-04	45.					
31	234.6	0.22675E	07	37.01	0.59048E	04	0.16544E-02	0.622E-04	45.					
32	237.3	0.22957E	07	36.88	0.59506E	04	0.16081E-02	0.606E-04	45.					
33	239.9	0.23239E	07	36.84	0.59961E	04	0.16284E-02	0.617E-04	45.					
34	242.5	0.23520E	07	36.57	0.60418E	04	0.16223E-02	0.595E-04	45.					
35	245.1	0.23800E	07	36.76	0.60882E	04	0.16803E-02	0.642E-04	45.					
36	247.8	0.24081E	07	36.76	0.61326E	04	0.14828E-02	0.654E-04	45.					

UNCERTAINTY IN REX=12997.   UNCERTAINTY IN F=0.05036 IN RATIO

RUN 071277-2 *** DISCRETE HOLE RIG *** NAS-3-14336 STANTON NUMBER DATA

TADB= 25.17 DEG C UINF= 17.13 M/S TINF= 25.04 DEG C
RHO= 1.137 KG/M3 VISC= 0.16054E-04 M2/S XVO= 23.3 CM
CP= 1012. J/KGK PR= 0.715

250C HSL M=0.4 P/D=5 TH=1 W/VCF(OPTIMUM)

PLATE	X	REX	TO	REENTH	STANTON NO	DST	DREEN	M	F	T2	THETA	DTH
1	127.8	0.11147E 07	41.84	0.17504E 04	0.25003E-02	0.474E-04	11.					
2	132.8	0.11689E 07	41.84	0.18746E 04	0.20831E-02	0.452E-04	20.	0.37	0.0120	40.83	0.940	0.018
3	137.9	0.12231E 07	41.87	0.25939E 04	0.18570E-02	0.441E-04	31.	0.38	0.0122	41.32	0.967	0.018
4	143.0	0.12773E 07	41.85	0.33250E 04	0.15777E-02	0.430E-04	40.	0.37	0.0121	41.40	0.973	0.018
5	148.1	0.13315E 07	41.93	0.40432E 04	0.13521E-02	0.420E-04	46.	0.37	0.0119	41.37	0.967	0.018
6	153.2	0.13857E 07	41.78	0.47420E 04	0.13380E-02	0.423E-04	52.	0.37	0.0121	41.42	0.978	0.018
7	158.2	0.14399E 07	41.95	0.54508E 04	0.10454E-02	0.412E-04	58.	0.37	0.0121	41.28	0.960	0.018
8	163.3	0.14941E 07	41.93	0.61373E 04	0.96397E-03	0.409E-04	63.	0.37	0.0118	41.42	0.970	0.018
9	168.4	0.15483E 07	42.03	0.68113E 04	0.93557E-03	0.406E-04	67.	0.37	0.0119	41.26	0.955	0.018
10	173.5	0.16024E 07	41.99	0.74738E 04	0.84515E-03	0.405E-04	71.	0.38	0.0122	41.24	0.956	0.018
11	178.6	0.16566E 07	42.08	0.81526E 04	0.81660E-03	0.402E-04	75.	0.38	0.0123	40.93	0.932	0.018
12	183.6	0.17106E 07	42.27	0.88126E 04	0.70323E-03	0.395E-04	79.	0.37	0.0121	40.89	0.920	0.018
13	187.5	0.17520E 07	40.47	0.94430E 04	0.59356E-03	0.245E-04	80.					
14	190.1	0.17799E 07	40.15	0.94595E 04	0.58556E-03	0.305E-04	80.					
15	192.7	0.18078E 07	40.15	0.94762E 04	0.61470E-03	0.303E-04	80.					
16	195.4	0.18359E 07	40.11	0.94937E 04	0.63261E-03	0.307E-04	80.					
17	198.0	0.18639E 07	40.03	0.95118E 04	0.66803E-03	0.317E-04	80.					
18	200.6	0.18918E 07	39.94	0.95312E 04	0.71464E-03	0.329E-04	80.					
19	203.2	0.19197E 07	39.90	0.95508E 04	0.69267E-03	0.317E-04	80.					
20	205.8	0.19477E 07	39.86	0.95713E 04	0.77373E-03	0.336E-04	80.					
21	208.5	0.19756E 07	39.82	0.95925E 04	0.74422E-03	0.334E-04	80.					
22	211.1	0.20035E 07	39.75	0.96143E 04	0.81202E-03	0.359E-04	80.					
23	213.7	0.20314E 07	39.65	0.96375E 04	0.85356E-03	0.370E-04	80.					
24	216.3	0.20594E 07	39.64	0.96611E 04	0.83409E-03	0.370E-04	80.					
25	218.9	0.20875E 07	39.62	0.96853E 04	0.89892E-03	0.389E-04	80.					
26	221.6	0.21154E 07	39.41	0.97101E 04	0.87617E-03	0.370E-04	80.					
27	224.2	0.21433E 07	39.62	0.97358E 04	0.96315E-03	0.407E-04	80.					
28	226.8	0.21712E 07	39.65	0.97638E 04	0.10435E-02	0.428E-04	80.					
29	229.4	0.21991E 07	39.48	0.97919E 04	0.96461E-03	0.392E-04	80.					
30	232.0	0.22270E 07	39.62	0.98196E 04	0.10147E-02	0.423E-04	80.					
31	234.6	0.22549E 07	39.60	0.98482E 04	0.10325E-02	0.425E-04	80.					
32	237.3	0.22830E 07	39.43	0.98770E 04	0.10350E-02	0.423E-04	80.					
33	239.9	0.23110E 07	39.43	0.99061E 04	0.10448E-02	0.430E-04	80.					
34	242.5	0.23389E 07	39.18	0.99355E 04	0.10568E-02	0.416E-04	80.					
35	245.1	0.23668E 07	39.31	0.99657E 04	0.11100E-02	0.457E-04	80.					
36	247.8	0.23947E 07	39.31	0.99947E 04	0.96454E-03	0.468E-04	80.					

UNCERTAINTY IN REX=12925. UNCERTAINTY IN F=0.05036 IN RATIO

RUN 071277-1 *** DISCRETE HOLE RIG *** NAS-3-14336 STANTON NUMBER DATA

2500 FSL M=0.4 P/D=5 TH=0 W/VCF(OPTIMUM)

RUN 071277-2 *** DISCRETE HOLE RIG *** NAS-3-14336 STANTON NUMBER DATA

2500 FSL M=0.4 P/D=5 TH=1 W/VCF(OPTIMUM)

LINEAR SUPERPOSITION IS APPLIED TO STANTON NUMBER DATA FROM
RUN NUMBERS 071277-1 AND 071277-2 TO OBTAIN STANTON NUMBER DATA AT TH=0 AND TH=1

PLATE	REXCOL	RE DEL2	ST(TH=0)	REXHOT	RE DEL2	ST(TH=1)	ETA	STCR	F-COL	STHR	F-HOT	LOGB
1	1120538.0	1760.2	0.002545	1114723.0	1750.4	0.002500	UUUUU	1.000	0.0000	1.000	0.0000	1.000
2	1175432.0	1856.8	0.002471	1168915.0	1873.9	0.002058	0.167	1.054	0.0130	0.878	0.0120	2.667
3	1229926.0	2040.3	0.002796	1223107.0	2630.5	0.001811	0.352	1.177	0.0131	0.763	0.0122	2.508
4	1284420.0	2193.7	0.002835	1277298.0	3381.0	0.001539	0.457	1.195	0.0132	0.649	0.0121	2.339
5	1338914.0	2346.9	0.002787	1331490.0	4114.6	0.001308	0.531	1.200	0.0127	0.563	0.0119	2.221
6	1393408.0	2497.4	0.002734	1395682.0	4832.7	0.001299	0.525	1.212	0.0129	0.576	0.0121	2.300
7	1447902.0	2642.5	0.002605	1439874.0	5553.2	0.001052	0.596	1.161	0.0129	0.469	0.0121	2.137
8	1502395.0	2784.9	0.002609	1494065.0	6262.9	0.000905	0.653	1.177	0.0127	0.408	0.0118	2.019
9	1556885.0	2924.0	0.002496	1548257.0	6952.9	0.000875	0.650	1.149	0.0128	0.403	0.0119	2.039
10	1611383.0	3058.1	0.002425	1602449.0	7640.6	0.000772	0.682	1.126	0.0129	0.358	0.0122	2.010
11	1665877.0	3190.1	0.002420	1656641.0	8343.9	0.000722	0.702	1.139	0.0129	0.340	0.0123	1.996
12	1720371.0	3323.8	0.002487	1710832.0	9042.6	0.000561	0.774	1.168	0.0126	0.264	0.0121	1.824
13	1761788.0	3423.8	0.002296	1752018.0	9719.7	0.000458	0.801	1.169		0.233		
14	1789851.0	3496.1	0.002135	1779527.0	9732.6	0.000462	0.784	1.132		0.245		
15	1817815.0	3546.4	0.002162	1807836.0	9745.9	0.000491	0.773	1.090		0.248		
16	1846115.0	3604.5	0.001974	1835879.0	9760.1	0.000525	0.734	1.076		0.286		
17	1874316.0	3659.9	0.001966	1863924.0	9775.3	0.000564	0.713	1.047		0.301		
18	1902286.0	3714.6	0.001925	1891832.0	9791.8	0.000618	0.679	1.029		0.330		
19	1930444.0	3767.7	0.001856	1919741.0	9808.8	0.000600	0.677	1.036		0.335		
20	1958505.0	3820.8	0.001927	1947650.0	9826.7	0.000682	0.646	1.034		0.366		
21	1986574.0	3873.6	0.001828	1975559.0	9845.5	0.000658	0.640	1.004		0.361		
22	2014638.0	3925.4	0.001860	2003468.0	9864.8	0.000728	0.608	1.019		0.399		
23	2042702.0	3978.2	0.001897	2031376.0	9885.8	0.000770	0.594	0.994		0.404		
24	2070532.0	4030.3	0.001810	2059420.0	9907.1	0.000756	0.582	1.019		0.426		
25	2099102.0	4081.9	0.001866	2087465.0	9929.1	0.000822	0.560	1.007		0.443		
26	2127167.0	4133.0	0.001769	2115373.0	9951.8	0.000805	0.545	1.034		0.470		
27	2155232.0	4184.1	0.001871	2143282.0	9975.5	0.000891	0.524	1.002		0.477		
28	2183296.0	4237.5	0.001933	2171191.0	10001.6	0.000973	0.496	1.014		0.511		
29	2211361.0	4293.0	0.001802	2199100.0	10027.7	0.000898	0.502	1.007		0.502		
30	2239425.0	4341.1	0.001838	2227009.0	10053.5	0.000949	0.484	1.018		0.526		
31	2267485.0	4393.1	0.001864	2254917.0	10080.3	0.000966	0.482	1.012		0.524		
32	2295550.0	4444.6	0.001801	2282961.0	10107.4	0.000974	0.459	1.002		0.542		
33	2323890.0	4495.5	0.001825	2311005.0	10134.7	0.000982	0.462	1.013		0.546		
34	2351555.0	4546.6	0.001813	2338914.0	10162.3	0.000996	0.451	1.017		0.559		
35	2380015.0	4598.4	0.001872	2366823.0	10190.9	0.001049	0.440	1.018		0.571		
36	2408083.0	4648.0	0.001657	2394732.0	10218.3	0.000909	0.451	1.042		0.572		

STANTON NUMBER RATIO BASED ON EXPERIMENTAL FLAT PLATE VALUE AT SAME X LOCATION

STANTON NUMBER RATIO FOR TH=1 IS CONVERTED TO COMPARABLE TRANSPIRATION VALUE
USING ALOG(1 + B)/B EXPRESSION IN THE BLOWN SECTION

RUN 072177-1 *** DISCRETE HOLE RIG *** NAS-3-14336   STANTON NUMBER DATA

TADB= 26.75 DEG C   UINF= 16.99 M/S   TINF= 26.66 DEG C
RHO= 1.173 KG/M3   VISC= 0.15633E-04 M2/S   XVO= 23.3 CM
CP= 1012. J/KGK   PR= 0.715

2500 HSL M=0.90 P/D=5 TH=0 W/VCF(OPTIMUM)

PLATE	X	REX	TO	REENTH	STANTON NO	DST	DREEN	M	F	T2	THETA	DTH
1	127.8	0.11355E 07	37.68	0.17830E 04	0.21116E-02	0.666E-04	8.					
2	132.8	0.11907E 07	37.58	0.18996E 04	0.21150E-02	0.672E-04	25.	0.92	0.0298	27.68	0.093	0.028
3	137.9	0.12459E 07	37.56	0.21821E 04	0.25454E-02	0.701E-04	42.	0.94	0.0303	27.77	0.101	0.028
4	143.0	0.13011E 07	37.56	0.24976E 04	0.27434E-02	0.716E-04	53.	0.91	0.0296	27.76	0.101	0.028
5	148.1	0.13563E 07	37.56	0.28105E 04	0.26316E-02	0.708E-04	63.	0.91	0.0295	27.86	0.110	0.028
6	153.2	0.14115E 07	37.49	0.31322E 04	0.25473E-02	0.706E-04	71.	0.90	0.0292	27.78	0.103	0.028
7	158.2	0.14667E 07	37.52	0.34360E 04	0.24343E-02	0.656E-04	78.	0.91	0.0296	27.82	0.107	0.028
8	163.3	0.15219E 07	37.56	0.37451E 04	0.24533E-02	0.695E-04	85.	0.91	0.0294	27.72	0.097	0.028
9	168.4	0.15771E 07	37.58	0.40380E 04	0.24401E-02	0.693E-04	91.	0.91	0.0294	27.80	0.104	0.028
10	173.5	0.16323E 07	37.62	0.43405E 04	0.23712E-02	0.666E-04	96.	0.90	0.0292	27.70	0.095	0.028
11	178.6	0.16875E 07	37.54	0.46256E 04	0.24097E-02	0.693E-04	102.	0.92	0.0299	27.85	0.109	0.028
12	183.6	0.17427E 07	38.17	0.49319E 04	0.21420E-02	0.640E-04	107.	0.90	0.0293	27.73	0.093	0.027
13	187.5	0.17846E 07	37.14	0.51406E 04	0.27647E-02	0.553E-04	109.					
14	190.1	0.18131E 07	37.09	0.52566E 04	0.25586E-02	0.943E-04	109.					
15	192.7	0.18415E 07	37.09	0.53316E 04	0.27068E-02	0.968E-04	109.					
16	195.4	0.18701E 07	37.52	0.54041E 04	0.23857E-02	0.883E-04	109.					
17	198.0	0.18986E 07	37.64	0.54714E 04	0.23766E-02	0.871E-04	109.					
18	200.6	0.19270E 07	37.64	0.55395E 04	0.23744E-02	0.866E-04	109.					
19	203.2	0.19555E 07	37.66	0.56052E 04	0.22408E-02	0.816E-04	109.					
20	205.8	0.19839E 07	37.75	0.56696E 04	0.22905E-02	0.835E-04	109.					
21	208.5	0.20123E 07	37.73	0.57340E 04	0.22327E-02	0.813E-04	109.					
22	211.1	0.20408E 07	37.79	0.57974E 04	0.22224E-02	0.820E-04	109.					
23	213.7	0.20692E 07	37.77	0.58607E 04	0.22218E-02	0.815E-04	109.					
24	216.3	0.20978E 07	37.85	0.59226E 04	0.21293E-02	0.790E-04	109.					
25	218.9	0.21263E 07	37.92	0.59836E 04	0.21560E-02	0.804E-04	109.					
26	221.6	0.21547E 07	37.73	0.60439E 04	0.20822E-02	0.759E-04	109.					
27	224.2	0.21832E 07	38.02	0.61040E 04	0.21397E-02	0.796E-04	109.					
28	226.8	0.22116E 07	38.10	0.61654E 04	0.21755E-02	0.808E-04	109.					
29	229.4	0.22400E 07	37.89	0.62255E 04	0.20451E-02	0.740E-04	109.					
30	232.0	0.22685E 07	38.19	0.62842E 04	0.20649E-02	0.783E-04	109.					
31	234.6	0.22969E 07	38.17	0.63439E 04	0.21070E-02	0.782E-04	109.					
32	237.3	0.23255E 07	38.00	0.64031E 04	0.20530E-02	0.758E-04	109.					
33	239.9	0.23540E 07	38.02	0.64615E 04	0.20523E-02	0.771E-04	109.					
34	242.5	0.23824E 07	37.68	0.65202E 04	0.20688E-02	0.747E-04	109.					
35	245.1	0.24109E 07	37.50	0.65795E 04	0.21038E-02	0.794E-04	109.					
36	247.8	0.24393E 07	37.90	0.66359E 04	0.18601E-02	0.793E-04	109.					

UNCERTAINTY IN REX=13138.   UNCERTAINTY IN F=0.05034 IN RATIO

RUN 072177-2 *** DISCRETE HOLE RIG *** NAS-3-14336 STANTON NUMBER DATA

TADB= 28.88 DEG C UINF= 17.05 M/S TINF= 28.75 DEG C
RHO= 1.164 KG/M3 VISC= 0.15823E-04 M2/S XVO= 23.3 CM
CP= 1013. J/KGK PR= 0.715

250C FSL M=0.90 P/D=5 TH=1 W/VCF(OPTIMUM)

PLATE	X	REX	TO	REENTH	STANTON NO	DST	DREEN	M	F	T2	THETA	DTH
1	127.8	0.11262E 07	42.46	0.17683E 04	0.23581E-02	0.554E-04	8.					
2	132.8	0.11609E 07	42.40	0.18912E 04	0.21301E-02	0.543E-04	39.	0.79	0.0256	42.19	0.984	0.023
3	137.9	0.12356E 07	42.31	0.33908E 04	0.22281E-02	0.552E-04	65.	0.84	0.0273	42.11	0.985	0.023
4	143.0	0.12904E 07	42.27	0.49851E 04	0.21885E-02	0.552E-04	89.	0.80	0.0260	42.14	0.990	0.023
5	148.1	0.13451E 07	42.35	0.65085E 04	0.19169E-02	0.535E-04	105.	0.81	0.0263	42.32	0.998	0.023
6	153.2	0.13555E 07	42.27	0.80454E 04	0.17847E-02	0.531E-04	120.	0.81	0.0263	42.39	1.009	0.023
7	158.2	0.14546E 07	42.40	0.95877E 04	0.14334E-02	0.511E-04	132.	0.82	0.0266	42.38	0.998	0.023
8	163.3	0.15094E 07	42.33	0.11106E 05	0.13703E-02	0.511E-04	144.	0.79	0.0255	42.50	1.013	0.023
9	168.4	0.15641E 07	42.44	0.12597E 05	0.13311E-02	0.506E-04	154.	0.81	0.0261	42.38	0.995	0.023
10	173.5	0.16189E 07	42.46	0.14091E 05	0.12793E-02	0.503E-04	164.	0.80	0.0259	42.40	0.995	0.023
11	178.6	0.16736E 07	42.54	0.15569E 05	0.12087E-02	0.498E-04	173.	0.83	0.0270	42.33	0.985	0.022
12	183.6	0.17284E 07	42.61	0.17088E 05	0.11463E-02	0.493E-04	182.	0.80	0.0259	42.33	0.979	0.022
13	187.5	0.17700E 07	40.89	0.18524E 05	0.10433E-02	0.381E-04	186.					
14	190.1	0.17982E 07	40.64	0.18553E 05	0.96237E-03	0.439E-04	186.					
15	192.7	0.18264E 07	40.64	0.18581E 05	0.10198E-02	0.442E-04	186.					
16	195.4	0.18547E 07	40.74	0.18609E 05	0.97957E-03	0.434E-04	186.					
17	198.0	0.18830E 07	40.74	0.18637E 05	0.10282E-02	0.446E-04	186.					
18	200.6	0.19112E 07	40.72	0.18666E 05	0.10476E-02	0.456E-04	186.					
19	203.2	0.19354E 07	40.58	0.18696E 05	0.10561E-02	0.443E-04	186.					
20	205.8	0.19676E 07	40.60	0.18727E 05	0.11313E-02	0.469E-04	186.					
21	208.5	0.19958E 07	40.55	0.18758E 05	0.10963E-02	0.461E-04	186.					
22	211.1	0.20240E 07	40.53	0.18790E 05	0.11557E-02	0.489E-04	186.					
23	213.7	0.20522E 07	40.45	0.18824E 05	0.12083E-02	0.503E-04	186.					
24	216.3	0.20805E 07	40.43	0.18858E 05	0.11999E-02	0.505E-04	186.					
25	218.9	0.21089E 07	40.45	0.18892E 05	0.12531E-02	0.523E-04	186.					
26	221.6	0.21371E 07	40.30	0.18927E 05	0.12253E-02	0.503E-04	186.					
27	224.2	0.21653E 07	40.43	0.18963E 05	0.13279E-02	0.542E-04	186.					
28	226.8	0.21934E 07	40.45	0.19002E 05	0.13911E-02	0.564E-04	186.					
29	229.4	0.22216E 07	40.32	0.19040E 05	0.12974E-02	0.517E-04	186.					
30	232.0	0.22498E 07	40.49	0.19077E 05	0.13692E-02	0.561E-04	186.					
31	234.6	0.22780E 07	40.45	0.19116E 05	0.14087E-02	0.566E-04	186.					
32	237.3	0.23064E 07	40.34	0.19156E 05	0.13748E-02	0.556E-04	186.					
33	239.9	0.23347E 07	40.32	0.19195E 05	0.14079E-02	0.569E-04	186.					
34	242.5	0.23629E 07	40.07	0.19235E 05	0.14134E-02	0.552E-04	186.					
35	245.1	0.23911E 07	40.20	0.19276E 05	0.14627E-02	0.602E-04	186.					
36	247.8	0.24193E 07	40.20	0.19315E 05	0.13216E-02	0.608E-04	186.					

UNCERTAINTY IN REX=13030. UNCERTAINTY IN F=0.05034 IN RATIO

.106

RUN 072177-1 *** DISCRETE HOLE RIG *** NAS-3-14336 STANTON NUMBER DATA

2500 FSL M=0.90 P/D=5 TH=0 W/VCF(OPTIMUM)

RUN 072177-2 *** DISCRETE HOLE RIG *** NAS-3-14336 STANTON NUMBER DATA

2500 FSL M=0.90 P/D=5 TH=1 W/VCF(OPTIMUM)

LINEAR SUPERPOSITION IS APPLIED TO STANTON NUMBER DATA FROM
RUN NUMBERS 072177-1 AND 072177-2 TO OBTAIN STANTON NUMBER DATA AT TH=0 AND TH=1

PLATE	REXCOL	RE DEL2	ST(TH=0)	REXHOT	RE DEL2	ST(TH=1)	ETA	STCR	F-COL	STHR	F-HOT	LOGR
1	1135471.0	1783.0	0.002112	1126150.0	1768.3	0.002358	UUUUU	1.000	0.0000	1.000	0.0000	1.000
2	1190671.0	1859.6	0.002113	1180897.0	1891.2	0.002130	*****	0.901	0.0298	0.908	0.0256	4.256
3	1245872.0	2029.1	0.002580	1235645.0	3413.1	0.002223	0.139	1.087	0.0303	0.936	0.0273	4.447
4	1301072.0	2177.8	0.002807	1290392.0	5029.2	0.002181	0.223	1.183	0.0296	0.919	0.0260	4.285
5	1356273.0	2330.2	0.002716	1345139.0	6566.3	0.001912	0.296	1.169	0.0295	0.823	0.0263	4.204
6	1411473.0	2476.0	0.002638	1399886.0	8105.9	0.001788	0.322	1.169	0.0292	0.792	0.0263	4.235
7	1466673.0	2621.2	0.002551	1454634.0	9635.4	0.001437	0.437	1.137	0.0296	0.641	0.0264	3.970
8	1521874.0	2762.7	0.002576	1509381.0	11157.2	0.001377	0.465	1.162	0.0294	0.621	0.0255	3.875
9	1577074.0	2904.6	0.002564	1564128.0	12629.8	0.001336	0.479	1.180	0.0294	0.615	0.0261	3.975
10	1632274.0	3044.2	0.002493	1618875.0	14130.6	0.001273	0.489	1.157	0.0292	0.591	0.0259	3.927
11	1687475.0	3183.3	0.002548	1673623.0	15615.4	0.001195	0.531	1.199	0.0299	0.563	0.0270	4.019
12	1742675.0	3315.9	0.002256	1728370.0	17156.2	0.001126	0.501	1.080	0.0293	0.529	0.0259	3.832
13	1784627.0	3420.6	0.002985	1769978.0	18623.2	0.001008	0.662	1.520		0.513		
14	1813056.0	3502.1	0.002742	1798173.0	18647.6	0.000930	0.661	1.453		0.493		
15	1841484.0	3582.4	0.002903	1826368.0	18674.6	0.000985	0.661	1.464		0.497		
16	1870050.0	3660.0	0.002547	1854699.0	18702.0	0.000951	0.627	1.388		0.518		
17	1898616.0	3732.3	0.002531	1883031.0	18729.5	0.001001	0.605	1.348		0.533		
18	1927044.0	3804.2	0.002527	1911226.0	18758.0	0.001021	0.596	1.350		0.545		
19	1955472.0	3874.0	0.002377	1939423.0	18787.0	0.001032	0.566	1.327		0.576		
20	1983900.0	3942.3	0.002423	1967615.0	18817.2	0.001108	0.543	1.301		0.594		
21	2012329.0	4010.5	0.002363	1995810.0	18848.0	0.001073	0.546	1.298		0.569		
22	2040757.0	4077.5	0.002345	2024005.0	18879.1	0.001134	0.517	1.285		0.621		
23	2069185.0	4144.1	0.002338	2052200.0	18911.9	0.001108	0.492	1.225		0.622		
24	2097751.0	4239.2	0.002236	2080531.0	18945.3	0.001181	0.472	1.258		0.665		
25	2126317.0	4273.2	0.002260	2108863.0	18979.4	0.001235	0.454	1.220		0.666		
26	2154748.0	4336.4	0.002181	2137058.0	19013.9	0.001208	0.446	1.274		0.706		
27	2183174.0	4399.2	0.002233	2165253.0	19049.4	0.001311	0.413	1.196		0.702		
28	2211602.0	4463.2	0.002266	2193447.0	19087.4	0.001375	0.393	1.191		0.723		
29	2240031.0	4525.8	0.002131	2221643.0	19124.9	0.001282	0.398	1.191		0.717		
30	2268455.0	4586.9	0.002167	2249837.0	19162.1	0.001355	0.375	1.201		0.750		
31	2296887.0	4648.9	0.002187	2278032.0	19200.9	0.001394	0.362	1.187		0.757		
32	2325453.0	4710.3	0.002131	2306364.0	19239.8	0.001361	0.361	1.186		0.758		
33	2354015.0	4770.9	0.002126	2334695.0	19278.7	0.001395	0.344	1.181		0.774		
34	2382447.0	4831.7	0.002144	2362890.0	19318.1	0.001400	0.347	1.203		0.785		
35	2410875.0	4893.2	0.002175	2391085.0	19358.6	0.001470	0.324	1.183		0.800		
36	2439303.0	4951.5	0.001922	2419280.0	19397.9	0.001311	0.318	1.209		0.824		

STANTON NUMBER RATIO BASED ON EXPERIMENTAL FLAT PLATE VALUE AT SAME X LOCATION

STANTON NUMBER RATIO FOR TH=1 IS CONVERTED TO COMPARABLE TRANSPIRATION VALUE
USING ALOG(1 + B)/B EXPRESSION IN THE BLOWN SECTION

RUN 082977-1 *** DISCRETE HOLE RIG *** NAS-3-14336 STANTON NUMBER DATA

TADB= 27.25 DEG C UINF= 16.80 M/S TINF= 27.12 DEG C
RHO= 1.164 KG/M3 VISC= 0.15723E-04 M2/S XVO= 26.1 CM
CP= 1016. J/KGK PR= 0.717

2500 FSL M=1.25 P/D=5 TH=0 W/VCF(OPTIMUM)

PLATE	X	REX	TO	REENTH	STANTON NO	DST	DREEN	M	F	T2	THETA	DTM
1	127.8	0.10858E 07	37.79	0.17531E 04	0.25346E-02	0.722E-04	5.					
2	132.8	0.11401E 07	37.77	0.18898E 04	0.25302E-02	0.726E-04	32.	1.24	0.0401	27.68	0.052	0.029
3	137.9	0.11944E 07	37.79	0.21456E 04	0.26869E-02	0.736E-04	54.	1.19	0.0385	27.75	0.059	0.029
4	143.0	0.12486E 07	37.73	0.242[illegible]E 04	0.29428E-02	0.764E-04	70.	1.26	0.0407	27.72	0.056	0.029
5	148.1	0.13025E 07	37.79	0.27[illegible]E 04	0.30522E-02	0.765E-04	83.	1.20	0.0389	27.84	0.067	0.029
6	153.2	0.13572E 07	37.73	0.301[illegible] 04	0.30361E-02	0.767E-04	94.	1.28	0.0415	27.72	0.056	0.029
7	158.2	0.14115E 07	37.79	0.33340E 04	0.28814E-02	0.751E-04	104.	1.21	0.0391	27.80	0.063	0.029
8	163.3	0.14657E 07	37.79	0.35994E 04	0.28699E-02	0.750E-04	113.	1.24	0.0400	27.72	0.056	0.029
9	168.4	0.15200E 07	37.77	0.38728E 04	0.29181E-02	0.755E-04	122.	1.19	0.0385	27.80	0.063	0.029
10	173.5	0.15743E 07	37.60	0.41606E 04	0.28369E-02	0.758E-04	129.	1.24	0.0402	27.70	0.055	0.029
11	178.6	0.16286E 07	37.75	0.44336E 04	0.28381E-02	0.750E-04	137.	1.20	0.0388	27.91	0.074	0.029
12	183.6	0.16828E 07	37.71	0.47433E 04	0.28672E-02	0.755E-04	144.	1.24	0.0400	27.76	0.060	0.029
13	187.5	0.17241E 07	35.28	0.49855E 04	0.27537E-02	0.939E-04	147.					
14	190.1	0.17520E 07	34.84	0.50682E 04	0.28395E-02	0.111E-03	147.					
15	192.7	0.17800E 07	34.84	0.51487E 04	0.29144E-02	0.113E-03	147.					
16	195.4	0.18081E 07	35.10	0.52224E 04	0.26411E-02	0.105E-03	147.					
17	198.0	0.18362E 07	35.10	0.53303E 04	0.26376E-02	0.104E-03	147.					
18	200.6	0.18641E 07	35.10	0.53736E 04	0.26327E-02	0.102E-03	147.					
19	203.2	0.18921E 07	35.24	0.54437E 04	0.24046E-02	0.949E-04	147.					
20	205.8	0.19200E 07	35.31	0.55114E 04	0.24332E-02	0.953E-04	147.					
21	208.5	0.19480E 07	35.35	0.55783E 04	0.23463E-02	0.921E-04	147.					
22	211.1	0.19759E 07	35.47	0.56427E 04	0.22800E-02	0.910E-04	147.					
23	213.7	0.20039E 07	35.41	0.57061E 04	0.22655E-02	0.903E-04	147.					
24	216.3	0.20320E 07	35.47	0.57682E 04	0.21751E-02	0.880E-04	147.					
25	218.9	0.20601E 07	35.54	0.58292E 04	0.21371E-02	0.886E-04	147.					
26	221.6	0.20880E 07	35.43	0.58891E 04	0.20919E-02	0.837E-04	147.					
27	224.2	0.21160E 07	35.66	0.59481E 04	0.21216E-02	0.860E-04	147.					
28	226.8	0.21439E 07	35.73	0.60074E 04	0.21232E-02	0.858E-04	147.					
29	229.4	0.21719E 07	35.62	0.60658E 04	0.20486E-02	0.813E-04	147.					
30	232.0	0.21998E 07	35.81	0.61231E 04	0.20491E-02	0.839E-04	147.					
31	234.6	0.22278E 07	35.79	0.61806E 04	0.20563E-02	0.833E-04	147.					
32	237.3	0.22559E 07	35.68	0.62372E 04	0.19902E-02	0.812E-04	147.					
33	239.9	0.22839E 07	35.68	0.62928E 04	0.19814E-02	0.815E-04	147.					
34	242.5	0.23119E 07	35.43	0.63482E 04	0.19781E-02	0.791E-04	147.					
35	245.1	0.23399E 07	35.60	0.64040E 04	0.20129E-02	0.841E-04	147.					
36	247.8	0.23678E 07	35.60	0.64567E 04	0.17502E-02	0.826E-04	147.					

UNCERTAINTY IN REX=12945. UNCERTAINTY IN F=0.05037 IN RATIO

RUN 082977-2 *** DISCRETE HOLE RIG *** NAS-3-14336   STANTON NUMBER DATA

TADB= 31.81 DEG C   UINF=   16.95 M/S   TINF= 31.68 DEG C
RHO= 1.144 KG/M3   VISC= 0.16138E-04 M2/S   XVO=   26.1 CM
CP=   1015. J/KGK   PR=   0.719

2500 HSL M=1.25 P/D=5 TH=1 W/VCF(OPTIMUM)

PLATE	X	REX	TO	REENTH	STANTON NO	DST	DREEN	M	F	T2	THETA	DTH
1	127.8	0.10672E 07	41.53	0.17230E 04	0.24724E-02	0.781E-04	5.					
2	132.8	0.11205E 07	41.68	0.18533E 04	0.24131E-02	0.766E-04	57.	1.14	0.0371	41.34	0.965	0.031
3	137.9	0.11738E 07	41.59	0.38972E 04	0.26972E-02	0.794E-04	97.	1.08	0.0349	41.21	0.961	0.031
4	143.0	0.12272E 07	41.55	0.58314E 04	0.27354E-02	0.800E-04	125.	1.14	0.0370	41.20	0.965	0.031
5	148.1	0.12805E 07	41.57	0.78801E 04	0.26314E-02	0.791E-04	148.	1.09	0.0352	41.38	0.981	0.031
6	153.2	0.13339E 07	41.59	0.98530E 04	0.22870E-02	0.764E-04	169.	1.16	0.0377	41.54	0.994	0.031
7	158.2	0.13872E 07	41.53	0.11967E 05	0.19885E-02	0.748E-04	188.	1.09	0.0353	41.51	0.998	0.032
8	163.3	0.14406E 07	41.51	0.13951E 05	0.18516E-02	0.741E-04	205.	1.12	0.0364	41.68	1.017	0.032
9	168.4	0.14939E 07	41.59	0.16021E 05	0.18382E-02	0.733E-04	220.	1.06	0.0344	41.55	0.996	0.031
10	173.5	0.15473E 07	41.55	0.17943E 05	0.17534E-02	0.733E-04	233.	1.10	0.0355	41.61	1.006	0.032
11	178.6	0.16006E 07	41.68	0.19535E 05	0.14907E-02	0.710E-04	246.	1.09	0.0353	41.50	0.981	0.031
12	183.6	0.16539E 07	41.63	0.21858E 05	0.13471E-02	0.707E-04	259.	1.10	0.0358	41.41	0.978	0.031
13	187.5	0.16945E 07	39.03	0.23768E 05	0.58682E-03	0.420E-04	265.					
14	190.1	0.17220E 07	38.59	0.23784E 05	0.58761E-03	0.555E-04	265.					
15	192.7	0.17494E 07	38.59	0.23800E 05	0.58427E-03	0.519E-04	265.					
16	195.4	0.17770E 07	38.57	0.23817E 05	0.63037E-03	0.525E-04	265.					
17	198.0	0.18046E 07	38.57	0.23835E 05	0.65687E-03	0.533E-04	265.					
18	200.6	0.18321E 07	38.57	0.23853E 05	0.65411E-03	0.540E-04	265.					
19	203.2	0.18596E 07	38.46	0.23871E 05	0.72007E-03	0.528E-04	265.					
20	205.8	0.18871E 07	38.46	0.23892E 05	0.76083E-03	0.535E-04	265.					
21	208.5	0.19145E 07	38.49	0.23912E 05	0.73172E-03	0.539E-04	265.					
22	211.1	0.19420E 07	38.48	0.23933E 05	0.78372E-03	0.573E-04	265.					
23	213.7	0.19655E 07	38.48	0.23955E 05	0.81486E-03	0.583E-04	265.					
24	216.3	0.19971E 07	38.48	0.23977E 05	0.80510E-03	0.589E-04	265.					
25	218.9	0.20247E 07	38.48	0.24001E 05	0.87978E-03	0.597E-04	265.					
26	221.6	0.20522E 07	38.44	0.24025E 05	0.86225E-03	0.591E-04	265.					
27	224.2	0.20796E 07	38.51	0.24049E 05	0.92473E-03	0.607E-04	265.					
28	226.8	0.21071E 07	38.53	0.24075E 05	0.97355E-03	0.614E-04	265.					
29	229.4	0.21346E 07	38.49	0.24101E 05	0.91881E-03	0.586E-04	265.					
30	232.0	0.21620E 07	38.53	0.24128E 05	0.99271E-03	0.631E-04	265.					
31	234.6	0.21895E 07	38.51	0.24155E 05	0.10275E-02	0.630E-04	265.					
32	237.3	0.22171E 07	38.48	0.24183E 05	0.99391E-03	0.632E-04	265.					
33	239.9	0.22447E 07	38.46	0.24211E 05	0.10230E-02	0.626E-04	265.					
34	242.5	0.22722E 07	38.26	0.24239E 05	0.10146E-02	0.611E-04	265.					
35	245.1	0.22957E 07	38.42	0.24268E 05	0.10818E-02	0.673E-04	265.					
36	247.8	0.23271E 07	38.42	0.24295E 05	0.92103E-03	0.667E-04	265.					

UNCERTAINTY IN REX=12723.   UNCERTAINTY IN F=0.05037 IN RATIO

RUN 082977-1 *** DISCRETE HOLE RIG *** NAS-3-14336 STANTON NUMBER DATA

2500 HSL M=1.25 P/D=5 TH=0 W/VCF(OPTIMUM)

RUN 082977-2 *** DISCRETE HOLE RIG *** NAS-3-14336 STANTON NUMBER DATA

2500 HSL M=1.25 P/D=5 TH=1 W/VCF(OPTIMUM)

LINEAR SUPERPOSITION IS APPLIED TO STANTON NUMBER DATA FROM
RUN NUMBERS 082977-1 AND 082977-2 TO OBTAIN STANTON NUMBER DATA AT TH=0 AND TH=1

PLATE	REXCOL	RE DEL2	ST(TH=0)	REXHOT	RE DEL2	ST(TH=1)	ETA	STCR	F-COL	STHR	F-HOT	LOGB
1	1085798.0	1753.1	0.002505	1067152.0	1723.0	0.002472	UUUUU	1.000	0.0000	1.000	0.0000	1.000
2	1140074.0	1889.9	0.002537	1120496.0	1853.2	0.002409	0.051	1.082	0.0401	1.027	0.0371	5.650
3	1194351.0	2031.7	0.002688	1173840.0	3566.0	0.002698	*****	1.132	0.0385	1.136	0.0349	5.578
4	1248627.0	2186.4	0.003009	1227184.0	5972.0	0.002725	0.094	1.268	0.0407	1.148	0.0370	5.823
5	1302903.0	2351.6	0.003081	1280529.0	8089.9	0.002619	0.150	1.326	0.0389	1.127	0.0352	5.675
6	1357180.0	2519.0	0.003086	1333873.0	10097.9	0.002277	0.262	1.368	0.0415	1.009	0.0377	5.832
7	1411456.0	2682.5	0.002938	1387217.0	12222.8	0.001985	0.324	1.310	0.0391	0.885	0.0353	5.370
8	1465732.0	2841.8	0.002934	1440561.0	14210.6	0.001860	0.366	1.323	0.0400	0.839	0.0364	5.424
9	1520009.0	3002.5	0.002998	1493906.0	16243.2	0.001816	0.392	1.375	0.0385	0.836	0.0344	5.289
10	1574285.0	3161.6	0.002873	1547250.0	18178.7	0.001754	0.389	1.334	0.0402	0.814	0.0355	5.395
11	1628562.0	3319.1	0.002931	1600594.0	20159.5	0.001481	0.495	1.380	0.0388	0.697	0.0353	5.172
12	1682838.0	3479.5	0.002978	1653939.0	22117.0	0.001313	0.559	1.400	0.0400	0.617	0.0358	5.030
13	1724088.0	3601.1	0.002912	1694480.0	24066.9	0.000538	0.815	1.483		0.274		
14	1752040.0	3683.9	0.003004	1721953.0	24081.7	0.000537	0.821	1.542		0.285		
15	1779593.0	3765.1	0.003085	1749425.0	24096.4	0.000532	0.828	1.556		0.268		
16	1808063.0	3851.3	0.002788	1777030.0	24111.8	0.000585	0.790	1.519		0.319		
17	1836168.0	3929.2	0.002782	1804636.0	24128.2	0.000613	0.780	1.482		0.326		
18	1864121.0	4006.6	0.002745	1832108.0	24145.1	0.000611	0.778	1.467		0.326		
19	1892073.0	4080.3	0.002528	1859580.0	24162.8	0.000682	0.730	1.411		0.381		
20	1920025.0	4151.5	0.002556	1887053.0	24182.2	0.000723	0.717	1.371		0.388		
21	1947978.0	4221.7	0.002464	1914525.0	24201.7	0.000696	0.718	1.353		0.382		
22	1975930.0	4289.3	0.002368	1941998.0	24221.6	0.000751	0.683	1.297		0.411		
23	2003883.0	4355.7	0.002372	1969470.0	24242.7	0.000782	0.670	1.243		0.410		
24	2031570.0	4420.7	0.002275	1997075.0	24264.1	0.000774	0.660	1.281		0.436		
25	2060558.0	4484.5	0.002283	2024681.0	24286.4	0.000851	0.627	1.232		0.459		
26	2088011.0	4546.9	0.002182	2052153.0	24309.6	0.000835	0.617	1.275		0.488		
27	2115963.0	4608.4	0.002209	2079626.0	24333.4	0.000898	0.594	1.183		0.481		
28	2143915.0	4670.1	0.002205	2107098.0	24358.8	0.000948	0.570	1.159		0.498		
29	2171868.0	4730.8	0.002131	2134571.0	24384.1	0.000894	0.581	1.191		0.499		
30	2199820.0	4790.4	0.002126	2162043.0	24409.8	0.000969	0.544	1.178		0.537		
31	2227773.0	4850.0	0.002132	2189515.0	24436.9	0.001004	0.529	1.157		0.545		
32	2255866.0	4908.7	0.002063	2217120.0	24464.1	0.000972	0.529	1.148		0.541		
33	2283548.0	4966.3	0.002052	2244725.0	24491.2	0.001002	0.512	1.139		0.556		
34	2311501.0	5023.6	0.002049	2272198.0	24518.6	0.000993	0.515	1.149		0.557		
35	2339453.0	5081.4	0.002081	2299671.0	24546.9	0.001061	0.490	1.132		0.577		
36	2367405.0	5135.9	0.001811	2327143.0	24573.9	0.000902	0.502	1.139		0.567		

STANTON NUMBER RATIO BASED ON EXPERIMENTAL FLAT PLATE VALUE AT SAME X LOCATION

STANTON NUMBER RATIO FOR TH=1 IS CONVERTED TO COMPARABLE TRANSPIRATION VALUE
USING ALOG(1 + B)/B EXPRESSION IN THE BLOWN SECTION

PUAC03177 VELOCITY AND TEMPERATURE PROFILES

RED =	0.11524E 07	REM =	2615.	REH =	1890.
XVO =	21.48 CM	DEL2 =	0.241 CM	DEH2 =	0.175 CM
UINF =	16.88 M/S	DEL99=	3.175 CM	DELT99 =	1.665 CM
VISC =	0.15564E-04 M2/S	DEL1 =	0.351 CM	UINF =	16.91 M/S
PORT =	3	H =	1.454	VISC =	0.15672E-04 M2/S
XLOC =	127.76 CM	CF/2 =	0.17028E-02	TINF =	25.87 DEG C
				TPLATE =	38.23 DEG C

Y(CM)	Y/DEL	U(M/S)	U/UINF	Y+	U+	Y(CM)	T(DEG C)	TBAR	TBAR
0.025	0.008	8.28	0.491	11.4	11.89	0.0127	37.51	0.058	0.942
0.030	0.010	8.60	0.510	13.6	12.35	0.0203	37.33	0.073	0.927
0.051	0.016	8.94	0.530	22.7	12.84	0.0305	37.21	0.082	0.918
0.056	0.018	9.35	0.554	25.0	13.42	0.0381	37.16	0.087	0.913
0.043	0.014	9.56	0.566	19.3	13.72	0.0508	37.11	0.091	0.909
0.076	0.024	9.80	0.581	34.1	14.07	0.0635	36.89	0.109	0.891
0.089	0.028	10.01	0.593	39.8	14.37	0.0762	33.50	0.382	0.618
0.102	0.032	10.14	0.601	45.5	14.57	0.0889	32.03	0.501	0.499
0.114	0.036	10.35	0.613	51.1	14.86	0.1143	30.74	0.606	0.394
0.127	0.040	10.51	0.623	56.8	15.09	0.1397	30.07	0.660	0.340
0.137	0.043	10.57	0.626	61.4	15.18	0.1651	29.72	0.689	0.311
0.157	0.050	10.76	0.638	70.5	15.45	0.1905	29.44	0.711	0.289
0.183	0.058	10.96	0.649	81.8	15.74	0.2159	29.23	0.728	0.272
0.208	0.066	11.18	0.663	93.2	16.06	0.2540	28.94	0.752	0.248
0.246	0.078	11.47	0.680	110.2	16.47	0.2921	28.75	0.767	0.233
0.297	0.094	11.76	0.697	133.0	16.89	0.3302	28.53	0.785	0.215
0.348	0.110	12.06	0.714	155.7	17.31	0.3556	28.43	0.793	0.207
0.411	0.130	12.37	0.733	184.1	17.77	0.3810	28.35	0.800	0.200
0.488	0.154	12.74	0.755	218.2	18.29	0.4191	28.21	0.811	0.185
0.577	0.182	13.05	0.774	258.0	18.75	0.4572	28.07	0.822	0.178
0.704	0.222	13.59	[illegible]	314.8	19.49	0.4953	27.94	0.833	0.167
0.831	0.262	14.01	0.830	371.6	20.11	0.5461	27.80	0.844	0.156
1.021	0.322	14.61	0.865	456.9	20.97	0.6350	27.56	0.863	0.137
1.212	0.382	15.14	0.897	542.1	21.74	0.7620	27.26	0.888	0.112
1.402	0.442	15.63	0.926	627.3	22.44	0.8890	27.01	0.908	0.092
1.593	0.502	16.05	0.951	712.6	23.04	1.0160	26.78	0.927	0.073
1.783	0.562	16.42	0.973	797.8	23.58	1.0795	26.68	0.935	0.065
1.847	0.582	16.46	0.975	826.2	23.63	1.2065	26.50	0.949	0.051
1.974	0.622	16.64	0.986	883.0	23.90	1.3970	26.27	0.968	0.032
2.037	0.642	16.68	0.989	911.4	23.96	1.5240	26.14	0.978	0.022
2.101	0.662	16.73	0.992	939.9	24.03	1.6510	26.02	0.988	0.012
2.228	0.702	16.80	0.995	996.7	24.12	1.7145	25.95	0.993	0.007
2.291	0.722	16.83	0.997	1025.1	24.16	1.7780	25.91	0.997	0.003
2.355	0.742	16.84	0.998	1053.5	24.19	1.8415	25.88	1.000	0.000
2.482	0.782	16.88	1.000	1110.3	24.23				

RUN 083177 *** DISCRETE HOLE RIG *** NAS-3-14336 STANTON NUMBER DATA

TADB= 25.38 DEG C UINF= 16.89 M/S TINF= 25.26 DEG C
RHO= 1.165 KG/M3 VISC= 0.15616E-04 M2/S XVO= 21.5 CM
CP= 1013. J/KGK PR= 0.715

26CC FSL FLAT PLATE P/D=10

PLATE	X	REX	TC	REENTH	STANTONNO	DST	DREEN	ST(THEO)	RATIO
1	127.8	0.11492E 07	38.13	0.18951E 04	0.23352E-02	0.590E-04	8.	0.20699E-02	1.128
2	132.8	0.12041E 07	38.15	0.20210E 04	0.22474E-02	0.584E-04	9.	0.20506E-02	1.096
3	137.9	0.12590E 07	38.15	0.21429E 04	0.21908E-02	0.580E-04	9.	0.20324E-02	1.078
4	143.0	0.13140E 07	38.11	0.22639E 04	0.22166E-02	0.583E-04	9.	0.20151E-02	1.100
5	148.1	0.13689E 07	38.17	0.23832E 04	0.21243E-02	0.576E-04	9.	0.19987E-02	1.063
6	153.2	0.14238E 07	38.21	0.24982E 04	0.20644E-02	0.571E-04	10.	0.19830E-02	1.041
7	158.2	0.14788E 07	38.17	0.26126E 04	0.21003E-02	0.574E-04	10.	0.19681E-02	1.067
8	163.3	0.15337E 07	38.15	0.27263E 04	0.20381E-02	0.572E-04	10.	0.19539E-02	1.043
9	168.4	0.15886E 07	38.13	0.28369E 04	0.19901E-02	0.570E-04	10.	0.19401E-02	1.026
10	173.5	0.16436E 07	39.13	0.29464E 04	0.19966E-02	0.570E-04	11.	0.19269E-02	1.036
11	178.6	0.16985E 07	36.15	0.30558E 04	0.19847E-02	0.569E-04	11.	0.19143E-02	1.037
12	183.6	0.17534E 07	38.13	0.31631E 04	0.19253E-02	0.567E-04	11.	0.19021E-02	1.012
13	187.5	0.17952E 07	37.43	0.32420E 04	0.18340E-02	0.650E-04	11.	0.18932E-02	0.969
14	190.1	0.18235E 07	37.18	0.32945E 04	0.18704E-02	0.694E-04	11.	0.18873E-02	0.991
15	192.7	0.18517E 07	37.18	0.33483E 04	0.19312E-02	0.705E-04	11.	0.18815E-02	1.026
16	195.4	0.18802E 07	37.39	0.34014E 04	0.18172E-02	0.679E-04	12.	0.18758E-02	0.969
17	198.0	0.19086E 07	37.39	0.34534E 04	0.18542E-02	0.685E-04	12.	0.18702E-02	0.991
18	200.6	0.19369E 07	37.39	0.35060E 04	0.18638E-02	0.689E-04	12.	0.18647E-02	1.000
19	203.2	0.19652E 07	37.37	0.35574E 04	0.17670E-02	0.652E-04	12.	0.18593E-02	0.950
20	205.8	0.19935E 07	37.37	0.36090E 04	0.18713E-02	0.684E-04	12.	0.18540E-02	1.009
21	208.5	0.20218E 07	37.37	0.36606E 04	0.17780E-02	0.657E-04	12.	0.18487E-02	0.962
22	211.1	0.20500E 07	37.41	0.37115E 04	0.18112E-02	0.679E-04	12.	0.18436E-02	0.982
23	213.7	0.20783E 07	37.30	0.37632E 04	0.18413E-02	0.680E-04	12.	0.18386E-02	1.002
24	216.3	0.21068E 07	37.35	0.38147E 04	0.17915E-02	0.673E-04	12.	0.18336E-02	0.977
25	218.9	0.21352E 07	37.37	0.38659E 04	0.18286E-02	0.688E-04	12.	0.18287E-02	1.000
26	221.6	0.21635E 07	37.16	0.39167E 04	0.17549E-02	0.645E-04	12.	0.18239E-02	0.962
27	224.2	0.21918E 07	37.43	0.39675E 04	0.18362E-02	0.685E-04	12.	0.18191E-02	1.009
28	226.8	0.22201E 07	37.62	0.40196E 04	0.18350E-02	0.694E-04	13.	0.18145E-02	1.014
29	229.4	0.22484E 07	37.39	0.40712E 04	0.18066E-02	0.655E-04	13.	0.18099E-02	0.998
30	232.0	0.22766E 07	37.64	0.41220E 04	0.17799E-02	0.675E-04	13.	0.18054E-02	0.986
31	234.6	0.23049E 07	37.60	0.41728E 04	0.18046E-02	0.674E-04	13.	0.18009E-02	1.002
32	237.3	0.23334E 07	37.47	0.42229E 04	0.17367E-02	0.652E-04	13.	0.17965E-02	0.967
33	239.9	0.23618E 07	37.41	0.42723E 04	0.17532E-02	0.663E-04	13.	0.17921E-02	0.978
34	242.5	0.23901E 07	37.09	0.43217E 04	0.17331E-02	0.630E-04	13.	0.17879E-02	0.969
35	245.1	0.24184E 07	37.37	0.43713E 04	0.17653E-02	0.674E-04	13.	0.17837E-02	0.992
36	247.8	0.24467E 07	37.37	0.44181E 04	0.15368E-02	0.678E-04	13.	0.17795E-02	0.864

///

RUN 090977-1 *** DISCRETE HOLE RIG *** NAS-3-14336   STANTON NUMBER DATA

TADB= 22.86 DEG C   UINF=   15.67 M/S   TINF= 22.74 DEG C
RHO= 1.182 KG/M3   VISC= 0.15352E-04 M2/S   XVO=   21.5 CM
CP=   1012. J/KGK   PR=   0.716

2600 MSL M=0.4 TH=0 P/D=10 W/VCP(OPTIMUM)

PLATE	X	REX	TO	REENTH	STANTON NO	DST	DREEN	M	F	T2	THETA	DTH
1	127.8	0.11540E 07	36.61	0.19031E 04	0.24275E-02	0.556E-04	8.					
2	132.9	0.12092E 07	36.57	0.20308E 04	0.22015E-02	0.545E-04	9.	0.43	0.0034	26.40	0.255	0.022
3	137.9	0.12643E 07	36.53	0.22052E 04	0.22932E-02	0.551E-04	10.	0.00	0.0034	36.53	0.255	0.023
4	143.0	0.13195E 07	36.53	0.23798E 04	0.22092E-02	0.546E-04	11.	0.52	0.0042	26.27	0.256	0.022
5	148.1	0.13746E 07	36.55	0.25628E 04	0.22823E-02	0.550E-04	12.	0.00	0.0042	36.55	0.256	0.022
6	153.2	0.14298E 07	36.61	0.27481E 04	0.22915E-02	0.548E-04	12.	0.40	0.0032	26.38	0.253	0.021
7	158.2	0.14853E 07	36.61	0.29185E 04	0.22011E-02	0.543E-04	13.	0.00	0.0032	36.61	0.253	0.022
8	163.3	0.15401E 07	36.55	0.30841E 04	0.21201E-02	0.541E-04	14.	0.53	0.0043	26.28	0.257	0.022
9	168.3	0.15953E 07	36.55	0.32530E 04	0.21727E-02	0.544E-04	15.	0.00	0.0043	36.55	0.257	0.022
10	173.5	0.16505E 07	36.52	0.34388E 04	0.20071E-02	0.536E-04	15.	0.39	0.0032	26.36	0.253	0.022
11	178.6	0.17056E 07	36.63	0.35994E 04	0.21425E-02	0.539E-04	16.	0.00	0.0032	36.63	0.253	0.022
12	183.5	0.17503E 07	36.52	0.37614E 04	0.20589E-02	0.539E-04	16.	0.89	0.0040	26.35	0.248	0.022
13	187.5	0.18027E 07	34.40	0.38976E 04	0.17575E-02	0.577E-04	17.					
14	190.0	0.18311E 07	34.00	0.40022E 04	0.17707E-02	0.565E-04	17.					
15	192.7	0.18595E 07	34.00	0.40539E 04	0.18598E-02	0.692E-04	17.					
16	195.4	0.18881E 07	34.11	0.41054E 04	0.17555E-02	0.668E-04	17.					
17	198.0	0.19166E 07	34.11	0.41561E 04	0.17968E-02	0.674E-04	17.					
18	200.5	0.19450E 07	34.11	0.42071E 04	0.17836E-02	0.575E-04	17.					
19	203.2	0.19734E 07	34.06	0.42574E 04	0.17457E-02	0.651E-04	17.					
20	205.8	0.20016E 07	34.09	0.43077E 04	0.17917E-02	0.668E-04	17.					
21	208.5	0.20302E 07	34.07	0.43584E 04	0.17715E-02	0.661E-04	17.					
22	211.0	0.20587E 07	34.13	0.44097E 04	0.17713E-02	0.574E-04	17.					
23	213.7	0.20871E 07	34.04	0.44599E 04	0.18252E-02	0.684E-04	17.					
24	216.3	0.21156E 07	34.06	0.45107E 04	0.17452E-02	0.555E-04	17.					
25	218.9	0.21442E 07	34.11	0.45612E 04	0.18092E-02	0.588E-04	17.					
26	221.6	0.21726E 07	33.96	0.46124E 04	0.17973E-02	0.565E-04	17.					
27	224.2	0.22010E 07	34.15	0.46537E 04	0.18217E-02	0.688E-04	17.					
28	226.8	0.22294E 07	34.27	0.47158E 04	0.18442E-02	0.701E-04	17.					
29	229.8	0.22578E 07	34.06	0.47569E 04	0.17406E-02	0.645E-04	17.					
30	232.0	0.22862E 07	34.28	0.48172E 04	0.17079E-02	0.605E-04	18.					
31	234.5	0.23146E 07	34.27	0.48685E 04	0.18203E-02	0.687E-04	18.					
32	237.0	0.23432E 07	34.15	0.49195E 04	0.17603E-02	0.560E-04	18.					
33	239.9	0.23717E 07	34.11	0.49598E 04	0.17600E-02	0.679E-04	18.					
34	242.5	0.24001E 07	33.83	0.50202E 04	0.17639E-02	0.649E-04	18.					
35	245.0	0.24205E 07	34.06	0.50711E 04	0.18187E-02	0.702E-04	18.					
36	247.8	0.24569E 07	34.06	0.51103E 04	0.16150E-02	0.708E-04	18.					

UNCERTAINTY IN REX=13625.   UNCERTAINTY IN F=0.00037 IN RATIO

RUN 090977-2 ***DISCRETE HOLE RIG***NAS-3-14336 STANTON NUMBER DATA

TADB= 24.37 DEG C UINF= 15.71 M/S TINF= 24.05 DEG C
RHO= 1.176 KG/M3 VISC= 0.15473E-04 M2/S XVO= 21.5 CM
CP= 1013. J/KGK PR= 0.716

2500 HSL M=0.4 TH=1 P/D=10 S/TCP(OPTIMUM)

PLATE	X	REX	TO	REENTH	STANTON NO	DST	DREEN	M	F	T2	THETA	DTH
1	127.8	0.11480E 07	36.53	0.18932E 04	0.24455E-02	0.516E-04	8.					
2	132.3	0.12028E 07	36.57	0.20181E 04	0.21094E-02	0.594E-04	10.	0.33	0.0027	36.95	1.030	0.025
3	137.9	0.12577E 07	36.67	0.22837E 04	0.20355E-02	0.586E-04	12.	0.33	0.0027	36.67	1.000	0.025
4	143.0	0.13126E 07	36.63	0.25453E 04	0.19570E-02	0.583E-04	14.	0.45	0.0036	37.03	1.002	0.025
5	148.1	0.13575E 07	36.67	0.28548E 04	0.18774E-02	0.577E-04	16.	0.33	0.0036	36.67	1.002	0.025
6	153.2	0.14223E 07	36.67	0.31625E 04	0.18759E-02	0.577E-04	18.	0.34	0.0028	36.81	1.011	0.025
7	158.2	0.14772E 07	36.63	0.34144E 04	0.17303E-02	0.572E-04	19.	0.00	0.0028	36.63	1.011	0.025
8	163.3	0.15321E 07	36.61	0.36607E 04	0.16713E-02	0.570E-04	20.	0.45	0.0036	37.05	1.035	0.025
9	168.4	0.15870E 07	36.55	0.39579E 04	0.16530E-02	0.571E-04	22.	0.00	0.0035	36.55	1.005	0.025
10	173.5	0.16418E 07	36.67	0.42552E 04	0.16701E-02	0.557E-04	23.	0.33	0.0027	36.67	1.000	0.025
11	178.5	0.15967E 07	36.55	0.44921E 04	0.15897E-02	0.569E-04	24.	0.01	0.0027	36.55	1.000	0.025
12	183.6	0.17516E 07	36.53	0.47257E 04	0.15911E-02	0.573E-04	25.	0.41	0.0033	36.74	1.016	0.025
13	187.5	0.17933E 07	35.39	0.49709E 04	0.12692E-02	0.473E-04	26.					
14	190.0	0.18216E 07	35.09	0.51904E 04	0.13483E-02	0.554E-04	26.					
15	192.7	0.18498E 07	35.09	0.52300E 04	0.14457E-02	0.575E-04	26.					
16	195.3	0.18782E 07	35.14	0.52704E 04	0.14097E-02	0.555E-04	26.					
17	198.0	0.19066E 07	35.14	0.53110E 04	0.14617E-02	0.580E-04	26.					
18	200.5	0.19349E 07	35.14	0.53523E 04	0.14567E-02	0.584E-04	26.					
19	203.2	0.19631E 07	35.03	0.53936E 04	0.14613E-02	0.570E-04	26.					
20	205.8	0.19914E 07	35.05	0.54357E 04	0.15152E-02	0.590E-04	26.					
21	208.5	0.20197E 07	35.05	0.54782E 04	0.14932E-02	0.585E-04	26.					
22	211.0	0.20479E 07	35.01	0.55210E 04	0.15377E-02	0.607E-04	26.					
23	213.7	0.20762E 07	34.99	0.55549E 04	0.15673E-02	0.516E-04	26.					
24	215.3	0.21046E 07	35.03	0.56085E 04	0.15182E-02	0.606E-04	26.					
25	218.9	0.21330E 07	35.05	0.56520E 04	0.15655E-02	0.522E-04	26.					
26	221.5	0.21512E 07	34.89	0.56955E 04	0.15755E-02	0.610E-04	26.					
27	224.2	0.21895E 07	35.10	0.57410E 04	0.15710E-02	0.524E-04	26.					
28	225.8	0.22179E 07	35.14	0.57862E 04	0.16276E-02	0.641E-04	26.					
29	229.4	0.22460E 07	34.95	0.58310E 04	0.15758E-02	0.593E-04	26.					
30	232.0	0.22743E 07	35.14	0.58752E 04	0.15733E-02	0.633E-04	26.					
31	234.6	0.23025E 07	35.14	0.59205E 04	0.16075E-02	0.533E-04	26.					
32	237.3	0.23309E 07	35.01	0.59556E 04	0.15035E-02	0.623E-04	26.					
33	239.9	0.23593E 07	35.01	0.60105E 04	0.15977E-02	0.530E-04	26.					
34	242.5	0.23876E 07	34.74	0.60553E 04	0.15763E-02	0.604E-04	26.					
35	245.0	0.24156E 07	34.93	0.61000E 04	0.16417E-02	0.658E-04	26.					
36	247.8	0.24441E 07	34.93	0.61445E 04	0.14093E-02	0.659E-04	26.					

UNCERTAINTY IN REX=13554. UNCERTAINTY IN F=0.05037 IN RATIO

RUN 090977-1 *** DISCRETE HOLE RIG *** NAS-3-14336 STANTON NUMBER DATA

2670 NSL M=0.4 TH=0 P/D=10 U/TCF(OPTIONS)

RUN 090977-2 *** DISCRETE HOLE RIG *** NAS-3-14336 STANTON NUMBER DATA

2670 NSL M=0.4 TH=1 P/D=10 U/TCF(OPTIONS)

LINEAR SUPERPOSITION IS APPLIED TO STANTON NUMBER DATA FROM
RUN NUMBERS 090977-1 AND 090977-2 TO OBTAIN STANTON NUMBER DATA AT TH=0 AND TH=1

PLATE	REXCOL	RE DEL2	ST(TH=0)	REXHOT	RE DEL2	ST(TH=1)	ETA	STCR	F-COL	STHR	F-HOT	LOAD
1	1153993.0	1903.1	0.002428	1147973.0	1893.2	0.002445	*****	1.000	0.0000	1.000	0.0000	1.000
2	1209155.0	2031.7	0.002234	1202847.0	2118.2	0.002113	0.054	0.994	0.0034	0.943	0.0027	1.457
3	1264317.0	2159.1	0.002309	1257722.0	2277.7	0.002047	0.143	1.090	0.0034	0.974	0.0027	1.462
4	1319479.0	2288.3	0.002224	1312596.0	2537.1	0.001957	0.143	1.035	0.0042	0.897	0.0036	1.568
5	1374642.0	2418.2	0.002416	1367473.0	2861.6	0.001898	0.216	1.137	0.0042	0.892	0.0036	1.594
6	1429804.0	2552.3	0.002433	1422345.0	3143.5	0.001809	0.224	1.170	0.0032	0.915	0.0028	1.483
7	1484966.0	2684.3	0.002365	1477219.0	3334.2	0.001762	0.263	1.126	0.0032	0.829	0.0028	1.101
8	1540129.0	2812.2	0.002273	1532094.0	3633.3	0.001685	0.259	1.115	0.0040	0.827	0.0036	1.551
9	1595291.0	2939.6	0.002345	1586968.0	3933.7	0.001673	0.286	1.170	0.0041	0.841	0.0036	1.581
10	1650453.0	3062.9	0.002123	1641843.0	4221.9	0.001678	0.239	1.063	0.0032	0.840	0.0027	1.409
11	1705615.0	3185.9	0.002363	1696717.0	4459.9	0.001588	0.322	1.179	0.0032	0.833	0.0027	1.367
12	1760777.0	3311.6	0.002218	1751591.0	4593.8	0.001595	0.283	1.152	0.0040	0.827	0.0033	1.524
13	1832731.0	3430.1	0.001923	1793296.0	4935.2	0.001276	0.337	1.049		0.635		
14	1891129.0	3454.7	0.001918	1921555.0	5152.3	0.001353	0.293	1.323		0.724		
15	1859518.0	3513.3	0.002033	1849817.0	5191.7	0.001450	0.275	1.336		0.751		
16	1889751.0	3565.6	0.001858	1878214.0	5232.2	0.001418	0.251	1.039		0.778		
17	1915513.0	3619.5	0.001913	1906612.0	5272.9	0.001465	0.233	1.330		0.793		
18	1945319.0	3673.8	0.001931	1934072.0	5314.3	0.001453	0.232	1.320		0.763		
19	1973827.0	3727.1	0.001842	1963132.0	5355.7	0.001466	0.255	1.363		0.820		
20	2001936.0	3780.1	0.001855	1991392.0	5397.9	0.001518	0.195	1.330		0.811		
21	2032245.0	3833.5	0.001859	2019651.0	5462.0	0.001491	0.201	1.257		0.830		
22	2058553.0	3886.3	0.001951	2047913.0	5483.3	0.001543	0.168	1.322		0.850		
23	2087752.0	3939.9	0.001918	2076174.0	5527.3	0.001573	0.183	1.339		0.852		
24	2115630.0	3993.0	0.001928	2104571.0	5571.3	0.001517	0.160	1.318		0.847		
25	2144154.0	4045.9	0.001881	2132949.0	5614.6	0.001568	0.171	1.334		0.853		
26	2172563.0	4099.2	0.001850	2161229.0	5658.1	0.001578	0.151	1.059		0.899		
27	2200971.0	4152.0	0.001937	2189489.0	5703.7	0.001576	0.175	1.338		0.857		
28	2229387.0	4207.1	0.001913	2217753.0	5743.3	0.001633	0.150	1.043		0.886		
29	2257783.0	4260.3	0.001823	2246013.0	5793.9	0.001539	0.155	1.378		0.852		
30	2285197.0	4312.6	0.001955	2274271.0	5839.2	0.001592	0.142	1.042		0.835		
31	2314536.0	4365.9	0.001932	2302531.0	5883.5	0.001610	0.149	1.349		0.872		
32	2341152.0	4418.7	0.001823	2330920.0	5928.7	0.001505	0.129	1.348		0.913		
33	2371598.0	4470.8	0.001845	2359326.0	5973.6	0.001590	0.130	1.353		0.937		
34	2399107.0	4523.0	0.001823	2387586.0	6019.4	0.001578	0.134	1.352		0.911		
35	2428515.0	4575.6	0.001670	2415846.0	6064.0	0.001600	0.125	1.362		0.920		
36	2456924.0	4626.1	0.001671	2444107.0	6137.0	0.001451	0.132	1.380		0.948		

STANTON NUMBER RATIO BASED ON EXPERIMENTAL FLAT PLATE VALUE AT SAME X LOCATION

STANTON NUMBER RATIO FOR TH=1 IS CONVERTED TO COMPARABLE TRANSPIRATION VALUE
USING ALOG(1 + B)/B EXPRESSION IN THE BLOWN SECTION

RUN 091077-1 *** DISCRETE HOLE RIG *** NAS-3-14336 STANTON NUMBER DATA

TADB= 24.52 DEG C UINF= 15.72 M/S TINF= 24.39 DEG C
RHO= 1.175 KG/M3 VISC= 0.15501E-04 M2/S XVO= 21.5 CM
CP= 1013. J/KGK PR= 0.715

2600 HSL M=0.90 TH=0 P/D=10 W/VCP (OPTIMUM)

PLATE	X	REX	TO	REENTH	STANTON NO	DST	DREEN	M	F	T2	THETA	DTH
1	127.9	0.11364E 07	37.37	0.18906E 04	0.24424E-02	0.594E-04	8.					
2	132.8	0.12012E 07	37.20	0.20173E 04	0.21803E-02	0.586E-04	10.	0.82	0.0067	28.67	0.334	0.023
3	137.9	0.12560E 07	37.12	0.22638E 04	0.23732E-02	0.601E-04	13.	0.00	0.0067	37.12	0.334	0.024
4	143.0	0.13108E 07	36.93	0.25136E 04	0.23013E-02	0.605E-04	16.	1.01	0.0082	28.80	0.352	0.024
5	148.1	0.13656E 07	36.95	0.27396E 04	0.23354E-02	0.610E-04	18.	0.00	0.0082	36.95	0.352	0.025
6	153.2	0.14204E 07	36.92	0.30884E 04	0.24069E-02	0.612E-04	21.	0.88	0.0071	28.78	0.350	0.024
7	158.2	0.14752E 07	37.05	0.33552E 04	0.23574E-02	0.603E-04	22.	0.00	0.0071	37.05	0.350	0.025
8	163.3	0.15300E 07	36.84	0.36199E 04	0.22572E-02	0.607E-04	24.	1.00	0.0081	28.75	0.350	0.024
9	168.4	0.15848E 07	36.97	0.39001E 04	0.23261E-02	0.605E-04	26.	0.00	0.0081	36.97	0.350	0.025
10	173.5	0.16396E 07	36.92	0.41795E 04	0.22216E-02	0.601E-04	27.	0.85	0.0069	28.71	0.345	0.024
11	178.6	0.16944E 07	37.05	0.44325E 04	0.22734E-02	0.598E-04	29.	0.00	0.0069	37.05	0.345	0.025
12	183.5	0.17492E 07	36.90	0.46874E 04	0.22883E-02	0.606E-04	30.	0.87	0.0070	28.76	0.350	0.024
13	187.5	0.17908E 07	35.03	0.49116E 04	0.16852E-02	0.633E-04	31.					
14	190.0	0.18191E 07	34.63	0.51003E 04	0.19234E-02	0.734E-04	31.					
15	192.7	0.18473E 07	34.63	0.51556E 04	0.19951E-02	0.753E-04	31.					
16	195.4	0.18756E 07	34.78	0.52101E 04	0.18597E-02	0.718E-04	31.					
17	198.0	0.19040E 07	34.78	0.52532E 04	0.18985E-02	0.725E-04	31.					
18	200.6	0.19322E 07	34.78	0.53166E 04	0.18835E-02	0.723E-04	31.					
19	203.2	0.19504E 07	34.76	0.53689E 04	0.18179E-02	0.693E-04	31.					
20	205.8	0.19887E 07	34.78	0.54211E 04	0.18739E-02	0.712E-04	31.					
21	208.5	0.20169E 07	34.78	0.54737E 04	0.18452E-02	0.702E-04	31.					
22	211.0	0.20451E 07	34.84	0.55257E 04	0.18353E-02	0.713E-04	31.					
23	213.7	0.20733E 07	34.74	0.55785E 04	0.18981E-02	0.724E-04	31.					
24	216.3	0.21017E 07	34.80	0.56309E 04	0.18112E-02	0.707E-04	31.					
25	218.9	0.21301E 07	34.82	0.56831E 04	0.18832E-02	0.720E-04	31.					
26	221.6	0.21583E 07	34.70	0.57357E 04	0.18391E-02	0.732E-04	31.					
27	224.2	0.21865E 07	34.88	0.57882E 04	0.18762E-02	0.725E-04	31.					
28	226.8	0.22147E 07	34.95	0.58419E 04	0.19270E-02	0.744E-04	31.					
29	229.3	0.22429E 07	34.76	0.58947E 04	0.18089E-02	0.683E-04	31.					
30	232.0	0.22712E 07	34.99	0.59454E 04	0.18550E-02	0.724E-04	31.					
31	234.5	0.22994E 07	34.99	0.59992E 04	0.18785E-02	0.724E-04	31.					
32	237.3	0.23277E 07	34.86	0.60516E 04	0.18349E-02	0.709E-04	31.					
33	239.9	0.23561E 07	34.82	0.61030E 04	0.18554E-02	0.720E-04	31.					
34	242.5	0.23843E 07	34.57	0.61558E 04	0.18257E-02	0.689E-04	31.					
35	245.1	0.24125E 07	34.78	0.62094E 04	0.18978E-02	0.746E-04	31.					
36	247.9	0.24408E 07	34.78	0.62590E 04	0.16023E-02	0.747E-04	31.					

UNCERTAINTY IN REX=13535. UNCERTAINTY IN F=0.05037 IN RATIO

RUN 091077-2 *** DISCRETE HOLE RIG *** NAS-3-14336 STANTON NUMBER DATA

TADB= 24.35 DEG C UINF= 15.72 M/S TINF= 24.24 DEG C
RHO= 1.175 KG/M3 VISC= 0.15487E-04 M2/S XVO= 21.5 CM
CP= 1013. J/KGK PR= 0.715

2600 BSL S=0.9 TH=1 P/D=10 W/TIP (OPTIMUM):

PLATE	X	REX	TO	REENTH	STANTON NO	DST	DREEN	M	F	T2	THETA	DTH
1	127.8	0.11471E 07	36.36	0.18917E 04	0.24524E-02	0.634E-04	8.					
2	132.8	0.12019E 07	36.42	0.20170E 04	0.21191E-02	0.611E-04	13.	0.77	0.0062	35.63	0.935	0.025
3	137.9	0.12568E 07	36.38	0.24541E 04	0.22093E-02	0.619E-04	18.	0.00	0.0062	36.38	0.935	0.026
4	143.0	0.13116E 07	36.38	0.28917E 04	0.21376E-02	0.614E-04	24.	0.97	0.0078	36.06	0.973	0.025
5	148.1	0.13664E 07	36.36	0.34239E 04	0.20623E-02	0.611E-04	29.	0.00	0.0078	36.36	0.973	0.026
6	153.2	0.14213E 07	36.40	0.39583E 04	0.22181E-02	0.618E-04	33.	0.82	0.0066	36.02	0.959	0.025
7	158.2	0.14761E 07	36.40	0.44295E 04	0.20947E-02	0.611E-04	36.	0.00	0.0066	36.40	0.959	0.026
8	163.3	0.15309E 07	36.46	0.48939E 04	0.19700E-02	0.601E-04	39.	0.94	0.0076	35.95	0.958	0.025
9	168.3	0.15858E 07	36.40	0.54002E 04	0.19516E-02	0.603E-04	43.	0.00	0.0076	36.40	0.958	0.026
10	173.5	0.16406E 07	36.38	0.59051E 04	0.19534E-02	0.604E-04	45.	0.83	0.0065	35.76	0.949	0.025
11	178.6	0.16954E 07	36.42	0.63453E 04	0.18542E-02	0.597E-04	47.	0.00	0.0065	36.42	0.949	0.025
12	183.6	0.17503E 07	36.36	0.67839E 04	0.18524E-02	0.600E-04	49.	0.84	0.0058	35.52	0.931	0.025
13	187.5	0.17919E 07	35.30	0.72050E 04	0.15349E-02	0.554E-04	50.					
14	190.1	0.18202E 07	35.07	0.75965E 04	0.15726E-02	0.510E-04	50.					
15	192.7	0.18484E 07	35.07	0.76407E 04	0.16028E-02	0.624E-04	50.					
16	195.4	0.18769E 07	35.16	0.75849E 04	0.15211E-02	0.603E-04	50.					
17	198.0	0.19052E 07	35.16	0.77283E 04	0.15537E-02	0.611E-04	50.					
18	200.6	0.19334E 07	35.16	0.77720E 04	0.15379E-02	0.609E-04	50.					
19	203.2	0.19616E 07	35.12	0.78150E 04	0.15012E-02	0.587E-04	50.					
20	205.8	0.19899E 07	35.12	0.78584E 04	0.15656E-02	0.507E-04	50.					
21	208.5	0.20181E 07	35.10	0.79023E 04	0.15407E-02	0.603E-04	50.					
22	211.1	0.20464E 07	35.09	0.79463E 04	0.15713E-02	0.622E-04	50.					
23	213.7	0.20745E 07	35.01	0.79915E 04	0.16269E-02	0.635E-04	50.					
24	216.3	0.21030E 07	35.07	0.80363E 04	0.15424E-02	0.619E-04	50.					
25	218.9	0.21314E 07	35.05	0.80310E 04	0.16201E-02	0.641E-04	50.					
26	221.6	0.21596E 07	34.89	0.81268E 04	0.16203E-02	0.629E-04	50.					
27	224.2	0.21878E 07	35.07	0.81729E 04	0.16423E-02	0.648E-04	50.					
28	226.8	0.22161E 07	35.12	0.82204E 04	0.17120E-02	0.671E-04	51.					
29	229.4	0.22443E 07	34.93	0.82672E 04	0.16041E-02	0.616E-04	51.					
30	232.0	0.22726E 07	35.14	0.83133E 04	0.16523E-02	0.657E-04	51.					
31	234.5	0.23008E 07	35.10	0.83607E 04	0.16996E-02	0.663E-04	51.					
32	237.3	0.23292E 07	34.99	0.84080E 04	0.16457E-02	0.648E-04	51.					
33	239.9	0.23575E 07	34.93	0.84550E 04	0.16816E-02	0.662E-04	51.					
34	242.5	0.23858E 07	34.67	0.85024E 04	0.16750E-02	0.637E-04	51.					
35	245.0	0.24140E 07	34.89	0.85505E 04	0.17270E-02	0.689E-04	51.					
36	247.8	0.24423E 07	34.89	0.85066E 04	0.15350E-02	0.591E-04	51.					

UNCERTAINTY IN REX=13544. UNCERTAINTY IN F=0.05037 IN RATIO

RUN 091077-1 *** DISCRETE HOLE RIG *** NAS-3-14336 STANTON NUMBER DATA

2600 NSL M=0.90 TH=0 P/D=10 U/VCP(OPTIMUM):

RUN 091077-2 *** DISCRETE HOLE RIG *** NAS-3-14336 STANTON NUMBER DATA

2600 NSL M=0.9 TH=1 P/D=10 U/VCP(OPTIMUM):

LINEAR SUPERPOSITION IS APPLIED TO STANTON NUMBER DATA FROM
RUN NUMBERS 091077-1 AND 091077-2 TO OBTAIN STANTON NUMBER DATA AT TH=0 AND TH=1

PLATE	REXCOL	RE DEL2	ST(TH=0)	REXHOT	RE DEL2	ST(TH=1)	ETA	STCR	F-COL	STHR	F-HOT	LOGB
1	1145494.0	1890.6	0.002442	1147105.0	1891.7	0.002452	0.000	1.000	0.0000	1.000	0.0000	1.999
2	1201203.0	2018.2	0.002216	1201938.0	2015.9	0.002111	0.047	0.986	0.0067	0.939	0.0062	2.115
3	1256773.0	2146.4	0.002454	1256771.0	2475.3	0.002192	0.110	1.125	0.0067	1.001	0.0062	2.110
4	1310932.0	2279.5	0.002303	1311604.0	2934.1	0.002125	0.112	1.203	0.0082	0.959	0.0078	2.286
5	1365692.0	2415.9	0.002588	1365437.0	3477.1	0.002348	0.207	1.216	0.0082	0.964	0.0078	2.343
6	1420431.0	2555.5	0.002518	1421270.0	4022.1	0.002209	0.121	1.218	0.0071	1.070	0.0066	2.319
7	1475203.0	2693.1	0.002535	1475132.0	4534.8	0.002091	0.170	1.193	0.0071	0.991	0.0065	2.207
8	1530130.0	2928.1	0.002421	1530935.0	4979.4	0.001953	0.193	1.188	0.0081	0.953	0.0075	2.347
9	1584799.0	2964.1	0.002541	1585769.0	5531.8	0.001925	0.242	1.277	0.0081	0.968	0.0076	2.387
10	1639593.0	3098.7	0.002372	1640601.0	6023.9	0.001939	0.182	1.188	0.0063	0.971	0.0055	2.296
11	1694398.0	3232.8	0.002522	1695424.0	6493.6	0.001813	0.279	1.271	0.0069	0.915	0.0065	2.186
12	1749199.0	3371.9	0.002539	1750267.0	6934.0	0.001819	0.293	1.318	0.0070	0.945	0.0068	2.275
13	1792845.0	3470.5	0.002301	1791943.0	7379.4	0.001499	0.283	1.143		0.817		
14	1819057.0	3530.5	0.002158	1823179.0	7795.7	0.001492	0.313	1.154		0.792		
15	1847239.0	3592.8	0.002225	1848418.0	7838.8	0.001563	0.297	1.152		0.837		
16	1875647.0	3652.9	0.002057	1875794.0	7891.9	0.001487	0.277	1.132		0.818		
17	1904335.0	3711.7	0.002131	1905173.0	7924.4	0.001519	0.277	1.133		0.919		
18	1932228.0	3770.8	0.002085	1933409.0	7957.1	0.001503	0.283	1.119		0.835		
19	1961449.0	3828.6	0.002033	1961648.0	8029.1	0.001469	0.267	1.134		0.831		
20	1989671.0	3886.0	0.002063	1989887.0	8051.6	0.001535	0.255	1.101		0.823		
21	2015373.0	3943.7	0.002025	2018126.0	8094.6	0.001510	0.255	1.139		0.910		
22	2045115.0	4000.4	0.001930	2046165.0	8137.8	0.001545	0.223	1.099		0.853		
23	2073335.0	4057.6	0.002057	2074504.0	8182.3	0.001599	0.222	1.117		0.853		
24	2101595.0	4114.5	0.001959	2102980.0	8225.3	0.001515	0.230	1.099		0.845		
25	2130750.0	4171.1	0.002037	2131355.0	8270.2	0.001593	0.218	1.118		0.871		
26	2159275.0	4227.7	0.001967	2159595.0	8315.3	0.001590	0.188	1.121		0.911		
27	2185497.0	4283.9	0.002011	2187834.0	8360.8	0.001619	0.196	1.096		0.841		
28	2214719.0	4341.3	0.002053	2216073.0	8407.6	0.001693	0.177	1.116		0.919		
29	2242941.0	4397.6	0.001920	2244312.0	8453.9	0.001503	0.179	1.068		0.875		
30	2271162.0	4452.7	0.001974	2272551.0	8499.3	0.001632	0.173	1.109		0.917		
31	2299381.0	4508.6	0.001933	2300790.0	8545.2	0.001682	0.152	1.099		0.932		
32	2327743.0	4564.2	0.001945	2329166.0	8592.9	0.001526	0.164	1.120		0.937		
33	2356101.0	4619.3	0.001957	2357542.0	8639.4	0.001664	0.150	1.116		0.930		
34	2384323.0	4674.0	0.001911	2385781.0	8696.9	0.001660	0.133	1.104		0.958		
35	2412545.0	4729.3	0.001999	2414020.0	8734.1	0.001710	0.144	1.129		0.966		
36	2440766.0	4782.5	0.001769	2442259.0	8779.7	0.001520	0.141	1.151		0.999		

STANTON NUMBER RATIO BASED ON EXPERIMENTAL FLAT PLATE VALUE AT SAME X LOCATION

STANTON NUMBER RATIO FOR TH=1 IS CONVERTED TO COMPARABLE TRANSPIRATION VALUE
USING ALOG(1 + B)/B EXPRESSION IN THE BLOWN SECTION

118

RUN080173 VELOCITY AND TEMPERATURE PROFILES

REX = 0.73550E 06 REM = 1826. REH = 1407.

XVC = 10.10 CM DEL2 = 0.286 CM DEH2 = 0.221 CM
UINF = 9.89 M/S DEL99= 2.436 CM DELT99 = 2.328 CM
VISC = 0.15478E-04 M2/S DEL1 = 0.413 CM UINF = 9.90 M/S
PORT = 3 H = 1.444 VISC = 0.15514E-04 M2/S
XLCC = 125.22 CM CF/2 = 0.18714E-02 TINF = 24.87 DEG C
TPLATE = 38.55 DEG C

Y(CM)	Y/DEL	U(M/S)	U/UINF	Y+	U+	Y(CM)	T(DEG C)	TBAR	TBAR
0.025	0.010	3.60	0.364	7.0	8.41	0.0127	35.44	0.227	0.773
0.033	0.014	3.97	0.401	9.1	9.27	0.0178	35.51	0.222	0.778
0.038	0.016	4.27	0.431	10.5	9.97	0.0254	34.86	0.270	0.730
0.046	0.019	4.55	0.460	12.6	10.64	0.0305	34.12	0.324	0.676
0.051	0.021	4.74	0.479	14.0	11.07	0.0381	33.19	0.392	0.608
0.058	0.024	4.94	0.500	16.1	11.55	0.0457	32.66	0.431	0.569
0.066	0.027	5.12	0.518	18.3	11.96	0.0533	31.99	0.479	0.521
0.071	0.029	5.22	0.528	19.7	12.20	0.0635	31.52	0.514	0.486
0.079	0.032	5.33	0.539	21.8	12.47	0.0711	31.18	0.539	0.461
0.089	0.036	5.41	0.547	24.6	12.65	0.0787	30.87	0.561	0.439
0.097	0.040	5.62	0.568	26.7	13.14	0.0889	30.56	0.584	0.416
0.104	0.043	5.81	0.587	28.8	13.57	0.1016	30.27	0.605	0.395
0.117	0.048	5.86	0.593	32.3	13.70	0.1143	30.01	0.624	0.376
0.127	0.052	5.89	0.595	35.1	13.76	0.1270	29.84	0.636	0.364
0.135	0.055	5.93	0.600	37.2	13.86	0.1524	29.67	0.664	0.336
0.147	0.060	6.06	0.613	40.7	14.16	0.1778	29.29	0.677	0.323
0.173	0.071	6.25	0.632	47.7	14.61	0.2032	29.08	0.692	0.308
0.211	0.087	6.42	0.649	58.3	15.00	0.2286	28.88	0.707	0.293
0.249	0.102	6.61	0.669	68.8	15.46	0.2540	28.70	0.720	0.280
0.287	0.118	6.71	0.678	79.3	15.68	0.2794	28.61	0.727	0.273
0.338	0.139	6.85	0.693	93.4	16.01	0.3048	28.39	0.742	0.258
0.376	0.154	6.96	0.704	103.9	16.28	0.3429	28.26	0.752	0.248
0.414	0.170	7.07	0.715	114.4	16.53	0.3683	28.15	0.760	0.240
0.465	0.191	7.18	0.726	128.5	16.78	0.4445	27.87	0.781	0.219
0.528	0.217	7.33	0.741	146.0	17.13	0.4953	27.71	0.793	0.207
0.592	0.243	7.48	0.757	163.6	17.49	0.5969	27.40	0.815	0.185
0.655	0.269	7.63	0.771	181.1	17.83	0.6604	27.23	0.827	0.173
0.719	0.295	7.79	0.788	198.7	18.21	0.7239	27.10	0.837	0.163
0.820	0.337	7.92	0.801	226.7	18.52	0.7874	26.92	0.850	0.150
0.909	0.373	8.07	0.816	251.3	18.87	0.8509	26.77	0.861	0.139
1.011	0.415	8.19	0.828	279.4	19.14	0.9271	26.63	0.871	0.129
1.062	0.436	8.30	0.840	293.6	19.41	1.0033	26.45	0.885	0.115
1.163	0.478	8.50	0.859	321.5	19.86	1.0795	26.33	0.893	0.107
1.290	0.530	8.71	0.880	356.6	20.35	1.1684	26.17	0.905	0.095
1.417	0.582	8.84	0.894	391.7	20.66	1.2954	26.00	0.917	0.083
1.608	0.660	9.07	0.918	444.4	21.21	1.4224	25.82	0.930	0.070
1.735	0.712	9.27	0.938	479.5	21.67	1.5494	25.67	0.941	0.059
1.925	0.790	9.47	0.957	532.1	22.13	1.7399	25.48	0.956	0.044
2.119	0.865	9.66	0.977	602.3	22.57	1.8669	25.34	0.965	0.035
2.370	0.973	9.79	0.990	655.0	22.88	2.0574	25.18	0.977	0.023
2.497	1.025	9.86	0.997	690.1	23.05	2.3114	25.02	0.989	0.011
2.560	1.051	9.90	1.001	707.6	23.14	2.6289	24.92	0.996	0.004
						2.883	24.87	1.000	0.000

RUN 080177 *** DISCRETE HOLE RIG *** NAS-3-14336 STANTON NUMBER DATA

TADB= 24.79 DEG C UINF= 9.87 M/S TINF= 24.74 DEG C
RHO= 1.176 KG/M3 VISC= 0.15502E-04 M2/S XVO= 10.1 CM
CP= 1013. J/KGK PR= 0.716

180C HSL FLAT PLATE P/D=5

PLATE	X	REX	TO	REENTH	STANTONNO	DST	DREEN	ST(THEO)	RATIO
1	127.8	0.74879E 06	38.53	0.13999E 04	0.23879E-02	0.943E-04	16.	0.22543E-02	1.059
2	132.8	0.78112E 06	38.53	0.14782E 04	0.24551E-02	0.950E-04	16.	0.22354E-02	1.098
3	137.9	0.81345E 06	38.55	0.15586E 04	0.25190E-02	0.956E-04	16.	0.22173E-02	1.136
4	143.0	0.84578E 06	38.49	0.16405E 04	0.25435E-02	0.961E-04	17.	0.22001E-02	1.156
5	148.1	0.87812E 06	38.49	0.17222E 04	0.25102E-02	0.958E-04	17.	0.21836E-02	1.150
6	153.2	0.91045E 06	38.46	0.18026E 04	0.24626E-02	0.955E-04	17.	0.21679E-02	1.136
7	158.2	0.94278E 06	38.46	0.18814E 04	0.24162E-02	0.950E-04	17.	0.21528E-02	1.122
8	163.3	0.97511E 06	38.42	0.19598E 04	0.23709E-02	0.948E-04	17.	0.21384E-02	1.109
9	168.4	0.10074E 07	38.42	0.20352E 04	0.23534E-02	0.946E-04	17.	0.21245E-02	1.108
10	173.5	0.10398E 07	38.40	0.21118E 04	0.23866E-02	0.950E-04	17.	0.21111E-02	1.131
11	178.6	0.10721E 07	38.44	0.21875E 04	0.22952E-02	0.939E-04	18.	0.20982E-02	1.094
12	183.6	0.11044E 07	38.46	0.22620E 04	0.23127E-02	0.940E-04	18.	0.20858E-02	1.109
13	187.5	0.11290E 07	38.17	0.23171E 04	0.21245E-02	0.870E-04	18.	0.20766E-02	1.023
14	190.1	0.11457E 07	38.10	0.23520E 04	0.20685E-02	0.896E-04	18.	0.20705E-02	0.999
15	192.7	0.11623E 07	38.10	0.23873E 04	0.21593E-02	0.903E-04	18.	0.20646E-02	1.046
16	195.4	0.11790E 07	38.29	0.24220E 04	0.20030E-02	0.863E-04	18.	0.20587E-02	0.973
17	198.0	0.11956E 07	38.29	0.24558E 04	0.20575E-02	0.874E-04	18.	0.20529E-02	1.002
18	200.6	0.12124E 07	38.29	0.24899E 04	0.20375E-02	0.869E-04	18.	0.20472E-02	0.995
19	203.2	0.12291E 07	38.29	0.25233E 04	0.19648E-02	0.831E-04	18.	0.20416E-02	0.962
20	205.8	0.12457E 07	38.26	0.25586E 04	0.20267E-02	0.858E-04	18.	0.20361E-02	0.996
21	208.5	0.12624E 07	38.30	0.25901E 04	0.19912E-02	0.844E-04	18.	0.20307E-02	0.981
22	211.1	0.12790E 07	38.29	0.26234E 04	0.20066E-02	0.862E-04	18.	0.20254E-02	0.991
23	213.7	0.12957E 07	38.25	0.26573E 04	0.20560E-02	0.877E-04	18.	0.20202E-02	1.018
24	216.3	0.13124E 07	38.27	0.26909E 04	0.19723E-02	0.854E-04	18.	0.20150E-02	0.979
25	218.9	0.13291E 07	38.34	0.27239E 04	0.19962E-02	0.870E-04	18.	0.20099E-02	0.993
26	221.6	0.13458E 07	38.15	0.27568E 04	0.19437E-02	0.827E-04	18.	0.20049E-02	0.969
27	224.2	0.13624E 07	38.38	0.27899E 04	0.20258E-02	0.874E-04	18.	0.20000E-02	1.013
28	226.8	0.13791E 07	38.48	0.28239E 04	0.20535E-02	0.886E-04	18.	0.19951E-02	1.029
29	229.4	0.13957E 07	38.20	0.28574E 04	0.19645E-02	0.826E-04	18.	0.19904E-02	0.987
30	232.0	0.14124E 07	38.53	0.28901E 04	0.19656E-02	0.842E-04	18.	0.19856E-02	0.990
31	234.6	0.14290E 07	38.51	0.29232E 04	0.20001E-02	0.861E-04	18.	0.19810E-02	1.010
32	237.3	0.14458E 07	38.42	0.29559E 04	0.19280E-02	0.838E-04	18.	0.19764E-02	0.976
33	239.9	0.14625E 07	38.40	0.29881E 04	0.19329E-02	0.844E-04	18.	0.19718E-02	0.980
34	242.5	0.14792E 07	38.13	0.30207E 04	0.19821E-02	0.830E-04	18.	0.19674E-02	1.007
35	245.1	0.14958E 07	38.32	0.30538E 04	0.19851E-02	0.876E-04	18.	0.19630E-02	1.011
36	247.8	0.15125E 07	38.32	0.30844E 04	0.16824E-02	0.887E-04	18.	0.19586E-02	0.859

RUN 080977-1 *** DISCRETE HOLE RIG *** NAS-3-14336 STANTON NUMBER DATA

TADB= 23.01 DEG C UINF= 9.83 M/S TINF= 22.97 DEG C
RHO= 1.184 KG/M3 VISC= 0.15334E-04 M2/S XVO= 10.1 CM
CP= 1013. J/KGK PR= 0.716

180C HSL P=0.4 P/D=5 TH=0 W/VCF(OPTIMUM)

PLATE	X	REX	TO	REENTH	STANTON NO	DST	DREEN	M	F	T2	THETA	DTH
1	127.8	0.75455E 06	38.55	0.14107E 04	0.24316E-02	0.859E-04	5.					
2	132.8	0.78713E 06	38.51	0.14872E 04	0.22651E-02	0.843E-04	7.	0.45	0.0147	26.20	0.208	0.019
3	137.9	0.81571E 06	38.49	0.16650E 04	0.25445E-02	0.874E-04	11.	0.40	0.0131	26.36	0.218	0.019
4	143.0	0.85229E 06	38.48	0.18409E 04	0.25519E-02	0.876E-04	13.	0.41	0.0133	26.25	0.211	0.019
5	148.1	0.88407E 06	38.46	0.20141E 04	0.24620E-02	0.867E-04	15.	0.40	0.0128	26.38	0.220	0.019
6	153.2	0.91744E 06	38.42	0.21861E 04	0.24772E-02	0.870E-04	16.	0.39	0.0127	26.29	0.215	0.019
7	158.2	0.95002E 06	38.42	0.23527E 04	0.22706E-02	0.848E-04	18.	0.43	0.0140	26.35	0.219	0.019
8	163.2	0.98260E 06	38.48	0.25255E 04	0.22094E-02	0.839E-04	19.	0.42	0.0136	26.27	0.213	0.019
9	168.4	0.10152E 07	38.59	0.26908E 04	0.21864E-02	0.830E-04	20.	0.40	0.0130	26.40	0.220	0.019
10	173.5	0.10478E 07	38.59	0.28536E 04	0.21360E-02	0.827E-04	22.	0.39	0.0125	26.30	0.213	0.019
11	178.6	0.10803E 07	38.57	0.30055E 04	0.20946E-02	0.824E-04	23.	0.38	0.0124	26.52	0.228	0.019
12	183.6	0.11124E 07	38.59	0.31700E 04	0.20876E-02	0.822E-04	24.	0.38	0.0122	26.41	0.220	0.019
13	187.5	0.11377E 07	38.23	0.33101E 04	0.22342E-02	0.876E-04	24.					
14	190.1	0.11545E 07	38.27	0.33459E 04	0.20364E-02	0.857E-04	24.					
15	192.7	0.11712E 07	38.27	0.33807E 04	0.21151E-02	0.857E-04	24.					
16	195.4	0.11881E 07	38.55	0.34144E 04	0.19318E-02	0.802E-04	24.					
17	198.0	0.12050E 07	38.59	0.34467E 04	0.19334E-02	0.805E-04	24.					
18	200.6	0.12217E 07	38.59	0.34790E 04	0.19134E-02	0.802E-04	24.					
19	203.2	0.12385E 07	38.51	0.35108E 04	0.18732E-02	0.771E-04	24.					
20	205.8	0.12553E 07	38.59	0.35427E 04	0.19325E-02	0.798E-04	24.					
21	208.5	0.12721E 07	38.57	0.35746E 04	0.18660E-02	0.775E-04	24.					
22	211.1	0.12889E 07	38.59	0.36063E 04	0.19083E-02	0.804E-04	24.					
23	213.7	0.13056E 07	38.48	0.36390E 04	0.19761E-02	0.818E-04	24.					
24	216.3	0.13225E 07	38.51	0.36714E 04	0.18816E-02	0.794E-04	24.					
25	218.9	0.13394E 07	38.59	0.37035E 04	0.19384E-02	0.821E-04	24.					
26	221.6	0.13561E 07	38.38	0.37355E 04	0.18800E-02	0.775E-04	24.					
27	224.2	0.13729E 07	38.65	0.37660E 04	0.19842E-02	0.832E-04	24.					
28	226.8	0.13897E 07	38.74	0.38020E 04	0.20644E-02	0.861E-04	24.					
29	229.4	0.14065E 07	38.55	0.38356E 04	0.19341E-02	0.786E-04	24.					
30	232.0	0.14232E 07	38.84	0.38680E 04	0.19286E-02	0.821E-04	24.					
31	234.6	0.14400E 07	38.82	0.39008E 04	0.19793E-02	0.828E-04	24.					
32	237.3	0.14569E 07	38.65	0.39338E 04	0.19408E-02	0.808E-04	24.					
33	239.9	0.14737E 07	38.65	0.39663E 04	0.19349E-02	0.816E-04	24.					
34	242.5	0.14905E 07	38.38	0.39990E 04	0.19564E-02	0.795E-04	24.					
35	245.1	0.15073E 07	38.55	0.40324E 04	0.20190E-02	0.854E-04	24.					
36	247.8	0.15241E 07	38.55	0.40636E 04	0.16969E-02	0.866E-04	24.					

UNCERTAINTY IN REX= 7673. UNCERTAINTY IN F=0.05294 IN RATIO

RUN 080977-2 *** DISCRETE HOLE RIG *** NAS-3-14336 STANTON NUMBER DATA

TADB= 24.17 DEG C UINF= 9.86 M/S TINF= 24.13 DEG C
RHO= 1.178 KG/M3 VISC= 0.15439E-04 M2/S XVO= 10.1 CM
CP= 1014. J/KGK PR= 0.716

1BCC HSL M=0.4 P/D=5 TH=1 W/VCF(OPTIMUM)

PLATE	X	REX	TO	REENTH	STANTON NO	DST	DREEN	M	F	T2	THETA	DTH
1	127.8	0.75109E 06	41.44	0.14042E 04	0.23016E-02	0.781E-04	5.					
2	132.8	0.78352E 06	41.46	0.14759E 04	0.21195E-02	0.762E-04	12.	0.38	0.0123	41.24	0.988	0.018
3	137.9	0.81595E 06	41.42	0.19352E 04	0.19511E-02	0.746E-04	21.	0.41	0.0133	41.49	1.004	0.018
4	143.0	0.84838E 06	41.40	0.24290E 04	0.17668E-02	0.730E-04	26.	0.37	0.0120	41.45	1.003	0.018
5	148.1	0.88081E 06	41.44	0.28723E 04	0.15235E-02	0.706E-04	30.	0.33	0.0106	41.42	0.999	0.018
6	153.2	0.91324E 06	41.44	0.32650E 04	0.14614E-02	0.703E-04	33.	0.34	0.0109	41.38	0.957	0.018
7	158.2	0.94567E 06	41.42	0.36618E 04	0.12397E-02	0.688E-04	37.	0.39	0.0125	41.38	0.958	0.018
8	163.3	0.97810E 06	41.44	0.41044E 04	0.10724E-02	0.677E-04	40.	0.40	0.0128	41.41	0.999	0.018
9	168.4	0.10105E 07	41.46	0.45536E 04	0.10456E-02	0.677E-04	43.	0.35	0.0114	41.27	0.969	0.018
10	173.5	0.10430E 07	41.40	0.49518E 04	0.97389E-03	0.673E-04	45.	0.35	0.0114	41.16	0.986	0.018
11	178.6	0.10754E 07	41.44	0.53487E 04	0.92533E-03	0.669E-04	48.	0.37	0.0119	40.93	0.971	0.018
12	183.6	0.11078E 07	41.46	0.57527E 04	0.86402E-03	0.665E-04	50.	0.37	0.0118	40.74	0.958	0.018
13	187.5	0.11225E 07	40.83	0.61438E 04	0.11173E-02	0.494E-04	51.					
14	190.1	0.11452E 07	40.77	0.61615E 04	0.10412E-02	0.533E-04	51.					
15	192.7	0.11655E 07	40.77	0.61798E 04	0.11044E-02	0.532E-04	51.					
16	195.4	0.11927E 07	40.77	0.61983E 04	0.11074E-02	0.533E-04	51.					
17	198.0	0.11954E 07	40.74	0.62174E 04	0.11805E-02	0.554E-04	51.					
18	200.6	0.12181E 07	40.74	0.62372E 04	0.11884E-02	0.564E-04	51.					
19	203.2	0.12328E 07	40.60	0.62572E 04	0.12041E-02	0.549E-04	51.					
20	205.8	0.12495E 07	40.62	0.62781E 04	0.12881E-02	0.581E-04	51.					
21	208.5	0.12662E 07	40.55	0.62993E 04	0.12509E-02	0.569E-04	51.					
22	211.1	0.12825E 07	40.57	0.63207E 04	0.13351E-02	0.606E-04	51.					
23	213.7	0.12996E 07	40.35	0.63436E 04	0.14392E-02	0.637E-04	51.					
24	216.3	0.13164E 07	40.43	0.63670E 04	0.13542E-02	0.620E-04	51.					
25	218.9	0.13332E 07	40.49	0.63900E 04	0.14043E-02	0.644E-04	51.					
26	221.6	0.13455E 07	40.20	0.64131E 04	0.13482E-02	0.613E-04	51.					
27	224.2	0.13666E 07	40.07	0.64382E 04	0.16549E-02	0.695E-04	51.					
28	226.8	0.13833E 07	40.55	0.64648E 04	0.15360E-02	0.698E-04	51.					
29	229.4	0.14000E 07	40.34	0.64902E 04	0.15015E-02	0.643E-04	51.					
30	232.0	0.14167E 07	40.57	0.65154E 04	0.15370E-02	0.679E-04	51.					
31	234.6	0.14334E 07	40.51	0.65412E 04	0.15776E-02	0.688E-04	51.					
32	237.3	0.14502E 07	40.41	0.65671E 04	0.15273E-02	0.674E-04	51.					
33	239.9	0.14670E 07	40.28	0.65929E 04	0.15546E-02	0.686E-04	51.					
34	242.5	0.14837E 07	40.11	0.66192E 04	0.15853E-02	0.670E-04	51.					
35	245.1	0.15004E 07	40.28	0.66461E 04	0.16342E-02	0.724E-04	51.					
36	247.8	0.15171E 07	40.28	0.66714E 04	0.13954E-02	0.740E-04	51.					

UNCERTAINTY IN REX= 7637. UNCERTAINTY IN F=0.05294 IN RATIO

RUN 080977-1 *** DISCRETE HOLE RIG *** NAS-3-14336 STANTON NUMBER DATA

1800 MSL M=0.4 P/D=5 TH=0 W/VCF(OPTIMUM)

RUN 080977-2 *** DISCRETE HOLE RIG *** NAS-3-14336 STANTON NUMBER DATA

1800 MSL M=0.4 P/D=5 TH=1 W/VCF(OPTIMUM)

LINEAR SUPERPOSITION IS APPLIED TO STANTON NUMBER DATA FROM
RUN NUMBERS 080977-1 AND 080977-2 TO OBTAIN STANTON NUMBER DATA AT TH=0 AND TH=1

PLATE	REXCOL	RE DEL2	ST(TH=0)	REXHOT	RE DEL2	ST(TH=1)	ETA	STCR	F-COL	STHR	F-HOT	LOGB
1	754546.3	1410.7	0.002432	751085.0	1404.2	0.002302	UUUUU	1.000	0.0000	1.000	0.0000	1.000
2	787126.1	1487.8	0.002304	783515.3	1475.9	0.002117	0.081	0.938	0.0147	0.862	0.0123	2.609
3	819705.8	1569.5	0.002706	815945.5	1939.9	0.001948	0.280	1.074	0.0131	0.773	0.0133	2.568
4	852285.5	1658.6	0.002766	848375.8	2432.1	0.001770	0.360	1.087	0.0133	0.696	0.0120	2.299
5	884865.2	1747.5	0.002720	880806.1	2874.3	0.001524	0.439	1.083	0.0128	0.607	0.0106	2.040
6	917444.9	1837.2	0.002760	913236.3	3267.4	0.001458	0.472	1.121	0.0127	0.592	0.0109	2.073
7	950024.7	1923.8	0.002558	945666.6	3665.2	0.001236	0.517	1.059	0.0140	0.511	0.0125	2.151
8	982604.4	2006.6	0.002523	978096.9	4108.8	0.001070	0.576	1.064	0.0136	0.451	0.0128	2.106
9	1015184.0	2087.8	0.002459	1010527.0	4558.4	0.001077	0.562	1.045	0.0130	0.458	0.0114	1.974
10	1047763.0	2167.9	0.002462	1042957.0	4960.1	0.000955	0.612	1.032	0.0125	0.400	0.0114	1.871
11	1080343.0	2247.8	0.002441	1075387.0	5361.3	0.000892	0.635	1.064	0.0124	0.389	0.0119	1.948
12	1112923.0	2327.6	0.002458	1107818.0	5775.1	0.000806	0.672	1.063	0.0122	0.348	0.0118	1.858
13	1137683.0	2399.3	0.002572	1132465.0	6180.8	0.001064	0.586	1.211		0.591		
14	1154462.0	2430.4	0.002330	1149166.0	6198.0	0.000994	0.573	1.126		0.480		
15	1171241.0	2470.4	0.002421	1165868.0	6215.1	0.001056	0.564	1.121		0.489		
16	1188100.0	2508.7	0.002142	1182650.0	6232.9	0.001069	0.501	1.070		0.534		
17	1204960.0	2544.8	0.002161	1199433.0	6251.4	0.001144	0.470	1.050		0.556		
18	1221735.0	2580.9	0.002133	1216135.0	6270.6	0.001154	0.459	1.047		0.566		
19	1238510.0	2616.2	0.002076	1232836.0	6290.1	0.001172	0.435	1.056		0.597		
20	1255256.0	2651.5	0.002128	1249538.0	6310.4	0.001257	0.409	1.049		0.620		
21	1272075.0	2686.7	0.002052	1266239.0	6331.1	0.001222	0.405	1.031		0.613		
22	1288853.0	2721.5	0.002091	1282941.0	6352.0	0.001276	0.390	1.042		0.636		
23	1305632.0	2757.0	0.002139	1299643.0	6374.5	0.001414	0.339	1.040		0.688		
24	1322492.0	2792.1	0.002041	1316425.0	6397.4	0.001329	0.349	1.035		0.674		
25	1339252.0	2826.9	0.002100	1333208.0	6420.1	0.001379	0.343	1.052		0.651		
26	1356120.0	2861.7	0.002041	1349909.0	6442.6	0.001323	0.352	1.050		0.680		
27	1372905.0	2896.3	0.002084	1366611.0	6467.4	0.001639	0.213	1.029		0.809		
28	1389687.0	2932.5	0.002224	1383313.0	6493.7	0.001511	0.321	1.083		0.736		
29	1406466.0	2968.5	0.002065	1400014.0	6518.8	0.001481	0.283	1.051		0.754		
30	1423245.0	3003.1	0.002056	1416716.0	6543.6	0.001487	0.277	1.046		0.756		
31	1440023.0	3038.0	0.002101	1433417.0	6569.0	0.001558	0.258	1.050		0.779		
32	1456803.0	3073.0	0.002066	1450200.0	6594.7	0.001508	0.270	1.072		0.782		
33	1473743.0	3107.6	0.002050	1466983.0	6620.1	0.001536	0.250	1.061		0.795		
34	1490522.0	3142.2	0.002069	1483684.0	6646.1	0.001568	0.242	1.044		0.791		
35	1507309.0	3177.5	0.002135	1500386.0	6672.7	0.001616	0.243	1.076		0.814		
36	1524075.0	3210.5	0.001788	1517087.0	6697.7	0.001381	0.228	1.063		0.821		

STANTON NUMBER RATIO BASED ON EXPERIMENTAL FLAT PLATE VALUE AT SAME X LOCATION

STANTON NUMBER RATIO FOR TH=1 IS CONVERTED TO COMPARABLE TRANSPIRATION VALUE
USING BLOG(1 + B)/B EXPRESSION IN THE BLOWN SECTION

RUN 080777-1 *** DISCRETE HOLE RIG *** NAS-3-14336 STANTON NUMBER DATA

TADB= 25.04 DEG C UINF= 9.86 M/S TINF= 24.99 DEG C
RHO= 1.178 KG/M3 VISC= 0.15499E-04 M2/S XVO= 10.1 CM
CP= 1012. J/KGK PR= 0.715

1800 HSL M=0.90 P/D=5 TH=0 W/VCF(OPTIMUM)

PLATE	X	REX	TO	REENTH	STANTON NO	DST	DREEN	M	F	T2	THETA	DTH
1	127.8	0.74841E 06	37.33	0.13992E 04	0.25384E-02	0.105E-03	5.					
2	132.8	0.78073E 06	37.39	0.14791E 04	0.24032E-02	0.103E-03	14.	0.98	0.0316	26.32	0.107	0.025
3	137.9	0.81304E 06	37.45	0.16760E 04	0.30157E-02	0.109E-03	23.	0.94	0.0305	26.42	0.115	0.024
4	143.0	0.84536E 06	37.43	0.18886E 04	0.31426E-02	0.111E-03	29.	0.93	0.0302	26.36	0.110	0.024
5	148.1	0.87767E 06	37.37	0.20969E 04	0.31123E-02	0.111E-03	34.	0.93	0.0301	26.46	0.119	0.025
6	153.2	0.90999E 06	37.28	0.23144E 04	0.32061E-02	0.113E-03	38.	0.92	0.0299	26.36	0.111	0.025
7	158.2	0.94230E 06	37.49	0.25208E 04	0.29255E-02	0.108E-03	42.	0.93	0.0302	26.42	0.115	0.024
8	163.3	0.97462E 06	37.51	0.27261E 04	0.28647E-02	0.107E-03	45.	0.91	0.0295	26.38	0.111	0.024
9	168.4	0.10069E 07	37.51	0.29217E 04	0.26918E-02	0.105E-03	49.	0.94	0.0303	26.40	0.113	0.024
10	173.5	0.10392E 07	37.35	0.31218E 04	0.28590E-02	0.108E-03	52.	0.92	0.0299	25.71	0.058	0.025
11	178.6	0.10716E 07	37.39	0.32689E 04	0.27581E-02	0.107E-03	54.	0.94	0.0303	26.45	0.118	0.025
12	183.6	0.11039E 07	37.37	0.34753E 04	0.28755E-02	0.108E-03	57.	0.93	0.0302	26.35	0.110	0.025
13	187.5	0.11284E 07	36.53	0.36535E 04	0.29519E-02	0.116E-03	59.					
14	190.1	0.11451E 07	36.90	0.37013E 04	0.27963E-02	0.117E-03	59.					
15	192.7	0.11617E 07	36.90	0.37491E 04	0.25356E-02	0.118E-03	59.					
16	195.4	0.11784E 07	37.24	0.37952E 04	0.25940E-02	0.109E-03	59.					
17	198.0	0.11952E 07	37.24	0.38389E 04	0.26590E-02	0.110E-03	59.					
18	200.6	0.12118E 07	37.28	0.38827E 04	0.25959E-02	0.108E-03	59.					
19	203.2	0.12284E 07	37.33	0.39248E 04	0.24522E-02	0.102E-03	59.					
20	205.8	0.12451E 07	37.43	0.39658E 04	0.24794E-02	0.103E-03	59.					
21	208.5	0.12617E 07	37.39	0.40074E 04	0.25043E-02	0.103E-03	59.					
22	211.1	0.12784E 07	37.49	0.40484E 04	0.24165E-02	0.103E-03	59.					
23	213.7	0.12950E 07	37.39	0.40892E 04	0.24825E-02	0.103E-03	59.					
24	216.3	0.13117E 07	37.45	0.41293E 04	0.23340E-02	0.992E-04	59.					
25	218.9	0.13285E 07	37.56	0.41684E 04	0.23550E-02	0.101E-03	59.					
26	221.6	0.13451E 07	37.33	0.42071E 04	0.22997E-02	0.959E-04	59.					
27	224.2	0.13617E 07	37.60	0.42460E 04	0.23669E-02	0.101E-03	59.					
28	226.8	0.13784E 07	37.71	0.42854E 04	0.23644E-02	0.101E-03	59.					
29	229.4	0.13950E 07	37.51	0.43242E 04	0.22925E-02	0.949E-04	59.					
30	232.0	0.14117E 07	37.73	0.43627E 04	0.23206E-02	0.998E-04	59.					
31	234.6	0.14283E 07	37.71	0.44017E 04	0.23670E-02	0.100E-03	59.					
32	237.3	0.14450E 07	37.58	0.44408E 04	0.23189E-02	0.984E-04	59.					
33	239.9	0.14618E 07	37.56	0.44793E 04	0.23071E-02	0.987E-04	59.					
34	242.5	0.14784E 07	37.31	0.45179E 04	0.23311E-02	0.966E-04	59.					
35	245.1	0.14950E 07	37.45	0.45574E 04	0.24114E-02	0.104E-03	59.					
36	247.8	0.15117E 07	37.45	0.45946E 04	0.20490E-02	0.104E-03	59.					

UNCERTAINTY IN REX= 7610. UNCERTAINTY IN F=0.05294 IN RATIO

RUN 080777-2 *** DISCRETE HOLE RIG *** NAS-3-14336 STANTON NUMBER DATA

TADB= 24.82 DEG C UINF= 9.86 M/S TINF= 24.78 DEG C
RHO= 1.179 KG/M3 VISC= 0.15479E-04 M2/S XVO= 10.1 CM
CP= 1012. J/KGK PR= 0.715

18CC FSL M=0.90 P/D=5 TH=1 W/VCF(OPTIMUM)

PLATE	X	REX	TO	REENTH	STANTON NO	DST	DREEN	M	F	T2	THETA	DTH
1	127.8	0.74905E 06	39.65	0.14004E 04	0.24136E-02	0.890E-04	5.					
2	132.8	0.78139E 06	39.58	0.14773E 04	0.23394E-02	0.886E-04	28.	0.93	0.0301	39.41	0.989	0.021
3	137.9	0.81373E 06	39.54	0.25176E 04	0.25423E-02	0.910E-04	47.	0.87	0.0283	39.47	0.995	0.021
4	143.0	0.84607E 06	39.58	0.35096E 04	0.25384E-02	0.904E-04	60.	0.86	0.0279	39.52	0.996	0.021
5	148.1	0.87842E 06	39.65	0.44865E 04	0.23683E-02	0.886E-04	70.	0.86	0.0278	39.49	0.989	0.021
6	153.2	0.91076E 06	39.62	0.54525E 04	0.23529E-02	0.886E-04	79.	0.87	0.0280	39.54	0.995	0.021
7	158.2	0.94310E 06	39.65	0.64232E 04	0.19288E-02	0.843E-04	87.	0.89	0.0289	39.36	0.980	0.021
8	163.3	0.97544E 06	39.77	0.73964E 04	0.16190E-02	0.812E-04	94.	0.85	0.0276	39.42	0.977	0.021
9	168.4	0.10078E 07	39.79	0.83202E 04	0.15653E-02	0.807E-04	101.	0.88	0.0284	39.31	0.968	0.021
10	173.5	0.10401E 07	39.84	0.92598E 04	0.15126E-02	0.800E-04	107.	0.86	0.0278	39.27	0.962	0.020
11	178.6	0.10725E 07	39.84	0.10174E 05	0.14611E-02	0.797E-04	112.	0.87	0.0282	39.06	0.948	0.020
12	183.6	0.11048E 07	39.52	0.11094E 05	0.13777E-02	0.787E-04	118.	0.86	0.0280	38.98	0.938	0.020
13	187.5	0.11254E 07	39.16	0.11969E 05	0.16062E-02	0.665E-04	120.					
14	190.1	0.11460E 07	39.06	0.11995E 05	0.14883E-02	0.650E-04	120.					
15	192.7	0.11627E 07	39.06	0.12020E 05	0.15721E-02	0.699E-04	120.					
16	195.4	0.11794E 07	39.25	0.12045E 05	0.14400E-02	0.666E-04	120.					
17	198.0	0.11962E 07	39.25	0.12070E 05	0.14960E-02	0.680E-04	120.					
18	200.6	0.12128E 07	39.25	0.12095E 05	0.15078E-02	0.688E-04	120.					
19	203.2	0.12295E 07	39.20	0.12120E 05	0.14443E-02	0.663E-04	120.					
20	205.8	0.12461E 07	39.24	0.12145E 05	0.15546E-02	0.690E-04	120.					
21	208.5	0.12628E 07	39.16	0.12171E 05	0.15562E-02	0.651E-04	120.					
22	211.1	0.12795E 07	39.14	0.12197E 05	0.16003E-02	0.722E-04	120.					
23	213.7	0.12961E 07	39.03	0.12225E 05	0.16723E-02	0.741E-04	120.					
24	216.3	0.13129E 07	39.01	0.12252E 05	0.16377E-02	0.734E-04	120.					
25	218.9	0.13296E 07	39.10	0.12280E 05	0.16693E-02	0.754E-04	120.					
26	221.6	0.13462E 07	38.89	0.12307E 05	0.16476E-02	0.724E-04	120.					
27	224.2	0.13629E 07	39.06	0.12336E 05	0.17679E-02	0.779E-04	120.					
28	226.8	0.13796E 07	39.14	0.12366E 05	0.18259E-02	0.802E-04	120.					
29	229.4	0.13962E 07	38.95	0.12396E 05	0.17437E-02	0.748E-04	120.					
30	232.0	0.14129E 07	39.12	0.12425E 05	0.18058E-02	0.801E-04	120.					
31	234.6	0.14295E 07	39.06	0.12456E 05	0.18832E-02	0.815E-04	120.					
32	237.3	0.14463E 07	38.95	0.12487E 05	0.19359E-02	0.801E-04	120.					
33	239.9	0.14630E 07	38.89	0.12518E 05	0.18744E-02	0.812E-04	120.					
34	242.5	0.14797E 07	38.65	0.12549E 05	0.18942E-02	0.798E-04	120.					
35	245.1	0.14963E 07	38.76	0.12582E 05	0.19848E-02	0.866E-04	120.					
36	247.8	0.15130E 07	38.76	0.12613E 05	0.17192E-02	0.881E-04	120.					

UNCERTAINTY IN REX= 7617. UNCERTAINTY IN F=0.05294 IN RATIO

RUN 080777-1 *** DISCRETE HOLE RIG *** NAS-3-14336   STANTON NUMBER DATA

1800 HSL M=0.90 P/D=5 TH=0 W/VCF(OPTIMUM)

RUN 080777-2 *** DISCRETE HOLE RIG *** NAS-3-14336   STANTON NUMBER DATA

1800 HSL M=0.90 P/D=5 TH=1 W/VCF(OPTIMUM)

LINEAR SUPERPOSITION IS APPLIED TO STANTON NUMBER DATA FROM
RUN NUMBERS 080777-1 AND 080777-2 TO OBTAIN STANTON NUMBER DATA AT TH=0 AND TH=1

PLATE	REXCOL	RE DEL2	ST(TH=0)	REXHOT	RE DEL2	ST(TH=1)	ETA	STCR	F-COL	STHR	F-HOT	LOGB
1	748411.3	1399.2	0.002538	749046.6	1400.4	0.002414	UUUUU	1.000	0.0000	1.000	0.0000	1.000
2	780726.1	1479.2	0.002411	781388.8	1477.3	0.002339	0.030	0.982	0.0316	0.953	0.0301	4.658
3	813040.9	1567.8	0.003075	813731.1	2528.2	0.002538	0.175	1.221	0.0305	1.008	0.0283	4.497
4	845355.8	1665.6	0.003223	846073.3	3524.6	0.002505	0.223	1.267	0.0302	0.985	0.0279	4.397
5	877670.6	1773.5	0.003209	878415.6	4506.6	0.002362	0.264	1.278	0.0301	0.941	0.0278	4.344
6	909985.4	1879.0	0.003318	910757.8	5480.3	0.002345	0.293	1.347	0.0299	0.952	0.0280	4.442
7	942300.3	1982.0	0.003054	943100.1	6455.2	0.001915	0.373	1.264	0.0302	0.793	0.0289	4.303
8	974615.1	2080.2	0.003027	975442.3	7446.0	0.001588	0.475	1.277	0.0295	0.670	0.0276	4.000
9	1006929.0	2175.0	0.002838	1007784.0	8389.6	0.001529	0.461	1.206	0.0303	0.650	0.0284	4.059
10	1039244.0	2269.1	0.002990	1040126.0	9356.9	0.001459	0.512	1.253	0.0299	0.611	0.0278	3.888
11	1071559.0	2364.2	0.002890	1072469.0	10302.9	0.001394	0.518	1.259	0.0303	0.607	0.0282	4.021
12	1103874.0	2460.6	0.003061	1104811.0	11258.0	0.001275	0.586	1.332	0.0302	0.551	0.0280	3.862
13	1128433.0	2536.5	0.003137	1129391.0	12196.3	0.001514	0.517	1.476		0.713		
14	1145075.0	2587.5	0.002976	1146047.0	12220.6	0.001398	0.530	1.439		0.676		
15	1161717.0	2638.3	0.003123	1162704.0	12244.6	0.001478	0.527	1.446		0.685		
16	1178440.0	2687.2	0.002752	1179441.0	12268.3	0.001361	0.506	1.374		0.679		
17	1195183.0	2733.6	0.002819	1196178.0	12291.4	0.001416	0.498	1.370		0.688		
18	1211865.0	2780.0	0.002745	1212834.0	12315.2	0.001433	0.478	1.347		0.703		
19	1228447.0	2824.4	0.002585	1229493.0	12338.9	0.001418	0.452	1.316		0.722		
20	1245090.0	2867.6	0.002606	1246146.0	12363.2	0.001491	0.428	1.285		0.735		
21	1261732.0	2911.3	0.002634	1262803.0	12388.1	0.001491	0.434	1.323		0.749		
22	1278374.0	2954.3	0.002529	1279459.0	12413.4	0.001544	0.389	1.260		0.770		
23	1295016.0	2997.0	0.002594	1296115.0	12439.7	0.001617	0.377	1.262		0.786		
24	1311735.0	3038.8	0.002430	1312852.0	12466.5	0.001590	0.346	1.232		0.806		
25	1328442.0	3079.5	0.002449	1329589.0	12493.2	0.001622	0.338	1.227		0.813		
26	1345104.0	3119.8	0.002389	1346246.0	12520.1	0.001603	0.329	1.229		0.825		
27	1361746.0	3160.1	0.002449	1362902.0	12547.9	0.001727	0.295	1.209		0.852		
28	1378288.0	3200.8	0.002438	1379558.0	12577.2	0.001789	0.266	1.187		0.871		
29	1395031.0	3240.5	0.002368	1396215.0	12606.4	0.001706	0.280	1.205		0.868		
30	1411673.0	3280.5	0.002391	1412871.0	12635.3	0.001770	0.260	1.217		0.901		
31	1428315.0	3320.7	0.002433	1429527.0	12665.5	0.001850	0.240	1.217		0.925		
32	1445038.0	3360.8	0.002385	1446264.0	12696.0	0.001803	0.244	1.237		0.935		
33	1461761.0	3400.4	0.002367	1463001.0	12726.4	0.001845	0.221	1.224		0.954		
34	1478403.0	3440.1	0.002391	1479658.0	12757.3	0.001864	0.220	1.206		0.941		
35	1495045.0	3480.6	0.002470	1496314.0	12789.2	0.001955	0.208	1.244		0.985		
36	1511687.0	3518.6	0.002094	1512970.0	12819.6	0.001697	0.190	1.245		1.008		

STANTON NUMBER RATIO BASED ON EXPERIMENTAL FLAT PLATE VALUE AT SAME X LOCATION

STANTON NUMBER RATIO FOR TH=1 IS CONVERTED TO COMPARABLE TRANSPIRATION VALUE
USING ALOG(1 + B)/B EXPRESSION IN THE BLOWN SECTION

RUN 080877-1 *** DISCRETE HOLE RIG *** NAS-3-14336 STANTON NUMBER DATA

TADB= 21.76 DEG C UINF= 9.80 M/S TINF= 21.72 DEG C
RHO= 1.191 KG/M3 VISC= 0.15209E-04 M2/S XVO= 10.1 CM
CP= 1011. J/KGK PR= 0.715

180C FSL M=1.25 P/D=5 TH=0 W/VCF(OPTIMUM)

PLATE	X	REX	TO	REENTH	STANTON NO	DST	DREEN	M	F	T2	THETA	DTH
1	127.8	0.75838E 06	35.43	0.14179E 04	0.25090E-02	0.957E-04	5.					
2	132.8	0.79113E 06	35.35	0.15004E 04	0.25311E-02	0.963E-04	16.	1.21	0.0390	23.27	0.114	0.022
3	137.9	0.82387E 06	35.49	0.17368E 04	0.30077E-02	0.101E-03	27.	1.26	0.0408	23.38	0.121	0.022
4	143.0	0.85662E 06	35.47	0.20014E 04	0.32845E-02	0.105E-03	34.	1.28	0.0413	23.32	0.117	0.022
5	148.1	0.88936E 06	35.49	0.22674E 04	0.33284E-02	0.105E-03	41.	1.25	0.0406	23.40	0.122	0.022
6	153.2	0.92211E 06	35.47	0.25427E 04	0.35464E-02	0.108E-03	46.	1.29	0.0419	23.31	0.116	0.022
7	158.2	0.95486E 06	35.52	0.28121E 04	0.31778E-02	0.103E-03	52.	1.28	0.0415	23.36	0.119	0.022
8	163.3	0.98760E 06	35.45	0.30783E 04	0.31961E-02	0.104E-03	56.	1.27	0.0412	23.28	0.114	0.022
9	168.4	0.10203E 07	35.41	0.33365E 04	0.32120E-02	0.104E-03	60.	1.27	0.0411	23.34	0.118	0.022
10	173.5	0.10531E 07	35.45	0.36022E 04	0.32890E-02	0.105E-03	64.	1.24	0.0402	23.19	0.107	0.022
11	178.6	0.10858E 07	35.47	0.38466E 04	0.30123E-02	0.101E-03	68.	1.27	0.0411	23.39	0.122	0.022
12	183.6	0.11186E 07	35.45	0.41124E 04	0.31552E-02	0.104E-03	71.	1.25	0.0405	23.32	0.117	0.022
13	187.5	0.11435E 07	34.55	0.43468E 04	0.32659E-02	0.124E-03	73.					
14	190.1	0.11603E 07	34.55	0.44000E 04	0.30280E-02	0.122E-03	73.					
15	192.7	0.11772E 07	34.57	0.44523E 04	0.31669E-02	0.123E-03	73.					
16	195.4	0.11941E 07	35.43	0.45022E 04	0.27476E-02	0.112E-03	73.					
17	198.0	0.12111E 07	35.45	0.45491E 04	0.28034E-02	0.112E-03	73.					
18	200.6	0.12280E 07	35.52	0.459[illegible]E 04	0.26928E-02	0.108E-03	73.					
19	203.2	0.12448E 07	35.62	0.46399E 04	0.25243E-02	0.101E-03	73.					
20	205.8	0.12617E 07	35.68	0.46825E 04	0.25642E-02	0.103E-03	73.					
21	208.5	0.12785E 07	35.68	0.47257E 04	0.25534E-02	0.102E-03	73.					
22	211.1	0.12954E 07	35.73	0.47681E 04	0.24776E-02	0.101E-03	73.					
23	213.7	0.13123E 07	35.68	0.48101E 04	0.24949E-02	0.101E-03	73.					
24	216.3	0.13292E 07	35.71	0.48513E 04	0.23849E-02	0.975E-04	73.					
25	218.9	0.13462E 07	35.85	0.48914E 04	0.23697E-02	0.984E-04	73.					
26	221.6	0.13630E 07	35.64	0.49308E 04	0.22934E-02	0.926E-04	73.					
27	224.2	0.13799E 07	35.52	0.49701E 04	0.23575E-02	0.973E-04	73.					
28	226.8	0.13968E 07	36.02	0.50098E 04	0.23450E-02	0.972E-04	73.					
29	229.4	0.14136E 07	35.79	0.50489E 04	0.22915E-02	0.919E-04	73.					
30	232.0	0.14305E 07	36.04	0.50877E 04	0.22402E-02	0.960E-04	73.					
31	234.6	0.14473E 07	35.98	0.51271E 04	0.23706E-02	0.971E-04	73.					
32	237.3	0.14643E 07	35.85	0.51666E 04	0.23393E-02	0.945E-04	73.					
33	239.9	0.14812E 07	35.81	0.52057E 04	0.23207E-02	0.960E-04	73.					
34	242.5	0.14981E 07	35.52	0.52450E 04	0.23378E-02	0.937E-04	73.					
35	245.1	0.15150E 07	35.68	0.52850E 04	0.24055E-02	0.100E-03	73.					
36	247.8	0.15318E 07	35.68	0.53226E 04	0.20381E-02	0.101E-03	73.					

UNCERTAINTY IN REX= 7712. UNCERTAINTY IN F=0.05294 IN RATIO

RUN 080877-2 *** DISCRETE HOLE RIG *** NAS-3-14336 STANTON NUMBER DATA

TADB= 24.75 DEG C UINF= 9.86 M/S TINF= 24.74 DEG C
RHO= 1.178 KG/M3 VISC= 0.15482E-04 M2/S XVO= 10.1 CM
CP= 1013. J/KGK PR= 0.716

1800 HSL M=1.25 P/D=5 TH=1 W/VCF(OPTIMUM)

PLATE	X	REX	TO	REENTH	STANTON NO	DST	DREEN	M	F	T2	THETA	DTH
1	127.8	0.74523E 06	38.51	0.14008E 04	0.24362E-02	0.949E-04	5.					
2	132.8	0.76158E 06	38.55	0.14827E 04	0.26273E-02	0.967E-04	35.	1.14	0.0369	38.73	1.013	0.023
3	137.9	0.81393E 06	38.51	0.27724E 04	0.23141E-02	0.936E-04	57.	1.19	0.0384	35.10	0.752	0.022
4	143.0	0.84628E 06	38.53	0.37877E 04	0.27778E-02	0.985E-04	73.	1.16	0.0374	38.77	1.017	0.023
5	148.1	0.87863E 06	38.48	0.51044E 04	0.27716E-02	0.987E-04	89.	1.15	0.0373	38.74	1.020	0.023
6	153.2	0.91098E 06	38.51	0.64245E 04	0.25609E-02	0.962E-04	102.	1.20	0.0387	38.76	1.018	0.023
7	158.2	0.94333E 06	38.57	0.77746E 04	0.21239E-02	0.915E-04	114.	1.20	0.0387	38.55	0.998	0.022
8	163.3	0.97568E 06	38.55	0.90903E 04	0.19317E-02	0.898E-04	125.	1.19	0.0386	38.62	1.005	0.023
9	168.4	0.10080E 07	38.67	0.10405E 05	0.17791E-02	0.879E-04	135.	1.20	0.0387	38.38	0.980	0.022
10	173.5	0.10404E 07	38.70	0.11688E 05	0.17610E-02	0.876E-04	144.	1.19	0.0382	38.38	0.977	0.022
11	178.6	0.10727E 07	38.70	0.12951E 05	0.15840E-02	0.862E-04	152.	1.20	0.0389	38.22	0.965	0.022
12	183.6	0.11051E 07	38.57	0.14219E 05	0.16102E-02	0.871E-04	160.	1.19	0.0385	38.03	0.961	0.022
13	187.5	0.11297E 07	37.62	0.15455E 05	0.15372E-02	0.654E-04	164.					
14	190.1	0.11463E 07	37.51	0.15480E 05	0.14167E-02	0.708E-04	164.					
15	192.7	0.11620E 07	37.52	0.15504E 05	0.14846E-02	0.699E-04	164.					
16	195.4	0.11797E 07	37.71	0.15528E 05	0.13324E-02	0.665E-04	164.					
17	198.0	0.11959E 07	37.66	0.15551E 05	0.14095E-02	0.676E-04	164.					
18	200.6	0.12131E 07	37.68	0.15574E 05	0.13798E-02	0.677E-04	164.					
19	203.2	0.12258E 07	37.64	0.15597E 05	0.13848E-02	0.652E-04	164.					
20	205.8	0.12485E 07	37.70	0.15620E 05	0.14055E-02	0.667E-04	164.					
21	208.5	0.12631E 07	37.66	0.15643E 05	0.14242E-02	0.675E-04	164.					
22	211.1	0.12758E 07	37.66	0.15667E 05	0.14232E-02	0.654E-04	164.					
23	213.7	0.12964E 07	37.58	0.15692E 05	0.14875E-02	0.710E-04	164.					
24	216.3	0.13132E 07	37.60	0.15716E 05	0.14290E-02	0.699E-04	164.					
25	218.9	0.13299E 07	37.68	0.15740E 05	0.14842E-02	0.714E-04	164.					
26	221.6	0.13466E 07	37.51	0.15765E 05	0.14800E-02	0.699E-04	164.					
27	224.2	0.13632E 07	37.68	0.15790E 05	0.15320E-02	0.731E-04	164.					
28	226.8	0.13799E 07	37.71	0.15816E 05	0.15870E-02	0.748E-04	164.					
29	229.4	0.13966E 07	37.54	0.15842E 05	0.15439E-02	0.710E-04	164.					
30	232.0	0.14132E 07	37.70	0.15868E 05	0.15870E-02	0.756E-04	164.					
31	234.6	0.14299E 07	37.66	0.15895E 05	0.16621E-02	0.769E-04	164.					
32	237.3	0.14466E 07	37.54	0.15922E 05	0.16275E-02	0.760E-04	164.					
33	239.9	0.14634E 07	37.51	0.15950E 05	0.16643E-02	0.772E-04	164.					
34	242.5	0.14800E 07	37.30	0.15978E 05	0.16537E-02	0.758E-04	164.					
35	245.1	0.14967E 07	37.41	0.16007E 05	0.17586E-02	0.820E-04	164.					
36	247.8	0.15133E 07	37.41	0.16034E 05	0.14555E-02	0.830E-04	164.					

UNCERTAINTY IN REX= 7618. UNCERTAINTY IN F=0.05294 IN RATIO

RUN 080877-1 *** DISCRETE HOLE RIG *** NAS-3-14336 STANTON NUMBER DATA

1800 MSL M=1.25 P/D=5 TH=0 W/VCF(OPTIMUM)

RUN 080877-2 *** DISCRETE HOLE RIG *** NAS-3-14336 STANTON NUMBER DATA

1800 MSL M=1.25 P/D=5 TH=1 W/VCF(OPTIMUM)

LINEAR SUPERPOSITION IS APPLIED TO STANTON NUMBER DATA FROM
RUN NUMBERS 080877-1 AND 080877-2 TO OBTAIN STANTON NUMBER DATA AT TH=0 AND TH=1

PLATE	REXCOL	RE DEL2	ST(TH=0)	REXHOT	RE DEL2	ST(TH=1)	ETA	STCR	F-COL	STHR	F-HOT	LOGB
1	758382.0	1417.9	0.002509	749232.7	1400.8	0.002436	UUUUU	1.000	0.0000	1.000	0.0000	1.000
2	791128.1	1500.2	0.002519	781583.0	1482.6	0.002626	*****	1.026	0.0390	1.070	0.0369	5.344
3	823672.5	1592.4	0.003114	813933.3	2754.8	0.002208	0.291	1.236	0.0408	0.876	0.0384	5.231
4	856618.9	1698.5	0.003363	846283.6	4075.1	0.002701	0.197	1.322	0.0413	1.062	0.0376	5.455
5	889264.3	1809.2	0.003402	878633.9	5375.3	0.002783	0.182	1.355	0.0406	1.109	0.0373	5.567
6	922109.6	1925.1	0.003677	910984.2	6667.4	0.002582	0.298	1.453	0.0419	1.048	0.0387	5.668
7	954855.0	2035.7	0.003317	943334.5	7995.2	0.002134	0.357	1.373	0.0415	0.883	0.0387	5.428
8	987600.4	2149.0	0.003362	975684.8	9313.4	0.001934	0.425	1.418	0.0412	0.816	0.0386	5.350
9	1020345.0	2259.8	0.003402	1008035.0	10621.6	0.001767	0.481	1.446	0.0411	0.751	0.0387	5.250
10	1053091.0	2372.6	0.002488	1040385.0	11929.4	0.001723	0.506	1.462	0.0402	0.722	0.0382	5.097
11	1085836.0	2482.1	0.003203	1072735.0	13219.2	0.001536	0.520	1.396	0.0411	0.669	0.0389	5.186
12	1118581.0	2590.6	0.003419	1105086.0	14528.5	0.001541	0.549	1.478	0.0405	0.666	0.0385	5.113
13	1143468.0	2676.2	0.003510	1129672.0	15811.9	0.001462	0.583	1.652		0.668		
14	1160232.0	2733.3	0.002256	1146332.0	15835.3	0.001347	0.586	1.574		0.651		
15	1177196.0	2789.5	0.003405	1162993.0	15858.3	0.001412	0.585	1.577		0.654		
16	1194161.0	2843.1	0.002948	1179734.0	15880.7	0.001271	0.569	1.472		0.635		
17	1211187.0	2893.4	0.003000	1196475.0	15902.5	0.001349	0.550	1.458		0.656		
18	1227551.0	2943.0	0.002878	1213135.0	15924.8	0.001323	0.540	1.413		0.649		
19	1244815.0	2990.0	0.002688	1229796.0	15946.8	0.001314	0.511	1.368		0.669		
20	1261675.0	3035.7	0.002728	1246456.0	15969.1	0.001355	0.503	1.345		0.668		
21	1278542.0	3081.6	0.002713	1263117.0	15991.9	0.001375	0.493	1.342		0.691		
22	1295400.0	3126.7	0.002627	1279777.0	16014.8	0.001377	0.476	1.309		0.686		
23	1312270.0	3171.2	0.002637	1296438.0	16038.3	0.001444	0.453	1.283		0.702		
24	1329216.0	3214.7	0.002520	1313179.0	16062.0	0.001387	0.449	1.278		0.703		
25	1346162.0	3257.0	0.002498	1329923.0	16085.4	0.001425	0.430	1.251		0.714		
26	1363025.0	3298.5	0.002409	1346580.0	16109.3	0.001445	0.400	1.239		0.743		
27	1375885.0	3339.7	0.002474	1363241.0	16133.9	0.001496	0.395	1.221		0.739		
28	1396753.0	3381.3	0.002452	1379901.0	16159.3	0.001554	0.366	1.194		0.757		
29	1413617.0	3422.2	0.002397	1396562.0	16184.9	0.001511	0.370	1.220		0.769		
30	1430491.0	3462.7	0.002399	1413222.0	16210.4	0.001556	0.351	1.220		0.792		
31	1447345.0	3503.8	0.002471	1429883.0	16237.0	0.001635	0.340	1.235		0.816		
32	1464291.0	3545.0	0.002405	1446624.0	16263.9	0.001598	0.336	1.248		0.829		
33	1481238.0	3585.7	0.002413	1463365.0	16290.9	0.001636	0.322	1.249		0.846		
34	1498100.0	3626.5	0.002429	1480025.0	16318.4	0.001666	0.314	1.225		0.840		
35	1514964.0	3668.1	0.002497	1496686.0	16346.8	0.001731	0.307	1.258		0.872		
36	1531828.0	3707.1	0.002115	1513346.0	16373.5	0.001472	0.304	1.257		0.875		

STANTON NUMBER RATIO BASED ON EXPERIMENTAL FLAT PLATE VALUE AT SAME X LOCATION

STANTON NUMBER RATIO FOR TH=1 IS CONVERTED TO COMPARABLE TRANSPIRATION VALUE
USING ALOG(1 + B)/B EXPRESSION IN THE BLOWN SECTION

RUN 073077-1 *** DISCRETE HOLE RIG *** NAS-3-14336 STANTON NUMBER DATA

TADB= 28.88 DEG C UINF= 10.00 M/S TINF= 28.84 DEG C
RHO= 1.155 KG/M3 VISC= 0.15896E-04 M2/S XVO= 10.1 CM
CP= 1013. J/KGK PR= 0.715

180C HSL M=1.50 P/D=5 TH=0 W/VCF(OPTIMUM)

PLATE	X	REX	TO	REENTH	STANTON NO	DST	CREEN	M	F	T2	THETA	DTH
1	127.8	0.74043E 06	40.00	0.13843E 04	0.24195E-02	0.113E-03	5.					
2	132.8	0.77240E 06	39.96	0.14613E 04	0.23981E-02	0.113E-03	22.	1.48	0.0479	29.64	0.073	0.028
3	137.9	0.80437E 06	40.03	0.16589E 04	0.30058E-02	0.119E-03	37.	1.44	0.0465	29.76	0.083	0.027
4	143.0	0.83634E 06	40.01	0.18838E 04	0.33625E-02	0.123E-03	47.	1.47	0.0475	29.73	0.080	0.027
5	148.1	0.86831E 06	39.98	0.21166E 04	0.35808E-02	0.126E-03	56.	1.45	0.0468	29.82	0.088	0.027
6	153.2	0.90028E 06	39.92	0.23657E 04	0.37571E-02	0.129E-03	63.	1.48	0.0479	29.75	0.082	0.028
7	158.2	0.93225E 06	39.86	0.26090E 04	0.35940E-02	0.127E-03	70.	1.46	0.0473	29.79	0.087	0.028
8	163.3	0.96422E 06	39.92	0.28574E 04	0.37275E-02	0.128E-03	76.	1.43	0.0461	29.71	0.079	0.028
9	168.4	0.99619E 06	40.03	0.30864E 04	0.32868E-02	0.122E-03	82.	1.47	0.0475	29.79	0.086	0.027
10	173.5	0.10282E 07	39.92	0.33326E 04	0.39675E-02	0.132E-03	87.	1.45	0.0469	29.71	0.079	0.028
11	178.6	0.10601E 07	40.01	0.35662E 04	0.32388E-02	0.122E-03	92.	1.43	0.0464	29.85	0.091	0.027
12	183.6	0.10921E 07	39.94	0.38040E 04	0.35375E-02	0.126E-03	97.	1.46	0.0471	29.78	0.085	0.028
13	187.5	0.11164E 07	39.25	0.40222E 04	0.34557E-02	0.136E-03	99.					
14	190.1	0.11329E 07	39.25	0.40760E 04	0.30755E-02	0.131E-03	99.					
15	192.7	0.11493E 07	39.25	0.41276E 04	0.31759E-02	0.130E-03	99.					
16	195.4	0.11659E 07	39.73	0.41753E 04	0.26133E-02	0.114E-03	99.					
17	198.0	0.11824E 07	39.75	0.42186E 04	0.26377E-02	0.112E-03	99.					
18	200.6	0.11989E 07	39.81	0.42608E 04	0.24633E-02	0.108E-03	99.					
19	203.2	0.12154E 07	39.84	0.43007E 04	0.23560E-02	0.102E-03	99.					
20	205.8	0.12318E 07	39.90	0.43397E 04	0.23732E-02	0.102E-03	99.					
21	208.5	0.12483E 07	39.90	0.43790E 04	0.23676E-02	0.103E-03	99.					
22	211.1	0.12647E 07	39.94	0.44175E 04	0.22912E-02	0.101E-03	99.					
23	213.7	0.12812E 07	39.92	0.44553E 04	0.22900E-02	0.101E-03	99.					
24	216.3	0.12978E 07	39.94	0.44926E 04	0.22331E-02	0.994E-04	99.					
25	218.9	0.13143E 07	40.05	0.45290E 04	0.21828E-02	0.987E-04	99.					
26	221.6	0.13306E 07	39.90	0.45646E 04	0.21371E-02	0.944E-04	99.					
27	224.2	0.13472E 07	40.13	0.46000E 04	0.21624E-02	0.975E-04	99.					
28	226.8	0.13637E 07	40.19	0.46357E 04	0.21627E-02	0.973E-04	99.					
29	229.4	0.13802E 07	40.03	0.46709E 04	0.21124E-02	0.928E-04	99.					
30	232.0	0.13966E 07	40.20	0.47059E 04	0.21288E-02	0.968E-04	99.					
31	234.6	0.14131E 07	40.20	0.47411E 04	0.21496E-02	0.966E-04	99.					
32	237.3	0.14296E 07	40.39	0.47764E 04	0.21230E-02	0.955E-04	99.					
33	239.9	0.14462E 07	40.09	0.48112E 04	0.20995E-02	0.953E-04	99.					
34	242.5	0.14626E 07	39.86	0.48459E 04	0.21150E-02	0.929E-04	99.					
35	245.1	0.14791E 07	39.98	0.48812E 04	0.21672E-02	0.953E-04	99.					
36	247.8	0.14956E 07	39.98	0.49140E 04	0.16008E-02	0.955E-04	99.					

UNCERTAINTY IN REX= 8760. UNCERTAINTY IN F=0.05287 IN RATIO

RUN 073077-2 *** DISCRETE HOLE RIG *** NAS-3-14336 STANTON NUMBER DATA

TADB= 22.14 DEG C UINF= 10.06 M/S TINF= 32.09 DEG C
RHO= 1.145 KG/M3 VISC= 0.16196E-04 M2/S XVO= 10.1 CM
CP= 1015. J/KGK PR= 0.716

1800 HSL M=1.50 P/D=5 TH=1 W/VCF(OPTIMUM)

PLATE	X	REX	TO	REENTH	STANTON NO	DST	DREEN	M	F	T2	THETA	DTH
1	127.8	0.73109E 06	44.26	0.13669E 04	0.24629E-02	0.106E-03	5.					
2	132.8	0.76266E 06	44.15	0.14453E 04	0.25063E-02	0.107E-03	42.	1.41	0.0457	43.85	0.976	0.026
3	137.9	0.79423E 06	44.18	0.29378E 04	0.29259E-02	0.111E-03	71.	1.36	0.0439	43.71	0.961	0.025
4	143.0	0.82579E 06	44.20	0.43638E 04	0.31120E-02	0.113E-03	90.	1.35	0.0438	43.75	0.963	0.025
5	148.1	0.85736E 06	44.20	0.57909E 04	0.30696E-02	0.112E-03	107.	1.36	0.0440	43.86	0.972	0.025
6	153.2	0.88893E 06	44.20	0.72331E 04	0.28442E-02	0.110E-03	121.	1.35	0.0438	43.93	0.978	0.026
7	158.2	0.92050E 06	44.15	0.86687E 04	0.24467E-02	0.106E-03	133.	1.34	0.0435	43.90	0.979	0.026
8	163.3	0.95206E 06	44.22	0.10037E 05	0.22243E-02	0.104E-03	145.	1.35	0.0437	44.02	0.984	0.026
9	168.4	0.98363E 06	44.17	0.11513E 05	0.21090E-02	0.103E-03	156.	1.37	0.0444	43.88	0.976	0.026
10	173.5	0.10152E 07	44.20	0.12948E 05	0.21066E-02	0.103E-03	166.	1.36	0.0440	43.86	0.972	0.025
11	178.6	0.10468E 07	44.11	0.14358E 05	0.17117E-02	0.100E-03	175.	1.38	0.0447	43.80	0.975	0.026
12	183.6	0.10783E 07	44.18	0.15769E 05	0.17666E-02	0.100E-03	184.	1.38	0.0446	43.82	0.970	0.026
13	187.5	0.11023E 07	44.22	0.17196E 05	0.17646E-02	0.791E-04	189.					
14	190.1	0.11188E 07	44.32	0.17223E 05	0.15737E-02	0.786E-04	189.					
15	192.7	0.11348E 07	44.32	0.17249E 05	0.16523E-02	0.768E-04	189.					
16	195.4	0.11512E 07	44.54	0.17274E 05	0.14477E-02	0.719E-04	189.					
17	198.0	0.11675E 07	44.54	0.17298E 05	0.14805E-02	0.720E-04	189.					
18	200.6	0.11838E 07	44.54	0.17322E 05	0.14443E-02	0.714E-04	189.					
19	203.2	0.12005E 07	44.49	0.17345E 05	0.14229E-02	0.688E-04	189.					
20	205.8	0.12163E 07	44.49	0.17369E 05	0.14930E-02	0.711E-04	189.					
21	208.5	0.12325E 07	44.45	0.17394E 05	0.15070E-02	0.720E-04	189.					
22	211.1	0.12488E 07	44.45	0.17418E 05	0.15200E-02	0.740E-04	189.					
23	213.7	0.12651E 07	44.45	0.17443E 05	0.15532E-02	0.754E-04	189.					
24	216.3	0.12814E 07	44.41	0.17468E 05	0.15420E-02	0.751E-04	189.					
25	218.9	0.12977E 07	44.49	0.17494E 05	0.15653E-02	0.765E-04	189.					
26	221.6	0.13140E 07	44.34	0.17519E 05	0.15456E-02	0.739E-04	189.					
27	224.2	0.13302E 07	44.51	0.17545E 05	0.16152E-02	0.778E-04	189.					
28	226.8	0.13465E 07	44.52	0.17572E 05	0.16853E-02	0.796E-04	189.					
29	229.4	0.13628E 07	44.41	0.17598E 05	0.15961E-02	0.747E-04	189.					
30	232.0	0.13790E 07	44.54	0.17625E 05	0.16599E-02	0.797E-04	189.					
31	234.6	0.13953E 07	44.32	0.17652E 05	0.17002E-02	0.801E-04	189.					
32	237.3	0.14116E 07	44.43	0.17680E 05	0.16802E-02	0.796E-04	189.					
33	239.9	0.14279E 07	44.41	0.17707E 05	0.17041E-02	0.803E-04	189.					
34	242.5	0.14442E 07	44.22	0.17735E 05	0.16939E-02	0.777E-04	189.					
35	245.1	0.14605E 07	44.32	0.17763E 05	0.17835E-02	0.847E-04	189.					
36	247.8	0.14767E 07	44.32	0.17790E 05	0.15044E-02	0.858E-04	189.					

UNCERTAINTY IN REX= 8649. UNCERTAINTY IN F=0.05287 IN RATIO

RUN 073077-1 *** DISCRETE HOLE RIG *** NAS-3-14336 STANTON NUMBER DATA

180C HSL M=1.50 P/D=5 TH=0 W/VCF(OPTIMUM)

RUN 073077-2 *** DISCRETE HOLE RIG *** NAS-3-14336 STANTON NUMBER DATA

180C HSL M=1.50 P/D=5 TH=1 W/VCF(OPTIMUM)

LINEAR SUPERPOSITION IS APPLIED TO STANTON NUMBER DATA FROM
RUN NUMBERS 073077-1 AND 073077-2 TO OBTAIN STANTON NUMBER DATA AT TH=0 AND TH=1

PLATE	REXCOL	RE DEL2	ST(TH=0)	REXHOT	RE DEL2	ST(TH=1)	ETA	STCR	F-COL	STHR	F-HOT	LOGB
1	740432.1	1384.3	0.002420	731093.6	1366.9	0.002463	UUUUU	1.000	0.0000	1.000	0.0000	1.000
2	772402.4	1461.2	0.002389	762660.6	1445.3	0.002509	*****	0.973	0.0479	1.022	0.0457	6.295
3	804372.7	1547.5	0.003013	794227.8	2972.7	0.002923	0.030	1.196	0.0465	1.180	0.0439	6.280
4	836342.0	1649.8	0.003396	825794.8	4452.5	0.003101	0.084	1.331	0.0475	1.219	0.0438	6.335
5	868313.3	1762.0	0.003629	857361.9	5933.7	0.003051	0.159	1.446	0.0468	1.215	0.0440	6.404
6	900283.6	1881.4	0.003844	888929.0	7411.5	0.002818	0.267	1.561	0.0479	1.144	0.0438	6.340
7	932253.9	2002.1	0.003702	920496.1	8877.3	0.002421	0.346	1.532	0.0473	1.002	0.0435	6.119
8	964224.3	2123.0	0.003866	952063.1	10323.6	0.002193	0.433	1.631	0.0461	0.925	0.0437	6.063
9	996194.6	2239.2	0.003357	983630.3	11771.3	0.002083	0.387	1.444	0.0475	0.885	0.0444	6.075
10	1028164.9	2359.6	0.004139	1015197.0	13238.0	0.002052	0.504	1.734	0.0469	0.860	0.0440	5.929
11	1060135.0	2479.5	0.003385	1046764.0	14686.6	0.001665	0.508	1.475	0.0464	0.726	0.0447	5.855
12	1092105.0	2592.9	0.003681	1078331.0	16151.1	0.001712	0.535	1.592	0.0471	0.740	0.0446	5.845
13	1116402.0	2681.6	0.003624	1102322.0	17599.0	0.001712	0.528	1.706		0.806		
14	1132867.0	2738.1	0.003230	1118579.0	17625.4	0.001527	0.527	1.561		0.738		
15	1145232.0	2792.1	0.003328	1134836.0	17650.8	0.001605	0.518	1.541		0.743		
16	1165876.0	2842.0	0.002730	1151172.0	17675.4	0.001411	0.483	1.363		0.705		
17	1182421.0	2887.2	0.002753	1167508.0	17698.6	0.001444	0.475	1.338		0.702		
18	1198884.0	2931.3	0.002587	1183765.0	17721.8	0.001412	0.454	1.270		0.693		
19	1215350.0	2972.8	0.002449	1200022.0	17744.7	0.001394	0.431	1.246		0.709		
20	1231815.0	3013.3	0.002466	1216279.0	17767.9	0.001465	0.406	1.216		0.722		
21	1248280.0	3054.0	0.002475	1232536.0	17791.9	0.001479	0.402	1.243		0.743		
22	1264745.0	3093.9	0.002368	1248793.0	17816.1	0.001496	0.368	1.180		0.745		
23	1281209.0	3132.9	0.002363	1265050.0	17840.7	0.001530	0.353	1.150		0.744		
24	1297754.0	3171.4	0.002302	1281306.0	17865.5	0.001520	0.340	1.167		0.771		
25	1314255.0	3208.9	0.002244	1297722.0	17890.5	0.001546	0.311	1.124		0.774		
26	1330763.0	3245.5	0.002196	1313979.0	17915.5	0.001527	0.305	1.130		0.786		
27	1347228.0	3281.8	0.002217	1330236.0	17940.9	0.001598	0.279	1.094		0.789		
28	1363693.0	3318.3	0.002210	1346493.0	17967.5	0.001670	0.244	1.076		0.813		
29	1380157.0	3354.4	0.002164	1362751.0	17993.9	0.001580	0.270	1.102		0.804		
30	1396622.0	3390.2	0.002176	1379008.0	18020.2	0.001645	0.244	1.107		0.837		
31	1413087.0	3426.2	0.002194	1395265.0	18047.3	0.001686	0.232	1.097		0.843		
32	1429831.0	3462.1	0.002167	1411600.0	18074.6	0.001666	0.231	1.124		0.864		
33	1446176.0	3497.6	0.002139	1427936.0	18101.9	0.001652	0.209	1.107		0.875		
34	1462641.0	3533.0	0.002157	1444193.0	18129.3	0.001681	0.221	1.088		0.848		
35	1479105.0	3569.0	0.002205	1460450.0	18157.4	0.001771	0.197	1.111		0.892		
36	1495570.0	3602.3	0.001839	1476708.0	18184.0	0.001495	0.187	1.083		0.889		

STANTON NUMBER RATIO BASED ON EXPERIMENTAL FLAT PLATE VALUE AT SAME X LOCATION

STANTON NUMBER RATIO FOR TH=1 IS CONVERTED TO COMPARABLE TRANSPIRATION VALUE
USING ALOG(1 + B)/B EXPRESSION IN THE BLOWN SECTION

RUN082277 VELOCITY AND TEMPERATURE PROFILES

REX =	0.15261E 06	REM =	519.	REH =	641.
XVO =	106.45 CM	DEL2 =	0.072 CM	DEH2 =	0.090 CM
UINF =	11.23 M/S	DEL99=	0.548 CM	DELT99 =	0.628 CM
VISC =	0.15688E-04 M2/S	DEL1 =	0.156 CM	UINF =	11.25 M/S
PORT =	3	H =	2.153	VISC =	0.15750E-04 M2/S
XLOC =	127.76 CM	CF/2 =	0.15450E-02	TINF =	23.53 DEG C
				TPLATE =	37.07 DEG C

Y(CM)	Y/DEL	U(M/S)	U/UINF	Y+	U+	Y(CM)	T(DEG C)	TBAR	TBAR
0.025	0.046	2.60	0.231	7.1	5.88	0.0127	34.85	0.164	0.836
0.038	0.069	3.17	0.282	10.7	7.18	0.0178	34.80	0.167	0.833
0.051	0.093	3.52	0.314	14.3	7.98	0.0279	34.74	0.172	0.828
0.064	0.116	4.02	0.358	17.9	9.12	0.0406	34.68	0.176	0.824
0.076	0.139	4.41	0.393	21.4	9.99	0.0610	34.22	0.210	0.790
0.089	0.162	4.74	0.422	25.0	10.74	0.0737	33.34	0.272	0.728
0.102	0.185	5.16	0.460	28.6	11.70	0.0864	32.51	0.337	0.663
0.114	0.208	5.50	0.489	32.2	12.45	0.0991	32.03	0.372	0.628
0.127	0.232	5.93	0.528	35.7	13.42	0.1118	31.26	0.429	0.571
0.140	0.255	6.24	0.556	39.3	14.14	0.1245	31.00	0.448	0.552
0.152	0.278	6.57	0.585	42.9	14.87	0.1499	30.10	0.515	0.485
0.178	0.324	7.26	0.646	50.0	16.44	0.1753	29.34	0.571	0.429
0.203	0.371	7.86	0.700	57.2	17.81	0.2134	28.36	0.643	0.357
0.229	0.417	8.42	0.750	64.3	19.07	0.2388	27.54	0.701	0.299
0.254	0.463	8.89	0.792	71.5	20.14	0.2642	26.94	0.748	0.252
0.279	0.509	9.26	0.825	78.6	20.98	0.2896	26.30	0.791	0.209
0.330	0.602	9.87	0.879	92.9	22.36	0.3277	25.65	0.844	0.156
0.368	0.672	10.24	0.912	103.6	23.20	0.3785	24.89	0.900	0.100
0.432	0.787	10.72	0.955	121.5	24.29	0.4293	24.39	0.937	0.063
0.495	0.903	10.98	0.977	139.4	24.87	0.4674	24.10	0.958	0.042
0.559	1.019	11.14	0.992	157.3	25.23	0.5055	23.93	0.971	0.029
0.622	1.135	11.23	1.000	175.1	25.44	0.5690	23.78	0.982	0.018
						0.632	23.66	0.990	0.010
						0.696	23.60	0.995	0.005
						0.759	23.57	0.997	0.003
						0.823	23.55	0.999	0.001
						0.886	23.53	1.000	0.000

RUN 082277 *** DISCRETE HOLE RIG *** NAS-3-14336 STANTON NUMBER DATA

TADB= 23.38 DEG C UINF= 11.37 M/S TINF= 23.33 DEG C
RHO= 1.154 KG/M3 VISC= 0.15731E-04 M2/S XVO= 105.5 CM
CP= 1013. J/KGK PR= 0.716

500 FSL FLAT PLATE P/D=5

PLATE	X	REX	TO	REENTH	STANTONNO	DST	DREEN	ST(THEO)	RATIO
1	127.8	0.16086E 06	36.12	0.64822E 03	0.30324E-02	0.934E-04	7.	0.30653E-02	0.989
2	132.8	0.19759E 06	36.88	0.75866E 03	0.29814E-02	0.886E-04	8.	0.29418E-02	1.013
3	137.9	0.23432E 06	36.71	0.86762E 03	0.29522E-02	0.892E-04	8.	0.28431E-02	1.038
4	143.0	0.27104E 06	36.74	0.97487E 03	0.28886E-02	0.884E-04	8.	0.27615E-02	1.046
5	148.1	0.30777E 06	36.80	0.10793E 04	0.27964E-02	0.873E-04	9.	0.26922E-02	1.039
6	153.2	0.34450E 06	36.80	0.11815E 04	0.27715E-02	0.871E-04	9.	0.26322E-02	1.053
7	158.2	0.38122E 06	36.76	0.12826E 04	0.27308E-02	0.869E-04	9.	0.25794E-02	1.059
8	163.3	0.41795E 06	36.71	0.13810E 04	0.26308E-02	0.863E-04	10.	0.25324E-02	1.039
9	168.4	0.45468E 06	36.65	0.14768E 04	0.25877E-02	0.863E-04	10.	0.24901E-02	1.039
10	173.5	0.49140E 06	36.53	0.15712E 04	0.25512E-02	0.866E-04	10.	0.24517E-02	1.041
11	178.6	0.52813E 06	36.71	0.16631E 04	0.24550E-02	0.848E-04	10.	0.24166E-02	1.016
12	183.6	0.56486E 06	36.72	0.17528E 04	0.24303E-02	0.845E-04	11.	0.23844E-02	1.019
13	187.5	0.59277E 06	35.60	0.18166E 04	0.22487E-02	0.832E-04	11.	0.23615E-02	0.952
14	190.1	0.61116E 06	35.41	0.18606E 04	0.21872E-02	0.892E-04	11.	0.23467E-02	0.932
15	192.7	0.62958E 06	35.41	0.19031E 04	0.22875E-02	0.906E-04	11.	0.23324E-02	0.981
16	195.4	0.64960E 06	35.62	0.19450E 04	0.21331E-02	0.876E-04	11.	0.23186E-02	0.920
17	198.0	0.66861E 06	35.62	0.19858E 04	0.21753E-02	0.875E-04	11.	0.23053E-02	0.944
18	200.6	0.68752E 06	35.62	0.20264E 04	0.21705E-02	0.876E-04	11.	0.22925E-02	0.947
19	203.2	0.70644E 06	35.60	0.20672E 04	0.20810E-02	0.835E-04	11.	0.22803E-02	0.913
20	205.8	0.72535E 06	35.62	0.21075E 04	0.21764E-02	0.867E-04	11.	0.22683E-02	0.960
21	208.5	0.74426E 06	35.60	0.21480E 04	0.21020E-02	0.845E-04	11.	0.22564E-02	0.932
22	211.1	0.76318E 06	35.62	0.21880E 04	0.21268E-02	0.867E-04	11.	0.22451E-02	0.947
23	213.7	0.78209E 06	35.58	0.22287E 04	0.21617E-02	0.874E-04	11.	0.22341E-02	0.968
24	216.3	0.80110E 06	35.62	0.22688E 04	0.20829E-02	0.854E-04	11.	0.22234E-02	0.937
25	218.9	0.82010E 06	35.70	0.23087E 04	0.21218E-02	0.873E-04	11.	0.22130E-02	0.959
26	221.6	0.83902E 06	35.52	0.23481E 04	0.20461E-02	0.825E-04	12.	0.22029E-02	0.929
27	224.2	0.85753E 06	35.75	0.23877E 04	0.21345E-02	0.872E-04	12.	0.21931E-02	0.973
28	226.8	0.87665E 06	35.85	0.24284E 04	0.21669E-02	0.885E-04	12.	0.21836E-02	0.993
29	229.4	0.89576E 06	35.70	0.24686E 04	0.20714E-02	0.824E-04	12.	0.21743E-02	0.953
30	232.0	0.91468E 06	35.52	0.25078E 04	0.20706E-02	0.858E-04	12.	0.21652E-02	0.956
31	234.6	0.93359E 06	35.51	0.25472E 04	0.20934E-02	0.855E-04	12.	0.21564E-02	0.971
32	237.3	0.95240E 06	35.77	0.25864E 04	0.20463E-02	0.837E-04	12.	0.21477E-02	0.953
33	239.9	0.97180E 06	35.77	0.26252E 04	0.20451E-02	0.844E-04	12.	0.21392E-02	0.956
34	242.5	0.99052E 06	35.52	0.26639E 04	0.20482E-02	0.816E-04	12.	0.21310E-02	0.961
35	245.1	0.10094E 07	35.70	0.27030E 04	0.20775E-02	0.868E-04	12.	0.21230E-02	0.979
36	247.8	0.10283E 07	35.70	0.27393E 04	0.17563E-02	0.870E-04	12.	0.21151E-02	0.830

RUN 082377-1 *** DISCRETE HOLE RIG *** NAS-3-14336 STANTON NUMBER DATA

TADB= 23.27 DEG C UINF= 11.33 M/S TINF= 23.21 DEG C
RHO= 1.182 KG/M3 VISC= 0.15376E-04 M2/S XVO= 105.5 CM
CP= 1012. J/KGK PR= 0.716

SCC HSL M=0.4 P/D=5 TH=0 W/VCF(OPTIMUM)

PLATE	X	REX	TO	REENTH	STANTON NO	DST	DREEN	M	F	T2	THETA	DTH
1	127.8	0.16402E 06	37.11	0.66096E 03	0.27656E-02	0.835E-04	4.					
2	132.8	0.20147E 06	37.16	0.76627E 03	0.28586E-02	0.840E-04	7.	0.43	0.0139	25.50	0.164	0.022
3	137.9	0.23852E 06	37.24	0.95972E 03	0.29222E-02	0.843E-04	12.	0.44	0.0144	25.56	0.167	0.022
4	143.0	0.27627E 06	37.09	0.11607E 04	0.29982E-02	0.857E-04	15.	0.44	0.0143	25.44	0.160	0.022
5	148.1	0.31362E 06	37.16	0.13566E 04	0.28371E-02	0.838E-04	17.	0.44	0.0141	25.52	0.166	0.022
6	153.2	0.35126E 06	37.20	0.15453E 04	0.28148E-02	0.834E-04	19.	0.42	0.0137	25.46	0.161	0.022
7	158.2	0.38671E 06	37.16	0.17330E 04	0.25848E-02	0.814E-04	21.	0.45	0.0147	25.54	0.167	0.022
8	163.3	0.42616E 06	37.14	0.19196E 04	0.24428E-02	0.805E-04	23.	0.43	0.0138	25.48	0.163	0.022
9	168.4	0.46361E 06	37.05	0.20924E 04	0.23477E-02	0.802E-04	25.	0.45	0.0145	25.50	0.166	0.022
10	173.5	0.50106E 06	37.09	0.22691E 04	0.22807E-02	0.795E-04	27.	0.44	0.0143	25.43	0.160	0.022
11	178.6	0.53850E 06	37.12	0.24154E 04	0.22427E-02	0.790E-04	28.	0.45	0.0145	25.60	0.171	0.022
12	183.6	0.57555E 06	37.11	0.26169E 04	0.22093E-02	0.793E-04	30.	0.43	0.0140	25.62	0.173	0.022
13	187.5	0.60441E 06	36.10	0.27721E 04	0.23081E-02	0.842E-04	30.					
14	190.1	0.62370E 06	35.98	0.28152E 04	0.21322E-02	0.866E-04	30.					
15	192.7	0.64256E 06	35.98	0.28575E 04	0.22254E-02	0.868E-04	30.					
16	195.4	0.66236E 06	36.25	0.28984E 04	0.20395E-02	0.816E-04	30.					
17	198.0	0.68174E 06	36.25	0.29377E 04	0.20633E-02	0.823E-04	30.					
18	200.6	0.70103E 06	36.25	0.29775E 04	0.20650E-02	0.825E-04	30.					
19	203.2	0.72031E 06	36.25	0.30165E 04	0.19757E-02	0.766E-04	30.					
20	205.8	0.73960E 06	36.27	0.30558E 04	0.20854E-02	0.822E-04	30.					
21	208.5	0.75689E 06	36.25	0.30950E 04	0.19765E-02	0.788E-04	30.					
22	211.1	0.77817E 06	36.27	0.31337E 04	0.20329E-02	0.820E-04	30.					
23	213.7	0.79746E 06	36.19	0.31736E 04	0.20987E-02	0.835E-04	30.					
24	216.3	0.81684E 06	36.23	0.32132E 04	0.20089E-02	0.812E-04	31.					
25	218.9	0.83622E 06	36.33	0.32525E 04	0.20552E-02	0.835E-04	31.					
26	221.6	0.85550E 06	36.13	0.32916E 04	0.20019E-02	0.794E-04	31.					
27	224.2	0.87479E 06	36.34	0.33313E 04	0.21032E-02	0.843E-04	31.					
28	226.8	0.89407E 06	36.46	0.33724E 04	0.21599E-02	0.867E-04	31.					
29	229.4	0.91336E 06	36.27	0.34130E 04	0.20453E-02	0.797E-04	31.					
30	232.0	0.93265E 06	36.55	0.34524E 04	0.20337E-02	0.833E-04	31.					
31	234.6	0.95193E 06	36.50	0.34922E 04	0.20938E-02	0.836E-04	31.					
32	237.3	0.97131E 06	36.28	0.35319E 04	0.20160E-02	0.812E-04	31.					
33	239.9	0.99069E 06	36.24	0.35710E 04	0.20287E-02	0.820E-04	31.					
34	242.5	0.10100E 07	36.12	0.36103E 04	0.20432E-02	0.800E-04	31.					
35	245.1	0.10293E 07	36.29	0.36503E 04	0.20974E-02	0.855E-04	31.					
36	247.8	0.10486E 07	36.29	0.36877E 04	0.17771E-02	0.861E-04	31.					

UNCERTAINTY IN REX= 1985. UNCERTAINTY IN F=0.05169 IN RATIO

RUN 082377-2 *** DISCRETE HOLE RIG *** NAS-3-14336   STANTON NUMBER DATA

TADB= 23.73 DEG C   UINF= 11.34 M/S   TINF= 23.67 DEG C
RHO= 1.180 KG/M3   VISC= 0.15417E-04 M2/S   XVO= 105.5 CM
CP= 1013. J/KGK   PR= 0.716

50C HSL M=0.4 P/D=5 TH=1 W/VCF(OPTIMUM)

PLATE	X	REX		TO	REENTH		STANTON NO	DST	DREEN	M	F	T2	THETA	DTH
1	127.8	0.16372E	06	40.07	0.65974E	03	0.28094E-02	0.737E-04	4.					
2	132.8	0.20110E	06	40.22	0.76148E	03	0.26342E-02	0.716E-04	14.	0.39	0.0127	40.08	0.991	0.019
3	137.9	0.23848E	06	40.19	0.13227E	04	0.22751E-02	0.687E-04	24.	0.42	0.0137	40.31	1.008	0.019
4	143.0	0.27586E	06	40.15	0.19203E	04	0.19553E-02	0.667E-04	31.	0.41	0.0132	40.25	1.008	0.019
5	148.1	0.31324E	06	40.17	0.24865E	04	0.17121E-02	0.647E-04	36.	0.39	0.0125	40.26	1.006	0.019
6	153.2	0.35061E	06	40.19	0.30181E	04	0.15810E-02	0.638E-04	41.	0.40	0.0130	40.29	1.006	0.019
7	158.2	0.38755E	06	40.15	0.35609E	04	0.13852E-02	0.627E-04	46.	0.44	0.0141	40.33	1.011	0.019
8	163.3	0.42537E	06	40.24	0.41432E	04	0.12066E-02	0.616E-04	50.	0.41	0.0134	40.32	1.[illegible]	0.019
9	168.4	0.46275E	06	40.34	0.46859E	04	0.11340E-02	0.609E-04	53.	0.41	0.0132	40.20	0.[illegible]	0.019
10	173.5	0.50013E	06	40.19	0.52196E	04	0.10630E-02	0.611E-04	57.	0.41	0.0134	40.09	0.994	0.019
11	178.6	0.53751E	06	40.15	0.57572E	04	0.11230E-02	0.614E-04	60.	0.40	0.0131	39.89	0.982	0.019
12	183.6	0.57489E	06	40.15	0.62760E	04	0.10369E-02	0.511E-04	63.	0.45	0.0146	39.78	0.978	0.019
13	187.5	0.60330E	06	38.86	0.68400E	04	0.93941E-03	0.404E-04	65.					
14	190.1	0.62255E	06	38.61	0.69583E	04	0.95121E-03	0.481E-04	65.					
15	192.7	0.64110E	06	38.61	0.68771E	04	0.10094E-02	0.484E-04	65.					
16	195.4	0.66114E	06	38.55	0.68970E	04	0.10558E-02	0.453E-04	65.					
17	198.0	0.68048E	06	38.55	0.69179E	04	0.11113E-02	0.512E-04	65.					
18	200.6	0.69973E	06	38.55	0.69395E	04	0.11300E-02	0.526E-04	65.					
19	203.2	0.71858E	06	38.34	0.69619E	04	0.11870E-02	0.519E-04	65.					
20	205.8	0.73823E	06	38.34	0.69856E	04	0.12750E-02	0.551E-04	65.					
21	208.5	0.75748E	06	38.30	0.70094E	04	0.11933E-02	0.533E-04	65.					
22	211.1	0.77673E	06	38.23	0.70336E	04	0.13227E-02	0.579E-04	65.					
23	213.7	0.79558E	06	38.17	0.70598E	04	0.13998E-02	0.601E-04	65.					
24	216.3	0.81533E	06	38.23	0.70863E	04	0.13464E-02	0.594E-04	65.					
25	218.9	0.83467E	06	38.25	0.71130E	04	0.14206E-02	0.617E-04	65.					
26	221.6	0.85392E	06	38.06	0.71404E	04	0.14172E-02	0.598E-04	65.					
27	224.2	0.87317E	06	38.25	0.71684E	04	0.14914E-02	0.637E-04	65.					
28	226.8	0.89242E	06	38.30	0.71982E	04	0.15989E-02	0.670E-04	65.					
29	229.4	0.91167E	06	38.13	0.72279E	04	0.14816E-02	0.611E-04	65.					
30	232.0	0.93092E	06	38.24	0.72558E	04	0.15212E-02	0.652E-04	65.					
31	234.6	0.95017E	06	38.22	0.72864E	04	0.15492E-02	0.653E-04	65.					
32	237.3	0.96952E	06	38.17	0.73161E	04	0.15320E-02	0.644E-04	65.					
33	239.9	0.98882E	06	38.17	0.73455E	04	0.15212E-02	0.647E-04	65.					
34	242.5	0.10081E	07	37.92	0.73752E	04	0.15397E-02	0.634E-04	65.					
35	245.1	0.10274E	07	38.08	0.74057E	04	0.16056E-02	0.684E-04	65.					
36	247.8	0.10466E	07	38.08	0.74345E	04	0.13846E-02	0.697E-04	65.					

UNCERTAINTY IN REX= 1981.   UNCERTAINTY IN F=0.05169 IN RATIO

Table of Contents

Chapter		Page

Appendix

RUN 082377-1 *** DISCRETE HOLE RIG *** NAS-3-14336 STANTON NUMBER DATA

50C HSL M=0.4 P/D=5 TH=0 W/VCF(OPTIMUM)

RUN 082377-2 *** DISCRETE HOLE RIG *** NAS-3-14336 STANTON NUMBER DATA

500 HSL M=0.4 P/D=5 TH=1 W/VCF(OPTIMUM)

LINEAR SUPERPOSITION IS APPLIED TO STANTON NUMBER DATA FROM
RUN NUMBERS 082377-1 AND 082377-2 TO OBTAIN STANTON NUMBER DATA AT TH=0 AND TH=1

PLATE	REXCOL	RE DEL2	ST(TH=0)	REXHOT	RE DEL2	ST(TH=1)	ETA	STCR	F-COL	STHR	F-HOT	LOGB
1	164022.8	661.0	0.002766	163719.9	659.7	0.002809	UUUUU	1.000	0.0000	1.000	0.0000	1.000
2	201470.9	767.1	0.002903	201398.8	761.4	0.002632	0.093	0.974	0.0139	0.883	0.0127	2.414
3	238515.0	878.6	0.003051	238477.8	1326.7	0.002275	0.254	1.033	0.0144	0.770	0.0137	2.385
4	276367.1	995.5	0.003193	275856.7	1920.6	0.002005	0.372	1.105	0.0143	0.694	0.0132	2.254
5	313815.2	1112.5	0.003054	313235.6	2483.1	0.001722	0.436	1.092	0.0141	0.616	0.0125	2.117
6	351263.3	1226.8	0.003054	350614.6	3012.2	0.001590	0.479	1.102	0.0137	0.574	0.0130	2.113
7	388711.4	1336.4	0.002798	387993.5	3552.5	0.001378	0.508	1.025	0.0147	0.504	0.0141	2.137
8	426155.4	1439.[illegible]	0.002694	425372.4	4129.2	0.001220	0.545	1.020	0.0138	0.464	0.0134	2.050
9	463607.6	1537.8	0.002587	462751.4	4673.7	0.001131	0.563	1.000	0.0145	0.437	0.0132	2.008
10	501055.6	1633.4	0.002519	500130.3	5207.4	0.001053	0.582	0.988	0.0143	0.413	0.0134	2.002
11	538503.8	1726.7	0.002468	537509.3	5747.5	0.001107	0.552	1.005	0.0145	0.451	0.0131	2.089
12	575951.8	1820.4	0.002532	574888.2	6276.2	0.001006	0.603	1.042	0.0140	0.414	0.0146	2.191
13	604412.4	1852.9	0.002600	603796.3	6849.4	0.000905	0.652	1.156		0.403		
14	623898.2	1941.2	0.002408	622546.4	6867.0	0.000921	0.617	1.101		0.421		
15	642583.9	1988.5	0.002485	641790.6	6885.3	0.000979	0.606	1.086		0.428		
16	662283.1	2033.8	0.002213	661139.9	6904.7	0.001332	0.534	1.037		0.484		
17	681742.6	2077.1	0.002266	680483.6	6925.1	0.001088	0.520	1.042		0.500		
18	701028.3	2120.8	0.002264	699733.8	6946.3	0.001107	0.511	1.043		0.510		
19	720314.1	2163.4	0.002144	718983.9	6968.2	0.001167	0.456	1.030		0.561		
20	739599.8	2205.9	0.002258	738234.0	6991.5	0.001295	0.444	1.038		0.577		
21	758885.9	2248.4	0.002144	757484.4	7014.9	0.001174	0.452	1.020		0.558		
22	778171.6	2290.2	0.002184	776734.5	7030.8	0.001305	0.403	1.027		0.614		
23	797457.3	2333.0	0.002249	795984.7	7064.7	0.001382	0.385	1.040		0.640		
24	816736.5	2375.4	0.002150	815328.1	7090.9	0.001332	0.380	1.032		0.640		
25	836216.0	2417.3	0.002191	834671.7	7117.2	0.001405	0.359	1.032		0.662		
26	855501.7	2459.0	0.002127	853921.8	7144.3	0.001403	0.340	1.039		0.686		
27	874787.4	2501.1	0.002234	873172.0	7172.0	0.001476	0.339	1.046		0.692		
28	894073.2	2544.7	0.002290	892422.1	7201.5	0.001585	0.305	1.051		0.731		
29	913359.3	2587.6	0.002166	911672.5	7230.9	0.001468	0.322	1.045		0.708		
30	932645.0	2629.2	0.002143	930922.6	7259.6	0.001508	0.296	1.035		0.729		
31	951930.8	2671.2	0.002210	950172.8	7288.9	0.001536	0.305	1.056		0.734		
32	971205.9	2713.0	0.002119	969516.2	7318.4	0.001520	0.283	1.036		0.743		
33	990489.4	2754.1	0.002137	988859.8	7347.6	0.001509	0.294	1.045		0.738		
34	1009575.0	2795.4	0.002146	1008109.0	7377.0	0.001548	0.279	1.048		0.756		
35	1029260.0	2837.4	0.002202	1027360.0	7407.3	0.001593	0.277	1.060		0.767		
36	1048546.0	2876.6	0.001861	1046610.0	7435.9	0.001375	0.261	1.059		0.783		

STANTON NUMBER RATIO BASED ON EXPERIMENTAL FLAT PLATE VALUE AT SAME X LOCATION

STANTON NUMBER RATIO FOR TH=1 IS CONVERTED TO COMPARABLE TRANSPIRATION VALUE
USING ALOG(1 + B)/B EXPRESSION IN THE BLOWN SECTION

RUN 082377-1 *** DISCRETE HOLE RIG *** NAS-3-14336 STANTON NUMBER DATA

TADB= 26.12 DEG C UINF= 11.62 M/S TINF= 26.06 DEG C
RHO= 1.143 KG/M3 VISC= 0.15983E-04 M2/S XVO= 105.5 CM
CP= 1014. J/KGK PR= 0.716

500 FSL M=0.9 P/D=5 TH=0 W/VCF(OPTIMUM)

PLATE	X	REX	TO	REENTH	STANTON NO	DST	DREEN	M	F	T2	THETA	DTH
1	127.8	0.16171E 06	38.29	0.65166E 03	0.28231E-02	0.936E-04	4.					
2	132.8	0.19864E 06	38.38	0.75647E 03	0.28546E-02	0.933E-04	16.	0.99	0.0319	27.19	0.092	0.025
3	137.9	0.23556E 06	38.34	0.98097E 03	0.34383E-02	0.991E-04	26.	0.93	0.0300	27.29	0.100	0.025
4	143.0	0.27248E 06	38.40	0.12209E 04	0.35361E-02	0.998E-04	33.	0.92	0.0299	27.19	0.092	0.025
5	148.1	0.30940E 06	38.38	0.14506E 04	0.34077E-02	0.986E-04	38.	0.91	0.0296	27.25	0.097	0.025
6	153.2	0.34632E 06	38.48	0.16792E 04	0.32351E-02	0.962E-04	43.	0.95	0.0306	27.17	0.090	0.025
7	158.2	0.38324E 06	38.40	0.18772E 04	0.30671E-02	0.953E-04	47.	0.93	0.0299	27.21	0.094	0.025
8	163.3	0.42016E 06	38.40	0.21125E 04	0.29710E-02	0.942E-04	51.	0.93	0.0301	27.17	0.090	0.025
9	168.4	0.45708E 06	38.42	0.23215E 04	0.29273E-02	0.937E-04	55.	0.92	0.0298	27.05	0.080	0.025
10	173.5	0.49401E 06	38.32	0.25159E 04	0.28375E-02	0.935E-04	59.	0.93	0.0300	25.92	-0.011	0.025
11	178.6	0.53093E 06	38.30	0.26078E 04	0.28265E-02	0.935E-04	62.	0.94	0.0303	27.02	0.079	0.025
12	183.6	0.56785E 06	38.44	0.27980E 04	0.27653E-02	0.916E-04	65.	0.90	0.0291	27.19	0.092	0.025
13	187.5	0.59551E 06	37.30	0.29744E 04	0.29114E-02	0.100E-03	66.					
14	190.1	0.61452E 06	37.11	0.30292E 04	0.28420E-02	0.112E-03	66.					
15	192.7	0.63354E 06	37.11	0.30843E 04	0.29466E-02	0.114E-03	66.					
16	195.4	0.65304E 06	37.43	0.31374E 04	0.26411E-02	0.106E-03	66.					
17	198.0	0.67215E 06	37.43	0.31881E 04	0.26825E-02	0.106E-03	67.					
18	200.6	0.69116E 06	37.43	0.32391E 04	0.26751E-02	0.105E-03	67.					
19	203.2	0.71018E 06	37.54	0.32893E 04	0.24870E-02	0.985E-04	67.					
20	205.8	0.72919E 06	37.60	0.33364E 04	0.25753E-02	0.101E-03	67.					
21	208.5	0.74821E 06	37.56	0.33851E 04	0.25392E-02	0.999E-04	67.					
22	211.1	0.76722E 06	37.58	0.34332E 04	0.25117E-02	0.100E-03	67.					
23	213.7	0.78624E 06	37.52	0.34813E 04	0.25366E-02	0.101E-03	67.					
24	216.3	0.80534E 06	37.56	0.35286E 04	0.24352E-02	0.980E-04	67.					
25	218.9	0.82445E 06	37.66	0.35752E 04	0.24539E-02	0.997E-04	67.					
26	221.6	0.84346E 06	37.43	0.36214E 04	0.24075E-02	0.950E-04	67.					
27	224.2	0.86248E 06	37.70	0.36676E 04	0.24478E-02	0.989E-04	67.					
28	226.8	0.88149E 06	37.77	0.37145E 04	0.24769E-02	0.998E-04	67.					
29	229.4	0.90051E 06	37.60	0.37609E 04	0.23995E-02	0.943E-04	67.					
30	232.0	0.91952E 06	37.81	0.38068E 04	0.24183E-02	0.985E-04	67.					
31	234.6	0.93854E 06	37.77	0.38532E 04	0.24591E-02	0.988E-04	67.					
32	237.3	0.95764E 06	37.62	0.38995E 04	0.23993E-02	0.964E-04	67.					
33	239.9	0.97675E 06	37.62	0.39451E 04	0.23949E-02	0.974E-04	67.					
34	242.5	0.99576E 06	37.33	0.39911E 04	0.24337E-02	0.953E-04	67.					
35	245.1	0.10148E 07	37.52	0.40377E 04	0.24644E-02	0.101E-03	67.					
36	247.8	0.10338E 07	37.52	0.40812E 04	0.21127E-02	0.101E-03	67.					

UNCERTAINTY IN REX= 1957. UNCERTAINTY IN F=0.05164 IN RATIO

RUN 082377-2 *** DISCRETE HOLE RIG *** NAS-3-14336 STANTON NUMBER DATA

TADB= 25.85 DEG C UINF= 11.61 M/S TINF= 25.79 DEG C
RHO= 1.144 KG/M3 VISC= 0.15958E-04 M2/S XVO= 105.5 CM
CP= 1014. J/KGK PR= 0.716

500 HSL P=0.9 P/D=5 TH=1 W/VCF(OPTIMUM)

PLATE	X	REX	TO	REENTH	STANTON NO	DST	DREEN	M	F	T2	THETA	DTH
1	127.8	0.16189E 06	40.05	0.65235E 03	0.29227E-02	0.832E-04	4.					
2	132.8	0.19885E 06	40.09	0.75772E 03	0.27790E-02	0.818E-04	30.	0.87	0.0282	40.24	1.010	0.022
3	137.9	0.23581E 06	39.98	0.19123E 04	0.28062E-02	0.825E-04	51.	0.85	0.0276	40.21	1.017	0.022
4	143.0	0.27277E 06	39.98	0.30532E 04	0.27468E-02	0.820E-04	65.	0.83	0.0270	40.23	1.018	0.022
5	148.1	0.30973E 06	39.98	0.41645E 04	0.24433E-02	0.795E-04	77.	0.85	0.0276	40.13	1.011	0.022
6	153.2	0.34669E 06	39.96	0.52839E 04	0.24371E-02	0.793E-04	88.	0.86	0.0279	40.22	1.019	0.022
7	158.2	0.38365E 06	40.07	0.64146E 04	0.18603E-02	0.747E-04	97.	0.90	0.0290	40.03	0.997	0.022
8	163.3	0.42061E 06	40.07	0.75530E 04	0.18375E-02	0.746E-04	105.	0.82	0.0265	40.10	1.002	0.022
9	168.4	0.45757E 06	39.92	0.86021E 04	0.18183E-02	0.752E-04	113.	0.86	0.0277	39.88	0.997	0.022
10	173.5	0.49453E 06	39.92	0.96830E 04	0.14620E-02	0.731E-04	120.	0.86	0.0277	39.88	0.997	0.022
11	178.6	0.53149E 06	40.11	0.10757E 05	0.14528E-02	0.722E-04	127.	0.87	0.0282	39.68	0.970	0.022
12	183.6	0.56845E 06	40.15	0.11822E 05	0.13879E-02	0.717E-04	132.	0.83	0.0268	39.43	0.950	0.021
13	187.5	0.59654E 06	39.16	0.12803E 05	0.14182E-02	0.566E-04	135.					
14	190.1	0.61558E 06	39.01	0.12829E 05	0.13373E-02	0.618E-04	135.					
15	192.7	0.63461E 06	39.01	0.12855E 05	0.13966E-02	0.613E-04	135.					
16	195.4	0.65374E 06	39.18	0.12881E 05	0.13054E-02	0.596E-04	135.					
17	198.0	0.67287E 06	39.18	0.12906E 05	0.13360E-02	0.605E-04	135.					
18	200.6	0.69190E 06	39.18	0.12932E 05	0.13690E-02	0.615E-04	135.					
19	203.2	0.71093E 06	39.08	0.12958E 05	0.13738E-02	0.597E-04	135.					
20	205.8	0.72997E 06	39.10	0.12985E 05	0.14520E-02	0.625E-04	135.					
21	208.5	0.74900E 06	39.05	0.13013E 05	0.14280E-02	0.621E-04	135.					
22	211.1	0.76804E 06	39.01	0.13041E 05	0.14354E-02	0.653E-04	135.					
23	213.7	0.78707E 06	38.89	0.13070E 05	0.15824E-02	0.678E-04	135.					
24	216.3	0.80620E 06	38.89	0.13099E 05	0.15336E-02	0.670E-04	135.					
25	218.9	0.82523E 06	38.95	0.13129E 05	0.15388E-02	0.694E-04	135.					
26	221.6	0.84436E 06	38.74	0.13160E 05	0.15508E-02	0.672E-04	135.					
27	224.2	0.86340E 06	38.93	0.13191E 05	0.16647E-02	0.713E-04	135.					
28	226.8	0.88243E 06	38.97	0.13223E 05	0.17489E-02	0.741E-04	135.					
29	229.4	0.90147E 06	38.76	0.13256E 05	0.16955E-02	0.698E-04	135.					
30	232.0	0.92050E 06	38.95	0.13289E 05	0.17309E-02	0.742E-04	135.					
31	234.6	0.93954E 06	38.87	0.13322E 05	0.17582E-02	0.751E-04	135.					
32	237.3	0.95866E 06	38.74	0.13356E 05	0.17553E-02	0.739E-04	135.					
33	239.9	0.97779E 06	38.70	0.13390E 05	0.17383E-02	0.753E-04	135.					
34	242.5	0.99682E 06	38.46	0.13424E 05	0.18187E-02	0.738E-04	135.					
35	245.1	0.10159E 07	38.59	0.13460E 05	0.18716E-02	0.799E-04	135.					
36	247.8	0.10349E 07	38.59	0.13493E 05	0.16326E-02	0.809E-04	135.					

UNCERTAINTY IN REX= 1559. UNCERTAINTY IN F=0.05164 IN RATIO

RUN 082377-1 *** DISCRETE HOLE RIG *** NAS-3-14336 STANTON NUMBER DATA

5CC HSL P=0.9 P/D=5 TH=0 W/VCF(OPTIMUM)

RUN 082377-2 *** DISCRETE HOLE RIG *** NAS-3-14336 STANTON NUMBER DATA

500 HSL P=0.9 P/D=5 TH=1 W/VCF(OPTIMUM)

LINEAR SUPERPOSITION IS APPLIED TO STANTON NUMBER DATA FROM
RUN NUMBERS 082377-1 AND 082377-2 TO OBTAIN STANTON NUMBER DATA AT TH=0 AND TH=1

PLATE	REXCOL	RE DEL2	ST(TH=0)	REXHOT	RE DEL2	ST(TH=1)	ETA	STCR	F-COL	STHR	F-HOT	LOGB
1	161714.8	651.7	0.002823	161887.1	652.4	0.002923	UUUUU	1.000	0.0000	1.000	0.0000	1.000
2	198635.9	756.6	0.002862	198847.6	757.7	0.002780	0.029	0.960	0.0319	0.932	0.0282	3.920
3	235557.0	874.1	0.003505	235808.1	1901.9	0.002815	0.197	1.187	0.0300	0.954	0.0276	3.932
4	272478.2	1005.6	0.003619	272768.5	3026.3	0.002761	0.237	1.253	0.0299	0.956	0.0270	3.931
5	309355.3	1137.2	0.003507	309729.0	4120.7	0.002458	0.259	1.254	0.0296	0.879	0.0276	3.938
6	346320.4	1263.2	0.003319	346689.5	5229.4	0.002420	0.271	1.158	0.0306	0.873	0.0279	3.485
7	383741.6	1363.7	0.003210	383650.0	6341.1	0.001871	0.417	1.175	0.0299	0.685	0.0290	3.792
8	420162.8	1499.5	0.003086	420610.4	7483.2	0.001837	0.405	1.173	0.0301	0.698	0.0265	3.682
9	457283.9	1612.8	0.003031	457570.9	8530.5	0.001818	0.400	1.171	0.0298	0.702	0.0277	3.839
10	494005.0	1722.1	0.002887	494531.4	9614.4	0.001458	0.495	1.131	0.0300	0.571	0.0277	3.622
11	530926.1	1828.4	0.002875	531491.9	10650.8	0.001429	0.503	1.171	0.0303	0.592	0.0282	3.792
12	567847.3	1933.8	0.002834	568452.4	11765.5	0.001328	0.532	1.166	0.0291	0.546	0.0268	3.615
13	595507.4	2015.2	0.003057	596542.4	12814.8	0.001350	0.558	1.359		0.600		
14	614521.8	2072.8	0.002989	615577.1	12839.7	0.001268	0.576	1.366		0.580		
15	633536.2	2130.7	0.003098	634611.7	12864.4	0.001326	0.572	1.354		0.579		
16	653342.6	2186.6	0.002771	653738.6	12868.9	0.001244	0.551	1.299		0.583		
17	672145.4	2239.7	0.002812	672865.6	12913.1	0.001295	0.539	1.293		0.595		
18	691163.8	2293.2	0.002802	691930.3	12937.9	0.001309	0.533	1.251		0.603		
19	710178.1	2344.5	0.002595	710934.9	12963.0	0.001323	0.490	1.247		0.636		
20	729192.5	2394.8	0.002685	729969.6	12989.0	0.001401	0.478	1.234		0.644		
21	748207.1	2445.6	0.002648	749004.4	13015.4	0.001377	0.480	1.260		0.655		
22	767221.5	2495.6	0.002612	768039.1	13042.3	0.001438	0.449	1.228		0.676		
23	786235.9	2545.5	0.002632	787073.7	13070.6	0.001539	0.415	1.217		0.712		
24	805242.4	2594.6	0.002523	806200.6	13099.5	0.001492	0.409	1.211		0.716		
25	824445.1	2642.8	0.002539	825327.6	13128.5	0.001549	0.390	1.196		0.730		
26	843463.5	2690.6	0.002487	844362.3	13158.0	0.001553	0.375	1.215		0.759		
27	862477.8	2738.3	0.002524	863398.9	13188.4	0.001629	0.355	1.183		0.763		
28	881492.2	2786.6	0.002548	882431.6	13220.2	0.001716	0.327	1.175		0.791		
29	900506.9	2834.3	0.002468	901466.4	13252.5	0.001668	0.324	1.191		0.805		
30	919521.2	2881.5	0.002485	920501.1	13284.5	0.001699	0.316	1.200		0.821		
31	938535.6	2929.1	0.002523	939535.7	13317.6	0.001768	0.299	1.205		0.845		
32	957842.1	2976.6	0.002462	958662.6	13350.9	0.001726	0.299	1.203		0.843		
33	976748.8	3023.4	0.002454	977789.6	13384.1	0.001760	0.283	1.200		0.861		
34	995763.2	3070.5	0.002494	996824.3	13417.9	0.001790	0.282	1.218		0.874		
35	1014777.0	3118.2	0.002520	1015858.0	13452.8	0.001865	0.260	1.213		0.898		
36	1033791.0	3162.8	0.002159	1034893.0	13485.9	0.001611	0.254	1.230		0.917		

STANTON NUMBER RATIO BASED ON EXPERIMENTAL FLAT PLATE VALUE AT SAME X LOCATION

STANTON NUMBER RATIO FOR TH=1 IS CONVERTED TO COMPARABLE TRANSPIRATION VALUE
USING BLOG(1 + B)/B EXPRESSION IN THE BLOWN SECTION

PUN 082677-1 *** DISCRETE HOLE RIG *** NAS-3-14336   STANTON NUMBER DATA

TADB= 24.46 DEG C   UINF=   11.46 M/S   TINF= 24.40 DEG C
RHO= 1.175 KG/M3   VISC= 0.15516E-04 M2/S   XVO= 105.5 CM
CP= 1012. J/KGK   PR=   0.715

500 HSL M=1.25 P/D=5 TH=0 W/VCF(OPTIMUM)

PLATE	X	REX	TO	REENTH	STANTON NO	DST	CREEN	M	F	T2	THETA	DTH
1	127.8	0.16434E 06	35.75	0.66222E 03	0.29020E-02	0.997E-04	4.					
2	132.8	0.20186E 06	35.85	0.77405E 03	0.30589E-02	0.100E-03	30.	1.81	0.0584	24.79	0.034	0.027
3	137.9	0.23538E 06	35.85	0.97466E 03	0.36947E-02	0.103E-03	52.	1.85	0.0598	24.86	0.040	0.027
4	143.0	0.27650E 06	35.79	0.12095E 04	0.40917E-02	0.112E-03	67.	1.81	0.0586	24.81	0.036	0.027
5	148.1	0.31442E 06	35.63	0.14423E 04	0.41358E-02	0.112E-03	80.	1.90	0.0615	24.85	0.039	0.027
6	153.2	0.35193E 06	35.75	0.16934E 04	0.44922E-02	0.117E-03	91.	1.76	0.0568	24.83	0.038	0.027
7	158.2	0.38645E 06	35.81	0.19381E 04	0.42762E-02	0.114E-03	100.	1.84	0.0596	24.89	0.042	0.027
8	163.3	0.42657E 06	35.81	0.21947E 04	0.43538E-02	0.115E-03	109.	1.83	0.0592	24.81	0.035	0.027
9	168.4	0.46445E 06	35.87	0.24341E 04	0.42260E-02	0.113E-03	117.	1.83	0.0594	24.83	0.037	0.027
10	173.5	0.50201E 06	35.61	0.26728E 04	0.40739E-02	0.111E-03	124.	1.80	0.0582	24.75	0.030	0.027
11	178.6	0.53553E 06	35.89	0.28895E 04	0.39340E-02	0.109E-03	131.	1.84	0.0555	24.87	0.040	0.027
12	183.6	0.57705E 06	35.85	0.31294E 04	0.40555E-02	0.111E-03	138.	1.77	0.0572	24.64	0.021	0.027
13	187.5	0.60557E 06	34.99	0.32888E 04	0.40124E-02	0.145E-03	141.					
14	190.1	0.62485E 06	34.91	0.33636E 04	0.37130E-02	0.145E-03	141.					
15	192.7	0.64421E 06	34.53	0.34406E 04	0.42527E-02	0.155E-03	141.					
16	195.4	0.66363E 06	35.49	0.35130E 04	0.32334E-02	0.129E-03	141.					
17	198.0	0.68305E 06	35.49	0.35765E 04	0.33248E-02	0.127E-03	141.					
18	200.6	0.70237E 06	35.49	0.36401E 04	0.32520E-02	0.124E-03	141.					
19	203.2	0.72165E 06	35.70	0.36999E 04	0.29319E-02	0.114E-03	141.					
20	205.8	0.74101E 06	35.75	0.37572E 04	0.29954E-02	0.115E-03	141.					
21	208.5	0.76034E 06	35.77	0.38147E 04	0.29488E-02	0.113E-03	141.					
22	211.1	0.77966E 06	35.63	0.38705E 04	0.28175E-02	0.110E-03	141.					
23	213.7	0.79898E 06	35.77	0.39250E 04	0.28154E-02	0.109E-03	141.					
24	216.3	0.81840E 06	35.83	0.39783E 04	0.26985E-02	0.106E-03	141.					
25	218.9	0.83781E 06	35.92	0.40305E 04	0.26973E-02	0.107E-03	141.					
26	221.6	0.85714E 06	35.73	0.40817E 04	0.25691E-02	0.100E-03	141.					
27	224.2	0.87646E 06	36.02	0.41321E 04	0.26251E-02	0.104E-03	141.					
28	226.8	0.89578E 06	36.12	0.41926E 04	0.26308E-02	0.104E-03	141.					
29	229.4	0.91511E 06	35.91	0.42327E 04	0.25756E-02	0.991E-04	141.					
30	232.0	0.93443E 06	36.17	0.42822E 04	0.25392E-02	0.102E-03	141.					
31	234.6	0.95375E 06	36.13	0.43316E 04	0.25668E-02	0.102E-03	141.					
32	237.3	0.97317E 06	35.58	0.43806E 04	0.24992E-02	0.951E-04	141.					
33	239.9	0.99258E 06	35.56	0.44287E 04	0.24730E-02	0.995E-04	141.					
34	242.5	0.10119E 07	35.64	0.44771E 04	0.25362E-02	0.978E-04	141.					
35	245.1	0.10312E 07	35.89	0.45259E 04	0.25043E-02	0.102E-03	141.					
36	247.8	0.10506E 07	35.89	0.45707E 04	0.21271E-02	0.101E-03	141.					

UNCERTAINTY IN REX= 1585.   UNCERTAINTY IN F=0.05164 IN RATIO

RUN 082677-2 *** DISCRETE HOLE RIG *** NAS-3-14336 STANTON NUMBER DATA

TACE= 26.62 DEG C UINF= 11.51 M/S TINF= 26.56 DEG C
RHO= 1.166 KG/M3 VISC= 0.15712E-04 M2/S XVO= 105.5 CM
CP= 1013. J/KGK PR= 0.715

500 HSL M=1.25 P/D=5 TH=1 W/VCF(OPTIMUM)

PLATE	X	REX	TO	REENTH	STANTON NO	DST	DREEN	M	F	T2	THETA	DTH
1	127.8	0.16293E 06	38.86	0.65654E 03	0.29782E-02	0.940E-04	4.					
2	132.8	0.20013E 06	38.89	0.76722E 03	0.29723E-02	0.937E-04	59.	1.66	0.0537	39.24	1.028	0.025
3	137.9	0.23732E 06	38.93	0.29408E 04	0.34770E-02	0.984E-04	102.	1.70	0.0551	38.99	1.004	0.025
4	143.0	0.27452E 06	38.86	0.51313E 04	0.35931E-02	0.100E-03	131.	1.64	0.0532	38.85	1.000	0.025
5	148.1	0.31172E 06	38.84	0.72436E 04	0.36467E-02	0.101E-03	155.	1.69	0.0548	38.76	0.994	0.025
6	153.2	0.34892E 06	38.84	0.93991E 04	0.33091E-02	0.973E-04	174.	1.58	0.0513	38.58	0.979	0.025
7	158.2	0.38612E 06	38.86	0.11391E 05	0.28455E-02	0.928E-04	191.	1.68	0.0545	38.34	0.958	0.025
8	163.3	0.42331E 06	38.55	0.13424E 05	0.25227E-02	0.894E-04	207.	1.67	0.0542	38.41	0.957	0.025
9	168.4	0.46051E 06	38.91	0.15443E 05	0.23305E-02	0.881E-04	221.	1.67	0.0540	38.23	0.945	0.025
10	173.5	0.49771E 06	38.70	0.17433E 05	0.26157E-02	0.917E-04	235.	1.66	0.0536	38.21	0.959	0.025
11	178.6	0.53491E 06	38.51	0.19429E 05	0.18766E-02	0.848E-04	247.	1.70	0.0549	37.97	0.924	0.025
12	183.6	0.57211E 06	38.40	0.21347E 05	0.15755E-02	0.862E-04	259.	1.62	0.0525	37.55	0.898	0.025
13	187.5	0.60038E 06	37.94	0.23155E 05	0.18749E-02	0.736E-04	264.					
14	190.1	0.61953E 06	37.85	0.23233E 05	0.17565E-02	0.782E-04	264.					
15	192.7	0.63845E 06	37.85	0.23264E 05	0.18131E-02	0.771E-04	264.					
16	195.4	0.65754E 06	38.08	0.23297E 05	0.16059E-02	0.722E-04	264.					
17	198.0	0.67719E 06	38.08	0.23328E 05	0.16341E-02	0.722E-04	264.					
18	200.6	0.69635E 06	38.08	0.23359E 05	0.16007E-02	0.716E-04	264.					
19	203.2	0.71550E 06	38.04	0.23389E 05	0.15515E-02	0.685E-04	264.					
20	205.8	0.73466E 06	38.04	0.23419E 05	0.16304E-02	0.708E-04	264.					
21	208.5	0.75382E 06	38.02	0.23450E 05	0.16149E-02	0.709E-04	264.					
22	211.1	0.77297E 06	38.00	0.23481E 05	0.16171E-02	0.724E-04	264.					
23	213.7	0.79213E 06	37.98	0.23513E 05	0.16456E-02	0.733E-04	264.					
24	216.3	0.81138E 06	37.96	0.23544E 05	0.16282E-02	0.733E-04	264.					
25	218.9	0.83063E 06	38.00	0.23576E 05	0.16653E-02	0.748E-04	264.					
26	221.6	0.84979E 06	37.83	0.23607E 05	0.16435E-02	0.722E-04	264.					
27	224.2	0.86895E 06	38.02	0.23643E 05	0.17137E-02	0.766E-04	264.					
28	226.8	0.88810E 06	38.10	0.23673E 05	0.17353E-02	0.768E-04	264.					
29	229.4	0.90726E 06	37.92	0.23706E 05	0.17225E-02	0.736E-04	264.					
30	232.0	0.92642E 06	39.11	0.23739E 05	0.17305E-02	0.775E-04	264.					
31	234.6	0.94557E 06	38.04	0.23773E 05	0.17920E-02	0.774E-04	264.					
32	237.3	0.96482E 06	37.92	0.23807E 05	0.17608E-02	0.772E-04	264.					
33	239.9	0.98407E 06	37.92	0.23840E 05	0.17461E-02	0.771E-04	264.					
34	242.5	0.10032E 07	37.70	0.23874E 05	0.17846E-02	0.758E-04	264.					
35	245.1	0.10224E 07	37.83	0.23909E 05	0.18103E-02	0.810E-04	264.					
36	247.8	0.10415E 07	37.83	0.23941E 05	0.15572E-02	0.818E-04	264.					

UNCERTAINTY IN REX= 1971. UNCERTAINTY IN F=0.05164 IN RATIO

RUN 082677-1 *** DISCRETE HOLE RIG *** NAS-3-14336 STANTON NUMBER DATA

500 HSL M=1.25 P/D=5 TH=0 W/VCF(OPTIMUM)

RUN 082677-2 *** DISCRETE HOLE RIG *** NAS-3-14336 STANTON NUMBER DATA

500 HSL M=1.25 P/D=5 TH=1 W/VCF(OPTIMUM)

LINEAR SUPERPOSITION IS APPLIED TO STANTON NUMBER DATA FROM
RUN NUMBERS 082677-1 AND 082677-2 TO OBTAIN STANTON NUMBER DATA AT TH=0 AND TH=1

PLATE	REXCOL	RE DEL2	ST(TH=0)	REXHOT	RE DEL2	ST(TH=1)	ETA	STCR	F-COL	STHR	F-HOT	LOGB
1	164336.3	662.2	0.002902	162927.4	656.5	0.002978	UUUUU	1.000	0.0000	1.000	0.0000	1.000
2	201856.9	774.1	0.003062	200125.4	767.3	0.002975	0.028	1.027	0.0584	0.998	0.0537	6.110
3	239375.7	901.0	0.003703	237323.4	2884.3	0.003481	0.060	1.254	0.0598	1.179	0.0551	6.612
4	276855.3	1047.6	0.004111	274521.4	5065.8	0.003594	0.126	1.423	0.0586	1.244	0.0532	6.670
5	314415.0	1202.7	0.004155	311719.4	7178.2	0.003645	0.123	1.486	0.0615	1.303	0.0548	7.063
6	351534.7	1365.8	0.004540	348917.4	9345.7	0.003292	0.275	1.638	0.0568	1.188	0.0513	6.590
7	389454.4	1532.3	0.004338	386115.4	11366.9	0.002797	0.355	1.588	0.0596	1.024	0.0545	6.609
8	426574.0	1697.0	0.004441	423313.4	13491.5	0.002437	0.451	1.688	0.0592	0.926	0.0542	6.549
9	464493.7	1861.0	0.004301	460511.4	15594.5	0.002224	0.482	1.662	0.0594	0.861	0.0540	6.466
10	502013.4	2019.1	0.004128	497709.4	17652.6	0.002539	0.385	1.618	0.0582	0.995	0.0536	6.787
11	539533.1	2171.5	0.004014	534907.4	19766.3	0.001744	0.566	1.635	0.0595	0.710	0.0549	6.422
12	577052.7	2324.6	0.004128	572105.4	21672.7	0.001769	0.571	1.698	0.0572	0.728	0.0525	6.310
13	605567.8	2441.6	0.004086	600375.9	23874.5	0.001658	0.594	1.817		0.738		
14	624856.4	2517.7	0.003781	619532.9	23905.3	0.001558	0.588	1.729		0.713		
15	644212.9	2596.2	0.004337	638669.9	23935.3	0.001566	0.639	1.856		0.685		
16	663625.2	2670.0	0.003290	657939.6	23964.1	0.001441	0.562	1.542		0.676		
17	683045.7	2734.5	0.003383	677109.6	23991.9	0.001463	0.568	1.555		0.672		
18	702368.3	2799.3	0.003309	696346.6	24019.7	0.001433	0.567	1.525		0.660		
19	721690.9	2860.1	0.002983	715503.5	24047.0	0.001412	0.526	1.432		0.678		
20	741013.5	2918.4	0.003043	734660.5	24074.8	0.001492	0.510	1.398		0.686		
21	760336.4	2976.8	0.002995	753817.7	24103.3	0.001480	0.506	1.425		0.704		
22	779655.0	3033.4	0.002859	772974.6	24131.8	0.001495	0.477	1.344		0.703		
23	798981.6	3088.7	0.002856	792131.6	24160.8	0.001527	0.465	1.321		0.706		
24	818297.8	3142.8	0.002736	811391.4	24190.0	0.001520	0.444	1.313		0.730		
25	837614.3	3195.6	0.002733	830631.4	24219.6	0.001561	0.429	1.288		0.736		
26	857136.9	3247.4	0.002622	849788.3	24249.4	0.001548	0.410	1.281		0.756		
27	876455.5	3298.5	0.002657	868945.3	24279.7	0.001622	0.390	1.245		0.760		
28	895782.1	3349.6	0.002631	888102.3	24311.1	0.001648	0.374	1.213		0.760		
29	915105.0	3400.3	0.002605	907259.4	24342.6	0.001636	0.372	1.257		0.790		
30	934427.6	3450.3	0.002567	926416.4	24374.0	0.001649	0.358	1.240		0.796		
31	953750.3	3500.2	0.002594	945573.4	24406.3	0.001714	0.339	1.239		0.819		
32	973166.4	3549.7	0.002525	964823.1	24438.9	0.001686	0.332	1.234		0.824		
33	992582.9	3598.3	0.002498	984073.1	24471.1	0.001672	0.331	1.222		0.818		
34	1011905.0	3647.3	0.002562	1003230.0	24503.5	0.001714	0.331	1.251		0.837		
35	1031228.0	3696.5	0.002528	1022387.0	24536.7	0.001749	0.308	1.217		0.842		
36	1050550.0	3741.7	0.002147	1041544.0	24567.9	0.001499	0.302	1.222		0.854		

STANTON NUMBER RATIO BASED ON EXPERIMENTAL FLAT PLATE VALUE AT SAME X LOCATION

STANTON NUMBER RATIO FOR TH=1 IS CONVERTED TO COMPARABLE TRANSPIRATION VALUE
USING ALOG(1 + B)/B EXPRESSION IN THE BLOWN SECTION

RUN 070677 VELOCITY PROFILE

REX = 0.11151E 07 REM = 2554.

XVC = 22.60 CM DEL2 = 0.234 CM
UINF = 16.79 M/S DEL99= 2.050 CM
VISC = 0.15393E-04 M2/S DEL1 = 0.327 CM
PORT = 3 H = 1.396
XLOC = 125.22 CM CF/2 = 0.10000E 01

Y(CM)	Y/DEL	U(M/S)	U/UINF	Y+	U+
0.025	0.012	7.22	0.430	277.0	0.43
0.028	0.014	7.29	0.435	304.7	0.43
0.030	0.015	7.35	0.438	332.4	0.44
0.033	0.016	7.59	0.452	360.1	0.45
0.038	0.019	8.07	0.481	415.5	0.48
0.043	0.021	8.42	0.502	470.9	0.50
0.048	0.024	8.74	0.520	526.3	0.52
0.053	0.026	8.96	0.534	581.7	0.53
0.058	0.029	9.17	0.546	637.1	0.55
0.071	0.035	9.51	0.566	775.6	0.57
0.079	0.038	9.61	0.572	858.7	0.57
0.084	0.041	9.86	0.587	914.1	0.59
0.097	0.047	10.03	0.597	1052.6	0.60
0.109	0.053	10.24	0.610	1191.1	0.61
0.135	0.066	10.49	0.625	1468.1	0.63
0.160	0.078	10.76	0.641	1745.1	0.64
0.185	0.090	11.01	0.656	2022.1	0.66
0.211	0.103	11.21	0.668	2299.1	0.67
0.236	0.115	11.38	0.678	2576.1	0.68
0.262	0.128	11.51	0.686	2853.1	0.69
0.312	0.152	11.83	0.705	3407.1	0.70
0.363	0.177	12.11	0.721	3961.1	0.72
0.401	0.196	12.28	0.731	4376.6	0.73
0.439	0.214	12.49	0.744	4792.1	0.74
0.478	0.233	12.67	0.755	5207.6	0.75
0.516	0.252	12.81	0.763	5623.1	0.76
0.566	0.276	13.10	0.781	6177.1	0.78
0.617	0.301	13.26	0.790	6731.1	0.79
0.681	0.332	13.51	0.805	7423.7	0.80
0.744	0.363	13.73	0.818	8116.2	0.82
0.808	0.394	13.97	0.832	8809.7	0.83
0.871	0.425	14.18	0.844	9501.2	0.84
0.998	0.487	14.56	0.867	10886.2	0.87
1.125	0.549	14.96	0.891	12271.2	0.89
1.252	0.611	15.32	0.912	13656.2	0.91
1.379	0.673	15.65	0.932	15041.2	0.93
1.506	0.735	15.89	0.947	16426.2	0.95
1.633	0.797	16.21	0.966	17811.2	0.97
1.760	0.859	16.40	0.977	19196.2	0.98
1.887	0.921	16.55	0.986	20581.2	0.99
2.014	0.983	16.66	0.993	21966.3	0.99
2.141	1.045	16.72	0.996	23351.3	1.00
2.268	1.107	16.73	0.997	24736.3	1.00
2.395	1.169	16.79	1.000	26121.3	1.00

RUN 070677 *** DISCRETE HOLE RIG *** NAS-3-14336 STANTON NUMBER DATA

TADB= 24.19 DEG C UINF= 16.79 M/S TINF= 24.06 DEG C
RHO= 1.183 KG/M3 VISC= 0.15407E-04 M2/S XVO= 22.8 CM
CP= 1012. J/KGK PR= 0.715

25CC LHSL FLAT PLATE P/D=5

PLATE	X	REX	TO	REENTH	STANTONNO	DST	DREEN	ST(THEO)	RATIO
1	127.8	0.11436E 07	36.46	0.96891E 02	0.34396E-02	0.688E-04	6.	0.31700E-02	1.085
2	132.9	0.11990E 07	36.44	0.28044E 03	0.31907E-02	0.670E-04	6.	0.27932E-02	1.142
3	137.9	0.12543E 07	36.46	0.45415E 03	0.30843E-02	0.661E-04	7.	0.26279E-02	1.174
4	143.0	0.13097E 07	36.46	0.62199E 03	0.29786E-02	0.653E-04	7.	0.25212E-02	1.181
5	148.1	0.13651E 07	36.44	0.78332E 03	0.28492E-02	0.644E-04	8.	0.24422E-02	1.167
6	153.2	0.14204E 07	36.46	0.93965E 03	0.27978E-02	0.640E-04	8.	0.23794E-02	1.176
7	158.2	0.14758E 07	36.44	0.10913E 04	0.26814E-02	0.633E-04	8.	0.23273E-02	1.152
8	163.3	0.15311E 07	36.46	0.12383E 04	0.26266E-02	0.628E-04	9.	0.22827E-02	1.151
9	168.4	0.15865E 07	36.48	0.13813E 04	0.25391E-02	0.621E-04	9.	0.22437E-02	1.132
10	173.5	0.16419E 07	36.52	0.15204E 04	0.24863E-02	0.616E-04	10.	0.22090E-02	1.126
11	178.6	0.16972E 07	36.50	0.16575E 04	0.24651E-02	0.616E-04	10.	0.21778E-02	1.132
12	183.6	0.17526E 07	36.46	0.17945E 04	0.24864E-02	0.619E-04	10.	0.21494E-02	1.157
13	187.5	0.17947E 07	35.37	0.18932E 04	0.20920E-02	0.719E-04	10.	0.21294E-02	0.982
14	190.1	0.18232E 07	35.18	0.19525E 04	0.20604E-02	0.761E-04	10.	0.21166E-02	0.973
15	192.7	0.18517E 07	35.28	0.20120E 04	0.21058E-02	0.775E-04	11.	0.21043E-02	1.001
16	195.4	0.18804E 07	35.33	0.20707E 04	0.20118E-02	0.744E-04	11.	0.20924E-02	0.962
17	198.0	0.19090E 07	35.33	0.21287E 04	0.20457E-02	0.754E-04	11.	0.20809E-02	0.983
18	200.6	0.19375E 07	35.33	0.21870E 04	0.20417E-02	0.753E-04	11.	0.20698E-02	0.986
19	203.2	0.19660E 07	35.35	0.22439E 04	0.19473E-02	0.717E-04	11.	0.20592E-02	0.946
20	205.8	0.19946E 07	35.39	0.23009E 04	0.20461E-02	0.749E-04	11.	0.20489E-02	0.999
21	208.5	0.20231E 07	35.35	0.23586E 04	0.19914E-02	0.730E-04	11.	0.20389E-02	0.977
22	211.1	0.20516E 07	35.39	0.24155E 04	0.19981E-02	0.746E-04	11.	0.20293E-02	0.985
23	213.7	0.20801E 07	35.28	0.24736E 04	0.20730E-02	0.756E-04	11.	0.20199E-02	1.026
24	216.3	0.21086E 07	35.41	0.25313E 04	0.19663E-02	0.738E-04	12.	0.20108E-02	0.978
25	218.9	0.21374E 07	35.43	0.25882E 04	0.20240E-02	0.752E-04	12.	0.20019E-02	1.011
26	221.6	0.21659E 07	35.35	0.26448E 04	0.19355E-02	0.715E-04	12.	0.19933E-02	0.971
27	224.2	0.21944E 07	35.51	0.27010E 04	0.20055E-02	0.744E-04	12.	0.19850E-02	1.010
28	226.8	0.22229E 07	35.60	0.27587E 04	0.20389E-02	0.761E-04	12.	0.19769E-02	1.031
29	229.4	0.22515E 07	35.39	0.28151E 04	0.19119E-02	0.695E-04	12.	0.19690E-02	0.971
30	232.0	0.22800E 07	25.66	0.28700E 04	0.19329E-02	0.730E-04	12.	0.19612E-02	0.986
31	234.6	0.23085E 07	35.64	0.29258E 04	0.19744E-02	0.735E-04	12.	0.19537E-02	1.011
32	237.3	0.23371E 07	35.49	0.29811E 04	0.19028E-02	0.709E-04	12.	0.19463E-02	0.978
33	239.9	0.23658E 07	35.47	0.30355E 04	0.19098E-02	0.720E-04	12.	0.19391E-02	0.985
34	242.5	0.23943E 07	35.18	0.30900E 04	0.19020E-02	0.692E-04	13.	0.19321E-02	0.984
35	245.1	0.24228E 07	35.43	0.31449E 04	0.19491E-02	0.744E-04	13.	0.19252E-02	1.012
36	247.8	0.24513E 07	35.37	0.31979E 04	0.17596E-02	0.756E-04	13.	0.19185E-02	0.917

RUN 070677 *** DISCRETE HOLE RIG *** NAS-3-14336 STANTON NUMBER DATA

TADB= 23.69 DEG C UINF= 16.78 M/S TINF= 23.56 DEG C
RHO= 1.185 KG/M3 VISC= 0.15363E-04 M2/S XVO= 22.8 CM
CP= 1011. J/KGK PR= 0.715

2500 UPSL M=0.4 TH=0 P/D=5 W/VCF(OPTIMUM)

PLATE	X	REX	TO	REENTH	STANTON NO	DST	REEN	M	F	T2	THETA	DTH
1	127.8	0.11459E 07	36.25	0.97084E 02	0.33716E-02	0.668E-04	6.					
2	132.8	0.12013E 07	36.17	0.26967E 03	0.28502E-02	0.633E-04	12.	0.45	0.0146	24.96	0.111	0.024
3	137.9	0.12568E 07	36.17	0.51946E 03	0.29204E-02	0.638E-04	19.	0.44	0.0144	25.03	0.116	0.024
4	143.0	0.13123E 07	36.13	0.77214E 03	0.28463E-02	0.635E-04	23.	0.45	0.0146	24.99	0.113	0.024
5	148.1	0.13678E 07	36.15	0.10181E 04	0.27155E-02	0.625E-04	27.	0.41	0.0134	25.10	0.122	0.024
6	153.2	0.14233E 07	36.17	0.12564E 04	0.25995E-02	0.616E-04	30.	0.43	0.0140	24.95	0.110	0.024
7	158.2	0.14787E 07	36.17	0.14835E 04	0.25168E-02	0.610E-04	33.	0.43	0.0140	25.07	0.120	0.024
8	163.3	0.15342E 07	36.15	0.17136E 04	0.24319E-02	0.606E-04	36.	0.45	0.0146	24.97	0.112	0.024
9	168.4	0.15897E 07	36.23	0.19356E 04	0.23045E-02	0.595E-04	39.	0.44	0.0142	25.00	0.113	0.024
10	173.5	0.16452E 07	36.19	0.21516E 04	0.22369E-02	0.593E-04	41.	0.45	0.0145	24.94	0.109	0.024
11	178.6	0.17006E 07	36.13	0.23632E 04	0.22248E-02	0.594E-04	44.	0.42	0.0135	25.12	0.124	0.024
12	183.6	0.17561E 07	36.17	0.25781E 04	0.21831E-02	0.590E-04	46.	0.43	0.0139	25.09	0.121	0.024
13	187.5	0.17983E 07	36.34	0.27644E 04	0.22549E-02	0.798E-04	47.					
14	190.1	0.18268E 07	36.46	0.28265E 04	0.20790E-02	0.752E-04	47.					
15	192.7	0.18554E 07	36.61	0.28864E 04	0.21114E-02	0.749E-04	47.					
16	195.4	0.18841E 07	36.83	0.29438E 04	0.19042E-02	0.692E-04	47.					
17	198.0	0.19128E 07	36.90	0.29997E 04	0.19343E-02	0.693E-04	47.					
18	200.6	0.19414E 07	36.93	0.30537E 04	0.19114E-02	0.687E-04	47.					
19	203.2	0.19700E 07	36.97	0.31069E 04	0.18067E-02	0.650E-04	47.					
20	205.8	0.19985E 07	37.01	0.31596E 04	0.18755E-02	0.672E-04	47.					
21	208.5	0.20271E 07	36.97	0.32124E 04	0.18192E-02	0.651E-04	47.					
22	211.1	0.20557E 07	37.07	0.32647E 04	0.18382E-02	0.672E-04	47.					
23	213.7	0.20843E 07	36.93	0.33184E 04	0.19167E-02	0.684E-04	47.					
24	216.3	0.21130E 07	37.03	0.33720E 04	0.18257E-02	0.667E-04	47.					
25	218.9	0.21417E 07	37.03	0.34252E 04	0.18948E-02	0.688E-04	47.					
26	221.6	0.21702E 07	36.86	0.34781E 04	0.18052E-02	0.646E-04	47.					
27	224.2	0.21984E 07	37.07	0.35311E 04	0.19019E-02	0.689E-04	47.					
28	226.8	0.22274E 07	37.16	0.35865E 04	0.19700E-02	0.716E-04	47.					
29	229.4	0.22560E 07	36.88	0.36413E 04	0.18636E-02	0.655E-04	47.					
30	232.0	0.22845E 07	37.16	0.36948E 04	0.18773E-02	0.688E-04	47.					
31	234.6	0.23131E 07	37.14	0.37491E 04	0.19209E-02	0.696E-04	47.					
32	237.3	0.23418E 07	36.93	0.38033E 04	0.18685E-02	0.674E-04	47.					
33	239.9	0.23705E 07	36.88	0.38571E 04	0.18515E-02	0.692E-04	47.					
34	242.5	0.23991E 07	36.48	0.39114E 04	0.19026E-02	0.665E-04	47.					
35	245.1	0.24277E 07	36.80	0.39659E 04	0.19073E-02	0.715E-04	47.					
36	247.8	0.24562E 07	36.52	0.40193E 04	0.18255E-02	0.751E-04	47.					

UNCERTAINTY IN REX=12815. UNCERTAINTY IN F=0.05036 IN RATIO

RUN 070677 *** DISCRETE HOLE RIG *** NAS-3-14336 STANTON NUMBER DATA

TADB= 23.78 DEG C UINF= 16.78 M/S TINF= 23.66 DEG C
RHO= 1.184 KG/M3 VISC= 0.15371E-04 M2/S XVO= 22.8 CM
CP= 1011. J/KGK PR= 0.715

2500 LPSL M=0.4 TH=1 P/D=5 W/VCF(OPTIMUM)

PLATE	X	REX	TO	REENTH	STANTON NO	DST	DREEN	M	F	T2	THETA	DTH
1	127.8	0.11454E 07	40.94	0.97046E 02	0.33016E-02	0.504E-04	6.					
2	132.8	0.12009E 07	40.77	0.26127E 03	0.26212E-02	0.466E-04	18.	0.39	0.0125	39.47	0.924	0.018
3	137.9	0.12563E 07	40.81	0.10359E 04	0.22539E-02	0.445E-04	31.	0.38	0.0124	39.99	0.952	0.018
4	143.0	0.13118E 07	40.76	0.18023E 04	0.18578E-02	0.428E-04	40.	0.38	0.0123	40.03	0.957	0.018
5	148.1	0.13672E 07	40.81	0.25528E 04	0.15909E-02	0.415E-04	47.	0.38	0.0122	39.96	0.951	0.018
6	153.2	0.14227E 07	40.94	0.32777E 04	0.13959E-02	0.405E-04	53.	0.37	0.0120	39.92	0.941	0.018
7	158.2	0.14782E 07	40.85	0.39779E 04	0.12348E-02	0.402E-04	58.	0.39	0.0126	39.86	0.942	0.018
8	163.3	0.15336E 07	40.77	0.47025E 04	0.11529E-02	0.401E-04	63.	0.38	0.0123	39.97	0.953	0.018
9	168.4	0.15891E 07	40.79	0.54164E 04	0.10745E-02	0.399E-04	68.	0.38	0.0124	39.73	0.938	0.018
10	173.5	0.16445E 07	40.87	0.61182E 04	0.98820E-03	0.395E-04	72.	0.39	0.0127	39.71	0.932	0.018
11	178.6	0.17000E 07	40.87	0.68272E 04	0.94383E-03	0.394E-04	76.	0.37	0.0120	39.25	0.906	0.018
12	183.6	0.17554E 07	40.94	0.74813E 04	0.84588E-03	0.390E-04	80.	0.38	0.0125	39.17	0.897	0.018
13	187.5	0.17976E 07	40.17	0.81368E 04	0.86867E-03	0.327E-04	82.					
14	190.1	0.18261E 07	39.98	0.81614E 04	0.85555E-03	0.357E-04	82.					
15	192.7	0.18547E 07	40.00	0.81864E 04	0.89503E-03	0.362E-04	82.					
16	195.4	0.18834E 07	40.03	0.82117E 04	0.86982E-03	0.355E-04	82.					
17	198.0	0.19121E 07	40.01	0.82374E 04	0.92947E-03	0.371E-04	82.					
18	200.6	0.19407E 07	40.01	0.82641E 04	0.93910E-03	0.377E-04	82.					
19	203.2	0.19692E 07	39.92	0.82909E 04	0.93086E-03	0.364E-04	82.					
20	205.9	0.19978E 07	39.96	0.83186E 04	0.10122E-02	0.392E-04	82.					
21	208.5	0.20263E 07	39.86	0.83471E 04	0.97833E-03	0.382E-04	82.					
22	211.1	0.20549E 07	39.82	0.83760E 04	0.10463E-02	0.410E-04	82.					
23	213.7	0.20834E 07	39.69	0.84071E 04	0.11235E-02	0.427E-04	82.					
24	216.3	0.21121E 07	39.77	0.84386E 04	0.10822E-02	0.424E-04	82.					
25	218.9	0.21408E 07	39.75	0.84704E 04	0.11384E-02	0.441E-04	82.					
26	221.6	0.21694E 07	39.59	0.85026E 04	0.11176E-02	0.421E-04	82.					
27	224.2	0.21980E 07	39.71	0.85358E 04	0.12019E-02	0.459E-04	82.					
28	226.8	0.22265E 07	39.75	0.85714E 04	0.12846E-02	0.489E-04	82.					
29	229.4	0.22551E 07	39.44	0.86073E 04	0.12258E-02	0.447E-04	82.					
30	232.0	0.22836E 07	39.71	0.86427E 04	0.12482E-02	0.480E-04	82.					
31	234.6	0.23122E 07	39.64	0.86791E 04	0.12939E-02	0.486E-04	82.					
32	237.3	0.23409E 07	39.41	0.87158E 04	0.12756E-02	0.478E-04	82.					
33	239.9	0.23696E 07	39.29	0.87528E 04	0.13113E-02	0.494E-04	82.					
34	242.5	0.23982E 07	38.93	0.87904E 04	0.13197E-02	0.476E-04	82.					
35	245.1	0.24267E 07	39.14	0.88290E 04	0.13625E-02	0.523E-04	82.					
36	247.8	0.24553E 07	39.14	0.88663E 04	0.12253E-02	0.539E-04	82.					

UNCERTAINTY IN REX=12810. UNCERTAINTY IN F=0.05036 IN RATIO

RUN 070677 *** DISCRETE HOLE RIG *** NAS-3-14336 STANTON NUMBER DATA

2500 UHSL P=0.4 TH=0 P/D=5 W/VCF(OPTIMUM).

RUN 070677 *** DISCRETE HOLE RIG *** NAS-3-14336 STANTON NUMBER DATA

2500 UHSL P=0.4 TH=1 P/D=5 W/VCF(OPTIMUM)

LINEAR SUPERPOSITION IS APPLIED TO STANTON NUMBER DATA FROM
RUN NUMBERS 070677 AND 070677 TO OBTAIN STANTON NUMBER DATA AT TH=0 AND TH=1

PLATE	REXCOL	RE DEL2	ST(TH=0)	REXHOT	RE DEL2	ST(TH=1)	ETA	STCR	F-COL	STHR	F-HOT	LOGB
1	1145868.0	97.1	0.003372	1145424.0	97.0	0.003302	UUUUU	1.000	0.0000	1.000	0.0000	1.000
2	1201344.0	270.5	0.002881	1200879.0	260.7	0.002600	0.098	0.903	0.0146	0.815	0.0125	2.225
3	1256821.0	434.0	0.003012	1256335.0	1085.9	0.002204	0.268	0.977	0.0144	0.715	0.0124	2.122
4	1312297.0	600.3	0.002981	1311790.0	1862.3	0.001804	0.395	1.001	0.0146	0.606	0.0123	2.012
5	1367774.0	762.7	0.002874	1367245.0	2658.8	0.001529	0.468	1.009	0.0134	0.537	0.0122	1.949
6	1423250.0	919.2	0.002768	1422700.0	3413.2	0.001317	0.524	0.989	0.0140	0.471	0.0120	1.655
7	1478727.0	1070.6	0.002694	1478155.0	4148.0	0.001150	0.573	1.005	0.0140	0.429	0.0126	1.893
8	1534204.0	1217.8	0.002610	1533610.0	4908.3	0.001072	0.589	0.994	0.0146	0.408	0.0123	1.859
9	1589680.0	1358.7	0.002471	1589065.0	5649.7	0.000994	0.598	0.973	0.0142	0.392	0.0124	1.877
10	1645157.0	1494.6	0.002428	1644520.0	6389.2	0.000888	0.634	0.976	0.0145	0.357	0.0127	1.871
11	1700633.0	1628.8	0.002410	1699975.0	7139.4	0.000815	0.662	0.978	0.0135	0.331	0.0120	1.770
12	1756110.0	1762.0	0.002393	1755430.0	7846.0	0.000681	0.715	0.962	0.0139	0.274	0.0125	1.693
13	1799277.0	1863.8	0.002479	1797576.0	8567.3	0.000693	0.720	1.185		0.331		
14	1826842.0	1931.7	0.002271	1826136.0	8587.2	0.000701	0.691	1.102		0.340		
15	1855412.0	1997.1	0.002302	1854695.0	8607.8	0.000742	0.678	1.093		0.353		
16	1884122.0	2059.6	0.002067	1883393.0	8629.0	0.000739	0.642	1.027		0.367		
17	1912831.0	2119.1	0.002092	1912091.0	8651.0	0.000803	0.616	1.023		0.392		
18	1941401.0	2178.6	0.002064	1940650.0	8674.2	0.000816	0.605	1.011		0.400		
19	1969972.0	2235.5	0.001944	1969210.0	8697.6	0.000820	0.578	0.958		0.421		
20	1998542.0	2292.5	0.002011	1997769.0	8722.2	0.000903	0.551	0.963		0.441		
21	2027113.0	2349.1	0.001951	2026329.0	8747.6	0.000872	0.553	0.980		0.438		
22	2055683.0	2405.1	0.001963	2054888.0	8773.6	0.000946	0.518	0.982		0.474		
23	2084254.0	2462.4	0.002041	2083447.0	8801.8	0.001023	0.499	0.985		0.496		
24	2112982.0	2519.4	0.001943	2112145.0	8830.5	0.000988	0.491	0.988		0.503		
25	2141672.0	2576.0	0.002014	2140843.0	8859.5	0.001043	0.482	0.995		0.515		
26	2170242.0	2632.1	0.001913	2169402.0	8889.2	0.001031	0.461	0.989		0.533		
27	2198812.0	2688.3	0.002012	2197962.0	8919.8	0.001113	0.447	1.003		0.555		
28	2227383.0	2746.7	0.002077	2226521.0	8953.0	0.001204	0.420	1.019		0.590		
29	2255954.0	2804.5	0.001964	2255081.0	8986.6	0.001145	0.417	1.027		0.599		
30	2284524.0	2860.9	0.001976	2283640.0	9019.6	0.001169	0.409	1.022		0.605		
31	2313094.0	2918.0	0.002013	2312200.0	9053.7	0.001215	0.399	1.023		0.615		
32	2341803.0	2975.0	0.001962	2340897.0	9088.2	0.001201	0.388	1.031		0.631		
33	2370514.0	3031.4	0.001983	2369595.0	9123.1	0.001238	0.376	1.038		0.648		
34	2399083.0	3088.3	0.001994	2398155.0	9158.6	0.001246	0.375	1.048		0.655		
35	2427653.0	3145.3	0.001996	2426714.0	9195.2	0.001316	0.339	1.021		0.675		
36	2456224.0	3201.2	0.001920	2455273.0	9230.5	0.001149	0.401	1.091		0.653		

STANTON NUMBER RATIO BASED ON EXPERIMENTAL FLAT PLATE VALUE AT SAME X LOCATION

STANTON NUMBER RATIO FOR TH=1 IS CONVERTED TO COMPARABLE TRANSPIRATION VALUE
USING ALOG(1 + B)/B EXPRESSION IN THE BLOWN SECTION

References

1. Esgar, J. B., Colladay, R. S., and Kaufman, A., "An Analysis of the Capabilities and Limitations of Turbine Air-Cooling Methods," NASA TND-5992, Sept. 1970.

2. Moffat, R. J., and Kays, W. M., "The Turbulent Boundary Layer on a Porous Plate: Experimental Heat Transfer with Uniform Blowing and Suction," Report NO. HMT-1, Thermosciences Div., Dept. of Mech. Engrg., Stanford Univ., 1967.

3. Simpson, R. L., Kays, W. M., and Moffat, R. J., "The Turbulent Boundary Layer on a Porous Plate: An Experimental Study of the Fluid Dynamics with Injection and Suction," Report No. HMT-2, Thermosciences Div., Dept. of Mech. Engrg., Stanford Univ., 1967.

4. Whitten, D. G., Kays, W. M., and Moffat, R. J., "The Turbulent Boundary Layer on a Porous Plate: Experimental Heat Transfer with Variable Suction, Blowing and Surface Temperature," Report No. HMT-3, Thermosciences Div., Dept. of Mech. Engrg., Stanford Univ., 1967.

5. Julien, H. L., Kays, W. M., and Moffat, R. J., "The Turbulent Boundary Layer on a Porous Plate: Experimental Study of the Effects of a Favorable Pressure Gradient," Report No. HMT-4, Thermosciences Div., Dept. of Mech. Engrg., Stanford Univ., 1969.

6. Thielbahr, W. H., Kays, W. M., and Moffat, R. J., "The Turbulent Boundary Layer: Experimental Heat Transfer with Blowing, Suction, and Favorable Pressure Gradient," Report No. HMT-5, Thermosciences Div., Dept of Mech. Engrg., Stanford Univ., 1969.

7. Kearney, D. W., Moffat, R. J., and Kays, W. M., "The Turbulent Boundary Layer: Experimental Heat Transfer with Strong Favorable Pressure Gradients and Blowing," Report No. HMT-12, Thermosciences Div., Dept. of Mech. Engrg., Stanford Univ., 1970.

8. Loyd, R. J., Moffat, R. J., and Kays, W. M., "The Turbulent Boundary Layer on a Porous Plate: An Experimental Study of the Fluid Dynamics with Strong Favorable Pressure Gradients and Blowing," Report No. HMT-13, Thermosciences Div., Dept. of Mech. Engrg., Stanford Univ., 1970.

9. Andersen, P. S., Kays, W. M., and Moffat, R. J., "The Turbulent Boundary Layer on a Porous Plate: An Experimental Study of the Fluid Mechanics for Adverse Free-Stream Pressure Gradients," Report No. HMT-15, Thermosciences Div., Dept. of Mech. Engrg., Stanford Univ., 1972.

10. Goldstein, R. J., "Film Cooling," Advances in Heat Transfer, 7:321-379, 1971.

11. Choe, M., Kays, W. J., and Moffat, R. J., "Turbulent Boundary Layer on a Full-coverage, Film-cooled Surface -- An Experimental Heat Transfer Study with Normal Injection," NASA Rep. CR-2642, 1976 (Also Stanford Univ., Dept. of Mech. Engrg., Report HMT-22).

12. Crawford, M. E., Kays, W. M., and Moffat, R. J., "Heat Transfer to a Full-coverage, Film-cooled Surface with 30° Slant-hole Injection," NASA Rep. CR-2786, 1976. (Also Stanford Univ., Dept. of Mech. Engrg. Report HMT-25).

13. Wieghardt, K., "Hot-Air Discharge for De-icing," AAF Translation, Report No. F-TS-919-Re, Wright Field, 1946.

14. Le Brocq, P. V., Launder, B. E., and Pridden, C. H., "Discrete Hole Injection as a Means of Transpiration Cooling -- An Experimental Study," Imp. Coll. Rep. HTS/71/37, 1971.

15. Metzger, D. E., Takeuchi, D. I., and Kuenstler, P. A., "Effectiveness and Heat Transfer with Full-coverage Film Cooling," J. Eng. Power, 95:180-184, 1973.

16. Mayle, R. E., and Camarata, F. J., "Multihole Cooling Film Effectiveness and Heat Transfer," J. Heat Transfer, 97: 534-538, 1975.

17. Metzger, D. E., and Fletcher, D. D., "Surface Heat Transfer Immediately Downstream of Flush, Non-tangential Injection Holes and Slots," AIAA, 5th Propulsion Joint Specialist Conference, USAF Academy, Colorado Springs, Colo, June, 1969, Paper 69-523.

18. Eriksen, V. L., "Film Cooling Effectiveness and Heat Transfer with Injection through Holes," NASA CR-72991, Aug. 1971.

19. Launder, B. E., and York, J., "Discrete Hole Cooling in the Presence of Free Stream Turbulence and Strong Favorable Pressure Gradient," HTS/73/9, Dept. of Mech. Engrg., Imperial College of Science and Technology, Jan. 1973.

20. Burggraf, F., and Huffmeier, R. W., "Film Effectiveness and Heat Transfer Coefficients for Injection from One and Two Rows of Holes at 35° to the Surface," AEG-Technical Information Series Report No. R70AEG351, General Electric Co., Lynn, Mass., Cincinnati, Ohio, August, 1970.

21. Nina, M. N. R., and Whitelaw, J. H., "The Effectiveness of Film Cooling with Three-Dimensional Slot Geometry," Gas Turbine Conference and Products Show, Houston, Texas, March 1971, ASME Paper No. 71-GT-11.

22. Ramsey, J. W., and Goldstein, R. J., "Interaction of a Heated Jet with a Deflecting Stream," NASA CR-72613, April 1970.

23. Metzger, D. E., Takeuchi, D. I., and Kuenstler, P. A., "Effectiveness and Heat Transfer with Full-Coverage Film Cooling," Trans. of ASME, J. Eng. Power, July 1973, pp. 180-184.

24. Goldstein, R. J., et al., "Film Cooling Following Injection through Inclined Circular Tubes," NASA CR-73612, 1969.

25. Eriksen, V. L., Eckert, E. R. G., and Goldstein, R. J., "A Model for Analysis of the Temperature Field Downstream of a Heated Jet Injected into an Isothermal Crossflow at an Angle of 90°," NASA CR-72990, 1971.

26. Pai, B. R., and Whitelaw, J. H., "The Prediction of Wall Temperature in the Presence of Film Cooling," Int. J. Heat Mass Transfer 14:409-426, 1971.

27. Patankar, S. V., Rastogi, A. K., and Whitelaw, J. H., "The Effectiveness of Three-dimensional Film-cooling Slots -- II. Predictions," Int. J. Heat Mass Transfer 16: 1673-1681, 1973.

28. Kline, S. J., and McClintock, F. A., "Describing Uncertainties in Single-Sample Expeirments," Mech. Engrg. 75:3-8, 1953.

29. Moffat, R. J., "Gas Temperature Measurement," Temperature -- Its Measurement and Control in Science and Industry. New York: Reinhold, 3:553-571, 1962.

30. Pimenta, M. M., Moffat, R. J., and Kays, W. M., "The Turbulent Boundary Layer: An Experimental Study of the Transport of Momentum and Heat with the Effect of Roughness," Report HMT-21, Thermosciences Div., Dept. of Mech. Engrg., Stanford Univ., 1975.

31. Colladay, R. S., "Importance of Combining Convection with Film Cooling," NASA TMX-67962, 1972.

32. Personal communication with M. E. Crawford, who did his Ph.D. thesis in "Heat Transfer to a Full-Coverage, Film-Cooled Surface with 30° Slant-Hole Injection," 1977.

32. Discussion with R. J. Moffat about "thermocouple probe."

1. Report No.	2. Government Accession No.	3. Recipient's Catalog No.
NASA CR-3103		

4\. Title and Subtitle HEAT TRANSFER TO A FULL-COVERAGE, FILM-COOLED SURFACE WITH COMPOUND-ANGLE (30^{o} AND 45^{o}) HOLE INJECTION

5\. Report Date February 1979

6\. Performing Organization Code

7. Author(s)
H. K. Kim, R. J. Moffat, and W. M. Kays

8\. Performing Organization Report No.
HMT-28

10\. Work Unit No.

9. Performing Organization Name and Address
Stanford University
Stanford, California 94305

11\. Contract or Grant No.
NAS3-14336

13\. Type of Report and Period Covered
Contractor Report

12. Sponsoring Agency Name and Address
National Aeronautics and Space Administration
Washington, D.C. 20546

14\. Sponsoring Agency Code

15\. Supplementary Notes
Final report. Project Manager, Raymond E. Gaugler, Fluid System Components Division, NASA Lewis Research Center, Cleveland, Ohio 44135.

16. Abstract
An experimental study of heat transfer was conducted on a turbulent boundary layer with full-coverage film cooling through an array of holes inclined at 30^{o} to the surface and 45^{o} to the flow direction (compound-angle injection). Heat transfer coefficients, based on $(t_{wall} - t_{stream})$, were measured over a range of injectant flows ($M = 0$ to $M = 1.5$) and Reynolds numbers ($1.6\times10^{5} \le Re_x \le 2.5\times10^{6}$) at velocities between 9.8 and 16.8 m/s. Data are presented for injectant temperature equal to the wall temperature and injectant temperature equal to the stream temperature. Superposition can be used to predict the Stanton number for any intermediate temperature. Compound-angle injection gives better thermal protection than in-line, slant-hole injection, but the beneficial effect is minimal in the first six rows of holes. For a value of $M = 0.37$ the heat transfer coefficient with compound-angle injection was the same as for the slant-angle injection after six rows, but was only one-half the slant-hole value after 11 rows. The data for compound-angle injection show the same general features as for slant-angle and normal injection. Within the blown region, Stanton number decreases rapidly, with the minimum at the last row of holes. Recovery is rapid after the last row of holes, with the heat transfer returning to a conventional smooth-plant correlation. The data for $M = 0.4$ show the lowest values of Stanton number. Pitch-to-diameter ratio of 10 provides less thermal protection than 5, for the same value of M.

17. Key Words (Suggested by Author(s))	18. Distribution Statement
Boundary layer; Heat transfer; Computer program; Turbulence; Numerical	Unclassified - unlimited STAR Category 34

19. Security Classif. (of this report)	20. Security Classif. (of this page)	21. No. of Pages	22. Price*
Unclassified	Unclassified	158	A08

* For sale by the National Technical Information Service, Springfield, Virginia 22161

NASA-Langley, 1979

END

June 12, 1981